Air, Water and Soil Quality Modelling for Risk and Impact Assessment

Edited by
Adolf Ebel
Teimuraz Davitashvili

Springer

This publication is supported by: The **NATO** Programme for **Security** through **Science**

Air, Water and Soil Quality Modelling for Risk and Impact Assessment

NATO Security Through Science Series

The Series is published by IOS Press, Amsterdam, and Springer Science and Business Media, Dordrecht, in conjunction with the NATO Public Diplomacy Division.

The Series is published by IOS Press, Amsterdam, and Springer Science and Business Media, Dordrecht, in conjunction with the NATO Public Diplomacy Division.

Sub-Series

A. **Chemistry and Biology** (Springer)
B. **Physics and Biophysics** (Springer)
C. **Environmental Security** (Springer)
D. **Information and Communication Security** (IOS Press)
E. **Human and Societal Dynamics** (IOS Press)

Meetings supported by the NATO STS Programme are in security-related priority areas of Defence Against Terrorism or Countering Other Threats to Security. The types of meeting supported are generally "Advanced Study Institutes" and "Advanced Research Workshops". The NATO STS Series collects together the results of these meetings. The meetings are co-organized by scientists from NATO countries and scientists from NATO's "Partner" or "Mediterranean Dialogue" countries. The observations and recommendations made at the meetings, as well as the contents of the volumes in the Series, reflect those of the participants in the workshop. They should not necessarily be regarded as reflecting NATO views or policy.

Advanced Study Institutes (ASI) are high-level tutorial courses to convey the latest developments in a subject to an advanced-level audience

Advanced Research Workshops (ARW) are expert meetings where an intense but informal exchange of views at the frontiers of a subject aims at identifying directions for future action

Following a transformation of the programme in 2004 the Series has been re-named and re-organised. Recent volumes on topics not related to security, which result from meetings supported under the programme earlier, may be found in the NATO Science Series

www.nato.int/science
www.springer.com
www.iospress.nl

Series C: Environmental Security

Air, Water and Soil Quality Modelling for Risk and Impact Assessment

edited by

Adolf Ebel
University of Cologne, Germany

and

Teimuraz Davitashvili
State University Tbilisi, Georgia

Printed on acid-free paper

CONTENTS

PREFACE

Environmental pollution by harmful anthropogenic substances and uncontrolled use of natural reserves have become a global problem and require substantial efforts for developing and applying efficient measures of control, mitigation and abatement. For achieving this goal predictions of possibly resulting risks and impacts are urgently needed for future environmental planning. Numerical models are convenient and indispensable tools for this purpose. Particularly due to public demand for improvement of environmental conditions (e.g. EU and UDA/EPA directives and recommendations) and due to the fact that the vulnerability of our complex modern society by manmade and natural hazards has dramatically grown during recent years, the need for reliable, complex and efficient models, which can be applied to such problems, is steadily increasing.

The majority of environmental quality models is focussing on selected isolated parts of the geo-system though impacts on one compartment usually also affect one or more other parts. There is a strong need to advance to an integral treatment of air, soil and water pollution by combining different models for different media. Furthermore it is imperative to develop and apply modern methods of control theory to environmental risk assessment in order to support mitigation and abatement measures in an optimal way.

Motivated by such considerations the NATO Advanced Research Workshop on "Air, Water and Soil Quality Modelling for Risk and Impact Assessment", was organized in Tabakhmela (Tbilisi), Georgia, from September 16 to 20, 2005, with the aim to address questions of joint environmental compartment modelling and applications of control theory to the assessment of environmental problems. It became a platform of lively and fruitful discussions. It is our hope that they will continue among the participants and stimulate further advancements of numerical environmental modelling and its application also beyond the small group which could be invited thanks to the support by the NATO Programme "Security Through Science". Three working groups analysed major problems and tasks of environmental modelling. There statements are found at the end of this volume and may be taken as a summary of the scientific outcome of the workshop.

The contributions to the proceedings are grouped in the following way. After an introductory paper issues concerning control theory and risk assessment are treated. Articles dealing with air, water and soil pollution modelling follow. The theoretical and modelling part is complemented by several papers concerned with actual environmental problems and their treatment. Goals and methods of integrated modelling are addressed, and views of future needs are found in the last part of the proceedings.

We are particularly grateful to the NATO Advisory Panel on Environmental Security for reviewing and approving the proposal of the Advanced Research Workshop.

We thank the members of the scientific and organizing committee for their contributions to planning and conductiing of the ARW. The committee was joined by

> Alexander Baklanov, DMI**,** Copenhagen, Denmark
> Ramaz Botchorishvili, VIAM, State University Tbilisi , Georgia
> Krassimir Georgiev, Bulgarian Academy of Sciences, Sofia
> David Gordeziani, VIAM, State University Tbilisi , Georgia
> Clemens Mensink, VITO, Mol, Belgium
> Ilya Tavkhelidze, VIAM, State University Tbilisi , Georgia
> Harry Vereecken, IGG, Agrosphere, Research Centre Juelich, Germany
> Zahari Zlatev, NERI, Roskilde, Denmark

Key lectures were delivered by Artash Aloyan, Alexander Baklanov, Carlos Borrego, Ramaz Botchorishvili, Teimuraz Davitashvili, Adolf Ebel, Krassimir Georgiev, David and Ekaterine Gordeziani, Wolfgang Joppich, Avtandil Kordzadze, Clemens Mensink, Roberto San José, Jirka Simunek, Sergej Zilitinkevich and Zahari Zlatev.

The Rhenish Institute for Environmental Research at the University of Cologne and the Tbilisi State University played an essential role for the preparation of the event and finally of the proceedings. Several participants helped to check and edit the articles collected in this book. Their substantial contribution to the publishing of the proceedings is gratefully acknowledged. We thank the NATO Public Diplomacy Division, particularly the Collaborative Programme Section with its Director Dr. Deniz Belen and ICS Programme Assistant Lynne Nolan, for patiently advising us and helping to solve the many problems originating from incompatibilities of the German and Georgian systems regarding the handling of organizational matters. Annelies Kersbergen from the Springer NATO Publishing Unit was always present with helpful advice and encouragement during the preparation of this volume.

We gratefully emphasize that the workshop would not have been so stimulating without the efforts of all participants to present excellent science at the workshop and that this book would not have been possible without the readiness of the authors to invest a considerable amount of time and energy in the preparation of attractive original articles.

Adolf Ebel and Teimuraz Davitashvili, Co-Directors of the ARW,
Cologne, Germany, and Tbilisi, Georgia,
September 2006

RISK AND EMERGENCY MODELLING FOR ENVIRONMENTAL SECURITY: GENERAL ASPECTS

CARLOS BORREGO*, JORGE HUMBERTO AMORIM
*CESAM, Department of Environment and Planning,
University of Aveiro, 3810-193 Aveiro, Portugal*

Abstract. The international instruments in the scope of environmental protection are not successful without taking into account the risk of natural hazards and terrorist attacks and their impact. Disaster reduction policies and measures need to be implemented, to enable societies to be resilient to natural and man-made hazards while ensuring that the development efforts do not increase the vulnerability to these hazards. Disaster reduction is therefore emerging as an important requisite for sustainable development. The need to have accurate tools supporting the development and implementation of adequate risk analysis, management and mitigation approaches, plans, methodologies and strategies give models a unique importance. In this context, the work is focused on some of the efforts made so far in the scope of risk and emergency modelling towards environmental security, at different spatial scales, from the atmosphere to aquatic systems.

Keywords: natural hazards; man-made hazards; risk analysis; emergency modelling; environmental security

_____

  * To whom correspondence should be addressed. Carlos Borrego, Department of Environment and Planning, University of Aveiro, 3810-193 Aveiro, Portugal; e-mail: borrego@ua.pt

1.   Introduction

As the world enters the 21st century, it faces critical levels of stresses to the resources of the planet. The former United Nations (UN) Secretary General Kofi Annan (2000) reflected a growing consensus of these realities when he wrote in his Millennium Report that «Freedom from want, freedom from fear, and the freedom of future generations to sustain their lives on this planet» are the three grand challenges facing the international community.

Nowadays, there is a growing concern about the frequency and the effects of both natural and human threats to the environment, human security and health and also to property. The attention to the problem is continuously brought by worldwide examples of extreme natural disasters, as floods, earthquakes, windstorms and droughts, identified as the most costly geo-hazards in terms of humanitarian costs and related damages; but also forest fires, volcanic eruptions, snow avalanches, landslides or even tsunamis. On the other hand, societies are learning to live with the constant threat of man-made disasters, either they have an accidental or deliberate origin, as in the case of terrorist attacks which is one of the major threats to world security for the current century. Also, the environmental crisis of this century can threat world stability. In fact, environmental problems clearly increase social and economic stresses while reducing possibilities for sustainable development, particularly in weak economies.

It is clear that the international instruments focused on environmental protection are not successful without taking into account the risks and the increasing costs of natural, environmental, technological and biological threats. Disaster reduction policies and measures need to be implemented, to enable societies to be resilient to natural hazards while ensuring that the development efforts do not increase the vulnerability to these hazards. Disaster reduction is therefore emerging as an important requisite for sustainable development. Consequently, there is evidence of greater official and public understanding that the threat of combined political, economical and environmental consequences of disasters demands more effective means to address vulnerability to current and emerging risks.

The need to have accurate tools supporting the development and implementation of adequate risk analysis, management and mitigation approaches, plans, methodologies and strategies give numerical models a unique importance. Within this context, the current document is focused on some of the efforts made so far in the scope of risk and emergency modelling towards environmental security, at different spatial scales, from the atmosphere to aquatic systems, and both at the scientific and institutional levels.

2.   Background

Recently, two natural disasters dramatically highlighted the importance of risk awareness, early warning, vulnerability reduction, and sustained attention to disaster and risk management. First, on 26 December 2004 the powerful earthquake and consequent tsunami that hit the Indian Ocean region, which resulted on a total estimate of 300,000 deaths and billions in material losses. Then, on 29 August 2005, the hurricane Katrina hit the coastal regions of Louisiana, Mississippi and Alabama with a strength that made it as one of the most destructive tropical cyclones ever in the United States. Subsequent flooding over most of the city of New Orleans, a large part of which lies below sea level, resulted in widespread damage and numerous deaths.

Also the disasters accidentally induced by human activity play a significant role on the overall scope of risk analysis and mitigation. An historical example was the accident occurred at the Chernobyl nuclear power plant in northern Ukraine on 26 April 1986, which originated a release of large amounts of radioactivity, primarily radioactive isotopes of caesium and iodine, that contaminated large areas of Belarus, the Russian Federation and Ukraine and other countries to a lesser extent, and exposed sizable populations to internal and external radiation doses (WHO, 2005). Another example, this one with a significant impact on the aquatic system, was the oil spill that occurred in 1979 in the gulf of Mexico, when the tanker IXTOC I spilled 560 thousands of tonnes of oil into the water, turning it as the 2nd largest oil spill of all-time, surpassed only by the deliberate release of oil during the 1991 Gulf War (NOAA, 1992). On the other hand, another type of man-made disaster that has grown in importance over the last years is related with the deliberate threat to human lives through terrorist attacks. In fact, the recent examples in the USA, Spain and United Kingdom, led to a new concept on security in the European and North-American territories.

The recognition of the international community of the necessity and the realistic potential for building the resilience of nations and communities to disasters was shown at the World Conference on Disaster Reduction (UN/ISDR, 2005), launched in January 2005, which was considered as a milestone in the progress in the broad areas of disaster risk reduction. Called for by the UN General Assembly and hosted by the Government of Japan, it brought together about 4,000 people from governmental and non-governmental bodies around the world, with participants from 168 States, 78 observer organizations, 161 NGOs and over 560 journalists. Through the adoption of a ten-year plan of action, the conference undertook a commitment to decrease substantially the loss in lives and social, economic and environmental assets of communities and countries around the world.

This strategy results from a greater official and public understanding that the threat of combined political, economic and environmental consequences of disasters demands more effective means to address vulnerability to current and emerging risks. Moreover, beyond general recognition and endorsement of these values, significantly greater commitment in practice is required. The current trends in vulnerability and in natural, environmental, technological and biological threats to societies reinforce the fact that they are often interrelated, and that they can result in widespread and compound effects. It is therefore crucial that those threats are taken into consideration when developing local risk reduction strategies.

3. Emergency preparedness and response models

The value of advanced technologies in the scope of disaster reduction and management is now widely recognized, mainly due to the fact that the performances of numerical models have risen significantly during the last decades, accompanying the technological development of remote sensing, geographic information systems, space-based observations, and information and communications technologies.

Modelling capabilities range from the relatively simple to the highly complex, varying with the type of application, the accuracy needed, the information available, the computational running time and the hardware requirements. Depending on their characteristics, models can be successfully applied in any of the stages of the disaster-management cycle, which is a core concept within environmental health management in disasters and emergencies. The objectives of such approach are to reduce, or avoid, losses from hazards; to assure prompt assistance to victims; and to achieve rapid and effective recovery. Main stages, also as their specific objectives, are summarized in Table 1.

TABLE 1. Objectives and examples of procedures taken during each stage of the disaster-management cycle (adapted from WHO, 2002).

Mitigation	Minimizing the effects of disaster
	Examples: building codes and zoning; vulnerability analyses; public education
Preparedness	Planning how to respond
	Examples: preparedness plans; emergency exercises/training; warning systems
Response	Efforts to minimize the hazards created by a disaster
	Examples: search and rescue; emergency relief
Recovery	Returning the community to normal
	Examples: temporary housing; grants; medical care

In this scope, and according to their characteristics, the application of modelling systems can be extremely valuable at different stages of an event:

- during the preparedness stage: for predicting the outcome of potential disaster scenarios, to improve pre-disaster planning, preparedness, communication and risk awareness for formulation of mitigation policies;
- during the response stage: for evaluating the hazard zone in a timescale ranging from minutes to some hours after the occurrence;
- in the post-event recovery and analysis stage: in the assessment of the impacts on human health and environment, in a period ranging from days to several months after the event.

4.   Some examples of modelling tools with application in the field of environmental security

One can find several examples of integrated numerical systems specifically oriented to risk and emergency modelling in the scope of environmental security. In this sense, this document doesn't intend to be an exhaustive list of the available tools; but, on the contrary, a brief state-of-the-art on some of the models that state the current effort and achievements on risk and emergency preparedness and response in the fields of natural and man-made disasters.

4.1. NATURAL DISASTERS

This section gives some examples of decision support tools developed in the scope of forest fires fighting, as also some modelling efforts in the field of other types of geo-hazards, as floods, volcanoes or landslides.

4.1.1. *Forest fires*

There are several examples of Forest Fire Decision Support Systems (FFDSS) that were developed for supporting the process of decision making during the management of forest fires, at different levels: risk assessment; simulation of fire and smoke behaviour and visibility impairment; and fire suppression decision support. This document summarises some FFDSS examples on each of the topics referred above. More information can be found in the work produced under the scope of the EC Research Project EUFIRELAB (Xanthopoulos et al., 2003).

In the scope of risk assessment, the SAFES Decision Support Tool, developed by the Greek company Algosystems, allows to estimate the

natural risk caused by natural factors such as vegetation, topography, etc; the human risk associated to human factors such as land-planning, accessibility of location, etc; the meteorological risk caused by meteorological factors (wind, air humidity, etc); and the degree of house protection, which is the level of protection of a specific house according to is construction, characteristics, surrounding environment, etc.

For the simulation of fire behaviour, F.M.I.S - An Integrated Software System for the Management of Forest Fires, developed by the same company gives the fire line evolution and the burned area according to the terrain and vegetation characteristics and the meteorological conditions.

Willing to couple the simulation of fire behaviour with smoke behaviour and visibility impairment, the Portuguese Universities of Aveiro and Coimbra worked together in order to develop DISPERFireStation, which is an integrated system capable of giving all the information related to fire progression, as in the case of FMIS, and additionally all the data needed to assess the air quality conditions, for instance through the representation of carbon monoxide (CO) or particulate matter concentrations three-dimensional (3D) fields, calculated according to fire progression, topography and meteorological data, and also the visibility conditions, which are simulated based on the extinction efficiencies of the emitted air pollutants (Valente et al., 2005).

In the scope of fire suppression decision support, the Intergraph Public Safety, from France, developed FIRETACTICS, a FFDSS that allows the optimisation of forest fire fighting operations, helping managers to make quick and documented decisions concerning the fire fighting plans, according to the available means.

As an example of a fire suppression decision support system, with a special focus on aerial fire fighting, the University of Aveiro and the Algosystems company developed under the scope of the EC research project ERAS an operational tool for the retardant aerial dropping modelling, which allows the simulation of the retardant ground pattern (concentration per square meter). This integrated system is prepared to be used in real time by the operational staff in order to improve the efficiency of suppression activities, and also as a training tool in the definition of good practices for the aerial application of retardants (Amorim et al., 2006).

4.1.2. *Other types of geo-hazards*

On the overall scope of natural disasters there are already interesting and promising developments on decision support tools applicable to avalanches, earthquakes, desertification, erosion, floods, windstorms, volcanic eruptions or even tsunamis. For instance, within floods modelling it is possible to generate 3D visualisations to determine flood levels at specified time

intervals. In the case of a tsunami, the DHI's MIKE 21 modelling system, owned by the DHI Software company, allows to simulate the region around the fault zone and the wave approach to the shore and consequent inundation of an urban area, allowing to have a first estimate of the possible consequences prior to or after the event.

In what relates to volcanoes, the Hybrid Single-Particle Lagrangian Integrated Trajectories model (HYSPLIT), from the NOAA Air Resources Laboratory, permits the modelling of the volcanic ash transport and its dispersion along the time for a given volcanic eruption.

Another example is the 3D modelling and visualisation of a given massive landslides, whether it is a real or hypothetical situation, which is another capability of nowadays' computer models. The overall objectives of this kind of studies are to determine what effect climate change has on the frequency of these events, to assess the physical impact of a landslide on the local environment, to develop a method for predicting their occurrence, and to determine why and how they occur.

4.2. MAN-MADE DISASTERS: ACCIDENTAL/DELIBERATE RELEASE OF HAZARDOUS AGENTS

This section is focused on risk and emergency models in the scope of both accidental and deliberate releases of hazardous agents to the atmosphere, water and soil.

4.2.1. *Accidental/deliberate release of chemical, biological or nuclear (C/B/N) agents to the atmosphere*

Modellers and emergency managers have long been concerned with tracking and predicting the atmospheric dispersion of hazardous agents originated by:

- accidental releases from industrial sites or during transport operations;
- terrorist attacks with mass destruction weapons, including the deliberate release of chemical, biological or nuclear (C/B/N) agents.

In the event of a chemical release to the atmosphere, whether planned or accidental, the ability to visualize the magnitude and extent of the chemical plume is critical. Consequently, models should be able to predict as accurately as possible the path and spread of different types of hazardous agents, in most cases in the absence of basic input information, providing a technical basis in any of the stages of an event:

- preparedness stage: training for response to threats against specific events such as the Olympics, or specific targets such as a nuclear power plant or a crowded city;

- response stage: for the immediate response to unanticipated emergency events. In this case, fast-response models are required;
- post-event recovery and analysis stage: for a detailed analysis of the wind flow and the contaminants dispersion behaviour after the accident, allowing to assess the expected impacts.

As an example of a model specifically developed for being applied in the preparedness stage, in this case in a specific event as the 2004 Olympic Games in Greece, the Northrop Grumman Information Technology developed a numerical tool capable of generating visualizations of surface dosage and probability of effect near Athens for an hypothetical terrorist attack with sarin gas.

When the objective is to simulate the effects of a potential accident on a specific target as a nuclear power plant, the Oak Ridge Evacuation Modeling System (OREMS), developed by the Oak Ridge National Laboratory, allows to simulate the evacuation plan through the calculation of the time required to evacuate a community, based on the population and average speed of the moving cars.

At the response stage, tools as the CT-Analyst, from the Naval Research Laboratory, estimates a given contaminant dispersion in a city downtown after a hypothetical terrorist attack. Also the Federal Emergency Management Information System (FEMIS), owned by the Pacific Northwest National Laboratory, performs a hazard analysis in response to a hypothetical chemical agent accidental release.

With application at the post-event recovery and analysis stage, more detailed and accurate models are available. One example is again the HYSPLIT model, which allowed, for instance, to perform the simulation of the evolution with time of the Caesium deposition after the Chernobyl accident. At a smaller scale, the FAST3D-CT model, from the Naval Research Laboratory, allows an high resolution simulation of the dispersion of the C/B/N agent released from an hypothetical terrorist attack in a given city centre.

Because it is impossible to anticipate all possible scenarios for an airborne release of an hazardous agent, and in many cases, the exact source location or nature may not be known initially, the advancement of technology in areas as meteorological forecasting, satellite communication, dispersion modelling, plume animation, and data storage, coupled with the rapid deployment of monitoring equipment, should give the needed support and a new insight into the problem.

4.2.2. *Accidental release of pollutants to the aquatic systems: Oil spills*

Although the number of large spills has significantly decreased during the last thirty years, their impacts on environment still persist, as in the case of physical and chemical alteration of natural habitats, lethal or sub-lethal effects on flora and fauna, and changes in biological communities resulting from oil effects on key organisms.

In 2002, the Prestige accident spilled 77 thousands of tonnes of heavy fuel oil into the sea, polluting the Galician coastline. The pollution then spread to the shores of Asturias, Cantabria and the Spanish Basque country, reaching the French coast. A week after the accident, more than 200 km of Atlantic coastline from the Spanish border to L'Ile d'Yeu were affected. The importance of this oil spill, among several others, is not also its magnitude and impact on public opinion, but also the opportunity that was given to test some of the models specifically developed for dealing with this kind of task, as it is the case of the Water Modelling System "Mohid", developed by MARETEC (Marine and Environmental Technology Research Centre) at Instituto Superior Técnico (IST), Portugal. This model allows to predict and simulate the trajectory and weathering of oil spills, which is essential to the development of pollution response and contingency plans, and to the evaluation of environmental impact assessments. In this specific case, this tool predicts the evolution and behaviour of the processes (transport, spreading and behaviour) and properties of the oil product spilled in water.

4.2.3. *Soil and groundwater contamination*

The soil and groundwater contamination can have different possible sources, as mining activities, the use of fertilisers and pesticides in agriculture, industrial activities, accidents, etc. As an example, the Visual MODFLOW Model, from the Scientific Software Group, allows to predict the contaminant transport in groundwater. Typical applications include the analysis, planning and management of a wide range of water resources and related environmental problems, such as the surface water impact from groundwater withdrawal, the river basin management and planning, environmental impact assessments, aquifer vulnerability mapping with dynamic recharge and surface water boundaries, groundwater management, floodplain studies, impact studies for changes in land use and climate, or impact studies of agricultural practices including irrigation, drainage and nutrient and pesticide management.

5. An overview on relevant institutional efforts in the scope of environmental security in Europe

Research related to hazards and disaster risks has expanded greatly during the past 10 years. This section provides examples of institutional support given to multinational and interdisciplinary research in the fields of natural and technological disasters in Europe.

The Global Monitoring for Environment and Security (GMES) is a joint initiative of the European Union and the European Space Agency (ESA), seeking to support the policy information needs through the following stages:

- mapping: consistent information from local to European scales;

- forecasting: systematic information on the short to long term evolution of Earth environment (air, water, resources);

- crisis management: real-time and secure information for civil protection and security.

The European Mediterranean Disaster Information Network (EU-MEDIN) is an initiative of the DG Research that intends to foster coordinated and increased access to data and expert know-how before, during, and after a disaster. It has also as main goal to enhance the coordination among the research and user communities for improved disaster preparedness and early warning, communication and rapid exchange of data and knowledge, in order to better mitigate and manage disasters.

The Natural and Environmental Disaster Information Exchange System (NEDIES) is a European Commission project developed in the framework of the DG JRC Institutional Programme "Safety and Emergency Management for Man-Made and Natural Hazards" aimed to support EU policies in the area of prevention, mitigation and management of natural risks and accidents. The major objectives are:

- supply the EU Commission with updated information about the occurrence of disasters and accidents, and their management;

- make available to the Civil Protection Services validated information on past disasters and accidents, their main consequences, methods and techniques relevant for the prevention of disasters, preparedness and response;

- provide an interdisciplinary platform for dialogue to facilitate the exchange of information between all the actors involved in the management of disasters and accidents;

- protect the citizens from disasters and accidents via the dissemination of targeted information on risk perception and awareness;

- constitute a common European repository of lessons learnt from disasters, with special focus on mitigation of disaster consequences.

Technology itself cannot guarantee security, but security without the support of technology is impossible. In today's technology-driven and knowledge-based world, excellence in research is a prerequisite for the ability to tackle the new security challenges. As a result, the technology base for defence, security and civil applications increasingly forms a continuum. Across it, applications in one area can often be transformed into applications in another. The challenge will be to take these initiatives forward and to develop them into a coherent approach. In this context, the establishment of an European Security Research Programme (ESRP) from 2007 onwards is crucial. Straddling civil and defence research, an ESRP should take advantage of both the duality of technologies and the growing overlap of defence and non-military security functions to bridge the gap between the various research sectors.

6. Conclusions

The power of current computational and communication resources means that we are able to create modelling and decision-support tools with unprecedented quality. In fact, during the past quarter century there have been many developments in scientific models and computer codes prepared to help predicting the ongoing consequences in the aftermath of many types of emergency: e.g. storms and flooding, chemical and nuclear accidents, epidemics such as SARS and terrorist attacks. Some of these models relate to the immediate events and can help in managing the emergency; others predict long-term impacts and thus can help to shape the strategy for returning to normality.

As a result of the developments on software and hardware performances, and on the technical skills of the personnel prepared to work with them, operational people can now benefit from the capabilities of models at any of the stages of an event: preparedness, response and post-event recovery and analysis. However, modelling the biosphere with ever-greater number of biotic and abiotic components remains a great challenge of our time, and some efforts are still needed, namely:

- an improvement in monitoring capability leading to better data and information access;
- a better understanding of events based on a more comprehensive integrated service bringing together diverse but complementary data sources and stakeholders;

- an improvement of models capacity, mainly at the operational level;

- technologically sophisticated countries and organizations need not only to encourage the wider application of technologies for disaster reduction in developing countries and for disaster-affected communities, but also to support fulfilment of associated human and technical requirements.

The development of improved models and technologies for hazard forecasting, analysis, planning, risk assessment and mitigation should contribute to reduce the impacts of hazards and risks and bring about improved disaster preparedness in the near future. In this sense, modellers should play an important role on the development of even more accurate numerical tools, which should be able to simulate the path and spread of hazardous agents, either they came from an accidental or a deliberate release; or to predict the potential consequences of a natural disaster. These operational tools should tackle the problem, in most cases in the absence of basic input information, providing a technical basis for the selection of emergency planning zones, public awareness areas, and recommendations supporting land-use activities, and emergency response pre-planning and event-planning tools to support field exercises and ensure that emergency response plans would be effective.

In today's globalised and complex world it is more vital than ever to have the decision support systems able to give reliable and timely information, in order to meet nowadays needs in security and environment. The development of improved models and technologies for hazard forecasting, risk assessment and mitigation should contribute for reducing impacts of hazards and risks and bring about improved disaster preparedness in the near future.

Acknowledgments

References

Amorim, J.H., Miranda, A.I., Borrego, C., Varela V., 2006, Recent developments on retardant aerial drop modelling for operational purposes, 5th International Conference on Forest Fire Research, November 24th - December 1st 2006, Figueira da Foz, Portugal.

Annan, K.A., 2000, "We the peoples", The role of the United Nations in the 21st Century, United Nations, Department of Public Information, New York, 80 p.

NOAA, 1992, Oil spill case histories 1967-1991, Summaries of significant U.S. and International spills, NOAA/Hazardous Materials Response and Assessment Division, Seattle, Washington; 224 p.

UN/ISDR, 2005, Building the resilience of nations and communities to disasters; United Nations Inter-Agency secretariat of the International Strategy for Disaster Reduction (UN/ISDR); Proceedings of the World Conference on Disaster Reduction 18-22 January 2005, Kobe, Hyogo, Japan; Geneva.

Valente, J., Miranda, A.I., Lopes, A.G., Borrego, C. and Viegas, D.X., 2005, A local-scale modelling system to simulate smoke dispersion, 6th Symposium on Fire and Forest Meteorology, 25-27 October, Canmore, AB, Canada.

WHO, 2002, Environmental health in emergencies and disasters: a practical guide. World Health Organization. B. Wisner, J. Adams (Eds), 252 p.

WHO, 2005, Health Effects of the Chernobyl Accident and Special Health Care Programmes; World Health Organization (WHO), Working Draft Report of the UN Chernobyl Forum Expert Group "Health" (EGH).

Xanthopoulos, G., Varela, V., Fernandes, P., Ribeiro, L., Guarnieri, F., 2003, Decision support systems and tools: a state of the art, Deliverable D-06-02, EUFIRELAB: Euro-Mediterranean Wildland Fire Laboratory, a "wall-less" Laboratory for Wildland Fire Sciences and Technologies in the Euro-Mediterranean Region; 41 p (available at www.eufirelab.org).

VARIATIONAL TECHNIQUE FOR ENVIRONMENTAL RISK/VULNERABILTY ASSESSMENT AND CONTROL

VLADIMIR PENENKO*, ELENA TSVETOVA
Institute of Computational Mathematics and Mathematical Geophysics of SD RAS, prospect Lavrentieva 6, 630090, Novosibirsk, Russia

Abstract. Logical schemes as well as constructive aspects of a variational methodology for problems of diagnostics, monitoring, and risk assessment are presented.

1. Introduction

Interaction between man and environment manifests itself in various forms. Recently the considerable attention has been focused on the research of human-induced changes of environmental quality because these changes, in turn, influence life quality and population health. The concept of ecological risks and vulnerability plays one of the key roles here. In reality the subject matter is more difficult and complicated. In general sense, we should formulate a trade-off between environmental protection and industrial development. From the mathematical point of view it is necessary to plan the character of man-nature interactions for the purpose of choosing optimal strategies according to the given goal functionals and restrictions. The effective tools to solve problems in such formulation are the

---

    *To whom correspondence should be addressed. Vladimir Penenko, Institute of Computational Mathematics and Mathematical Geophysics of SD RAS, prospect Lavrentieva 6, 630090, Novosibirsk; e-mail: Penenko@sscc.ru

comprehensive models of environmental evolution. In the world there are some different ways to solve the problems of this class[1-3].

In the paper the concept and the methods developed at the Institute of Computational Mathematics and Mathematical Geophysics SD RAS to study the nature processes and to solve interconnected problems of ecology and climate are presented.

The traditional approach to solve environmental problems is usually based on forward modelling. Despite of wide use of this approach, methods of forward modelling cannot provide comprehensive assessment of all the complex questions arising in nature protection with modern standards. The specific features of ecological forecasting and design demand the combined use of forward and inverse methods. Such methods are generated by variational principles together with the methods of sensitivity, optimization, and control. This enables to construct an open modelling system as well as to provide effective ways of its realization on modern computers[4-9].

2.   Statement of the problem

A rather broad spectrum of environmental protection problems exists. This scientific field unites many disciplines such as physics, chemistry, ecology, biology, economy, mathematics, etc. Here we present the mathematical tool intended to combine diverse knowledge in this interdisciplinary issue. The relevant processes are described by hydrodynamic models of the climatic system, models of transport and transformation of moisture, chemically and optically active pollutants in gas and aerosol phase. To handle the process models and monitoring systems with the purpose of treating the interactions between them both in the forward and inverse modes, we assume that all elements of the system (i.e. models and observations) can contain uncertainties and errors. In this case, it is natural to construct the algorithms for realization of such communications that proceed from conditions of minimization of some total measure of uncertainties and errors. For the description of processes and their mathematical models we introduce some types of objects such as a state function $\boldsymbol{\varphi} = \{\varphi_i(\mathbf{x},t),\ i=\overline{1,n}\} \in Q(D_t)$, model parameters $\mathbf{Y} \in \mathrm{R}(\mathrm{D}_t)$, and an adjoint functions $\boldsymbol{\varphi}^* = \{\varphi_i^*(\mathbf{x},t),\ i=\overline{1,n_c}\} \in Q^*(D_t)$, $n_c \geq n$. Here D_t is the domain of definition of spatial coordinates and time, $D_t = D \times [0,\overline{t}\,]$, D is the area of change of spatial coordinates $\mathbf{x} = (x_1, x_2, x_3)$, $[0,\overline{t}\,]$ is the time interval; $Q(D_t)$ is the space of the state functions satisfying the boundary conditions at the boundary Ω_t of the area D_t. The functional space $Q^*(D_t)$ is adjoint to the space of the state functions $Q(D_t)$, $R(D_t)$ is the range of

admissible values of parameters. The domain D_t is considered to be in three variants: a sphere, a hemisphere or limited areas on the sphere.

In the paper the purpose of the detailed description of all elements of the system is not pursued. The various aspects can be found in[2-5].

Here we consider only those models which are directly describing the processes of heat, moisture, radiation, and pollutants transport and transformation in the atmosphere as follows:

$$L\boldsymbol{\varphi} \equiv \frac{\partial \boldsymbol{\pi}\varphi_i}{\partial t} + \mathrm{div}\boldsymbol{\pi}(\varphi_i\, \mathbf{u} - \mu_i \mathrm{grad}\, \varphi_i) + \boldsymbol{\pi}((H\boldsymbol{\varphi})_i - f_i(\mathbf{x},t) - r_i) = 0, \ \ i = \overline{1,n}. \quad (1)$$

Here φ_i are the potential temperature, the mixing ratio of humidity in the atmosphere (water vapour, cloud water, rain water, snow and ice crystals), the concentration of pollutants in gas and aerosol phase); $\mathbf{f} = \{f_i(\mathbf{x},t)\}$ is the function of heat, moisture and pollutants sources; $\mathbf{r} = \{r_i\}$ are the functions describing uncertainty and errors of the models; $\mathbf{u} = (u_1, u_2, u_3)$ is the velocity vector; $\boldsymbol{\pi}$ is the function depending on the coordinate system; $\mu_i = (\mu_1, \mu_2, \mu_3)_i$ are the coefficients of turbulent exchange for a substance φ_i in the coordinate direction $\mathbf{x} = \{x_i\}, i = 1,3$; $H(\boldsymbol{\varphi})$ is the nonlinear matrix operator which describes the local processes of transformation of the corresponding substances. The functions $\mathbf{u}, \mu_i, f_i$ and input data of initial and boundary conditions are included in vector $\mathbf{Y}$.

To take into account the formation and transformation of aerosols (nucleation, coagulation, condensation, etc.), one more variable, i.e. the size of particles, is introduced. Besides, the new members having integro-differential structure are added to the operator of transformation.

The processes of dry and wet deposition are considered in the vertical terms of the transport operator. An example of the base cycle of chemical transformation of a multicomponent mixture of pollutants for typical conditions in the atmosphere of industrial regions is presented in[5,10].

The initial conditions at $t = 0$, the boundary conditions, and the model parameters can be written in the form:

$$\boldsymbol{\varphi}^0 = \boldsymbol{\varphi}_a^0 + \boldsymbol{\xi}(\mathbf{x}), \ (R_b(\boldsymbol{\varphi}))_i - g_i = \varepsilon_i, \ \ i = \overline{1,n}, \ \ \mathbf{Y} = \mathbf{Y_a} + \boldsymbol{\zeta}(\mathbf{x},t), \qquad (2)$$

where $\boldsymbol{\varphi}_a^0$ and $\mathbf{Y_a}$ are the set of the prior estimations of the initial fields $\boldsymbol{\varphi}^0$ and the vector of parameters $\mathbf{Y}$; $\boldsymbol{\xi}(\mathbf{x}), \boldsymbol{\zeta}(\mathbf{x},t)$ are the errors and uncertainty of initial fields and parameters; R_b are the operators of boundary conditions, and g_i, ε_i are functions describing sources and uncertainty at the boundary Ω_t of the domain D_t. To include observational data in the model system it is necessary to formulate a functional dependence between the data of measurements and the state functions in the forward and inverse modes

$$\Psi_m = [\mathbf{W}(\varphi)]_m + \eta(\mathbf{x}, t), \tag{3}$$

where Ψ_m is the set of measured values; $[\mathbf{W}(\varphi)]_m$ is the set of observational models; $\eta(\mathbf{x}, t)$ are the errors and uncertainty of these models and data. The values Ψ_m are defined on the set of points $D_t^m \in D_t$. The symbol $[\ ]_m$ denotes the operation of data transfer from D_t to D_t^m.

3. The variational formulation of models of processes

Integration of all models in a united system is carried out by means of variational principles.

Therefore, along with the differential formulation of the problem, we use the variational formulation of the model (Eqs.1 - 2)[4]

$$I(\varphi, \mathbf{Y}, \varphi^*) = \int_{D_t} (L(\varphi), \varphi^*) dDdt = 0. \tag{4}$$

The integral identity (Eq. 4) is constructed with the use of boundary and initial conditions. Having executed all necessary transformations in Eq. (4) for the model (Eqs. 1–2), we finally receive integral identity in the form of

$$I(\varphi, \mathbf{Y}, \varphi^*) \equiv \sum_{i=1}^{n} \left\{ (\Lambda\varphi, \varphi^*)_i + \int_{D_t} (H(\varphi)_i - f_i - r_i)\varphi_i^* \pi dDdt \right\} = 0, \tag{5}$$

$$(\Lambda\varphi, \varphi^*)_i \equiv \left\{ \int_{D_t} \left\{ 0.5 \left[(\varphi^* \frac{\partial \pi\varphi}{\partial t} - \varphi \frac{\partial \pi\varphi^*}{\partial t}) + (\varphi^* \,\mathbf{div}\, \pi\varphi\mathbf{u} - \varphi \,\mathbf{div}\, \pi\varphi^*\mathbf{u}) \right] + \right.$$

$$\left. \pi\mu \,\mathbf{grad}\, \varphi \,\mathbf{grad}\, \varphi^* \right\} dDdt + \int_D 0.5\varphi\, \varphi^* \pi dD \Big|_0^{\bar{t}} + \tag{6}$$

$$\int_{\Omega_t} (0.5\varphi u_n - \mu \frac{\partial \varphi}{\partial n})\varphi^* \pi d\Omega dt + \int_{\Omega_t} ((R_b\varphi) - g - \varepsilon)\varphi^* \pi d\Omega dt \right\}_i.$$

u_n is the normal to the boundary component of the velocity vector. Discrete approximations of Eqs. (5) - (6) are constructed in such a way that they should keep the basic properties incorporated in integrated identity.

4. Variational principles in the problems of environment protection

To formulate the variational principles we introduce a set of functionals which express the generalized characteristics of the processes and mathematical models. For the purposes of monitoring, forecasting, management and designing let us define a set of such characteristics by means of the functionals of a general type

$$\Phi_k(\varphi) = \int_{D_t} F_k(\varphi)\chi_k(\mathrm{x},t)dDdt \equiv \left(F_k(\varphi), \chi_k(\mathrm{x},t)\right), \quad k=1,...,K, \; K \geq 1, \; (7)$$

where $F_k(\varphi)$ are the functions of the given form defined and differentiated on the set of the model state functions $Q(D_t)$, $\chi_k(\mathrm{x},t) \geq 0$ are the weight functions, $\chi_k \in Q^*(D_t)$ and $\chi_k(\mathrm{x},t)dDdt$ are the corresponding measures of Radon and Dirac in $D_t^{h\;11}$. At a suitable choice of the functions $F_k(\varphi)$ and $\chi_k(\mathrm{x},t)dDdt$ in Eq. (7) by means of the functionals of this type, it is possible to describe the various generalized global, distributed and local characteristics of the system behaviour, as well as the ecological restrictions on the environment quality, the results of observations of various types, the criteria of management and designing, the criteria of model quality etc[6,9].

 "Quality" functionals help us to include the data of observations (Eq. 3) to the modelling system for goals of data assimilation and parameter identification. Usually they are defined as an estimation of a measure of all uncertainties in the structure of Eq. (3)

$$\Phi_0(\varphi) = \left(\left(\Psi_m - [\mathbf{W}(\varphi)]_m\right)^{\mathrm{T}} \chi_0 \mathbf{S}\left(\Psi_m - [\mathbf{W}(\varphi)]_m\right)\right)_{D_t^m}, \qquad (8)$$

where index T denotes the transposing, $\mathbf{S}$ is a weight matrix for formation of scalar product on the set of the observed data of the various nature. It is the positive definite Hermitian matrix, χ_0 is the weight function defining a configuration of the space-time support of observation D_t^m in D_t and a measure for representation of Eq. (8) in the form of Eq. (7). To locate the sources and design observations in addition to the functionals of Eq. (8), it is necessary to introduce the sequence of the functionals of the type of Eq. (7). Each of them describes the individual observation in the structure of Eq. (3).

 The functionals of the following types are introduced for the solution to the problems of optimization of nature protection activity, control of environmental quality and ecological designing in the presence of constrains[6]. Using the definition (Eq. 7), we write down them both as equalities and inequalities

$$\Phi_{ri}(\varphi) = \int\limits_{D_t} F_{ri}(\varphi)\chi_{ri}(x,t)dDdt \leq 0, \quad i = \overline{1,n_c} \ , \qquad (9)$$

where functions $F_{ri}(\varphi)$ are defined in such a way that all the integrated, local, and distributed restrictions on the state functions could be accounted by means of Eq. (9), n_c is the total number of restrictions. In particular, the equality in Eq. (9) takes place when it is necessary to consider the restrictions in the form of inequalities distributed in D_t

$$\psi_i(\varphi,\mathbf{x},t) \leq 0, \quad i = \overline{1,n_\psi} \ , \qquad (10)$$

where $\psi_i(\varphi,\mathbf{x},t)$ are continuous and, in general, nonlinear functions, n_ψ is the number of these inequalities. Due to high dimension of the problems the direct inclusion of distributed inequalities into the algorithms poses the principle difficulties. To overcome them the local constraints (Eq. 10) are transformed to the equivalent integral form of Eq. (9) with the strict equality to 0. In such a way, all the distributed constraints are involved into the general scheme of variational principles and sensitivity methods with the use of adjoint problems regardless of the state function dimension[6].

For convenience of the algorithm construction, all functionals of Eqs. (7) – (9) are formed by the same principle as inner product, i.e. they are written in the form of global integrals on the domain D_t with the integrand expressions defined in the space of the state functions and with non-negative weight functions taken from the corresponding adjoint spaces. From the variational principle point of view numerical models are considered as the constraints on the class of functions and as connections between parameters and the state functions.

Thus, the basic set of concepts and base elements of the modelling system are defined. Now it is possible to formulate a variational principle to link all elements and algorithms in a uniform system.

The essence of variational principle is expressed as follows. It is necessary to define the basic sensitivity relations for the chosen set of functionals to the variations of input parameters of the models and external forcing so that they would be independent on the variations of the first order of the state functions, adjoint functions, and functions of uncertainty of corresponding objects. The functionals and models can be linear as well as nonlinear in relation to the state functions. However, while parameters (including sources) are varied, the estimations of the functionals should always be stationary in relation to the first order variations of the state functions, the adjoint functions, and functions of uncertainty of corresponding objects. The conditions of such stationary state define mutually coordinated structure of numerical schemes for the basic models and the adjoint problems generated by the variational principle.

It is convenient to generate all algorithms for realization of the variational principle on the basis of the set of extended functionals which unite the functionals and models in discrete form[4]

$$\tilde{\Phi}^h(\boldsymbol{\varphi}) = \Phi_k^h(\boldsymbol{\varphi}) + \mathbf{I}^h(\boldsymbol{\varphi}, \mathbf{Y}, \boldsymbol{\varphi}^\bullet), \ k = \overline{1, K}, \ K \geq 1, \tag{11}$$

where the index h denotes discrete analogs.

The formulated variational principle has universal character. Its concrete content is defined by the set of functionals and variational formulations of models in the form of integral identity (Eq. 4).

5. Application of forward and inverse modelling

To formulate the statements of inverse problems and to construct the algorithms for their solution we take advantage of optimization theory and techniques of variational calculus. The main functional for organization of modelling system is formulated by analogy with Eq. (11) in such a way that all models and the accessible data considered in it, as well as the influence of uncertainties being in them, are minimized

$$\tilde{\Phi}_k^h(\boldsymbol{\varphi}, \boldsymbol{\varphi}^\bullet, \mathbf{Y}, \boldsymbol{\eta}, \mathbf{r}, \boldsymbol{\xi}, \boldsymbol{\zeta}) = \alpha_0 \Phi_k^h(\boldsymbol{\varphi}) + 0.5 \Big\{ \alpha_1 (\boldsymbol{\eta}^T M_1 \boldsymbol{\eta})_{D_t^m} + \alpha_2 (\mathbf{r}^T M_2 \mathbf{r})_{D_t^h}$$
$$+ \alpha_3 (\boldsymbol{\xi}^T M_3 \boldsymbol{\xi})_{D^h} + \alpha_4 (\boldsymbol{\zeta}^T M_4 \boldsymbol{\zeta})_{R^h(D_t^h)} \Big\}^h + \Big[\mathbf{I}^h(\boldsymbol{\varphi}, \mathbf{Y}, \boldsymbol{\varphi}^*) \Big]_{D_t^h}. \tag{12}$$

Here the first term represents the target functional of the type of Eq. (7) or Eq. (9), the four following members express, in total, a measure of uncertainties of the model of observations, the models of processes, initial data and parameters, accordingly. We remind that all input parameters of models and sources of external influences are included in the vector $\mathbf{Y}$. The last term contains the description of numerical model in variational formulation. $M_i, i = \overline{1,4}$ are the positive definite weight matrixes. $\alpha_i, i = \overline{0,4}$ are parameters given to describe the structure of the algorithm. The discrete analogs of the functionals (Eqs. 11–12) are constructed with the use of weak approximation, splitting, and decomposition. Finally, the discrete approximations of models and algorithms for modelling are obtained from the stationary conditions for the extended functionals $\tilde{\Phi}_k^h$ to the variations of different components.

(**1**) One can get the approximations for the main problems and methods of forward modelling from the stationary conditions for the functionals $\tilde{\Phi}_k^h$ to the variations of the adjoint function components: $\partial \tilde{\Phi}_k^h / \partial \boldsymbol{\varphi}^* = 0$.

(**2**) The adjoint problems and inverse modelling approximations can be obtained from the stationary conditions for the functionals $\tilde{\mathbf{\Phi}}_k^h$ to the variations of the state function components $\left\{ \partial \tilde{\Phi}_k^h / \partial \boldsymbol{\varphi} = 0, \ \boldsymbol{\varphi}_k^*(\mathrm{x})\big|_{t=\bar{t}} = 0 \right\}$.

(**3**) If uncertainty is present in the model, then the stationary conditions to the variations of the components of these functions give the system of equations for uncertainty estimations with the help of measured data incorporated in the functionals (Eq. 12) through the corresponding sensitivity functions (SF): $\partial \tilde{\Phi}_k^h / \partial \mathbf{U} = 0$, where $\mathbf{U} = \{\mathbf{r}, \xi, \zeta, \varepsilon\}$ is the uncertainties functions.

(**4**) The stationary conditions to the variations of model parameters, including sources of external influences, lead to the system of the equations for finding these parameters with the use of actual information. In essence, these are the algorithms of feedback realization from the functionals to the model parameters using the SFs: $\Gamma_k = \partial I^h(\boldsymbol{\varphi}, \mathbf{Y}, \boldsymbol{\varphi}_k^*) / \partial \mathbf{Y}$ or $\Gamma_k = \partial \tilde{\Phi}_k^h / \partial \mathbf{Y}$.

The operations of differentiation in items (**1**)-(**4**) are carried out for each of grid components of the state functions, the adjoint functions, and parameters. Structurally they are realized by means of Gateaux derivatives for the functionals of Eqs. (11)-(12) with respect to each of their functional arguments. The system obtained is the central kernel of the computing technology for forward and inverse modelling for the risk and control problems.

The relations between the variations $\delta \Phi_k^h(\boldsymbol{\varphi})$ and the variations of model parameters are described by the sensitivity relations and realized by means of SFs. Their expressions are defined by the coefficients at the variations of the corresponding parameters in the basic sensitivity relation for $\tilde{\Phi}_k^h(\boldsymbol{\varphi})$ written according to three stationary conditions specified above

$$\delta \Phi_k^h(\boldsymbol{\varphi}) \equiv \frac{\partial}{\partial \alpha} I^h(\boldsymbol{\varphi}, Y + \alpha \ \delta Y, \ \boldsymbol{\varphi}_k^*)\big|_{\alpha=0} \equiv (\boldsymbol{\Gamma}_k, \delta Y) \equiv \sum_{i=1}^{N} \Gamma_{ki} \delta Y_i . \quad (13)$$

Here α is a real parameter, $\delta \mathbf{Y}$ is a vector of parameter variations, $\boldsymbol{\varphi}_k^*$ is the solution of the adjoint problem (item (**2**)) corresponding to the functional $\Phi_k^h(\boldsymbol{\varphi})$. The algorithms for the construction of the basic sensitivity relations and SFs for the problems of the considered class are described in[4,6,12].

The equations of a feedback are produced after the calculation of the sensitivity relations (Eq. 13) for all functionals of Eqs. (7), (9) participating in the statements of the problem. Starting from the methods of control theory and following[4,6], we put down these equations in the form

$$\frac{\partial \mathbf{Y}}{\partial t} = -\aleph \boldsymbol{\Gamma}_k , \quad\quad\quad\quad (14)$$

where Γ_k are the SFs for target functionals, and $\aleph$ is a coefficient of proportionality. The correction of the right hand side of Eq. (14) is made if the restriction functionals (Eq. 9) are present. The gradient projection method is used for these purposes[6].

The methods of sensitivity theory can be directly used for estimation of ecological risks and vulnerability of territories in relation to the influence of anthropogenic factors considered in the models of processes, such as the changes of heat sources, moisture, air quality and changes of the characteristics of the Earth surface.

The sensitivity functions are calculated through the solutions of the main and adjoint problems for the model (items **1**–**2**) with undisturbed values of input data. And consequently, they have the deterministic character. But the variations of parameters, initial and boundary conditions and sources may be both deterministic and stochastic.

For a quantitative estimation of ecological risks we introduce some threshold values for functional variations (Eq. 13). Let us denote them as Δ_k^s, $k = \overline{1, K}$. Then, the situations may be considered as conditionally ecologically safe if the following inequalities are true for them

$$\left| \delta \Phi_k \right| \le \Delta_k^s .$$ (15)

Otherwise, the situations may be classified as that of ecological risk. It follows from Eq. (13), that the check of the inequalities of "ecological well-being" (Eq. 15) does not cause the difficulties if the sensitivity functions and quantitative information on variations of parameters are available. In case of the deterministic variations of sources and parameters, the estimation of magnitude of functional variations can be calculated by formulas

$$\left| \delta \Phi_k \right| \le \sum_{i=1}^{N} \left| \Gamma_{ki} \right| \left| \delta Y_i \right| .$$ (16)

Using these estimations together with inequalities of Eq. (15) it is possible to make the direct conclusion whether the situation refers to a category of well-being or risk. If variations of parameters and sources have stochastic character, the estimations become more complicated in comparison with the deterministic case, as it is necessary to work with multi dimensional spaces of SFs and parameters with stochastic disturbances[9].

The SFs give new quality in studying direct relations and feedback in the simulated system. Their analysis is expedient for carrying out together with the state functions.

6.   Risk assessment and observability of territories using AERONET

Let us consider an example of modelling scenario showing some applications of the presented methodology, in particular for: 1) estimation of risk and vulnerability of territories; 2) estimation of observability of territories by means of a monitoring system and solution of inverse problems; 3) identifying sources by inverse modelling.

The Siberian part of the global observational system AERONET[13-14] is of great interest in this context and can conveniently be used for this task. Some features of AEROSIBNET[14] are taken into account for the choice of receptors and formation of target functionals. Nine industrial Siberian cities from the Ural Mountains up to the Pacific Ocean containing aerosol monitoring stations are taken as the receptors for risk assessment.

The ground-based stations equipped with Sun/sky photometers are the basis of the monitoring network. They measure vertically integrated optical spectral properties of the atmosphere and the concentration of aerosol particles as a function of size. To describe these integrated data we define functionals of the type of Eq. (7) which contain both the corresponding model of observation in the form of Eq. (3) and the weight functions showing the position of monitoring devices in time and space.

The variational principle for studying the target functionals with the use of the models of transport and transformation of aerosols and the SFs gives the scan-out of the information incorporated in target functionals in the phase space. It enables to develop effective procedures of data assimilation for the estimation of atmospheric conditions, for estimation of risks/-vulnerability and for the organization of control strategies.

The realization of scenarios is carried out employing a system of global models of chemical tracer transport in the atmosphere[12]. The models are used in forward and inverse modes within the frame of the basic algorithm (items (**1**)-(**4**)). The atmospheric circulation was simulated using NCEP/NCAR reanalysis data[15] and our dynamical model[16]. Fast data assimilation procedures[17] were applied in the model with 20 levels in the vertical. A time step of 30 minutes was used.
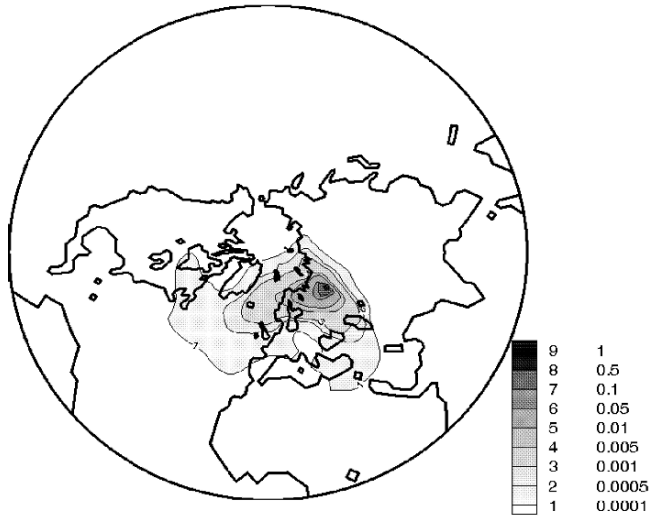
Figure 1. The sensitivity function (reference values) for monitoring stations placed in Ekaterinburg.
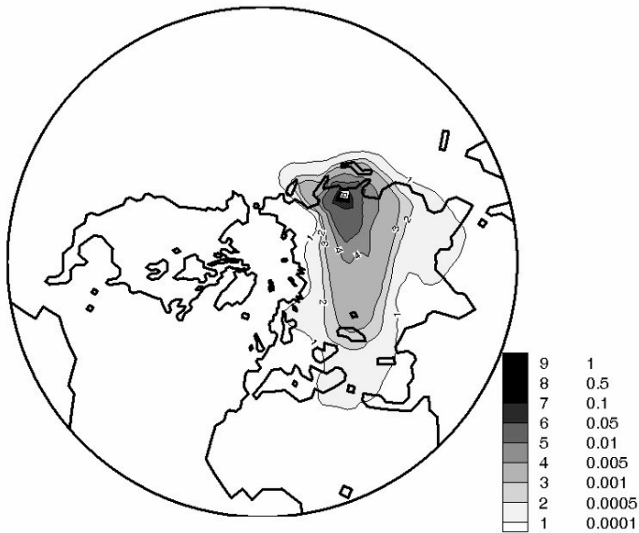
Figure 2. The same as in Fig. 1, but for Ussuriisk.
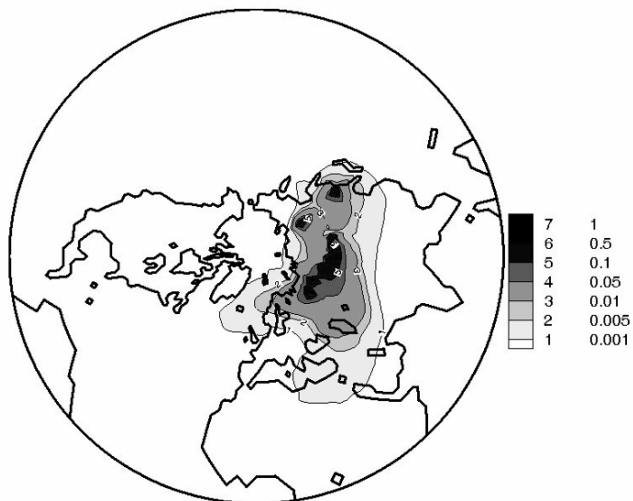
Figure 3. The function of total observability of territories by means of nine monitoring sites.
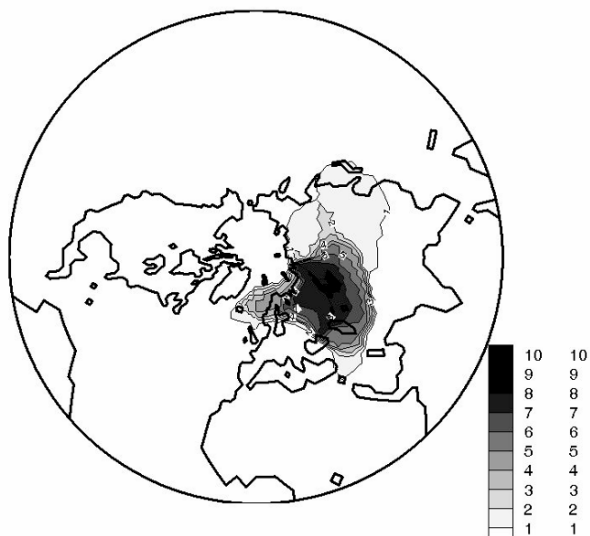
Figure 4. The location function of sources which could release the aerosols observed by all the measuring sites.

Results derived for this scenario are presented in Figs. 1–4. The sensitivity-risk-observability functions are shown in Figs. 1–2 for two monitoring stations (from nine) placed in the receptor area. The territory is considered as an observable one for a monitoring station if it is met by the carrier of the sensitivity function for this station. The risk function for a receptor in relation to sources coincides with the function of observability. Figure 3 gives the function of total observability of the territory by means of these 9 stations in relation to the ground sources of pollution. In Fig. 4 the location function of sources of aerosols derived from the data observed in the receptor area is presented. The location function of sought sources is formed from overlapping of the carriers of the sensitivity function for separate functionals. The function shows the number of monitoring stations which can observe the same area. The values of this function are the sum of the characteristic functions constructed for each observability function. There are 9 stations in our scenario. It means that integer-value location function can vary from 0 to 9. The areas with the highest level of the significance have to contain the sources. Most probably these sources released the aerosols which were measured by these stations.

Thus the proposed way of treating observational data allows one to get the estimations of risk/observability domains of large extension. This is due to the fact that propagation of information from vertically integrated functionals to space-time domains is carried out in the frame work of inverse modelling.

If AERONET is used in such an approach, it is possible to get information about the sources of pollution from large territories. This is especially important for the northern regions and Siberia where regular observations of environmental quality are hard to achieve.

7.   Final remark

To conclude we note that future studies should be carried out for the class of problems connected with the choice of the optimal strategy of environmental quality control aiming at sustainable development. This sort of problems can successfully be solved with the methods based on variational principles.

Acknowledgements

References

1. *Climate Change 2001.* Synthesis report. (Cambrige University Press, UK, 2003).
2. G. I. Marchuk, *Mathematical Modelling in Environmental Problems* (Nauka, Moscow 1982).
3. G. I. Marchuk, *Adjoint Equations and Analysis of Complex Systems* (Kluwer Academic Publishers, Dordrecht, 1995).
4. V. V. Penenko, *Methods of Numerical Modelling of Atmospheric Processes* (Gidrometeoizdat, Leningrad, 1981).
5. V. V. Penenko and A. E. Alojan. *Models and methods for environment protection problems* (Nauka, Novosibirsk, 1985).
6. V. V. Penenko, Numerical models and methods for the solution of problems of ecological forecasting and design, *Review of Applied and Industrial Mathematics* 1(6), 917– 941 (1994).
7. V. V. Penenko, Methodology of inverse modeling for the problems of climate changes and environmental protection. In: *Advanced mathematics: computations and applications* (NCC Publisher, Novosibirsk, 1995), pp . 358–367.
8. V. Penenko, A. Baklanov, and E.Tsvetova, Methods of sensitivity theory and inverse modeling for estimation of source parameters. *FGCS,* 18, 661– 671 (2002).
9. V. V. Penenko and E. A. Tsvetova, Mathematical models for studying risks of environment pollution, *Appl. Mech. Tech. Phys.* 45 (2), 136 –146 (2004).
10. V. V. Penenko, E. A. Tsvetova, G. I. Skubnevskaja et al., Numerical modelling of chemical kinetics and transport of polluting impurity in the atmosphere of industrial regions . *Chemistry in interest of sustainable development* 5, 535–539 (1997).
11. L. Schwartz, *Analyse Mathematique* (Hermann,1967).
12. V. V. Penenko and E. A. Tsvetova, Mathematical models for studies of interactions in system of Lake Baikal and the atmosphere of the region, *Appl. Mech. Tech. Phys.* 40 (2), 137–147 (1999).
13. B. N. Holben and co-authors, AERONET- a federated instrument network and data archive for aerosol characterization, *Remote Sens. Environ.* 66, 1–16 (1998).
14. S. M. Sakerin, D. M. Kabanov, M. V. Panchenko, B. Holben, A. V. Smirnov, V. V. Koshelev, Variation of aerosol characteristics of atmospheric depth by AEROSIBNET data, Proceedings of SPIE 6160**,** (2005), in press.
15. E. Kalney, M. Kanamitsu, R. Kistler et al., The NCEP/NCAR 40-year reanalysis project, *Bull. Am. Meteorol. So.* 77, 437–471 (1996).
16. V. V. Penenko and E. A. Tsvetova, Preparation of data for ecological studies with the use of reanalysis, *Atmos. Ocean Opt*. 12(5), 447–449 (1999).
17. V. V. Penenko and E. A. Tsvetova, Variational fast data assimilation algorithms, Research Activities in Atmospheric and Oceanic Modeling. WGNE Blue Book Web (2002); http://www.cmc.ec.gc.ca/rnp/wgne 01–48.

ENVIRONMENTAL RISK AND ASSESSMENT
MODELLING – SCIENTIFIC NEEDS
AND EXPECTED ADVANCEMENTS

ALEXANDER BAKLANOV
Danish Meteorological Institute, DMI, Lyngbyvej 100,
DK- 2100, Copenhagen, Denmark; e-mail: alb@dmi.dk

Abstract. Environmental risk and impact assessment and prediction modelling is one of the most important instruments in the environmental security management and preparedness, and it needs further development in the quickly changing world and society. Most of the previous studies in this field considered, as a rule, only separate aspects of the risk and impact assessments. New realities and problems in the environmental security, as well as increasing scientific knowledge and power of modern supercomputer facilities, request a new generation of the assessments and prediction tools for the risk and impact assessments. Some new trends, advantages and perspectives in the risk and impact assessment and forecasting methodology (including the integrated and multidisciplinary approaches, health and combined effects of different risk and impact factors, source-receptor, sensitivity and vulnerability problems, and meteorological advances for urban air quality forecasting and assessments) are discussed in the paper.

Keywords: integrated modelling; probabilistic risk; urban air quality, health effects; adjoint methods; source-receptor; sensitivity and vulnerability studies

1. Introduction

Environmental risk and impact assessment and prediction modelling is one of the most important instruments in the environmental security management and preparedness, and it needs further development in the

quickly changing word and society. Most of the previous studies in this field considered, as a rule, one of the following aspects of the risk and impact assessments:

- Studies of impact on the environment considered the concentrations of harmful pollutants or factors, or their deposition characteristics as the main indicators, which were recalculated in the terms of the critical loads or levels.
- Risk studies as a rule were realised either as case studies or as a probabilistic risk assessment. Both methods have advantages and disadvantages.
- Assessments were realised on one specific scale: local, regional or global, and did not considered the possible scales interactions.
- As a rule, forecasting and assessment systems were focused on one of the environment impact types: atmospheric, water or soil pollution.

New realities and problems in the environmental security, as well as increasing scientific knowledge and power of modern supercomputer facilities, request a new generation of the assessments and prediction tools for the risk and impact assessments.

The following new trends, advantages and perspectives in the risk and impact assessment and forecasting methodology, needed for realization, are discussed in the paper:

- Integrated approach for risk assessments and predictions;
- Health effects are among the most important issues, consideration of the population exposure as a simple indicator;
- Combined effects of different risk and impact factors (air, water, soil, nutrition pathways, noise, radiation, geophysical and meteorological factors, health, etc.);
- Multidisciplinary approach => combined indicators of the risk and impact; effects on different aspects of the environment, man and society (environmental, health, social, economical, risk perception, etc.);
- Source-Receptor, sensitivity and vulnerability problems => direct and inverse modelling methodology, adjoint problem, methods of sensitivity and perturbation theories;
- Scale interaction: from local to regional and global scales, feedbacks between different scale and type of processes (e.g., local impact => global effects => local processes; aerosol effects on climate from urban to global scale);
- Meteorological advances and systems for urban air quality forecasting and assessments: from integrated UAQIFS to health and chemical weather forecast.

Examples of different relevant studies and projects (where the author was involved), focusing on further development of the above-mentioned advance impact assessment and forecasting methodologies and systems are presented and discussed. The following projects are among them:

- Joint studies in the Novosibirsk Computing Center of Siberian Division of Russian Academy of Sciences (Baklanov, 1988; Penenko and Baklanov, 2001; Penenko et al., 2002).
- NARP Arctic Risk study: Atmospheric Transport Pathways, Vulnerability and Possible Accidental Consequences from the Nuclear Risk Sites in the European Arctic (multi-disciplinary network studies) (AR-NARP, 2003; Baklanov, 2002; Baklanov et al., 2003; Baklanov and Mahura, 2004);
- NKS NordRisk: Nuclear risk from atmospheric dispersion in Northern Europe (Lauritzen et al., 2006);
- 6FP EU CA EnviroRISKS: Man-induced Environmental Risks: Monitoring, Management and Remediation of Man-made Changes in Siberia Siberia (Baklanov and Gordov, 2005; Baklanov, 2006a);
- 5FP EU project FUMAPEX: Integrated Systems for Forecasting Urban Meteorology, Air Pollution and Population Exposure (Baklanov, 2004, 2006b; Baklanov et al., 2002b, 2006a);
- IIASA Radiation Safety of the Biosphere project Kola Assessment Study (KAS) (Baklanov et al., 1996, 2002a; Bergman and Baklanov, 1998) and Far-East Russia FARECS studies (Mahura et al., 2005a);
- Swedish ÖCB RW project: Risk and Nuclear Waste: nuclear problems, risk perceptions of, and societal responses to nuclear waste in the Barents region (Baklanov and Bergman, 1999; OCB, 2000);
- Danish ARGOS project: Accident Reporting and Guidance Operational System (Hoe et al., 2000, 2002; Baklanov et al., 2005a);
- 5FP project ENSEMBLE: Methods to Reconcile Disparate National Forecasts of Medium and Long Range Dispersion (Galmarini et al., 2004);
- INTAS project: Assessment of potential risk of environmental radioactive contamination in northern Europe from terrestrial nuclear units in north-west Russia (Baklanov et al., 2006b).

2. Suggested methodological approaches and models

The quality of the air pollution modelling/forecast and the Air Quality Information and Forecasting Systems (AQIFS) critically depends on:
  (i) the mapping of emissions,
  (ii) the air pollution (APM) and chemical transport (CTM) models, and
  (iii) the meteorological fields in the considered areas.
    The main problem in forecasting air quality is the prediction of episodes with high pollutant concentration in urban areas where most of the well-known methods and models, based on in-situ meteorological measurements, fail to realistically produce the meteorological input fields for the urban air pollution (UAP) models.

2.1. URBAN AIR QUALITY INFORMATION AND FORECASTING SYSTEMS

About 70% of the European population leaves in cities. A major share of anthropogenic sources of pollutants originates from conurbations. These pollutants have not only local effects (on human health, material, ecosystem), but may impact all the way to the regional (acidification, euthrophication) and global scales (atmospheric composition, climate changes). Urban areas present a challenge to the atmospheric scientists - both experimentalists and modellers - as typically urban areas have high roughness elements penetrating well above the surface layer, heterogeneous distribution of surface features with wide variation in surface fluxes of heat, moisture, momentum and pollutants. Additionally, the structure of the conurbation may trigger the local meteorological circulations and processes (e.g., heat island, enhanced production of condensation nuclei) as well as enhanced vertical motions resulting in longer residence time of atmospheric compounds.

As model resolution is increasing towards a few kilometres or finer and various end-users are expecting better targeted meteorological forecasts and products, it has become a necessity to be able to account for, describe and simulate urban effects and processes in various meteorological and air pollution models. On the other hand, this has brought new requirements for observations and measuring strategy in order to be able to describe, simulate and forecast meteorological and concentration fields in urban areas. Integration of these aspects will greatly benefit the development of urban air quality information and forecasting systems (UAQIFS) for a variety of applications and end-users.

Modern numerical weather prediction (NWP) and meso-meteorological models (MetM) able to resolve urban-scale processes are considered to be the main tools in future urban air pollution (UAP) forecasting and assessments because they allow for sufficiently high spatial and temporal resolution and can trace back the linkages between sources and impacts. The ongoing European project FUMAPEX (fumapex.dmi.dk) focuses on the evaluation and improvement of meteorological modelling and pre-processing for urban areas.

The following urban features can influence the atmospheric flow, microclimate, turbulence regime and, consequently, the transport, dispersion, and deposition of atmospheric pollutants within urban areas:

(1) local-scale non-homogeneities, sharp changes of roughness and heat fluxes,
(2) the building effect in reducing wind velocity,
(3) redistribution of eddies, from large to small, due to buildings,
(4) trapping of radiation in street canyons,
(5) effect of urban soil structure on diffusivities of heat and water vapour,
(6) anthropogenic heat fluxes, including the urban heat island effect,
(7) urban internal boundary layers and the urban mixing height (MH),
(8) different gas and particle deposition efficiencies for different types of the urban surfaces (walls, roofs, streets, etc.),

(9) effects of pollutants (including aerosols) on urban meteorology and climate,

(10) urban effects on clouds and precipitation.

Accordingly, the following aspects of urban effects were considered by the FUMAPEX project in the improved urban-scale NWP and meteorological models (Baklanov et al., 2005c): (i) higher spatial grid resolution and model downscaling, (ii) improved physiographic data and land-use classification, (iii) calculation of effective urban roughness and urban heat fluxes, (iv) urban canopy and soil sub-models, (v) MH in urban areas.

2.2. INTEGRATED MODELLING AND CHEMICAL WEATHER FORECASTING

In general sense it is suggested to consider air quality as a combination and integration at least of the following factors: air pollution, urban climate & meteorological conditions and population exposure. This is reasonable to consider them together due to the facts that:

(i) meteorology is the main source of uncertainty in UAP and emergency preparedness models,

(ii) complex and combined effects of meteorological and pollution components on human health (for example, in France in the hot summer 2003 with a large number of mortality cases),

(iii) effects of pollutants/aerosols on urban climate and meteorological events (precipitation, thunderstorms, etc.).

Quantification of the combined effect of bio-meteorological factors together with the effects of air pollution is a major issue. In this context two levels of the integration strategy are considered (Figure 1):

1. Off-line integration of Urban Meteorology, Air Pollution and Population Exposure models for urban air pollution forecast and emer-gency preparedness, which is the main issue e.g. in the FUMAPEX project.

2. On-line integration of meteorological models and atmospheric aerosol & chemical transport models with consideration of the feed-backs of air pollution (e.g. urban aerosols) on meteorological processes and urban climate. This direction is developed by several research organisations and considered in the COST728 (http://www.cost728.org). This will lead to a new generation of models for "chemical weather forecasting".

One example of the on-line integrated MetM-CTM systems - Enviro-HIRLAM - is developing by DMI (Baklanov et al., 2004). Recently they have developed a new version of the meteorological model HIRLAM with on-line integrated tracer (Chenevez et al., 2004) and have implemented a versatile aerosol-cloud module and heterogeneous chemistry in their Atmospheric Chemical Transport Model (Gross & Baklanov, 2004).
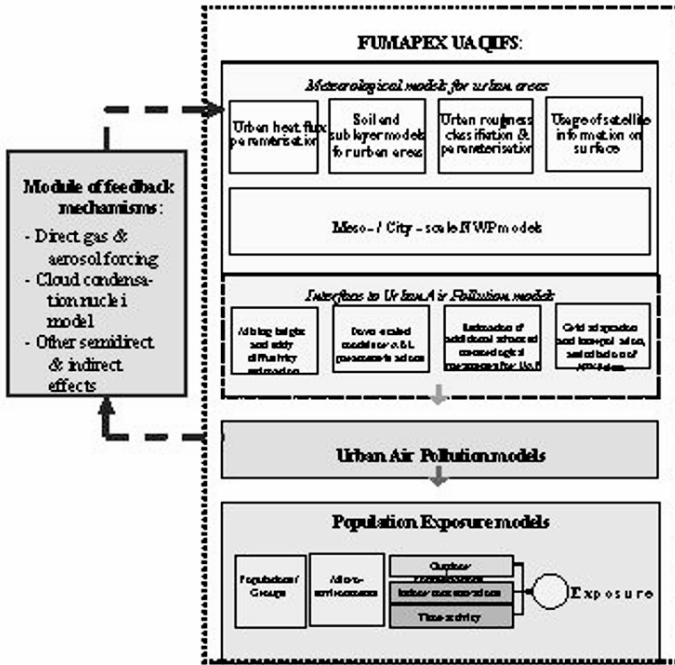
Figure 1. Extended FUMAPEX scheme of the improvements of meteorological forecasts (NWP) in urban areas, interfaces and integration with UAP and population exposure models for urban air quality information forecasting and information systems (UAQIFS).

2.3. HEALTH RISK ASSESSMENTS

Ambient pollutant concentrations are associated with significant health effects on urban, as well as rural, populations (Samoli et al., 2005). Compliance with air quality standards, however, while being a useful administrative tool in air quality management, is nevertheless not sufficient to protect the general public from the excess morbidity and mortality currently caused by air pollution.

Exposure is the mediating link between man and the environment; the health effects actually having a causal association with air pollution must be caused by personal exposures of the affected individuals (Ott, 1995). Personal exposures have been, however, found to correlate poorly with ambient air quality (see e.g. Kousa et al., 2002). Personal exposures differ from ambient air quality, as characteristically a majority of time is spent in indoor environments, where the building envelope filters some of the ambient pollution, and indoor pollution sources affect air quality.

The presence of individuals in the vicinity of the emission sources, especially in traffic, may also substantially increase exposure, compared with the data at fixed monitoring sites. As a result, air quality modelling needs to be integrated with population time-activity and mobility models to estimate actual exposure distributions caused by ambient pollution even in situations when ambient air quality standards are met. This was one of the main objectives of the FUMAPEX work (Hänninen, 2005; Hänninen et al., 2005).

The main novel element of the UAQIFS system developed in FUMAPEX (Baklanov et al., 2006a) is the presentation of an improved type of UAQIFS which integrates all the required forecast steps from emissions and meteorological data to atmospheric pollution and population exposure. The previous experience and corresponding publications suggested some integrated systems: starting from atmospheric dispersion models integrated with population exposure models for environmental assessments (e.g., Coulson et al., 2005) or from meteorological models to atmospheric pollution forecast for urban areas without consideration of the health effects (e.g., Berge et al., 2002; Byun and Ching, 1999). For emergency preparedness modelling there are integrated systems that account for the NWP, accidental contamination and population doses, but they consider mostly the regional scale processes and did not included the urban features, e.g. the urban meteorology (e.g., RODOS, 2000).

In FUMAPEX (Baklanov et al., 2006a) for the first time an integrated system encompasses emissions, urban meteorology and population exposure for urban air pollution episode forecasting, the assessment of urban air quality and health effects, and for emergency preparedness issues for urban areas. Such an integration increases the quality of the air pollution forecast in urban areas.

Air quality modelling, linked with population exposure evaluation, can provide a relevant support to urban air quality management and critical conditions recovery planning. These modelling tools may be applied on two temporal scales. On the one hand, short-term urban air quality forecasts are compared with air quality guidelines on a daily basis and can therefore be used to create warning systems and plan mitigation actions to prevent severe episodic situations. On the other hand, air quality modelling systems are employed for long-term air quality evaluation needed for urban planning, the design and management of transportation networks, industrial sites and residential areas, in order to minimise unacceptable risk to public health.

2.4. SOURCE-RECEPTOR MODELLING FOR ENVIRONMENT AND HEALTH RISK ASSESSMENTS

Estimation of regions with high potential risk/vulnerability from different risk sites is important for long-term planning socio-economical

development of territories and emergency systems. The concept of ecological risk/vulnerability of territories with respect to anthropogenic impact is actively used in recent environmental investigations. The problem of risk assessment becomes especially urgent in connection with different accidents of radioactive, chemical and biological nature (e.g. due to terror acts). One of the most important aspects of this problem is the source term estimation for emergency response systems. E.g., after the Algeciras accident in Spain (30 May 1998) many European monitors measured peaks of radiation, but during several days the reason was unknown. A similar situation applies to the Chernobyl disaster.

Such accidents show the necessity to develop constructive methods for estimation of an unknown source term based on monitoring data, and prediction and assessment of risk/vulnerability levels for various risk sites and situations under conditions of both ordinary and extraordinary anthropogenic loads.

Methods of numerical modelling are widely spread for the solution of pollution problems, including the source-receptor relationship problem. Two approaches are usually used: Lagrangian and Eulerian. Lagrangian models allow to calculate the trace of the individual particle or ensemble of particles moving together with air masses. Eulerian approach gives the distribution of concentration of pollutants, released from a given set of sources, in a chosen domain. These two approaches are not alternative; they supplement each other. Each approach has its own advantages and drawbacks and application areas.

Depending on the goal of investigation, forward and inverse procedures of modelling are distinguished. The methods of forward modelling are traditionally used for the solution of forecast and assessment problems. For their realization, the values of all input parameters of the models, boundary and initial conditions, sources of the external and internal forcing have to be given. Forward problems are used to study the processes of propagation of perturbations from various sources. These are so-called source-receptor problems. The spatial-time domains, where perturbations are observed, play role of zones-receptors. The methodology of inverse modelling is mainly oriented towards diagnosis and solution of inverse problems. Its value is that it starts from the result (receptor) and moves to the sources and causes. From the viewpoint of ecological safety, the inverse problems of the receptor-source type are of interest, since they allow to determine the degree of the potential danger of contamination of the zone-receptor by pollutants entering it and to identify sources of this danger. In combination with the forward modelling, the inverse approach opens up new prospects of extending the class of relevant problems and developing as well as organizing interactive technologies for their control and mitigation.

Source-receptor data can be evaluated: a) statistically or b) in combination with monitoring data to derive sources or other model

variables. The common back-trajectory technique, suitable only for Lagrangian models, is an example of such inverse studies. Most of western scientists use these techniques for the discussed problem. The Novosibirsk scientific school of Acad. G.I. Marchuk (Marchuk, 1982, 1995; Penenko, 1981) in Russia suggested a new, very elegant theoretical method for inverse modelling, based on variational principles with adjoint equations and suitable for both Eulerian and Lagrangian models.

The methodology of source–receptor relations (SRR) is actively developed during the last decades and becomes very popular among Western scientists as well (e.g., Robertson and Lange, 1998; Pudykiewicz, 1998; Baklanov, 2000). In particular, the variational principles combined with decomposition, splitting and optimisation techniques are used for construction of numerical algorithms (Penenko, 1981; Baklanov, 1988). The novel aspects are the sensitivity theory and inverse modelling for environmental problems, which use the solution of the corresponding adjoint problems for the given set of functionals and models (Penenko and Baklanov, 2001; Penenko et al., 2002). The methodology proposed provides optimal estimations for objective functionals, which are criteria of the atmospheric quality and (or) informative quality of measurements.

The Danish Emergency Response Model for Atmosphere (DERMA), developed by DMI originally in the direct mode, is also tested in the inverse (adjoint) mode for different resolutions and grid domains for forecast and for long-term simulation of source-receptor relationship for various pollutants including nuclear, chemical, biological etc. danger (Sørensen, 1998; Baklanov and Sørensen, 2001). Among 28 models from most of European countries, USA, Canada and Japan, which contributed to model validations based on the European Tracer EXperiment (ETEX), the DMI's DERMA model was emphasised as performing excellently (Graziani et al., 1998).

2.5. COMPLEX NUCLEAR RISK ASSESSMENT AND VULNERABILITY EVALUATION

New methodological approach for multidisciplinary nuclear risk and vulnerability assessments based on the GIS integration was suggested in the Arctic Risk project (Rigina and Baklanov, 2002; Baklanov et al., 2003, 2005b) for estimation of nuclear risk to the population in the Nordic countries in case of a severe accident at the nuclear risk sites (NRSs) (Figure 2). The main focus was on the evaluation of the atmospheric transport and deposition of radioactive pollutants from NRSs. The method developed was derived from a probabilistic point of view. The main question addressed was: *What is the probability for radionuclide atmospheric transport, deposition and impact to different neighbouring regions and countries in case of an accident at a risk site?*
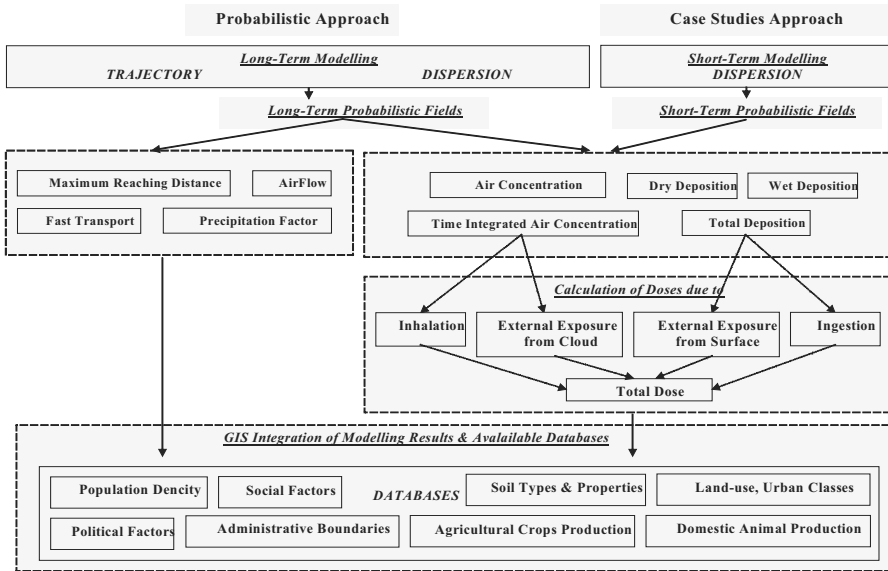
Figure 2. General scheme of probabilistic assessment of risk sites' impact.

To answer this question a set of different tools was tested and applied:
(i) *Trajectory Modelling* - to calculate multiyear forward trajectories
originated over the locations of selected risk sites; (ii) *Dispersion Modelling*
- for long-term simulation and case studies of radionuclide transport from
hypothetical accidental releases at sites; (iii) *Cluster Analysis* - to identify
atmospheric transport pathways from sites and its temporal variability; (iv)
Probability Fields Analysis - to construct annual, monthly, and seasonal
NRS impact indicators to identify the most impacted and sensitive
geographical regions; (v) *Specific Case Studies* - to estimate consequences
for the environment and population after a hypothetical accident; (vi)
Vulnerability Evaluation to Radioactive Deposition - to describe its
persistence in the ecosystems with a focus on the transfer of certain radio-
nuclides into the food chains of key importance for the intake and exposure
for a whole population and certain population groups; (vii) *Risk Evaluation
and Mapping* - to analyse environmental, social, economical, etc.
consequences for different geographical areas and various population
groups taking into account social-geophysical factors and probabilities, and
using demographic databases based on GIS analysis.

   This methodology was tested on examples of the risk sites located in
Arctic, Sub-Arctic, and Northern Europe (Baklanov et al., 2002a;

Mahura and Baklanov, 2003; Mahura et al., 2005a,b). The sites included the nuclear power plants' reactors, nuclear reprocessing plant, nuclear submarine, decommissioning site, and former nuclear weapons testing site. Recently the methodology was extended to other types of environmental risk sites (e.g. Mahura et al., 2006).

2.6. AIR QUALITY MODELLING AS A NATURAL PART OF THE CLIMATE CHANGE MODELLING

The role of greenhouse gases (such as water vapour, CO_2, O_3 and CH_4) and aerosols in climate change has been highlighted as a key area of future research (IPCC 2001, AIRES 2001). Uncertainties in emission projections of gaseous pollutants and aerosols (especially secondary organic components) need to be addressed urgently to advance our understanding of climate forcing (Semazzi 2003). In relation to aerosols, their diverse sources, complex physicochemical characteristics and large spatial gradients make their role in climate forcing particularly challenging to quantify. In addition to primary emissions, secondary particles, such as nitrates, sulphates and organic compounds, also result from chemical reactions involving precursor gases such as SO_x, DMS, NOx, volatile organic compounds and oxidising agents including ozone. One consequence of the diverse nature of aerosols is that they exhibit negative (e.g. sulphates) as well as positive (e.g. black carbon) radiative forcing characteristics (IPCC 2001; Jacobson 2001). Although much effort has been directed towards gaseous species, considerable uncertainties remain in size dependent aerosol compositional data, physical properties as well as processes controlling their transport and transformation, all of which affect the composition of the atmosphere (Penner et al., 1998, Shine 2000, IPCC2001). Probably one of the most important sources of uncertainty relates to the indirect effect of aerosols as they also contribute to multiphase and microphysical cloud processes, which are of considerable importance to the global radiative balance (Semazzi 2003).

In addition to better parameterisation of key processes, improvements are required in regional and global scale modelling (IPCC 1996; Semazzi 2003). Resolution of regional climate information from atmosphere-ocean general circulation models remains a limiting factor. Vertical profiles of temperature, for example, in climate and air quality models need to be better described. Such limitations hinder the prospect of reliably distinguishing between natural variability (e.g. due to natural forcing agents, solar irradiance and volcanic effects) and human-induced changes caused by emissions of greenhouse gases and aerosols over multi-decadal timescales (Semazzi 2003, NAS 2001). Consequently, the current predictions of the impact of air pollutants on climate, air quality and ecosystems or of extreme events are unreliable (e.g. Watson et al., 1997). Therefore it is very important in the future research to address all the key

areas of uncertainties so as provide an improved modelling capability over regional and global scales and an improved integrated assessment methodology for formulating mitigation and adaptation strategies.
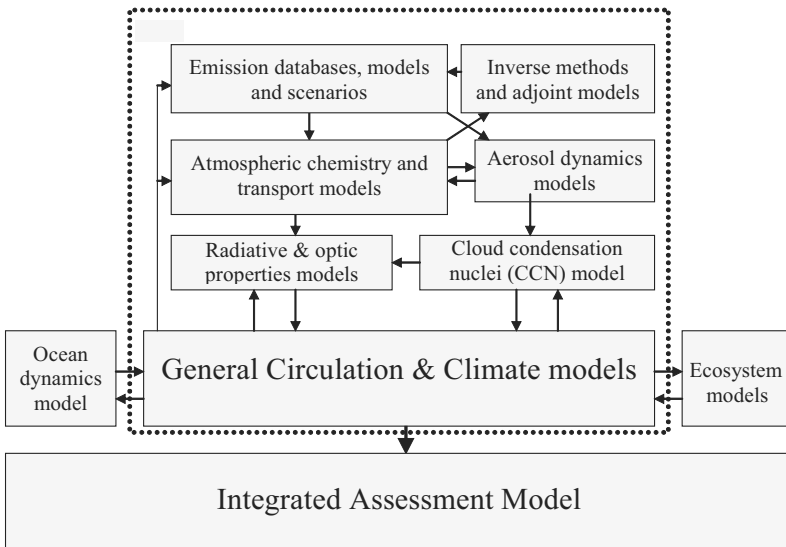
Figure 3. Integrated (on-line coupled) modelling system structure for assessment / predicting climate change and atmospheric composition.

In this concern, one of the important tasks is to develop a modelling instrument of coupled 'Atmospheric chemistry / Aerosols' and 'Atmospheric Dynamics / Climate' models for integrated studies (see Figure 3).

3. Conclusions

New realities and problems in the environmental security, as well as increasing scientific knowledge and power of modern supercomputer facilities, request a new generation of the assessments and prediction tools for the risk and impact assessments.

Some new trends, advantages and perspectives in the environmental risk and impact assessment and forecasting methodology were analysed in the paper based on the author experience. It is suggested to consider:

- Integrated approach for risk assessments and predictions;
- Incorporation of the health effects and population exposure into models;
- Combined effects of different risk and impact factors (air, water, soil, nutrition pathways, radiation, geophysical and meteo- factors, health, etc.);
- Multidisciplinary approach based on combined indicators of the risk and impact; effects on different aspects of the environment, man and society (environmental, health, social, economical, risk perception, etc.);

- Source-Receptor, sensitivity and vulnerability problems, based on direct and inverse modelling methodology, sensitivity and perturbation theories;
- Scale interaction: from local to regional and global scale, feedbacks between different scale and type of processes (e.g. aerosol effects on environment and climate from urban to global scale);
- Meteorological advances and systems for urban air quality forecasting and assessments: from integrated UAQIFS to health and chemical weather forecast.

Acknowledgments

References

AIRES, 2001, *AIRES in ERA*, European Commission, EUR 19436.

AR-NARP, 2003, Atmospheric transport pathways, vulnerability and possible accidental consequences from the nuclear risk sites in the European Arctic (Arctic Risk) NARP project; http://glwww.dmi.dk/f+u/luft/eng/arctic-risk/main.html.

Baklanov, A., 1988, *Numerical modelling in mine aerology*, Apatity: KSC RAS, 200 p. (in Russian)

Baklanov, A., 2000, Modelling of the atmospheric radionuclide transport: local to regional scale. *Numerical Mathematics and Mathematical Modelling*, INM RAS, Moscow, Russia, **2**: 244–266.

Baklanov, A., 2002, Methodologies for multidisciplinary nuclear risk and vulnerability assessments in the Arctic and Sub-Arctic. *NATO Science Series, Ser IV Earth and Env. Sci.*, **31**(2003): 385–405.

Baklanov, A., 2004, European FUMAPEX project: 'Integrated Systems for Forecasting Urban Meteorology, Air Pollution and Population Exposure', European Association for the Science of Air Pollution, *EURASAP Newsletter*, **52**: 6–36.

Baklanov, A. (Editor), 2006a, *Enviro-RISKS: Man-induced Environmental Risks: Monitoring, Management and Remediation of Man-made Changes in Siberia*. EU Coordination Action 1st Report. DMI Sci. Report, Feb. 2006, Copenhagen, 89 p.

Baklanov, A. (Editor), 2006b, *FUMAPEX: Integrated Systems for Forecasting Urban Meteorology, Air Pollution and Population Exposure*. EC 5FP project Final Sci. Report. In 3 volumes. DMI, Copenhagen, Jan. 2006.

Baklanov, A. and Bergman, R., 1999, Radioactive Sources in the Barents Euro-Arctic Region: Are there reasons to be concerned? Chapter XI at the *NEBI Yearbook: North European and Baltic Sea Integration*, Copenhagen, Springer-Verlag, pp. 171–192.

Baklanov A.A. and Gordov, E.P., 2005, Enviro–RISKS - Man-induced Environmental Risks: Monitoring, Management and Remediation of Man-made Changes in Siberia (FP6 INCO CA project, 2005–2008). *The Bulletin of the Russian National Committee for IGBP*, No 4, 2005, Vladivostok, Dalnauka Printing House.

Baklanov, A., and Mahura, A., 2004, Assessment of possible airborne impact from risk sites: methodology for probabilistic atmospheric studies, *Atmospheric Chemistry and Physics*, **4(2)**: 485–495.

Baklanov, A., and Sørensen, J.H., 2001, Parameterisation of radionuclide deposition in atmospheric dispersion models, *Phys. Chem. Earth (B)* **26**: 787–799.

Baklanov, A., Bergman, R. and Segerstahl, B., 1996, *Radioactive sources in the Kola region: Actual and potential radiological consequences for man*, IIASA, Final Report, Laxenburg, Austria, December 1996, 260 p.

Baklanov, A., Mahura, A., Jaffe, D., Thaning, L., Bergman, R., Andres, R., 2002a, Atmospheric Transport Patterns and Possible Consequences for the European North after a Nuclear Accident. *Journal of Environment Radioactivity,* **60**: 23–48.

Baklanov, A., Rasmussen, A., Fay, B., Berge, E. and Finardi, S., 2002b, Potential and Shortcomings of Numerical Weather Prediction Models in Providing Meteorological Data for Urban Air Pollution Forecasting. *Water, Air and Soil Poll.: Focus,* **2**(5–6): 43–60.

Baklanov A., Mahura A., Sørensen J.H., 2003, Methodology for Prediction and Estimation of Consequences of Possible Atmospheric Releases of Hazardous Matter: Kursk Submarine Study. *Atmospheric Chemistry and Physics*, **3**: 747–762.

Baklanov, A., Gross, A., Sørensen, J.H., 2004, Modelling and forecasting of regional and urban air quality and microclimate. *J. Computational Technologies*, **9**: 82–97.

Baklanov, A., Sørensen, J.H., Hoe, S., Amstrup, B., 2005a, Urban meteorological modelling for nuclear emergency preparedness. *J. Environment Radioactivity*, **85**: 154–170.

Baklanov, A., Sørensen, J.H., and Mahura, A., 2005b, Long-Term Dispersion Modelling: Methodology for Probabilistic Atmospheric Studies, *Environmental Modelling and Assessment*, In Review.

Baklanov, A., Mestayer, P., Clappier, A., Zilitinkevich, S., Joffre, S., Mahura, A., 2005c, On parameterizations of urban atmosphere sublayer in meteorological models. *Atmospheric Chemistry and Physics Discussions,* **5**: 12119–12176.

Baklanov, A., Hänninen, O., Slørdal, L.H., Kukkonen, J., Bjergene, N., Fay, B., Finardi, S., Hoe, S.C., Jantunen, M., Karpinen, A., Rasmussen, A., Skouloudis, A., Sokhi, R.S., Sørensen, J.H., 2006a, Integrated systems for forecasting urban meteorology, air pollution and population exposure. *Atmospheric Chemistry and Physics Discussions*, **6**: 1867–1913.

Baklanov, A., Morozov, S., Mahura, A., Rigina, O., Nazarenko, L., Tausnev, N., Koshkin, V., Fedorenko, Yu., 2006b, *Modelling of possible environmental consequences of accidents on nuclear risk sites in the European Arctic*. Publisher: Russian Academy of Sciences. (In Russian)

Berge, E., Walker, S.-E., Sorteberg, A., Lenkopane, M., Eastwood, S., Jablonska, H.I. and Køltzow, M.Ø., 2002, A real-time operational forecast model for meteorology and air quality during peak air pollution episodes in Oslo, Norway. *Water, Air and Soil Pollution Focus,* **2**: 745–757.

Bergman, R. and Baklanov, A., 1998, *Radioactive sources in main radiological concern in the Kola-Barents region*. FRN/FOA publication, Stockholm, 1998. 80 p.

Byun, D.W. and Ching, J.K.S. (Editors), 1999, *Science Algorithms of the EPA Models-3 Community Multiscale Air Quality (CMAQ) Modelling System*. EPA/600/R-99/030, Washington, DC.

Chenevez, J., Baklanov, A., Sørensen, J.H., 2004, Pollutant transport schemes integrated in a numerical weather prediction model: Model description and verification results. *Meteorological Applications,* **11**(3): 265–275.

Coulson, G., Bartonova, A. Bøhler, T., Broday, D.M., Colbeck, I., Fløisand, I., Fudala, J., Hollander, W., Housiadas, Ch., Lazaridis, M. and Smolik, J., 2005, Exposure Risks from Pollutants in Domestic Environments: The Urban Exposure Project, *Indoor Built. Environ.* **14**(3–4): 209–213.

Galmarini, S., R. Bianconi, W. Klug, T. Mikkelsen, R. Addis, S. Andronopoulos, P. Astrup, A. Baklanov, J. Bartniki, J.C. Bartzis, R. Bellasio, F. Bompay, R. Buckley, M. Bouzom, H. Champion, R. D'Amours, E. Davakis, H. Eleveld, G.T. Geertsema, H. Glaab, M. Kollax, M. Ilvonen, A. Manning, U. Pechinger, C. Persson, E. Polreich, S. Potemski, M. Prodanova, J. Saltbones, H. Slaper, M.A. Sofiev, D. Syrakov, J.H. Sørensen, L. Van der Auwera, I. Valkama, R. Zelazny, 2004, Ensemble Dispersion Forecasting, Part I: Concept, Approach and Indicators. *Atmos. Environ.* **38**: 4607–4617.

Graziani, G., Klug, W. and Moksa, S., 1998, *Real-Time Long-Range Dispersion Model Evaluation of the ETEX First Release*. EU JRC.

Gross, A. and Baklanov A., 2004, Modelling the influence of dimethyl sulphide on the aerosol production in the marine boundary layer, *International Journal of Environment and Pollution,* **22**: 51–71.

Hänninen, O., 2005, *Probabilistic Modelling of PM2.5 Exposures in the Working Age Population of Helsinki Metropolitan Area.* Publications of the National Public Health Institute (KTL) A10/2005. PhD dissertation.

Hänninen, O.O., Lebret, E., Tuomisto, J.T., Jantunen, M.J., 2005, Characterization of model error in the simulation of PM2.5 exposure distributions of the working age population in Helsinki, Finland. *Journal of the Air & Waste Management Association,* **55**: 446–457.

Hoe S., Müller, H. and Thykier-Nielsen, S., 2000, Integration of dispersion and radioecological modelling in ARGOS NT. In: *Proceedings of IRPA 10, Tenth International Congress of the International Radiation Protection Association*, Hiroshima, Japan, May 14–19, 2000.

Hoe, S.C., Müller, H., Gering, F., Thykier-Nielsen, S. and Sørensen, J.H., 2002, ARGOS 2001 a Decision Support System for Nuclear Emergencies. In: *Proceedings of the Radiation Protection and Shielding Division Topical Meeting*, April 14–17, 2002, Santa Fe, New Mexico, USA.

IPCC, 1996, Impacts, adaptations and mitigation of climate change: scientific technical analyses. In: *Watson RT, Zinyowera MC, Moss RH, editors. Contributing working group II, 2nd assessment report, Intergovernmental Panel on Climate Change.* Cambridge (UK): Cambridge Univ. Press; 880 p.

IPCC, 2001, Climate change 2001: the scientific basis. In: *Houghton JT, Ding Y, Griggs DJ, Noguer M, van der Linden PJ, Dai X, Maskell K, Johnson CA, editors. Contributing working group I, 3rd assessment report, Intergovernmental Panel on Climate Change.* Cambridge (UK): Cambridge Univ. Press. 881 p.

Jacobson, M., 2001, Strong radiative heating due to the mixing state of black carbon in atmospheric aerosols, *Nature*, **409**: 695–697.

Kousa, A., Oglesby, L., Koistinen, K., Kunzli, N., Jantunen, M., 2002, Exposure chain of urban air PM2.5 - associations between ambient fixed site, residential outdoor, indoor, workplace and personal exposures in four European cities in the EXPOLIS-study. *Atmospheric Environment*, **36**: 3031–3039.

Lauritzen, B., Baklanov, A., Mahura, A., Mikkelsen, T., Sørensen, J.H., 2006, K-model description of probabilistic long-range atmospheric transport in the Northern Hemisphere. *Atmospheric Environment*, accepted.

Mahura A. and Baklanov A., 2003, Probabilistic Indicators of Atmospheric Transport for Regional Monitoring and Emergency Preparedness Systems. *Environment International,* **29/8**: 1063–1069.

Mahura A.G., Baklanov, A.A., Sørensen, J.H., Parker, F.L., Novikov, V., Brown, K., Compton*,* K.L., 2005a, Assessment of Atmospheric Transport and Deposition Patterns Related to Russian Pacific Fleet Operations. *Environmental Monitoring and Assessment*, **101**: 261–287.

Mahura, A., Baklanov, A., Sørensen, J.H., 2005b, Long-Term Dispersion Modelling: Assessment of Atmospheric Transport and Deposition Patterns from Nuclear Risk Sites in Euro-Arctic Region, *Journal of Computational Technolo*gy, **10**: 112–134.

Mahura, A., Baklanov, A., Sørensen, J.H., Svetlov, A., Koshkin, V., 2006, Assessment of long-range transport and deposition from Cu-Ni smelters in Russian North. *The same issue*.

Marchuk, G.I., 1982, Mathematical modeling in the environmental problems. Moscow, Nauka (in Russian).

Marchuk, G.I., 1995, Adjoint equations and analysis of complex systems. Kluver Academic Publication.

NAS, 2001, *Climate change science: an analysis of some key questions*. Washington (DC): National Academy of Sciences National Academy Press. 28 p.

Ott, W.R., 1995, Human exposure assessment: the birth of a new science. *Journal of Exposure Analysis and Environmental Epidemiology* **5**: 449–472.

Penenko, V. and Baklanov, A., 2001, Methods of sensitivity theory and inverse modeling for estimation of source term and nuclear risk/vulnerability areas *Lecture Notes in Computer Science*, **2074**: 57–66.

Penenko, V., Baklanov, A. and Tsvetova, E., 2002, Methods of sensitivity theory and inverse modeling for estimation of source term. *Future Generation Computer Systems*, **18**: 661–671.

Penenko, V.V., 1981, *Methods of numerical modeling of the atmospheric processes*. Leningrad, Gidrometeoizdat (in Russian).

Penner J.E. et al., 1998, Climate forcing by carbonaceous and sulphate aerosols, *Clim. Dynamics,* **14**: 839–851.

Pudykiewicz, J.A., 1998: Application of adjont tracer transport equations for evaluating source parameters, Atmos. Environ. 32: 3039–3050.

Rigina, O., and Baklanov, A., 2002, Regional radiation risk and vulnerability assessment by integration of mathematical modelling and GIS-analysis, *Environment International*, **27**: 527–540.

Robertson, L. and Lange, J., 1998, Sourse function estimate by means of a variational data data assimilation applied to the ETEX-I tracer experiment, *Atmos. Environ*. **32**: 4219.

RODOS, 2000, RODOS: *Decision support system for off-site nuclear emergency management in Europe*. Edited by J. Ehrhardt and A. Weiss. Final project report. EC DG Research, EURATOM, EUR 19144 EN, 259 p.

Samoli, E., Analitis, A., Touloumi, G., Schwartz, J., Anderson, H.R., Sunyer, J., Bisanti, L., Zmirou, D., Vonk, J.M., Pekkanen, J., Goodman, P., Paldy, A., Schindler, C., Katsouyanni, K., 2005, Estimating the Exposure-Response Relationships between Particulate Matter and Mortality within the APHEA Multicity Project. *Env Health Pers.,* **113**(1): 88–95.

Semazzi, F., 2003, Air quality research: perspective from climate change modelling research. *Environment International* **29**: 253– 261.

Shine, K.P., 2000, Radiative forcing of climate change, *Space Sci. Rev.* **94**: 363–373.

Sørensen J.H., 1998, Sensitivity of the DERMA Long-Range Gaussian Dispersion Model to Meteorological Input and Diffusion Parameters, *Atmospheric Environment*, **32**: 4195–4206.

Watson R.T. et al., 1997, *The regional impacts of climate change: an assessment of vulnerability*. Special Report for the Intergovernmental Panel on Climate Change.

CONTROL THEORY AND ENVIRONMENTAL RISK ASSESSMENT

ARTASH E. ALOYAN*, V.O. ARUTYUNYAN
Institute of Numerical Mathematics, RAS, Gubkin str., 8, Moscow, 119991, Russia

Abstract. Two environmental protection problems are considered. The first one is related to control theory and optimization focusing on minimization of damage to the environment, and the second one is concerning numerical modelling of the dynamics and transformation of atmospheric gaseous pollutants and aerosols. The wind field and turbulence parameters are calculated from a 3D mesoscale hydrodynamic model.

1. Introduction

Mathematical modelling of atmospheric gas-aerosol variability and the environmental impact of atmospheric pollutants constitute an important problem in atmospheric science. The atmosphere is a complex dynamical system with various dynamical and physico–chemical processes, which are conditioned both by atmospheric circulation and transformation of gaseous pollutants and aerosols (chemical reactions and kinetic processes of nucleation, condensation and coagulation). The atmospheric pollution by gaseous pollutants and aerosol particles poses a problem of reducing their negative impact on the environment. An efficient method of solving this

---

*To whom correspondence should be addressed. A.E. Aloyan, Institute of Numerical Mathematics, RAS, Gubkin str., 8, Moscow, 119991, Russia; e-mail: aloyan@inm.ras.ru

type of problems is the sensitivity analysis for specific areas based on adjoint functions, which allows one to separate zones of environmental concern. Another important problem is the optimization of emission source magnitudes in order to minimize the environmental damage. In this paper, these problems are considered employing the system of atmospheric models developed in the Institute of Numerical Mathematics, RAS.

2. Pollution transport and transformation model

2.1. GOVERNING EQUATIONS

Let us consider the equation of pollution transport in the atmosphere:

$$\frac{\partial \varphi}{\partial t} = F_i - div\, u\varphi + \frac{\partial}{\partial x} K_x \frac{\partial \varphi}{\partial x} + \frac{\partial}{\partial y} K_y \frac{\partial \varphi}{\partial y} + \frac{\partial}{\partial z} K_z \frac{\partial \varphi}{\partial z} \tag{1}$$

where $\{u,v,w\}$ are the components of wind velocity, F_i describes the intensity of emissions, and K_x, K_y and K_z are the coefficients of turbulent diffusion. The equation is solved in the domain

$$D_t = D \times [0,T],\, D = \{(x,y,\sigma): x \in [-X,X],\, y \in [-Y,Y],\, \sigma \in [0,H]\}$$

under the corresponding initial and boundary conditions:

$$K_z \frac{\partial \varphi}{\partial z}\Big|_{z=h} = \frac{1}{r_a + r_b + r_c}\left(\varphi - \varphi_{surf}\right)$$

$$\varphi_i\big|_\Gamma = \varphi_i^b \quad \text{if } u_n < 0,$$

$$\frac{\partial \varphi_i}{\partial n}\Big|_\Gamma = \varphi_i^b \quad \text{if } u_n \geq 0. \tag{2}$$

$$\varphi_i = \varphi_i^0 \quad \text{for } t = 0,$$

$$\varphi_i = \varphi_i^b \quad \text{for } z = H$$

Here r_a, r_b, and r_c are the aerodynamic, quasi-laminar, and surface resistances, u_* is the dynamical velocity, and h is height of the surface layer. Equation (1) is coupled with 3D hydrodynamic equations.

Let us consider the following functional of the solution:

$$J = \int_0^T dt \int_D p\,\varphi\,dD \tag{3}$$

where p is a given function

$$p = \begin{cases} p_0, & (x,y,z) \in G \\ 0, & (x,y,z) \notin G \end{cases}, \quad p_0 > 0,\; G \subset D. \tag{4}$$

This functional describes the total concentration of pollutants in a selected subdomain G within the entire domain D, weighted by p_0. The domain G corresponds to the zone of pollution assessment. Depending on the selection of this domain, different characteristics of the pollution field can be obtained (Marchuk, 1982; Marchuk and Aloyan, 1995; Marchuk et al., 2005).

2.2. ADJOINT PROBLEM

To estimate the functional J, we use an approach based on the adjoint method (Marchuk, 1982; Marchuk and Aloyan, 1989):

$$-\frac{\partial \varphi^*}{\partial t} = P_i - divu\varphi^* + \frac{\partial}{\partial x} K_x \frac{\partial \varphi^*}{\partial x} + \frac{\partial}{\partial y} K_y \frac{\partial \varphi^*}{\partial y} + \frac{\partial}{\partial z} K_z \frac{\partial \varphi^*}{\partial z} \qquad (5)$$

with boundary conditions similar to those in Eq. (2).

The adjoint function allows us to estimate the rate of potential danger of atmospheric pollution in the domain G, for given meteorological conditions. The total amount of in the given area can be determined by the adjoint function: $J = \int_0^T dt \int_D F\varphi^* dD$. The function φ^* is a weight function describing the contribution of each source to atmospheric pollution in the subdomain G. This contribution is equal to the product of the emission magnitude to the value of φ^*. By its values, we can divide the whole domain into areas with respect to the danger of atmospheric pollution impacts in the domain G.
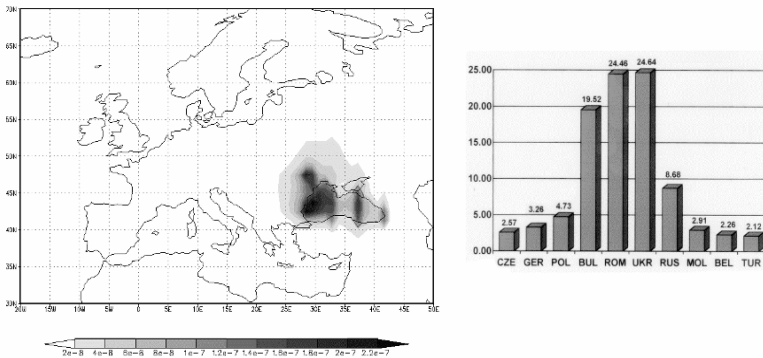
Figure 1. Sensitivity function for the Black Sea region and percentage distribution of sulphuric pollution.

Using this model, numerical experiments were performed for different regions (Marchuk and Aloyan, 1995; Marchuk et al., 2005). Some results of the numerical calculations are presented below. Figure 1 presents the results of transboundary transport calculations for the territory of the Black Sea.

Also, a histogram showing the percentage contribution of each country to the sulphuric pollution is shown.

Let us consider an optimization problem for the control of emission source magnitudes with some criteria and constraints of ecological and economic character being imposed.

2.3.   OPTIMIZATION PROBLEM (NONLINEAR APPROXIMATION)

Assume that we have n sources of admixtures with emission rates Q_i ($i=1,2,…,n$) in domain D_t. We select an ecologically significant subdomain $G \subseteq D_t$ and consider the functionals

$$\alpha_i^c = \alpha_i^c f_1(\varphi), \quad \alpha_i = \alpha_i f_2(\varphi),$$

where $f_1(j)$ and $f_2(j)$ are given functions of concentration (risk level), characterizing the amount of damage ecological criteria. The total environmental damage is usually assumed to linearly depend on the pollution. However, the actual dependence often proves to be nonlinear (Balatskiy, 1979). Here is a simple example: let some amount of pollutants be deposited on a forest of area S, which leads to the destruction of αQ-portion of the forest. By damage, we mean the costs needed to restore the destroyed fraction of forest. The costs are assumed to be proportional to the time of restoration. Also assume that the forest grows in a geometric progression with the factor $\delta = 1 + \beta$. Then, we obtain the expression

$$S = S(1-\alpha Q)(1+\beta)^t \qquad t = \frac{\ln \dfrac{1}{1-\alpha Q}}{\ln(1+\beta)}.$$

If 20-percent of the forest is destroyed and the forest growth factor is 1.1, the time of restoration is 2.34 years. If we take 50-percent damage, the time will be 7.27 years.

By statistical data, the dependence of damage to housing stock by dust (x_1) and sulphuric anhydride (x_2) has the form:

$\ln y = 7.62 + 0.87 \ln x_1 + 1.27 \ln x_2.$

For convenience, we assume that damage is a quadratic function of the total concentration. In the protected zone and the remaining area the function is defined as (Aloyan and Perekhodtsev, 2000):

$$Y^c = \sum_{i=1}^{n} (\alpha_i^c Q_i)^2 \qquad\qquad Y_0 = \sum_{i=1}^{n} (\alpha_i Q_i)^2$$

where (α_i^c and (α_i are damage coefficients in the protected zone G and the total area D.

The optimization problem is

$$Y^c = \sum_{i=1}^n (\alpha_i^c Q_i)^2 \to \min_{e_i}$$

under the following constraints

$$0 \le Q_i \le \tilde{Q}_i \qquad k_1 Y_0 \le \sum_{i=1}^n \alpha_i Q_i \le k_2 Y_0$$

where k1 and k2 are coefficients characterizing the desirable level of damage reduction.
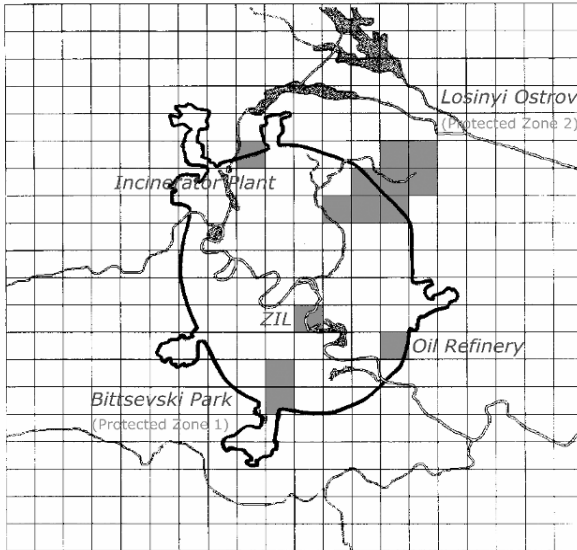
Figure 2. Pollution sources and protected zones in the Moscow region.

To solve this problem, the method of nonlinear programming is used

$$Q(x) = p^T x + x^T C x \to \min,$$
$$Ax \le b,\ x \ge 0$$

This model was applied to the problem of damage minimization of in the Moscow region, including three pollution sources (incinerator plant, oil

refinery, and motor-car plant) and two protected zones (*Bittesvski park* and *Losini Ostrov*) (Fig. 2).

In Fig. 3, we demonstrate the emission reduction ratio for a 10% damage-reduction control. Here, only gaseous pollutants were used. However, the actual control problems are more complex, particularly if human-health criteria are used, which include some uncertainties. This is connected with the fact that the effect of aerosol particles with different ion composition and size distribution on human organs is diverse.

Protected Zone: *Bittsevski Park*

Source	Q	Q⁻	Q/Q⁻
Oil Refinery	223.78	3278	0.07
Incinerator Plant	1167.13	3514	0.33
ZIL Motor Plant	195.27	3086	0.06

Protected Zone: *Losinyi Ostrov*

Source	Q	Q⁻	Q/Q⁻
Oil Refinery	1446.90	3278	0.44
Incinerator Plant	418.75	3514	0.12
ZIL Motor Plant	3086	3086	0.15

Figure 3. Emission reduction ratio for a 10% control (unit is g/s). Q- is the value of primary emission and Q is the value of emission after optimization.

3. Combined model of gas-aerosol dynamics

Let us now formulate the combined model of gas and aerosol dynamics in the atmosphere. These processes are described using main equations of pollution transport, chemical transformation and aerosol formation with condensation/evaporation, coagulation, and nucleation. The chemical model describes both gas and aqueous phase chemical processes including mass-exchange processes on the gas-aerosol (drop) interface. In the general form, the system of model equations can be written as

$$\frac{\partial C_i}{\partial t} + u_j \frac{\partial C_i}{\partial x_j} = F_i^{\,gas} - P_i^{\,nucl} - P_i^{\,cond} + P_i^{\,phot}$$

$$+ \frac{\partial}{\partial x_1} K_{11} \frac{\partial c_i}{\partial x_1} + \frac{\partial}{\partial x_2} K_{22} \frac{\partial c_i}{\partial x_2} + \frac{\partial}{\partial x_3} K_{33} \frac{\partial c_i}{\partial x_3};$$

$$\frac{\partial \varphi_k}{\partial t} + (u_j - \delta_{j3} w_g) \frac{\partial \varphi_k}{\partial x_j} = F_k^{\,aer} + P_k^{\,nucl} + P_k^{\,cond} + P_k^{\,coag}$$

$$+ \frac{\partial}{\partial x_1} K_{11} \frac{\partial \varphi_k}{\partial x_1} + \frac{\partial}{\partial x_2} K_{22} \frac{\partial \varphi_k}{\partial x_2} + \frac{\partial}{\partial x_3} K_{33} \frac{\partial \varphi_k}{\partial x_3}.$$

where $x_1 = x$, $x_2 = y$, and $x_3 = z$; C_i ($i = 1, N_g$) and φ_k ($k = 1, N_a$) are the concentrations of gaseous species and aerosols, N_g and N_a are the numbers of gaseous components and aerosol fractions, respectively; w_g is the gravitational settling; F^{gas} and F^{aer} describe the emission source magnitudes of gaseous species and aerosols; P^{nucl}, P^{cond}, P^{coag}, and P^{phot} are the operators of nucleation (in the system H_2O–H_2SO_4–NH_3), condensation, coagulation, and photochemical transformation (involving gas- and aqueous-phase chemical processes), respectively. The condensation and coagulation processes are solved using nonequilibrium particle-size distributions (Aloyan and Piskunov, 2005). The photochemical model includes a total of 200 gas-phase reactions, 26 equilibrium dissociation reactions, 61 reactions in drops, and 9 photodissociation reactions. The model includes a total of 30 particle size bins, representing the size range from 0.05 to 1.5 micrometers.

The coagulation is considered for a system of mixture composed of two species (sulphuric acid and water). In this case, the kinetic equation of coagulation can be written as (Piskunov et al., 1997; Aloyan and Piskunov, 2005):

$$\frac{\partial C(g, \alpha, t)}{\partial t} = \frac{1}{2} \int_0^g \int_0^\alpha K(g-s, \alpha-\beta; s, \beta) C(g-s, \alpha-\beta) C(s, \beta) ds d\beta$$

$$- C(g, \alpha, t) \int_0^\infty \int_0^\infty K(g, \alpha; s, \beta) C(s, \beta) ds d\beta, \qquad (6)$$

where g is the total mass of particles, α is the mass of emitted admixtures, K is the coagulation coefficient, and $C(g, \alpha, t)$ is the total concentration of particles. Explicitly separating the contributions of admixtures and composite particles to the total concentration yields

$$C(g,\ \alpha,\ t) = c(g,\ t)\ \delta(g - \alpha) + c_c(g,\ \alpha,\ t) \qquad (7)$$

where $c(g,\ \alpha,\ t)$ is the concentration of admixture particles with a total mass g and an admixture mass α, $c_c(g,\ \alpha,\ t)$ is the concentration of composite particles, and α is the mass of substance (admixture) in the particle. Inserting Eq. (7) into Eq. (6), we obtain more suitable equations for numerical calculations.

The kinetic equation for the distribution function is

$$\frac{\partial c}{\partial t} + \frac{\partial}{\partial g}(v_g c) = J(g,t)\delta[g - g_*(t)];\qquad (8)$$

where v_g is the growth rate of particles with a total mass of g, J is the nucleation rate, and g_* is the mass of the critical-size drop.

Then, the combined equations of gas- and aqueous-phase chemical processes are applied taking into account the mass-exchange at the gas-particle interface.
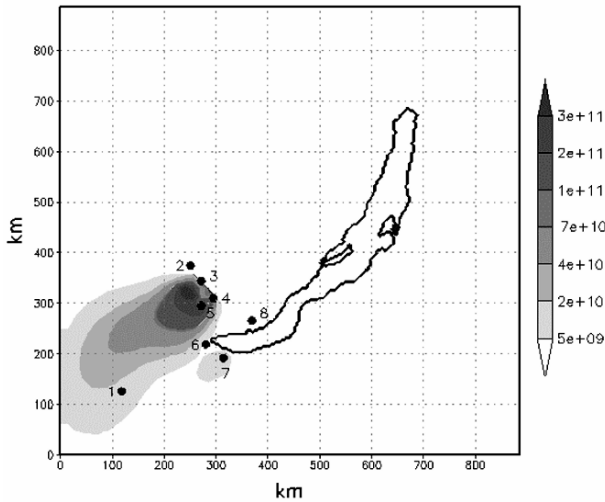
Figure 4. Concentration of sulphuric acid.

4.   Numerical results

The numerical calculations were performed for the Baikal Lake region (Russia). A total of five large industrial emission sources were considered including the species SO_2, NO, CO, etc. Apart from the fact that this region is characterized by complex topography and covers the unique water area of Lake Baikal, there are large local sources of SO_2 emissions. This leads to enhanced nucleation and new-particle formation patterns. The following

input parameters were used in the calculations: the horizontal size of the computational domain is 900 × 900 km, the horizontal step is 15 km, the height is 2050 m, and the number of vertical layers is 20.

In Fig. 4, we demonstrate the concentration of sulphuric acid for t = 24 h. In the Baikal region, the sulphuric acid vapour concentration is much higher than the threshold value for the formation of nucleation-mode particles. When the temperature decreases, the nucleation rate increases, while the rate decreases with decreasing relative humidity.
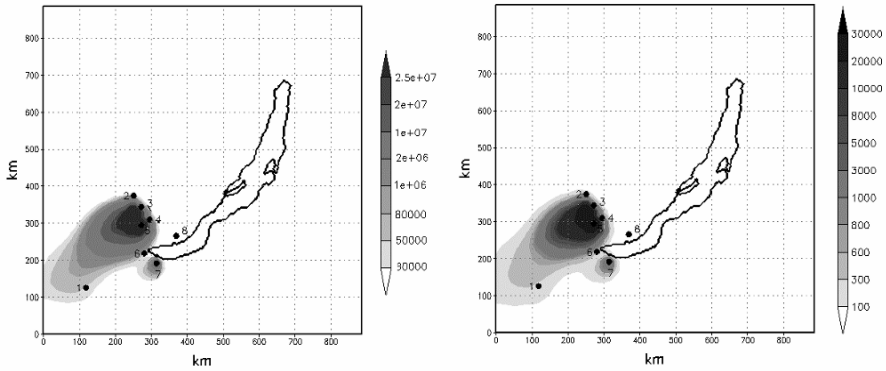
Figur 5. Aerosol particle concentrations (0.31 and 2.06 μm).

In Fig. 5, we demonstrate the number concentrations of aerosol particles with radii 0.31 and 2.6 micrometers. The numerical results indicate that smaller drops have higher acidity values.

To reproduce the complex atmospheric circulation in this region, a nonhydrostatic mesoscale hydrodynamic model is used. We have performed a comparison between the calculated and observed data on the ion composition of sulphate particles (Fig. 6). The observation data are represented by the total concentration of H^+ protons accumulated on the filter during a 7-day period with no account of the particle-size distribution. The calculation results were integrated over all particle sizes. And the observation data were collected for the town of Irkutsk and Mondy background station.

5. Conclusion

Using an optimization model with adjoint functions, efficient algorithms for the control of emission source magnitudes were constructed. If the dependence of damage on pollution concentration is quadratic, the problem of damage optimization has a nonzero solution; i.e., one can avoid closing any plant under control. The numerical experiments indicated that our model can be used for studying the regional-scale dynamics and kinetics of
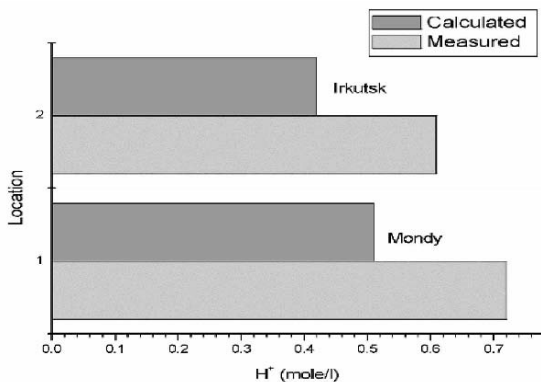
Figure 6. Calculated and measured H+ protons.

gas pollutants and aerosols in the atmosphere. The gas- and aqueous-phase chemical model successfully reproduces the ion composition of sulphate aerosol particles.

Acknowledgments

References

Aloyan, A. E., and Perekhodtsev, D. M., 2000, Mathematical modelling of pollution transport in the atmospheric boundary layer and control of emission source magnitudes. In: *Problems of Atmospheric Boundary Layer Physics and Air Pollution*, Hydrometeoizdat, St.-Petersburg, pp. 43–57.

Aloyan, A. E., and Piskunov, V. N., 2005, Modelling the regional dynamics of gaseous admixtures and aerosols, *Izvestiya, Atmospheric and Oceanic Physics* **41**(3):296–307.

Balatskiy, O. F., 1979, *Technical Progress, Chemistry, and Environment,* Khimiya, Moscow.

Marchuk, G. I., 1982, *Mathematical Modelling in the Problem of Environment,* Nauka, Moscow.

Marchuk, G. I., and Aloyan, A. E., 1989, Mathematical modelling in ecological problems, Preprint No. 234, DNM, USSR Acad. Sci., Moscow, pp. 1–36.

Marchuk, G. I., and Aloyan, A. E., 1995, Global transport of pollutants in the atmosphere, *Izv. Russ. Acad. Sci.: FAO* **31**(5):597–606.

Marchuk, G. I., Aloyan, A. E., and Arutyunyan, V. O., 2005, Adjoint equations and transboundary transport of pollutants, *Ecol. Vest. Nauch. Tsentr. ChES* **2**:54–64.

Piskunov, V. N., Golubev, A. I., Goncharov, E. A., and Ismailova, N. A., 1997, Kinetic modelling of composite particles coagulation, *J. Aerosol Sci.* **28**:1215–1231.

AIR QUALITY MODELS FOR RISK ASSESSMENT
AND EMERGENCY PREPARDNESS–INTEGRATION
INTO CONTROL NETWORKS

ROBERTO SAN JOSÉ[*], J.L. PÉREZ
*Environmental Software and Group, Computer Science
School, Technical University of Madrid), Campus de
Montegancedo, Boadilla del Monte 28660 Madrid (Spain)*

R.M. GONZÁLEZ
*Department of Meteorology and Geophysics
Faculty of Physics, Complutense University of Madrid
Ciudad Universitaria 28040 Madrid (Spain)*

Abstract. Different programmes related to air quality risk management and emergency situations are currently in operation at European level. Intensive research is currently in operation related to integration of air quality and air quality and meteorological observational networks to provide efficient, robust and confident air quality forecasts for emergency and risk assessment situations. Different EU programmes are currently ongoing with several objectives into such integration. The GMES programme is focusing on Global Monitoring for Environment and Security. This programme is supported by European Space Agency and EU Commission (FP6 EU Programme). Also a specific programme supported by EU into the 6th Framework Programme and in the area of Information Technologies is supporting several projects focusing on Risk & Management on Environmental Issues. In this contribution we will show the results of integration of new telecommunication technologies (mobile technologies, SMS, GPRS, 3G-UMTS, WAP, etc.) to produce integrated air quality services for the citizen and also for environmental authorities. In this

_____

*To whom correspondence should be addressed. R. San José, Environmental Software and Modelling Group, Computer Science School, Technical University of Madrid), Campus de Montegancedo, Boadilla del Monte 28660 Madrid (Spain); e-mail: roberto@fi.upm.es

application we show the OPANA V2 model (OPerational Atmospheric Numerical pollution model for urban and regional Areas) which includes the MEMO model (University of Karlsruhe, Germany) and the chemistry module SMVGEAR (University of Los Angeles, USA) which has been implemented into MEMO in on-line mode. This model was used into APNEE and APNEE-TU IST EU 5th Framework Programme which focused on the integration of mobile telecommunication technologies and air quality forecasting systems.

1.   Introduction

Different tools have been developed in the last years in order to provide an integrated Air Quality Management tool for environmental authorities at different levels in the administration such as municipalities, counties, regions, autonomous communities, states, continental and global levels. The environmental modelling and particularly the air quality modelling and assessment is a particular complex matter which integrates many different tools from several scientific classical areas. The integration is generally provided by sophisticated information technology tools which assures a robust, efficient and reliable capability to combine the different capabilities of each of the tools. In order to provide an efficient response to air quality emergencies and risks, the quality and quantity of the different unit tools which are forming the final integrated air quality management tools should be formed by "state-of-the-art" applications. However, for risk management and emergency air quality situations it would be necessary to combine quality with effectiveness in order to account for the limitations in computer capabilities nowadays.

Figure 1 shows a scheme of the different elements creating a robust, reliable and efficient Air Quality Management Tool to be used for risk assessment and emergency situations. This scheme shows the integration between air quality models and mobile telecommunication technologies to produce air quality warning message to the public by using mobile technologies. The actual research lines are focusing on the integration of satellite data which covers a large extension of model domains into the air quality modelling systems by using different "assimilation" techniques such as 3DVAR or (more computer costly efficient) 4DVAR. However, for emergency situations a combination between sophisticated models which are running operationally under daily or periodic basis and fast-Gaussian-Lagrangian (Collins et al., 1997) air quality dispersion models is desirable.

These Gaussian-Lagrangian model are general less computationally expensive and can provide information about the forecasted impact of emission sources in an efficient way by using background information provided by sophisticated operational 3D air quality models (Gardner et al., 1997) . This combination seems to be the most efficient approach for air quality risk assessment and emergency situations.
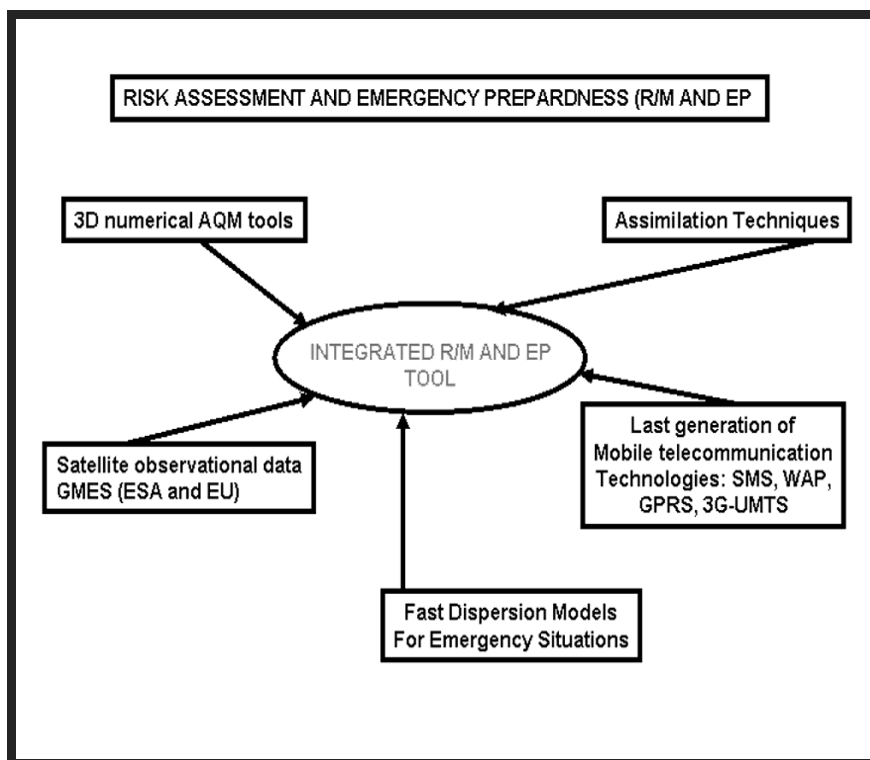
Figure 1. Different elements to consider to create an air quality management tool for risk management and emergency situations.

The well-known Gaussian plume models such as ISCT3, AERMOD, DEGADIS (EPA, US) or Lagrangian models such as CALPUFF (EPA, USA) or FLEXPART or FLEXTRA (Technical University of Munich, Germany) models are more appropriate for this purposes. In risk management applications, background concentrations and proper meteorological data are essential to obtain accurate, reliable and confident results. For emergency purposes such as dense or/and gas releases in explosions, proper meteorological data is an essential input to forecast accurately the time and location of the impact of the dangerous gas emission.

A proper continental meteorological and air quality model information to provide accurate boundary and initial conditions to regional and local model applications has been developed. Some examples are shown from APNEE and APNEE-TU IST EU projects (5th Framework Programme) which integrated sophisticated mobile telecommunication techniques with continental meteorological and air quality applications and fast-response dispersion tools.

In this contribution we are showing the construction of an integrated platform using real-time satellite data from TOM's satellite, real-time air quality monitoring data, three dimensional air quality models such as OPANA V2 (MEMO-SMVGEAR) or OPANA V3 (MM5-CMAQ), (Gery et al., 1989; Lagner et al., 1998, Roemer M. et al., 1996; San José et al., 1994, 1996;) fast-response modelling tools (Gaussian and/or Lagrangian model applications such as DEGADIS, AERMOD and CALPUFF, and an integrated software platform to manage the air pollution warning messages to citizens and environmental authorities (APNEE). Figure 2 shows an example of the different components for an specific application in Madrid (Spain) during the APNEE EU project.
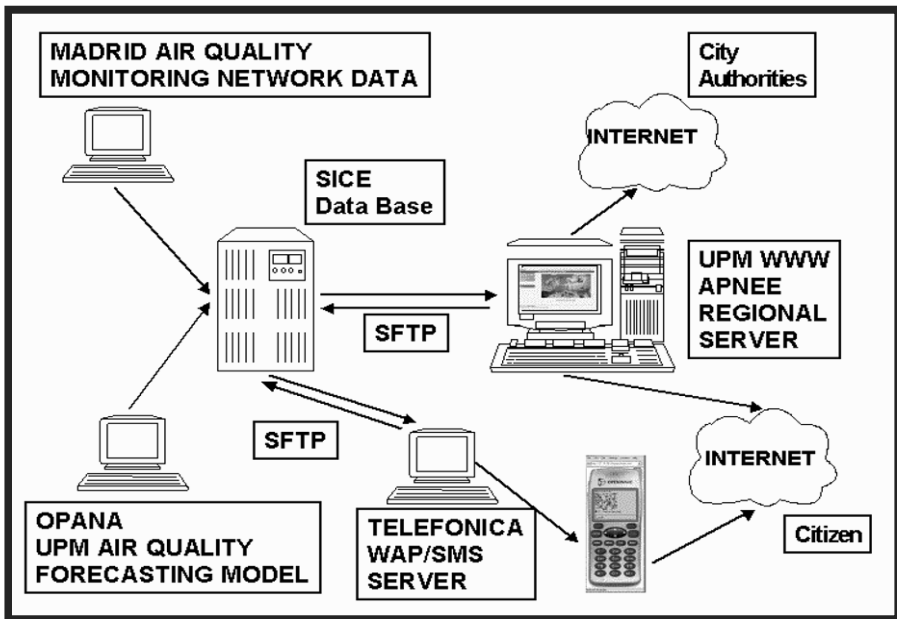
Figure 2. Madrid Air Quality warning system as developed in APNEE EU IST Project (2000-2004).

2.   The APNEE and APNEE-TU projects

The APNEE project was funded by the European Commission during the 5th Framework Programme and APNEE-TU project was funded immediately after the ending of APNEE as a take-up action. APNEE ended on 2002 and APNEE-TU ended in 2004. Different countries were involved and represented by air quality authorities at city and regional levels, air quality service companies and environmental research and university groups. In the case of Spain, City of Madrid was involved during the APNEE project and Andalusia and Canary Islands (Spain) Autonomous Communities were involved in APNEE-TU. These sites served as pilot sites to test the different air quality applications and integrated tools created and developed during APNEE project. An example of the situation before APNEE and after APNEE can be seen in Figures 3 and 4. This was applicable to all the sites and countries involved at European level.
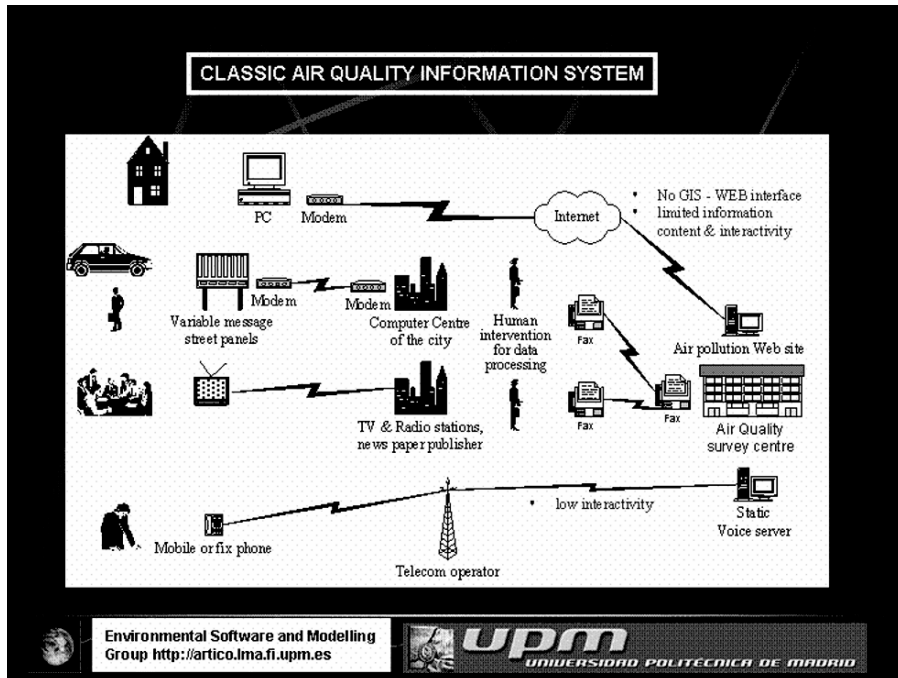
Figure 3. Scheme showing the technological situation before APNEE related to the technologies used to provide air quality information to public and different users.
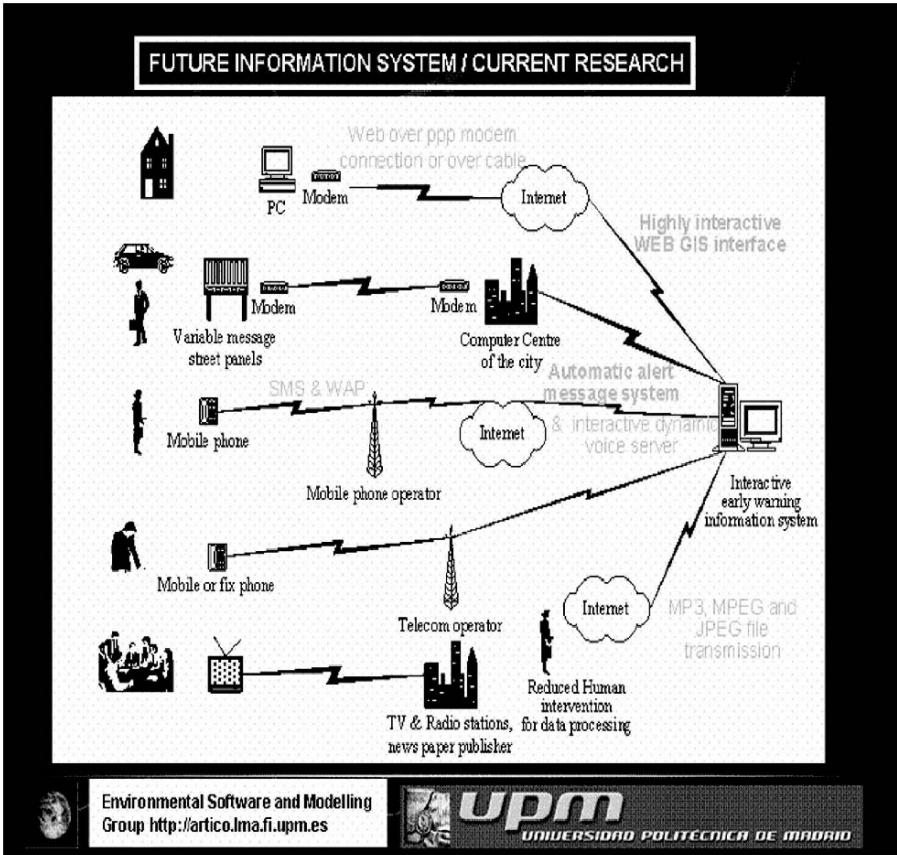
Figure 4. Scheme showing the technological situation after APNEE related to the technologies used to provide air quality information to public and different users.

APNEE and APNEE-TU in the Spanish application produced several services such as WAP and SMS alerts related to urban and regional air quality indexes for Madrid City, Andalusia and Canary Islands regions. In Figure 5 we observe a summary of different services related to telecommunication technologies with application into the Air Quality Warning systems to be used for emergency and risk management applications.
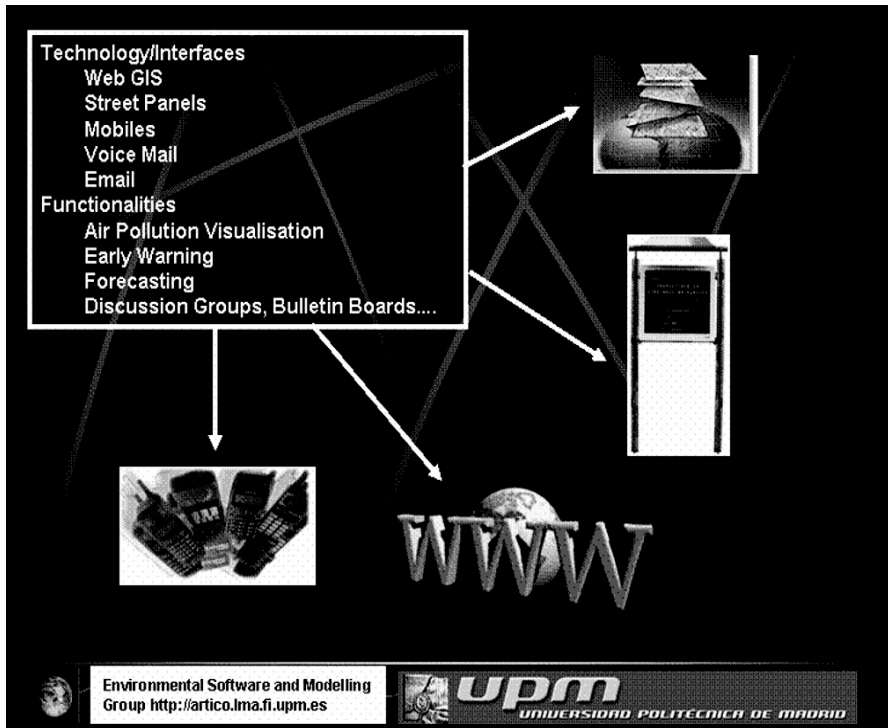
Figure 5. Telecommunication technologies as a fundamental vehicle to serve for integrated air quality applications for risk and emergency management tools.

3. Air quality management systems

Different air quality systems are in operation in Europe such as RIU (University of Cologne) which produces a daily European and local air quality forecast (see Figure 6); DMU-THOR which is used in Denmark and produced by the Danish Environmental Research Institute; UK Air Quality Forecasts prepared by the UK Department of Environment, etc. These tools are operating mainly on the Internet and are providing daily forecasts for the next 24–72 hours at national and local levels. However several additional features should be incorporated in the future to improve not only the quality of the forecasts but also the way that the citizens and general public is receiving the information. (Schmidt et al., 2001; Stockwell et al., 1977).

In Spain our group has developed different air quality forecast systems for different applications such as cities, regions and/or industrial plants. We have developed since 1995 Internet based Air Quality Forecasting systems for Madrid City and Community, Bilbao, Asturias, Andalusia Community,

Canary Islands Community, Las Palmas de Gran Canaria Municipality (Spain), Leicester City Council (UK) and Quito (Ecuador). These applications continue to be in operation either by the own users or from our laboratory. The last implementation was down in 2004 for Las Palmas de Gran Canaria (Canary Islands, Spain) as shown in Figure 7. This last application uses MM5-CMAQ as Air Quality System which is the "state-of-the-art" in air quality modelling. This site includes a sophisticated 4D Internet visualization system which was developed based on VISAD Java libraries. See Figure 8.
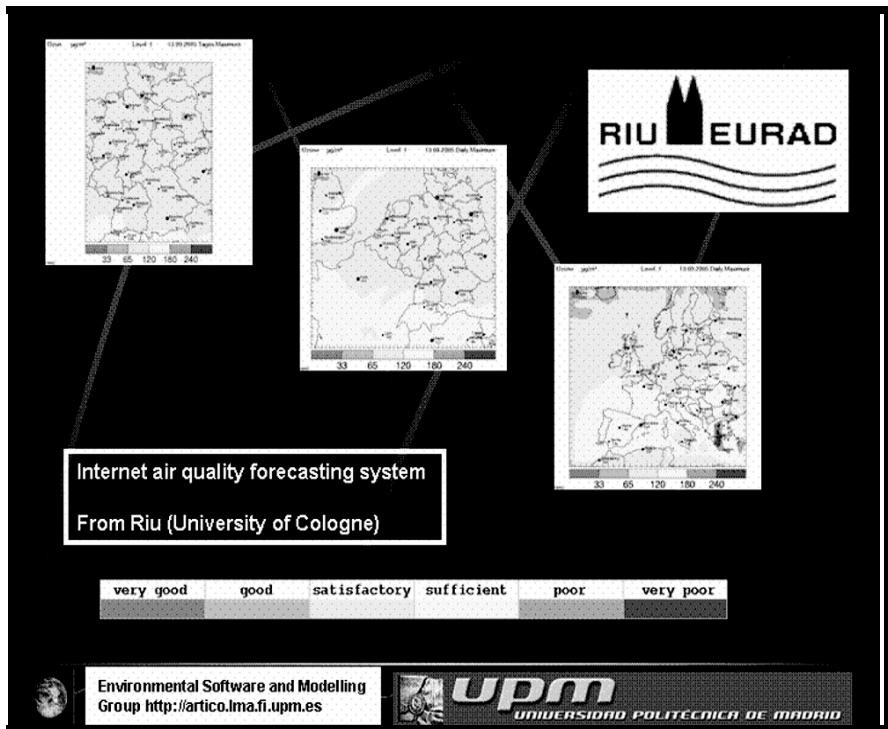
Figure 6. RIU (University of Cologne) air quality forecasts system for different domains.

The air quality information systems developed in Spain by UPM include sophisticated mapping-GIS tools to locate a geographical location and produce air quality forecast graphics at user demand. It also includes hourly surface maps for pollutant. Three levels of information are provided: a) Forecasted Air Quality Indexes for a full day b) Detailed surface and pollutant time series for a geographical location and c) 4D visualization.

At this stage, in some cases all levels are visualized but in other cases the some visualization levels are restricted to Municipal environmental authorities.
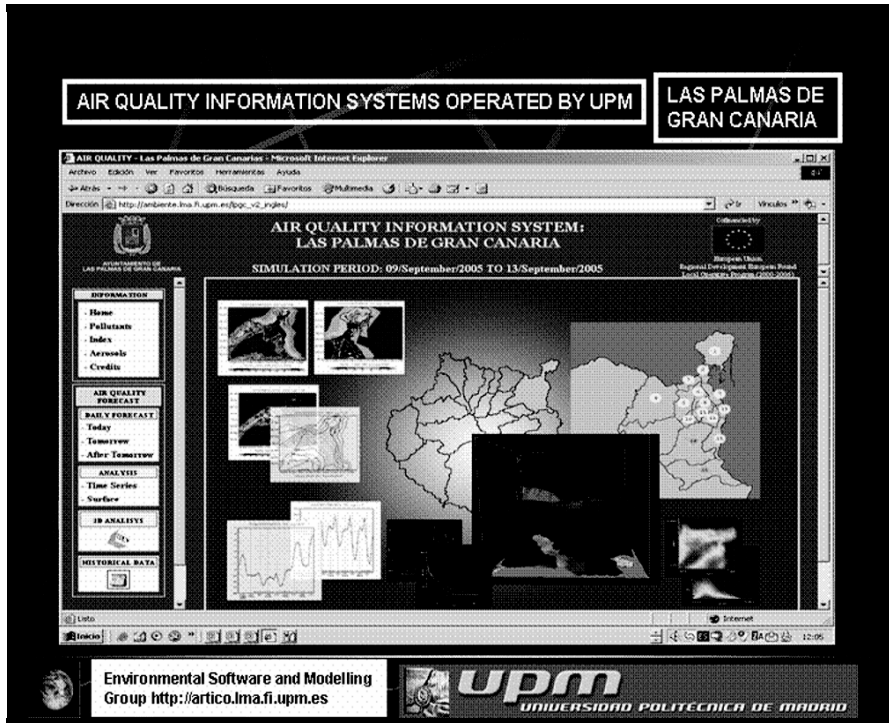
Figure 7. Home site for Las Palmas de Gran Canaria Municipality (Canary Islands, Spain) to provide daily air quality forecasts.

4. Industrial air quality forecasting applications

A EUREKA project led by UPM was held in 2001-2004 with the participation of INDRA S.A: Spanish software company and Institute of Physics (Lithuania). The project was titled TEAP (A tool to evaluate the air quality impact of industrial plants). This tool uses last generation of air quality models such as MM5 (for meteorology) and CMAQ (for 3D dispersion). Since the air quality processes are highly non-linear, the impact of an industrial plant is extracted from the differences between ON and OFF scenarios. In other words, the impact is extracted between the results of two simultaneous simulations which includes all anthropogenic and biogenic sources in an identical way but in ON scenario the expected emissions for the next 96 hours are included and in OFF scenario these

industrial emissions are not included. The differences provide a detailed time and spatial analysis of the impact of the industrial emissions in air concentrations in time and space and provides a qualitative and quantitative evaluation of the portion in air concentrations due to the emissions of the industrial plant. This approach is consistent with the use of sophisticated models. This approach is computationally expensive but provides an accurate and detailed information at spatial and temporal levels. The increase in computer power and in the use of cluster platforms are making cheaper this approach in the coming years. In Figure 9 we observe the home site of the TEAP EUREKA project. And in Figure 10 we observe the home page for the first real application of the TEAP EUREKA project. The system is providing industrial impact air quality forecasts for a power plant in the south area of Madrid Community located in Aceca (Toledo). The system is operating since last July, 2005 and providing air quality impact forecasts in the web for the companies (Iberdrola and Unión Fenosa) and environmental authorities (Environmental Council of Castilla-La Mancha). See Figure 10.
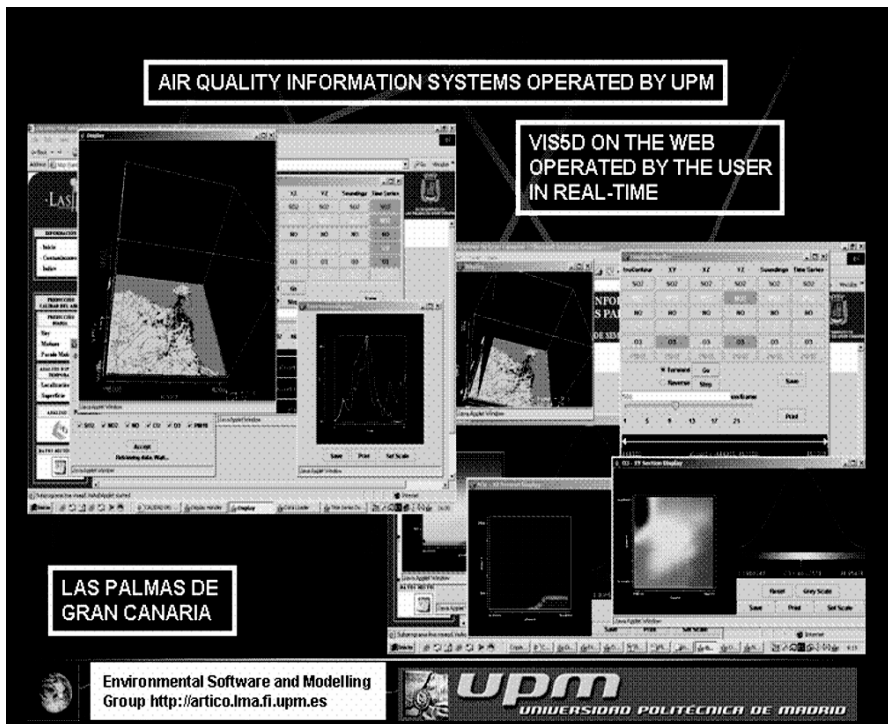
Figure 8. Sohisticated 4D visualization system on the Internet by using VISAD Java libraries for Las Palmas de Gran Canaria (Canary Islands, Spain).

Figure 9. TEAP EUREKA home page.

5. Conclusions

An intense research and technical activity is carrying on related to the development of integrated air quality systems focused to risk assessment and emergency situations. The needs to produce reliable, efficient and robust tools is based on the integration of telecommunication, satellite and a combination of sophisticated air quality models and fast-response dispersion and impact tools. These integrated models require a huge amount of information related to Geographic Information Systems and real-time data sets related to traffic information, industrial emissions and tertiary and domestic activity related to emission of pollutants to the atmosphere. Technologies such as GPS and real-time traffic counting should be incorporated to create these integrated air quality tools for risk management and emergency situations.
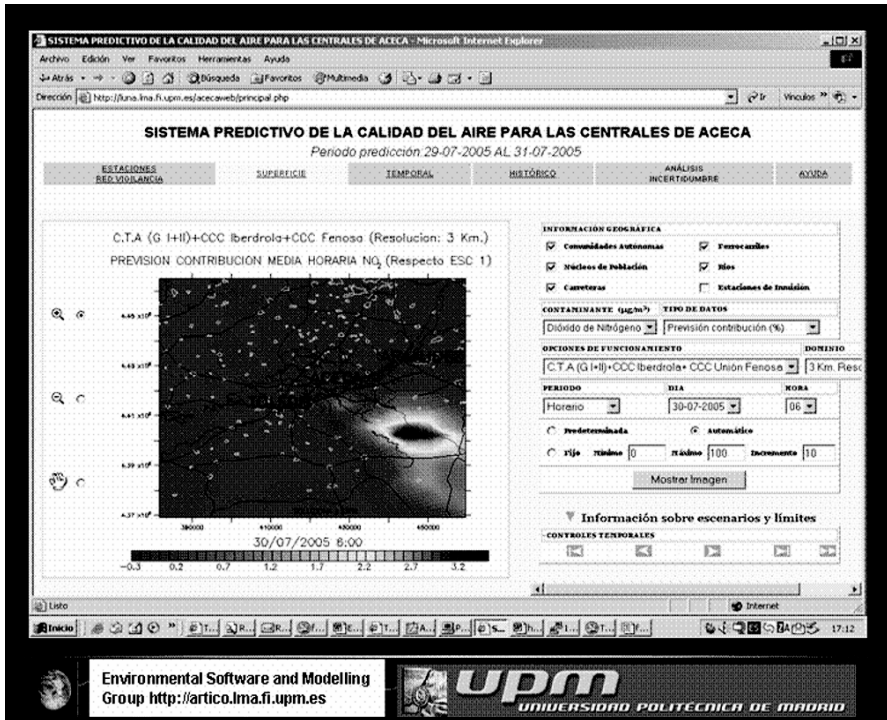
Figure 10. Industrial Impact Air Quality Forecasting System implemented in Aceca Power plant (Toledo, Castilla - La Mancha, Spain).

References

Collins, W.J., Stevenson, D.S., Johnson, C.E., and Derwent, R.G., 1997, Tropospheric ozone in a global scale3D Lagrangian model and its response to NOx emission controls. *J. Atmos. Chem.* **86:**223–274.

Gardner, R.K., Adams, K., Cook, T., Deidewig, F., Ernedal, S., Falk, R., Fleuti, E., Herms, E., Johnson, C., Lecht, M., Lee, D., Leech, M., Lister, D., Masse, B., Metcalfe, M., Newton, P., Schmidt, A., Vandenberg, C., and van Drimmelen, R., 1997, The ANCAT/EC global inventory of NOx emissions from aircraft, *Atmospheric Environment* **31:**1751–1766.

Gery, M.W., Whitten, G.Z., Killus, J.P., and Dodge, M.C., 1989, A photochemical kinetics mechanism for urban and regional scale computer , *Journal of Geophysical Research* **94, D10:**12925–12956.

Langner, J., Bergstrom, R., and Pleijel, K., 1998, European scale modelling of sulfur, oxidized nitrogen and photochemical oxidants. Model development and evaluation for the 1994 growing season, SMHI report RMK No. 82. Swedish Met. And Hydrol. Inst., SE-601 76 Norrkoping, Sweden.

Roemer, M., Boersen, G., Builtjes, P., and Esser, P., 1996, The budget of ozone and precursors over Europe calculated with the LOTOS model, TNO publication P96/004, Apeldoorn, The Netherlands.

San José, R., Rodriguez, L., Moreno, J., Palacios, M., Sanz, M.A., and Delgado, M., 1994, Eulerian and photochemical over Madrid area in a mesoscale context, in: *Air Pollution II, Vol. 1, Computer Simulation, Computational Mechanics Publications,* Baldasano, Brebbia, Power and Zannetti., eds., pp. 209–217.

San José, R., Cortés, J., Moreno, J., Prieto, J.F., and González, R.M., 1996, Ozone over a large city by using a mesoscale Eulerian model: Madrid case study, in: *Development and Application of Computer Techniques to Environmental Studies, Computational Mechanics Publications*, Zannetti and Brebbia, eds., pp. 309–319.

Schmidt, H., Derognat, C., Vautard, R., and Beekmann, M., 2001, A comparison of simulated and observed ozone mixing ratios for the summer 1998 in Western Europe. *Atmospheric Environment* **35:**6277–6297.

Stockwell, W., Kirchner, F., Kuhn, M., and Seefeld, S., 1977, A new mechanism for regional atmospheric chemistry modelling. *J. Geophys. Res*. **102:**25847–25879.

INTEGRATED ASSESSMENT MODELLING: APPLICATIONS OF THE IMPACT PATHWAY METHODOLOGY

CLEMENS MENSINK*, LEO DE NOCKER, KOEN DE RIDDER
*VITO - Flemish Institute for Technological Research,
Boeretang 200, B-2400 Mol, Belgium*

Abstract. The impact pathway methodology integrates the input of different scientific disciplines within a consistent calculation framework as developed in the ExternE community. In this contribution, the methodology is used to evaluate the impact of two different land use development scenarios in terms of traffic flows, air quality, human exposure to air pollution and associated external costs. In the uncontrolled 'urban-sprawl' scenario, the urbanized area increases by almost 75%. For the 'satellite-city' scenario, where the urban development is controlled and directed to 5 five existing towns, the urban land use changes are increasing with 9%. A detailed analysis shows that the urban-sprawl scenario results in an exposure *reduction* of 5.7% due the movement of people from locations with high concentrations of particulate matter to locations with lower particulate matter concentrations. A reduction of 1.4% was found for the satellite-city scenario. The dominant driver of these exposure changes appears to be the population moving from the relatively polluted conurbation to less-polluted areas.

---

*To whom correspondence should be addressed. Clemens Mensink, VITO – Flemish Institute for Technological Research, Boeretang 200, B-2400 Mol, Belgium; e-mail: clemens.mensink@vito.be

1.   Introduction

Integrated assessment can be defined as an interdisciplinary process of combining, interpreting and communicating knowledge from diverse scientific disciplines in such a way that the whole cause-effect chain of a problem can be evaluated from a synoptic perspective with two characteristics: (i) it should have added value compared to single disciplinary assessment; and (ii) it should provide useful information to decision makers (Munn, 2002). In ambient air quality policies, one of the main concerns to policy makers is to know the possible impact of potential emission reduction strategies on pollutant concentrations. Tools that are needed to obtain this information, i.e. evaluating the impact of abatement strategies and mobility scenarios on particulates, ozone and other pollutants, must provide fast assessments at low computational costs. In this way a large number of scenarios can be evaluated.

Over the past years, we contributed to the development of an integrated assessment approach to evaluate the impact of emissions from energy use and road transport emissions on air quality on an urban and regional scale. The framework for this assessment is the impact pathway methodology. We discuss the principles and characteristics of the impact pathway methodology and the steps and tools that are involved in the methodology in section 2. The impact pathway method follows the fate of pollutants along the steps in the DPSIR chain: Drive (human activities), Pressure (emissions), State (air quality and exposure), Impact (health, economic) and Response (policy). The evaluation of environmental impacts is based on the accounting framework of the European ExternE project. Using the ExternE methodology, estimations of the environmental damage costs related to the impacts can be provided (Friedrich and Bickel, 2001). The calculation framework for external costs results from a series of European research projects, starting in 1991 and still ongoing for further development, extension and refinement.

In section 3 the methodology will be illustrated by an application in a policy context, with special attention to the impact of mobility scenarios on road transport emissions and air quality. The application focuses on the assessment of different land use development scenarios in terms of traffic flows, air quality and associated external costs for the German Ruhr area. This assessment was carried out within the EU Fifth Framework Programme research project BUGS (Benefits of Urban Green Spaces) (BUGS, 2004). The inter-related issues of urban sprawl, traffic congestion, noise, and air pollution are major socio-economic problems faced by most European cities. Road traffic, which is one of the most important sources of air pollution inside urbanised areas, is greatly determined by the distribution of population and working places inside and around the urban centre. Moreover, through their impact on surface properties such as

moisture availability, roughness, and albedo, cities also alter atmospheric turbulence and wind fields. Within BUGS, a methodology has been developed to assess and compare different land use development scenarios - in particular those related to urban sprawl - in terms of air quality (De Ridder et al., 2004).

Starting from an analysis of the existing socio-economic as well as the surface parameters, scenarios are created for which simulations are performed using a traffic flow model, a traffic emission model, and a regional air quality model. In the end, an economic evaluation of the various air pollution-related health impacts and damage costs is done by means of the ExternE-methodology. In the first scenario, an extreme case of urban sprawl is implemented in which the relative size of the urbanised area increases from 26 to 44%. Population and jobs are re-distributed accordingly. In the second scenario, the same amount of people and jobs are re-distributed in five satellite cities created from existing smaller towns around the central Ruhr area. Results for the two scenarios are presented and discussed in section 4.
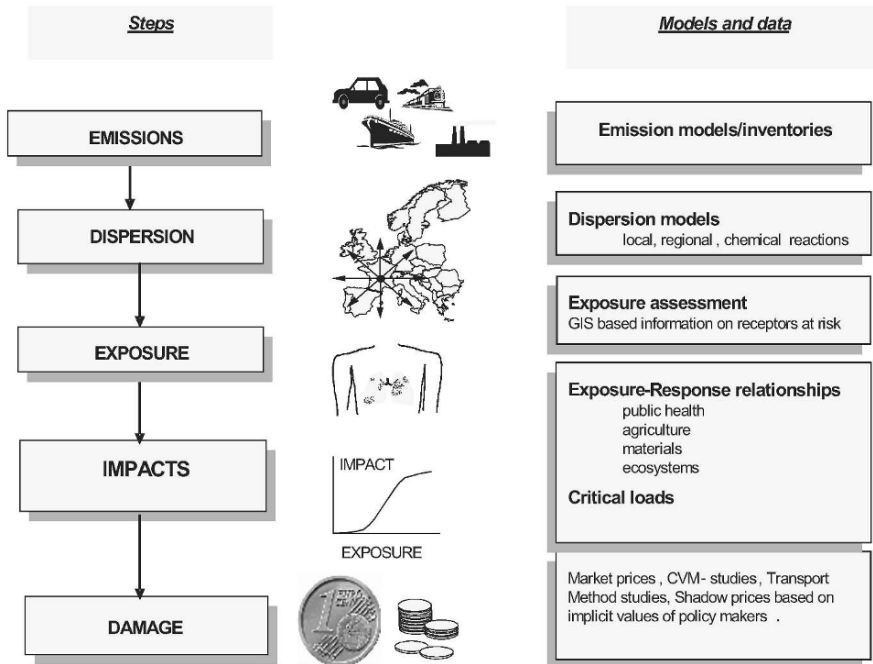
Figure 1. Presentation of the impact pathway methodology.

2. Methodology

The ExternE method for calculating external costs of energy and transport was developed between 1991 and 1995 within the European Commission's Joule Programme. Initially this method of calculation was confined to quantifying the external costs of electricity generation. In 1996-1997 this ExternE methodology was applied in all EU member states to the greatest diversity of energy carriers.

Within this framework VITO implemented this methodology for the external costs of the coal, gas and nuclear fuel cycle. Since 1996 the ExternE methodology has also been expanded to include transport.

TABLE 1. Effects and pollutants included in the impact pathway methodology.

Impact category	Pollutant	Effects included
Public health: mortality	PM SO_2, O_3 carcinogens	Reduced life-expectancy Acute mortality Fatal cancers
Public health: morbidity	PM PM, CO PM, SO_2 O_3 O_3 Carcinogens	Mild respiratory effects in asthmatics Chronic respiratory illness Restricted activity days (RAD's) Congestive heart failure in elderly Hospital admissions Asthma attacks, minor RAD's Non-fatal cancers
Materials	SO_2	Wearing of building materials (natural stone, limestone, sandstone, paint, zinc, rendering, mortar, galvanised steel)
Crops	SO_2, O_3 Acid deposition NO_x, SO_x	Yield change (potato, rice, rye, oats, tobacco, barley, wheat, sugar beet & sunflower) Increased liming of farmland Fertilising effects
Global warming	CO_2, N_2O CH_4	Health impacts, mortality, economic damages

The ExternE calculation framework is based on the '*impact pathway method*' (DPSIR chain) as illustrated in Figure 1. This method systematically maps the pathway running from an emission to damage to people, buildings, crops or ecosystems. In a first stage an inventory is made of all significant emissions and other direct impacts for all links in the fuel chain.

The second stage concerns the dispersion of chemical reactions from those pollutants on a local, regional or global scale. Then, based on exposure-effect relationships (or dose-response relationships), the effects of the increased concentrations of pollutants on health, buildings, crops and ecosystems (for example rise in illness phenomena or diminished yield of agricultural crops) is calculated. Table 1 shows the pathways (or end points) that are included in the methodology. Finally these impacts are valued in terms of money by reference to market prices or estimated values. This valuation is based on the 'willingness to pay' and can be estimated using methods from environmental economics (Contingent Valuation, Transport-ation cost method, shadow price calculations using implicit values of policy makers).

The impact pathway methodology integrates the input of different scientific disciplines within a consistent calculation framework. This detailed bottom-up approach makes it possible to calculate external costs for a specific technology and location. While this might make the method very data-intensive, it makes it appropriate for comparing different technologies, fuels, locations, etc. against each other. It allows a detailed cost-benefit analysis of policy measures. The calculation framework reflects the state-of-the-art in these disciplines, including the uncertainties.

In the European Union, ExternE is increasingly recognised as the authoritative reference for quantifying impacts from air pollution. It was used by the European Commission to prepare the air quality directives (European Community, 1996) and national emission ceilings, as well as various emission control strategies for transport and cars and an integrated product policy. This broad acceptance on the policy level underlines the success of the past ExternE activities, but at the same time requires the integration of new scientific findings into the existing framework to improve and maintain the high level of reliability and acceptance of this technology assessment tool. The methodology has continuously been improved, integrating various new scientific findings into the existing framework (e.g. the results of the 'ExternE Core/Transport' project, the current 'NewExt' project and the new 'ExternE-Pol project'). In addition, related projects like NEEDS, RECORDIT, UNITE, GREENSENSE, OMNIITOX and ECOSIT have developed new achievements. Furthermore teams have developed improvements and new approaches in various national projects.

3. Application

A series of numerical simulations was performed to evaluate the impact of two urban development scenarios on air quality and related human exposure, using the impact pathway methodology. Compact and polycentric

city forms are associated with minimal consumption of land and energy, and are often promoted as the more sustainable and hence preferred mode of urban development. The opposite type of urban development can be characterized as 'urban sprawl'. It results in a significant increase in built-up surface.
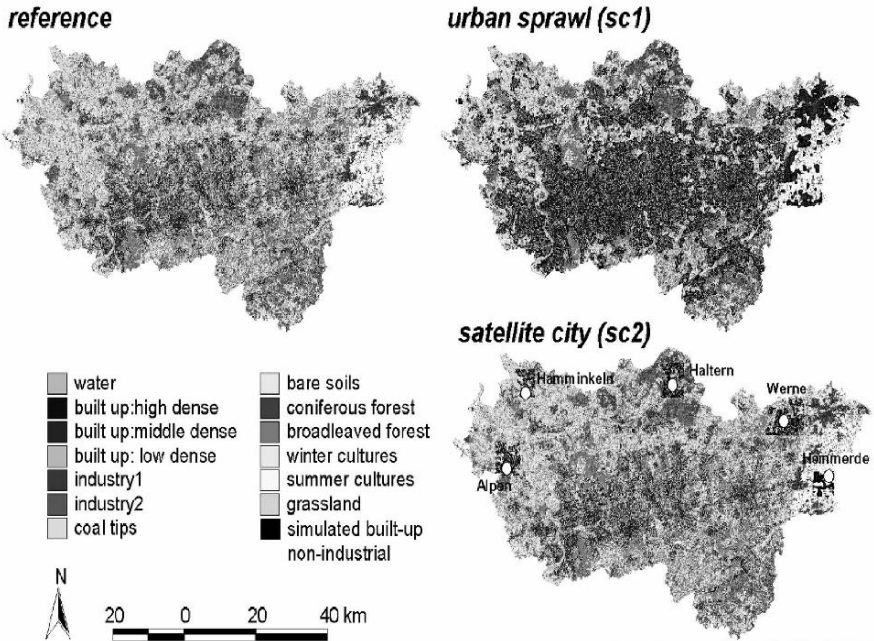
Figure 2. Land use categories of the reference state and the two scenarios. The dark band extending in the east-west direction in the central portion of the domain corresponds with the urbanised areas.

The 'urban sprawl' scenario (sc 1) supposes a continuation of the current process of people leaving the highly occupied central part of a city to settle in the greener surroundings. In a second scenario, referred to as 'satellite cities' (sc 2), persons and jobs were displaced to five existing towns located near the core of the urban area.

The area that was selected to study these two scenarios, consists of a highly urbanised region in the Ruhr area, located in the north-western part of Germany in central North Rhine-Westphalia with a total population in excess of 5.5 million. The choice for this particular area was mainly motivated by its size and importance, as well as its conversion potential.

Figure 2 shows the changes in land use for the two scenarios compared to the reference state. For the urban-sprawl situation (sc 1), the urbanised area in the study domain increases by almost 75%, hence land consumption is rather drastic. For the satellite-city scenario (sc 2), urban land use changes are much lower, around 9%. The resulting land use maps for each scenario were used to model the corresponding spatial distribution of people and jobs.

Models dealing with land use, traffic flows, and atmospheric dispersion were applied, first under conditions representative of the actual urbanised area, and subsequently for the two urban development scenarios. The impact of the scenarios with respect to air quality was evaluated, including an estimate of human exposure to air pollution and the associated external costs.

Traffic flow modelling was done with a traditional four-step methodology, which contains sub-models that deal with trip generation, trip distribution, mode choice and traffic assignment. Trip generation or travel demand models calculate, based on the spatial distribution of population, jobs, and activities, the amount of travel that a population will undertake, distinguishing between different zones and using information regarding their characteristics to determine the number of trips that will originate or end in each zone. The first step in the traffic modelling activities was the creation of a simplified network for the study domain, consisting of highways and other major roads.

The number of trips to and from each zone (i.e., the traffic volume) was calculated for a 24-hour period. For the reference situation, the number of car trips was calculated from the number of inhabitants and jobs as well as the average number of daily car trips per inhabitant or per job. As a next step, matrices were created containing the traffic volumes between zones in the area. This was done using a so-called gravity model, which calculates the number of trips between any two zones following the number of trips produced in each zone as well as the number of trips attracted to each zone, the probability of travel between two zones decreasing with their distance. Information regarding the traffic relations between individual zones was then used to calculate the traffic relations on individual road segments. To obtain realistic spatial distribution of traffic loads for the reference case, a calibration procedure was carried out using data from the most recent traffic census.

In order to simulate the effect of the scenarios on traffic volumes and their spatial distribution, the traffic origins and destinations for each zone were recalculated based on the changes in land use, number of inhabitants and number of jobs. The road network and the traffic zones were taken identical as for the reference state. The main result of the traffic simulations is that, owing mainly to the increased average travel distance to get from home to work, passenger car traffic increased by 17% for the urban-sprawl scenario, and by 15% for the satellite-city scenario.

The methodology to compute regional-scale air quality is based on computer simulations with the atmospheric dispersion model AURORA (Mensink et al., 2001), which receives relevant meteorological data from the Advanced Regional Prediction System (ARPS), a non-hydrostatic mesoscale atmospheric model developed at the University of Oklahoma (Xue et al., 2000, 2001). AURORA contains modules representing transport, and (photo-) chemistry, and has nesting capabilities. The chemistry module is the Carbon-Bond IV-model, which lumps together different chemical species into single components in order to reduce the computing-time. An advanced land surface scheme (De Ridder and Schayes, 1997) was incorporated in AURORA to account for the impact of land use changes on atmospheric circulations and pollutant dispersion. The surface scheme calculates the interactions between the land surface and the atmosphere, including the effects of vegetation and soils, on the surface energy balance, and was specifically adapted to better represent urban surfaces.

A three-week period, 1-20 May 2000, was selected to perform the simulations on. This period was characterized by the presence of a blocking anticyclone over southern Scandinavia, producing weak south-easterly winds, clear skies, and moderately high temperatures over the Ruhr area. The nice weather ended abruptly on the 17th, when a cold front swept over the area. Emissions from industry, shipping and building heating were obtained from the 'Landesumweltamt Nordrhein-Westfalen', the local environmental administration. Traffic-related emissions were calculated using the MIMOSA model (Mensink et al., 2000; Lewyckyj et al., 2004), which uses the COPPERT III methodology to calculate geographically and temporally distributed traffic emissions using traffic information (including fluxes of vehicles and their speeds) from the traffic flow model (see above). Apart from anthropogenic emissions, biogenic emissions from forests (isoprene) were also calculated. The simulations carried out here focused on ground-level ozone and fine particulate matter, both pollutants being recognised as having major effects on human health.

4. Results and discussion

Air quality simulations performed by means of the AURORA model were validated by comparing model results with available observations from two stations (Bottrop and Essen) in the area that measured ozone (see Figure 3). Even though the simulations overestimate the ozone peak concentrations rather systematically by up to a few ten percent, the diurnal cycle as well as the behaviour of the model over the entire three-week period is rather satisfactory, and well in line with results produced by models of this type.

In particular the difference of night time concentrations between the two locations, which is due to the titration effect (reduction of ozone by traffic-related NO emissions) caused by the more intensive traffic at Bottrop, is well captured by the model, meaning that the spatial distribution of traffic emissions as well as the chemical processes accounted for in the model perform correctly.
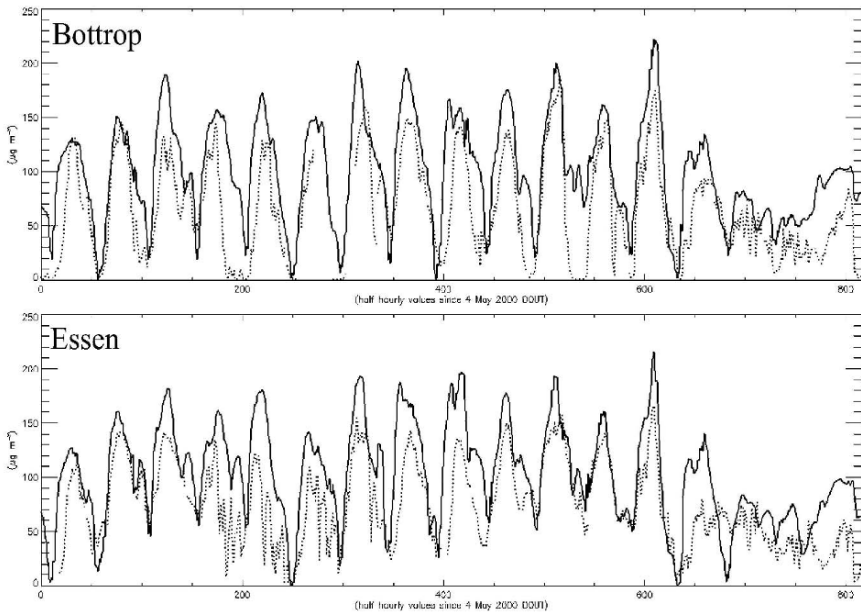
Figure 3. Simulated (solid line) as compared to observed (dotted line) ground-level ozone concentrations for the stations Bottrop (upper panel) and Essen (lower panel).

After the successful completion of the simulations for the reference case, the AURORA model was run on the urban-sprawl and satellite-city scenarios established previously, using the modified land use characteristics as well as the correspondingly modified traffic flows as inputs. The calculated pollutant emissions, largely traffic-related in this area, underwent increases of the same order as the increases of the traffic flows themselves.

The simulated change of ground-level ozone and of primary particulate matter is shown in Figure 4. With respect to ozone, the largest changes are seen to occur for the urban-sprawl scenario. Owing to the dominating south-easterly wind direction during this episode, an increased ozone plume is simulated north-west of the agglomeration. The titration effect,

on the other hand, slightly depresses ozone concentrations in the central portion of the domain, i.e., where the highest population densities occur. As a result, the average exposure to ozone pollutants (calculated as the average of the concentrations, spatially weighted with population density) remained almost unchanged – they increased by 0.3% – between the reference case and the urban-sprawl scenario (Figure 5). Also in the satellite-city scenario the changes are minimal (decrease by 0.45%), despite the increased domain-average emissions.
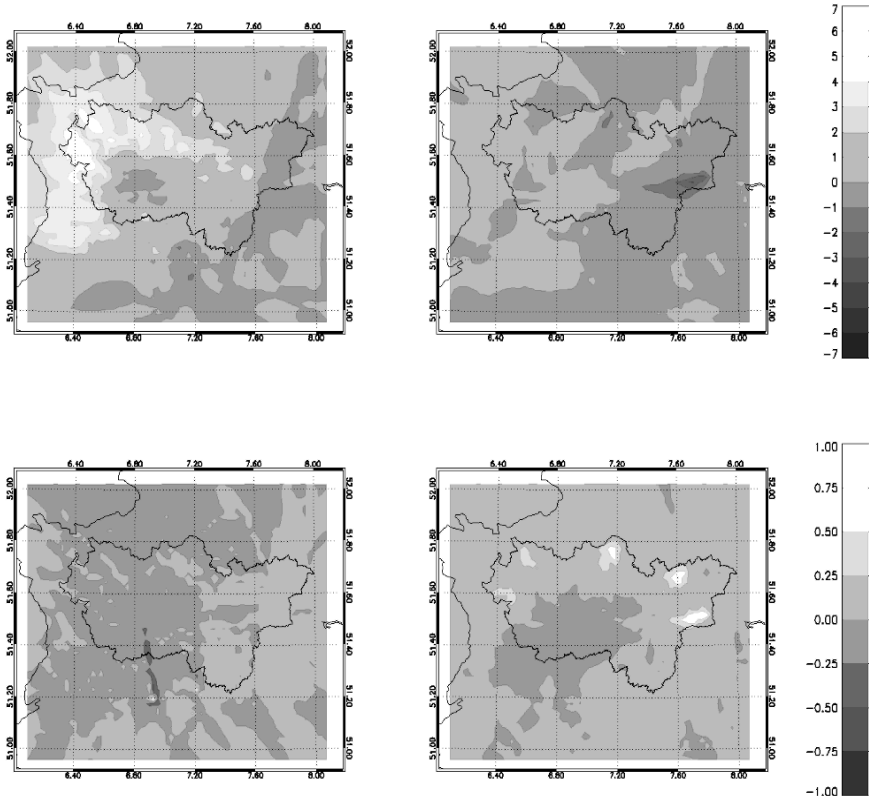
Figure 4. Concentration change (in µg/m³) of ozone (upper panels) and PM10 (lower panels) for scenario 1 (left panels) and scenario 2 (right panels). Positive values indicate an increase of the considered scenario compared to the reference situation.

With respect to fine particulate matter, the effect of the scenarios is perhaps not so clear (Figure 4). Whereas the satellite-city scenario clearly exhibits local spots of (a very modest) increase of this pollutant, the concentration patterns in the urban-sprawl case appear almost unaltered. A detailed analysis shows that there is a slight overall increase of

domain-average concentration. However, the effects on human exposure to this pollutant are not so straightforward: whereas one would intuitively associate increased emissions and the ensuing increased domain-average concentrations with increased human exposure values, the contrary is seen to occur. Indeed, a detailed analysis shows that the urban-sprawl scenario results in an exposure *reduction* of 5.7%, and a reduction of 1.4% for the satellite-city case (Figure 5). The dominant driver of these exposure changes appears to be the movement of people from locations with high to locations with lower particulate matter concentrations. Stated otherwise,
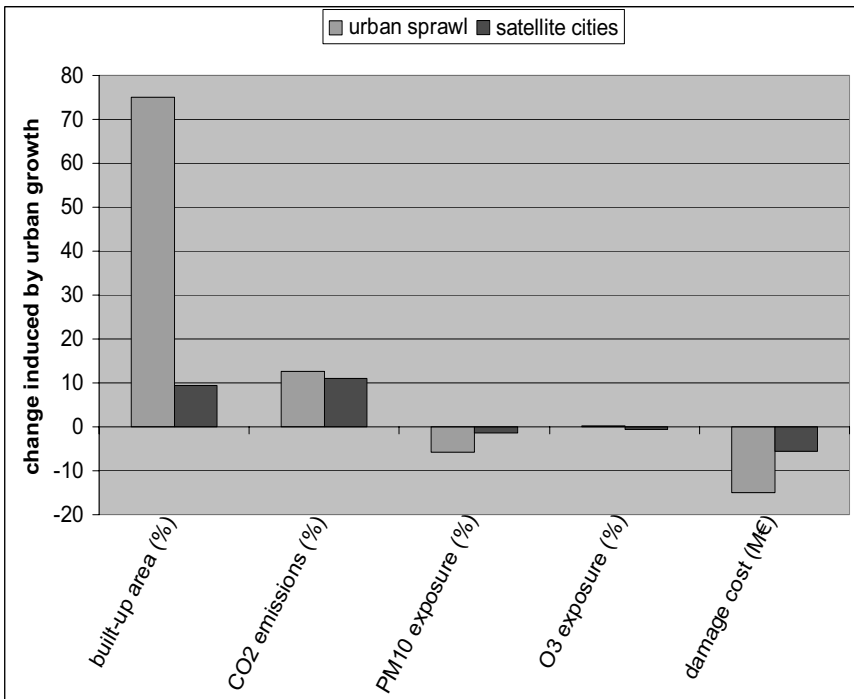
Figure 5. Overview of the changes induced by the urban-sprawl and satellite-city scenarios, for the indicators listed on the horizontal axis. All changes are expressed as a percentage increase compared to the reference case, except the damage cost, which is expressed in M€.

the global exposure decreases when a portion of the population moves from the relatively polluted conurbation to less-polluted areas.

The air pollution-related public health damage, together with changes in CO_2 emissions, were used for the calculation of the damage costs using the ExternE methodology (see also Table 1). The emissions in CO_2 increase in both scenarios, though slightly more so for the urban sprawl scenario, when compared to the reference state. This results in higher damage costs related to global change. The changes in damage costs of public health related to primary particulate matter and ground-level ozone are determined by the changes in exposure which reflect the combined effect of changes in concentrations and changes in population at a specific location in the study area. Because of the dominant effect of relocating people to less polluted areas, the urban development patterns presented in both scenarios result in a positive effect in the public health damage costs, especially for the urban sprawl scenario. In the calculation of the total damage costs, the effects of exposure changes to particulate matter were dominant, owing to the severe health impacts attributed to this pollutant. As a result, the total avoided damage costs range between 5.6 M€ and 15.0 M€ for, respectively, the satellite city scenario and the urban sprawl scenario when compared to the reference state (Figure 5).

5.   Conclusions

By using state of the art knowledge from a wide range of different sciences, the impact pathway methodology has always been in the forefront of quantifying impacts from air pollution. Expertise from ExternE has proven to be an important corner stone for other activities related to evaluation of air quality, energy and transport systems, policy measures in these fields and risk assessment in general. The conclusion that total externalities are dominated by the public health impacts from emissions of particulate matter, and the fact that particulate matter has become one of the priority pollutants in the EU air quality policies, led to the development of specific knowledge and methods to quantify the health impacts of air pollution in terms of costs for society and quality related health indicators.

The dominant role of particulate matter and health impacts is also shown in the application of the impact pathway method for two urban development scenarios, as discussed in this paper.

Compact and polycentric city forms are associated with minimal consumption of land and energy, hence they are often promoted as being the more sustainable and hence preferred mode of urban development. In this context, a series of numerical simulations was performed to evaluate the impact of two urban development scenarios – urban sprawl and the creation of satellite cities – on air quality and related human exposure.

Working on a highly urbanised area in the German Ruhr area, models dealing with satellite data processing (to map land use and relevant socio-economic indicators), traffic flows, pollutant emission and their dispersion in the atmosphere were applied, under conditions representative of the urbanised area as it is today.

Urban sprawl and satellite-city scenarios were defined and implemented using spatial modelling techniques. The resulting updated maps of the area were then used as input for the traffic and atmospheric dispersion simulations, which showed that total traffic kilometres and associated emissions increased by up to almost 17%. As a consequence, the domain-average pollutant concentrations also increased, though by a smaller amount.

However, despite these global concentration increases, an analysis of human exposure to atmospheric pollution revealed that both scenarios considered here lead to *lower* rather than higher exposure values. While not contesting the evident advantages of compact or polycentric cities with respect to a host of sustainability indicators, these results indicate that compact/polycentric cities may also induce adverse effects, which should be taken into account by policy makers when making choices regarding urban development scenarios.

References

BUGS ,2004, http://www.vito.be/bugs/

De Ridder, K., Lefebre, F., Bañuelos, A., Pérez-Lacorzana, J.M., Dufek, J., Adamec, V., Damsgaard, O., Thierry, A., Bruse, M., Bürger, M., Weber, C. and Hirsch, J., 2004, An integrated methodology to assess the benefits of urban green space, *Science of the Total Environment*, **334–335**: 489–497.

De Ridder, K., and Schayes, G., 1997, The IAGL land surface model, *Journal of Applied Meteorology*, **36**: 167–182.

European Community, 1996, Council Directive 96/62/EC of 27 September 1996 on ambient air quality assessment and management, *Official Journal of the EC,* L 296, 21/11/1996, pp. 55–63.

Friedrich, R. and Bickel, P. (ed.), 2001, *Environmental External Costs of Transport*, Springer Verlag, Heidelberg.

Lewyckyj, N., Colles, A., Janssen, L. and Mensink, C., 2004, MIMOSA: a road emission model using average speeds from a multi-modal traffic flow model, **in:** R. Friedrich and S. Reis (Eds.): *Emissions of air pollutants, Measurements, Calculations and Uncertainties*, pp. 299–304, Springer Verlag, Berlin, Heidelberg, New York.

Mensink C., K. De Ridder, N. Lewyckyj, L. Delobbe, L. Janssen, P. Van Haver, 2001, Computational aspects of air quality modelling in urban regions using an optimal resolution approach (AURORA). *Large-scale scientific computing – lecture notes in computer science*, **2179**: 299–308.

Mensink, C., De Vlieger, I. and Nys, J., 2000, An urban transport emission model for the Antwerp area, *Atmospheric Environment*, **34**: 4595–4602.

Munn, T., 2002, *Encyclopedia of Global Environmental Change*.

Xue, M., Droegemeier, K.K. and Wong, V., 2000, The Advanced Regional Prediction System (ARPS) - A multiscale nonhydrostatic atmospheric simulation and prediction tool. Part I: Model dynamics and verification. *Meteorology and Atmopheric Physics*, **75**: 161–193.

Xue, M., Droegemeier, K.K., Wong, V., Shapiro, A., Brewster, K., Carr, F., Weber, D., Liu, Y. and Wang, D.-H., 2001, The Advanced Regional Prediction System (ARPS) - A multiscale nonhydrostatic atmospheric simulation and prediction tool. Part II: Model physics and applications. *Meteorology and Atmopheric Physics*, **76**: 134–165.

ADVANCED AIR POLLUTION MODELS AND THEIR APPLICATION TO RISK AND IMPACT ASSESSMENT

ADOLF EBEL*, MICHAEL MEMMESHEIMER,
HERMANN J. JAKOBS, HENDRIK FELDMANN
*Rhenish Institute for Environmental Research at the
University of Cologne (RIU), Aachener Str. 209, 50931
Cologne (Koeln), Germany*

Abstract. A large number of risks, with which society is confronted at present and will even more be exposed to in the course of future industrial development and growth of agricultural activity due to increasing population worldwide, is caused by anthropogenic emissions of primary air pollutants and precursors of secondary ones. Numerical model systems simulating chemistry and transport of minor constituents in the atmosphere have been developed which have mainly been used for air quality analysis in the past and are now more and more converted to forecast tools for the atmospheric environment. Such air quality (AQ) models have the potential to be applied with fast response to emergency cases like chemical or power plant accidents. Comprehensive assessment of risks and possible impacts can be carried out and used for mitigation or prevention of hazardous impacts. Requirements for the design of advanced AQ models for the treatment of such problems are discussed and some examples demonstrating the spectrum of possible applications are presented. Necessary steps for future improvements of model design and performance are briefly mentioned.

Keywords: air pollution; air quality; chemistry transport model; CTM; emergency modelling; response time; meteorology; forecast; troposphere; anthropogenic emission; oil fields; Chernobyl; evaluation

*To whom correspondence should be addressed. Adolf Ebel, RIU/University of Cologne, Aachener Str. 209, 50931 Cologne, Germany; e-mail: eb@eurad.uni-koeln.de

83

1. Introduction

Numerical chemistry transport models (CTMs) for the atmosphere are an indispensable tool for assessing risks and impacts of air pollution. Risks originate from a multitude of anthropogenic activities and natural causes. They may considerably differ in temporal and spatial scales. Sources of emissions leading to harmful impacts exhibit a wide range of physical and chemical characteristics. For instance, sudden events at certain points or narrow locations – like explosions in a factory or volcanic eruptions – require a treatment quite different from that of a hazardous smog episode in a larger region. Furthermore, short-term effects in the vicinity of a point source after an accident like the spread of clouds containing harmful gases call for another modelling strategy than long-term impacts, e.g. through the growth of the dose of a pollutant leading to the deterioration of ecosystems.

It is obvious that the broad spectrum of atmospheric phenomena and processes involved in hazardous events cannot be treated in a single model but needs a hierarchy of models to cover all aspects which should be taken into account for risk and impact assessment pertaining to the atmospheric environment.

Gaussian type dispersion models have proven to be a convenient tool for fast response calculations regarding the assessment of impacts in the close vicinity of a source in the case of accidents which can be described by abruptly increased point source emissions. They may also be used for statistical assessment of possible impacts around locations where a risk of emission accidents exists. Such numerical approaches and their application as emergency models and control tools have widely been discussed in the literature. They consist of fast and computationally less demanding algorithms. Yet the focus of this paper is put on a different type of models, namely three-dimensional time dependent chemical transport models of Eulerian or Lagrangian type. Such models allow a more rigorous and comprehensive treatment of the complex system of processes which have to be taken into account for reliable air pollution risk and impact assessment.

2. Principle features of advanced air quality models for risk and impact assessment

In this section we try to identify the most essential properties to be exhibited by models which are intended to be applied to risk and impact assessment as well as the treatment of emergency cases. It is helpful to analyse actual events which happened in the past and have been investigated with the help of three-dimensional numerical models.

The nuclear reactor accident in Chernobyl represents an illuminating case in this context. A simulation of the spread of the radioactive cloud has been carried out by Hass et al., (1990) among others. Observations of the cloud were used to test the performance of atmospheric transport models in an **A**tmospheric **T**ransport **E**valuation **S**tudy (ATMES, Klug et al., 1992). A controlled transport and modeling experiment was carried out in the framework of the **E**uropean **T**racer **Ex**periment (ETEX, Girardi et al., 1998). The studies of the Chernobyl accident showed that knowledge of modifications of exhaust characteristics, in particular exhaust height, by meteorological conditions was essential not only for far field estimates but also for near source simulations. This requires realistic treatment of the free troposphere. Also impacts of area sources caused, for instance, by forest, bush and bog fires or by burning oil fields (as it happened during the Gulf wars or as they may occur any time in Iraq and elsewhere due to terrorist action; see Section 3 and Fig. 1) can only reliably be treated when transport and chemistry of the free troposphere is well represented in the applied model. In specific cases it may even be necessary to extend the model up to lower stratospheric levels, e.g. when impacts resulting from intercontinental transport of pollutants are considered (Stohl and Trickl, 1999).

Besides the possibility to include the free troposphere in various degrees of perfection, three-dimensional numerical AQ models offer a large flexibility regarding their adjustment to reliable treatment of specific risk and impact problems. For defining specific properties of specialized models for this purpose it is convenient to classify them with respect to their design for near source and small-scale applications and meso- (regional) to large-scale (hemispheric and global) simulations. Essential requirements and characteristics of models designed for small-scale applications are
in case of an emergency:

- Immediate response to alerts (implies constraints for the degree of complexity of the model due to minimizing the compute time)
- Meteorology: nowcasting
- High horizontal resolution
- Vertical extension may be reduced depending on intended application (only atmospheric boundary layer or up to middle troposphere)
- Without chemistry or with highly simplified chemical mechanism
- Small scale dynamical and transport processes well represented, particularly in the ABL
- Detailed orography and land use formulation
- Source parameters as accurate as possible

in case of (statistical) risk analysis:

- Fast response not essential, therefore
- Explicit calculations and thus higher complexity possible
- Meteorology from analyses or simulations of past periods
- Inclusion of relevant processes in the free troposphere
- Extended chemical mechanism
- Other features as for emergency applications

As regards the treatment of meso- and large-scale impacts the models should fulfil the following conditions if applied
in case of an emergency:

- Response time as short as possible regarding, in particular, regional impacts
- Meteorology: regional to global forecasts
- Adaptation of resolution to regions of increasing seize around the location of accident (nesting, dynamical grids)
- Inclusion of the free troposphere
- Full chemistry, adjusted to composition of accidental release
- Suitable parameterization of subgrid processes in the ABL (e.g. turbulent transport) and free troposphere (e.g. clouds, rain)
- Orography and land use parameters according to the resolution of the model
- Source parameters as accurate as possible

In case of risk assessment and impact analyses on larger scales the main restriction to the complexity of model applications is given by the limitation of available computer resources. Rather complex advanced model systems are available at several places for detailed and long-term risk and impact simulations. Of course, calculations with increased complexity are also possible for risk and impact studies with small-scale and local models since no time limit is set by fast response requirements.

3.   Available advanced models

Among the many existing air quality model systems only those are suitable for emergency and risk analysis which are able to provide or use meteorological forecasts. Impact analyses are possible with past

meteorological analyses. It is not intended to provide a comprehensive overview of suitable models in this article. Only a few hints are given here where the interested reader will find information which will lead him to relevant publications or internet addresses.

Krueger (2000) has compiled a list of European chemical forecast activities. A selection of models mentioned in the list (EM, EURAD, EUROS, LOTOS, MATCH, REM3/CALGRID) has been compared in an aerosol simulation study by Hass et al., (2003). Prediction skills of several European ozone forecast models have been investigated by Tilmes et al., (2002). Russell and Dennis (2000) reviewed several American and European models applied to historical case studies, but capable to be run in the forecast mode. Syrakov et al., (2003) describe a Bulgarian Emergency Response System (BERS) which is using an inert tracer approach. American initiatives to carry out numerical air quality prediction started in Canada (Pudykiewicz et al., 1997, 2003). New real-time Eulerian photochemical numerical forecast systems are under development in the USA (McHenry et al., 2004, Vaughan et al., 2004).

4. Applications

4.1. MODEL USED FOR DEMEONSTRATION (EURAD)

Numerical emergency and risk studies have usually been carried out in a retrospective approach to demonstrate that air quality models are able to handle hazardous events. Model preparedness for possible occurrence of such events in a given region, say Europe or a part of it, needs considerable advance investments for the generation of adequate data sets allowing realistic simulation of actual emergency situations resulting, in particular, from industrial activities. Industrial and military data protection may form a barrier difficult to overcome by modelling institutions or groups trying to develop publicly available model systems for environmental and societal security.

Some examples are selected to illustrate the applicableness of advanced models to risk and impact assessment problems. They are chosen from simulations with a model system which has been developed and employed by the authors, namely the **Eur**opean **A**ir Quality **D**ispersion model system (EURAD; Ebel, 2002; Ebel et al., 2004). It consists of a chemical transport model (EURAD CTM2; Hass, 1991), the **M**eso-scale **M**eteorological Model, Version **5** (MM5; Grell et al., 1993) and the **E**URAD**E**mission **M**odel (EEM, Memmesheimer et al., 1991). EMM provides gridded hourly emission data as input to the CTM.

In its basic version EURAD covers the major part of Europe with coarse resolution. The method of sequential nesting is used (Jakobs et al., 1995) to simulate the atmospheric composition in smaller domains. Meteorological

initial and boundary conditions are obtained for the coarse resolution version from ECMWF or NMC analyses. Emission input data have been derived from available European and regional inventories (EMEP, GENEMIS or regional emission data sets, depending on the details of air quality simulations). Recently, a hemispheric version of the system has been developed. Nested calculations are usually carried out with resolution of 125 km (so-called coarse grid), 25 km (nest 1) and 5 km (nest 2). For special applications to local problems a resolution of 1 km may be employed. It may be combined with a higher resolving model with meteorological parameterizations adapted to finer grid calculations (Brücher et al., 2000). The standard model version has 23 layers between the surface and 100 hPa, where 15 are found below an altitude of 3000 m. The height of the lowest layer is about 40 m. The chemical mechanism usually applied in CTM2 is either RADM2 with 63 gas phase species (Stockwell et al., 1990) or RACM (77 species, Stockwell et al., 1997). The latter one is used when secondary organic aerosols are included in the simulations. The aerosol module attached to the CTM is MADOC (**M**odal **A**erosol **D**ynamic Model with **O**rganic Components and **C**louds) consisting of a modal aerosol dynamic mechanism with inorganic chemistry (Ackermann et al., 1998; Binkowski and Roselle, 2003), a cloud-aerosol interaction module (Friese et al., 2000) and a **S**econdary **O**rganic **A**erosol **M**odule (SORGAM; Schell et al., 2001). The CTM calculates hourly concentrations of ozone and other gaseous pollutants and various aerosol parameters (PM_{10}, $PM_{2.5}$, composition of the organic and inorganic fractions of suspended particles).

4.2. EXAMPLES OF APPLICATIONS

In Section 2 we mentioned the simulation of the spread of the radioactive cloud after the nuclear reactor accident in Chernobyl as an example. It was a challenging case for the application of pure transport and chemical transport models like EURAD still years after the accident occurred since it allowed comprehensive evaluation of impact assessments based on numerical simulations. As one of the outcomes, the sensitivity of the assessment of (radioactive) impacts to the parameterization of subgrid processes controlling convection and precipitation became clearly evident.

The aerosol cloud exhibited in Fig. 1 was simulated in the framework of a precautionary study of risks resulting from possible attacks on oil fields in Iraq. Depending on the meteorological situation and the duration of fires such events may lead to serious health effects which could be mitigated by early warning using the model prediction of the spreading aerosol cloud. This application also demonstrated the benefit of system flexibility with respect to quick changes of the model domain.
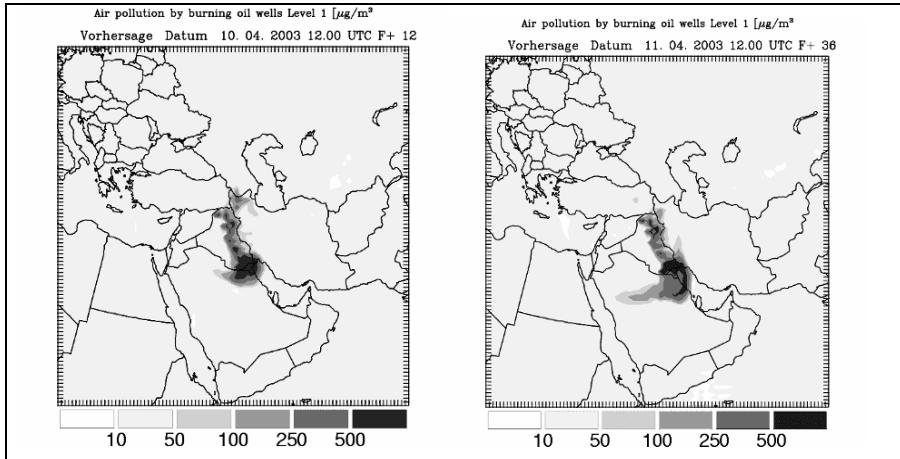
Figure 1. Forecast of dispersion of hypothetical oil fire emissions in Iraq using the meteorology of April 10 and 11, 2003. Aerosol is chosen as a tracer. Left panel: 12 hours after the start of the fire. Right panel: 36 hours after the start. Low level emissions assumed.

In contrast to sudden hazardous events like the power plant explosion in Chernobyl represented by a point source in numerical models there are numerous area sources with low but long lasting emissions (e.g. waste disposal sites, animal husbandry) imposing high doses of tormenting or harmful substances on the neighbouring population. One can assess the possible impacts of exposure to such substances by simulating transport and chemistry with reduced and/or elevated emissions. Figure 2 shows the result of a simulation demonstrating the reduced impact of ammonia emissions on the surroundings of an area source whose strength is cut by 50%. The calculations were performed using the nesting option of EURAD. Such studies have also been carried out for other substances, among them aerosols, on different spatial and temporal scales (Ebel et al., 2005).

5. Conclusions

The reliability of models applied to risk and impact assessment needs systematic control through regular evaluation. It is common to use data from operational ground stations, e.g. of the European EMEP or national networks, for checking the performance air quality models. It is important to extend the evaluation, which is usually restricted to surface conditions,

to higher levels as it has occasionally been done with airborne observations from field campaigns or satellite measurements. As an example, the performance of EURAD model system in the upper atmospheric boundary layer was evaluated together with other models employing air craft measurements (Schaller et al., 2001) from the BERLIOZ field campaign (Becker et al., 2002).
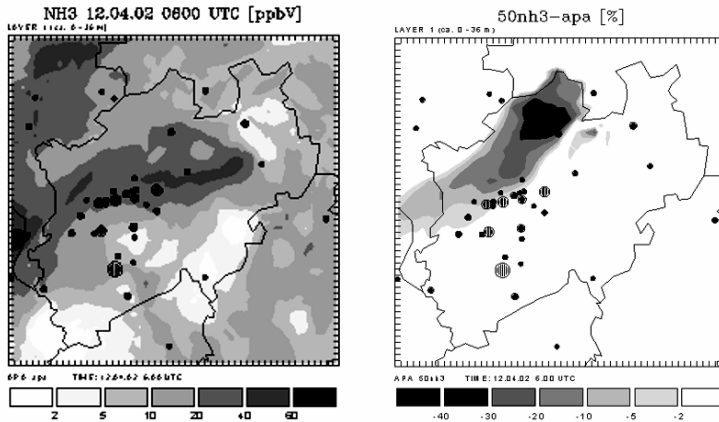
Figure 2. Assessment of the impact of NH_3 emissions for a day in April 2002 assuming a reduction of 50% of normal source strength in a small area located at the northern boundary of the model domain (state North-Rhine Westfalia). Nested calculation with the EURAD model system. Left panel: NH_3 mixing ratio, basic emission scenario. Right panel: Decrease of mixing ratio after emission reduction.

A practical and realistic approach to a large-scale (continental-wide) atmospheric emergency warning system would be the formation of a network of local and smaller meso-scale models with fast response capabilities for near field risk and impact assessment, embedded in one or several larger regional models for the estimation of far field effects. This requires homogenization of model input and output data among participating institutions and, of course, high and safe transmission capacities for efficient data exchange.

Since strong interrelationships exist between hazardous impacts on soil as well as open and ground water it is desirable that more comprehensive interfaces between models of anthropogenic impacts on the earth system compartments atmosphere, hydro/cryosphere, geosphere and biosphere will be designed now and that algorithms will be developed in future which allow treating these environmental regimes in a single model interactively.

References

Ackermann, I.J., Hass, H., Memmesheimer, M ., Ebel, A., Binkowski, F.B., and Shankar, U., 1998, Modal Aerosol dynamics model for Europe: Development and first applications. *Atmos. Environm*. **32:**2891–2999.

Becker, A., Scherer, B., Memmesheimer, M., and Geiss, H., 2002, Studying the city plume of Berlin on 20 July 1998 with three different modelling approaches*, J. Atmos. Chem.* **42:**41–70.

Binkowski, F.S., and Roselle, S.J., 2003, Models-3 Community Multiscale Air Quality (CMAQ) model aerosol component, 1. Model description, *J. Geophys. Res*. **108:** NO. D6, 4183, doi:10.129/2001JD001409.

Brücher, W., Kessler, C., Kerschgens, M.J., and Ebel, A., 2000, Simulation of traffic induced air pollution on regional to local scales. *Atmos. Environ*. **34:** 4675–4681.

Ebel, A., 2002, Changing atmospheric environment, changing views – and an air quality model's response on the regional scale, in: *Air Pollution Modeling and its Application XV,* C. Borrego and G. Schayes, eds., Kluwer Academic/Plenum Publ., New York, pp. 25–36.

Ebel, A., Memmesheimer, M., Friese, E., Jakobs, H.J., Feldmann, H., Kessler, C., and Piekorz, G., 2004, Analysis of seasonal changes of atmospheric aerosols on different scales in Europe using sequentially nested simulations, in: *Proceedings of the 27th NATO/CCMS ITM on Air Pollution Modelling and its Application,* Banff, Canada, 25–29 Oct. 2004, in print.

Ebel, A., Memmesheimer, M., Friese, E., Jakobs, H.J., Feldmann, H., Kessler, C., and Piekorz, G., 2005, Long-term Atmospheric Aerosol Simulations - Computational and Theoretical Challenges, in: *Proceedings of the 5th Internat. Conf. on Large-Scale Scientific Computations,* Sozopol, Bulgaria, 6–10 June 2005, in print.

Friese, E., Memmesheimer, M., Ackermann, I.J., Hass, H., Ebel, A., and Kerschgens, M.J., 2000, A study of aerosol/cloud interactions with a comprehensive air quality model, *J. Aerosol Sci.* **31:** Suppl 1, 54–55.

Girardi, F., Graziani, G., van Velzen, D., Galmarini, S., Mosca, S., Bianconi, R., Bellasio, R., Klug, W., and Fraser, G., eds., 1998, *ETEX, The European Tracer Experiment*, Joint Research Centre, European Commission, Italy.

Grell, A.G., Dudhia, J., and Stauffer, D.R., 1993, *A description of the fifth-generation PennState/NCAR Mesoscale Model (MM5),* NCAR Techn. Note, NCAR/TN-398+1A.

Hass, H., Memmesheimer, M., Geiss, H., Jakobs, H.J., Laube, M., and Ebel, A., 1990, Simulation of the Chernobyl radioactive cloud over Europe using the EURAD model*, Atmos. Environ.* **24A:**673–692.

Hass, H., 1991, *Description of the EURAD Chemistry Transport Model, version 2 (CTM2),* Mitteil. Inst. Geophys. Meteor., Universitaet zu Koeln, no. 83.

Hass, H., van Loon, M., Kessler, C., Stern, R., Matthijsen, J., Sauter, F., Zlatev, Z., Langner, J., Foltescu, V., and Schaap, M., 2003*, Aersolsol modelling: results and intervomparison from European regional-scale modelling systems,* EUROTRAC-2 ISS, Munich.

Jakobs, H.J., Feldmann, H., Hass, H., and Memmesheimer, M., 1995, The use of nested models for air pollution studies: an application of the EURAD model to a SANA episode, *J. Appl. Met.* **34:**1301–1319.

Klug, W., G. Graziani, G. Grippa, D. Pierce, and C. Tassone, eds., 1992, *Evaluation of long range atmospheric transport models using environmental radioactivity data from the Chernobyl accident. The ATMES Report*, Elsevier Science Publishers, Linton Rd., Essex, England.

Krueger, B., 2000, Bernd Krueger's link list. Tropospheric ozone forecasts; http://homepage.boku.ac.at/krueger/ozontrop.htm.

McHenry, J.N., Ryan, W.F., Seaman, N.L., Coats jr., C.J., Pudikiewicz, J., Arunachalam, S., and Vukovich, J.M., 2004, A real time Eulerian photochemical model forecast system, *Bull. Americ. Met. Soc.* **85:** 525–548.

Memmesheimer, M., Tippke, J., Ebel, A., Hass, H., Jakobs, H.J., and Laube, M., 1991, On the use of EMEP emission inventories for European scale air pollution modelling with the EURAD model, in: *EMEP Workshop on Photo-oxidant Modelling for Long-Range Transport in Relation to Abatement Strategies*, Berlin, April 1991, pp. 307–324.

Pudykiewicz, J., Kallaur, A., and Smolarkiewicz, P.K., 1997, Semi-Lagrangian modeling of tropospheric ozone, *Tellus* **49B:**231–248.

Pudykiewicz, J., et al., 2003, Operational air quality forecasting in Canada: Numerical-model-guidance for ground-level ozone and particulate matter, http://ams.confex.com/ams/ annual2003/techprogram/paper_54490.htm

Russel, A., and Dennis, R., 2000, NASTRO critical review of photochemical models and modeling, Atmos. Environm. **34:**2283–2324.

Schaller, E., Schlünzen, K.H., and Ebel, A., 2001, Evaluierungsstrategien für Chemie-Transport-Modelle*, Promet* **27, 1/2:**17–30.

Schell, B., Ackermann, I.J., Hass, H., Binkowski, F.S., and Ebel, A., 2001, Modeling the formation of secondary organic aerosol within a comprehensive air quality modeling system*. J. Geophys. Res*. **106:**28275–28293.

Stockwell, W.R., Middleton, P., and Chang, J.S., 1990, The second generation regional acid deposition model chemical mechanism for regional air quality modelling, *J. Geoph. Res.* **95:**16343–16367.

Stockwell, W.R., Kirchner, F., and Kuhn, M., 1997, A new mechanism for regional atmospheric chemistry modeling. *J. Geophys. Res.* **102:**25847–25879.

Stohl, A., and Trickl, T., 1999, A textbook example of long-range transport: Simultaneous observation of ozone maxima of stratospheric and North American origin in the free troposphere over Europe, *J. Geophys. Res.* **104:**30445–30462.

Syrakov, D., Prodanova, M., and Slavov, K., 2003, Description and performance of Bulgarian emergency response system in case of nuclear accident (BERS), Intern. J. Environm. Poll. **20:**283–296.

Tilmes, S., J. Brandt, F. Flatoy, R. Bergström, J. Flemming, J. Langner, J.H. Christensen, L.M. Frohn, O. Hov, I. Jacobsen, E. Reimer, R. Stern, and J. Zimmermann, 2002, Comparison of five Eulerian Air Pollution Forecasting Systems for the summer of 1999 using the German ozone monitoring data, *J. Atmos. Chem.* **42:** 91–121.

Vaughan, J., Lamb, B., Frei, C., Wilson, R., Bowman, C., Figueroa-Kaminsky, C., Otterson, S., Boyer, M., Mass, C., Albright, M., Koenig, J., Collingwood, A., Gilroy, M., and Maykut, N., 2004, A numerical daily air quality forecast system for the Pacific Northwest, *Bull. Americ. Met. Soc.* **85:** 549–561.

DISPERSION MODELLING OF ATMOSPHERIC CONTAMINANTS RESULTING FROM TERRORIST ATTACKS AND ACCIDENTAL RELEASES IN URBAN AREAS

ANA MARGARIDA COSTA[*], ANA ISABEL MIRANDA,
CARLOS BORREGO

*CESAM, Department of Environment and Planning,
University of Aveiro, 3810 Aveiro (Portugal)*

Abstract. After the September 11th, 2001, it has become clear that a new type of event can also trigger the need for rapid response and exposure, environmental and human health impact analysis. The use of specific numerical tools, such as computational fluid dynamic (CFD) models, combined with exposure studies can contribute to the simulation of the effect of a terrorist attack on local air quality and on human health, in an urban area. The main objective of this study is the development of an exposure module to chemical agents and its integration in the CFD model VADIS, in order to estimate the cumulative exposure and the number of persons exposed above specific limit values of Sulphur Mustard HD agent. The improved numerical model was applied to a selected case study in the Lisbon urban area, in order to determine the effects on the population, as a result of a terrorist attack scenario with chemical agent Sulphur Mustard HD. The number of inhabitants exposed to HD agent concentrations above 100 mg.min.m^{-3}, capable of causing the first noticeable effects, above the medium incapacitating dosage (ICt50) of

‾‾‾‾‾‾
  * To whom correspondence should be addressed. Ana Margarida Costa, Department of Environment and Planning, Campus Universitário de Santiago, Universidade de Aveiro, 3810-193 Aveiro, Portugal; e-mail: anamarg@dao.ua.pt

150 mg.min.m^{-3} and the lethal concentration LCt50 of 15000 mg.min.m^{-3} were determined.

1. Introduction

Emergency response protocols have always been associated with natural disasters, industrial accidents, war situations, and other events, but these were rarely considered for deliberate acts of terror against an unsuspecting public. After the September 11th, 2001, it has become clear that a new type of event can also trigger the need for rapid response and exposure, environmental and human health impact analysis.

Chemical and Biological (C/B) weapons, previously considered to be of interest mainly to military planners, are now a topic of public and institutional interest (Kadlec et al., 1997). Potential effects of a C/B terrorist event vary widely, depending on the agent used, the effectiveness of its dissemination, the target struck, and the public reaction to the event. These agents can be divided into three categories: biological agents, biological toxins and chemical agents (Raber et al., 2001).

One of the chemical agents with possible usage in case of a terrorist attack is Sulphur Mustard Agent HD. This gas was first developed in the 19th century and introduced as chemical warfare agent in 1917 during World War I. Exposure to this gas by inhalation and/or skin contact produces several symptoms, such as, blisters on the skin and airway damage, or even death, with no specific treatment available. The duration of exposure will regulate the gravity of the effects (Shea and Gottron, 2004).

The use of CFD (Computational Fluid Dynamics) models with the capability to simulate the atmospheric transport of contaminants and the population exposure, in urban areas, can allow emergency management, law enforcement and action planning and training to respond to potential terrorist attacks and accidents involving toxic industrial chemicals.

Since people spend most of their time indoors, and in different indoor places depending on their age and activity, it is essential to evaluate the concentration of the C/B agent not only in open air, but also in different indoor locations, defined as microenvironments (Borrego et al., 2004a).

The main objective of this study is the development of an exposure module to chemical agents and its integration in the CFD model VADIS, in order to estimate the cumulative exposure and the number of persons

exposed above specific limit values of Sulphur Mustard HD agent. The numerical system was applied to a selected case study in the Lisbon urban area, in order to determine the effects on the population, as a result of a terrorist attack scenario with chemical agent Sulphur Mustard HD. The number of inhabitants exposed to HD concentrations above 100 mg.min.m^{-3}, capable of causing the first noticeable effects, above the medium incapacitating dosage (ICt_{50}=150 mg.min.m^{-3}) and lethal concentration (LCt_{50}=15000 mg.min.m^{-3}) were determined.

2.   Methodology

An exposure module to chemical agents was developed and included in VADIS CFD model taking into account information on modelled concentrations of the chemical agent on the ambient air, population data and the definition of microenvironments (Figure 1).
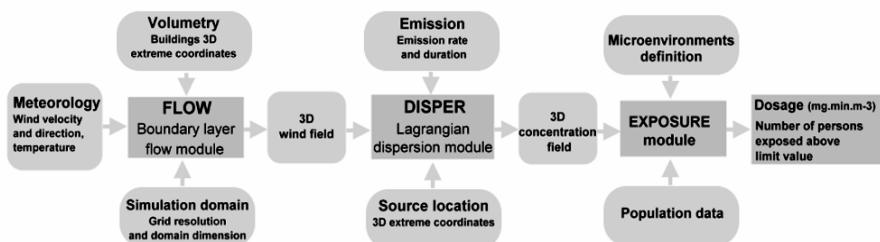
Figure 1. Schematic representation of VADIS model, including the input and output data of FLOW, DISPER and EXPOSURE modules.

2.1. VADIS CFD MODEL

VADIS is a CFD model, developed at the University of Aveiro, that allows the evaluation of flow and pollutants dispersion fields in urban geometries due to volume, area and point sources. Its structure is based in a FLOW module for the estimation of 3D meteorological fields, and a DISPER module for the determination of 3D pollutant concentration fields (Borrego et al., 2004b). Figure 1 presents the input and output data of FLOW and DISPER modules.

The model has been validated with wind tunnel measurements and more recently, was applied to the Lisbon downtown area, demonstrating a good performance in the calculation of flow and dispersion around obstacles under variable wind conditions when compared with measured values at the air quality station (Borrego et al., 2003).

2.2. EXPOSURE MODULE

The exposure module is constructed to predict and to assess the cumulative exposure distribution from modelled chemical agent concentrations in different microenvironments of an urban area and from the number of persons present in the same environments.

2.2.1. *Concentration data*

The chemical agent concentration is one of the main inputs for the exposure quantification. It is distinguished between the ambient air (outdoor) concentrations provided by the DISPER module, and indoor concentrations calculated through empirical indoor/outdoor (I/O) relations. In total, five different microenvironments are distinguished in the exposure model: residence; office; school; transport and outdoor. The I/O empirical relations used to calculate the indoor concentrations are different for each micro-environment.

It was only possible to define for Sulphur Mustard agent HD exposure quantification, I/O relations for transport and buildings (includes residence, school and office) microenvironments, based on an extensive bibliographic survey. Specifically, it was considered that 30% and 40% of the outdoor HD agent concentration enters the buildings and the transport microenvironment, respectively (adapted from URL1). This methodology can be applied to other C/B agents if the outdoor/indoor relations are known.

2.2.2. *Population data and microenvironments definition*

The main objective of the population data processing is to obtain temporal and spatial distributions of habitants within the study domain. Diverse information is used for this purpose including statistical data on population age groups, mobility data and employment information focused on the description of the proportion of time spent by the population in the various microenvironments. In this data processing the emphasis is to characterise the population groups and not an individual.

The exposure module considers population time-activity data in the form of a daily profile with varying hourly population fraction for each microenvironment. The exposure module uses the population profile together with the microenvironments regular grid to calculate spatial distribution of habitants for each hour. The total number of habitants vary during the day due to income and outcome fluxes related with activity and mobility data. The main result of the population processing module is the number of persons in each grid cell for each simulation hour (Borrego et al., 2004a).

2.2.3. *Cumulative exposure estimation*

The effect of a chemical warfare agent on a person depends on his cumulative dose or how much agent the body takes in or absorbs. Dose tends to be a scientific concept used in laboratory studies and is practically impossible to measure in the field.

On the other hand, it is possible to calculate the dosage in the field. Dosage is defined as the cumulative exposure or the concentration of chemical agent to which a person is exposed in a certain microenvironment integrated over the time of exposure (URL1):

$$Dosage\ (mg.\min.m^{-3}) = C_{agent} \times T\ ,$$

where C_{agent} is the concentration of gas present in the ambient air ($mg.m^{-3}$) and T is the time of exposure (min).

It is possible to define three dosages of interest for Sulphur Mustard Agent HD: Medium lethal dosage ($LCt_{50}=1500$ $mg.\min.m^{-3}$), kills 50% of exposed, unprotected personnel; Median Incapacitating dosage ($ICt_{50}=150$ $mg.\min.m^{-3}$), disables 50% of exposed, unprotected personnel; and First Noticeable Effects (FNE=100 $mg.\min.m^{-3}$), corresponds to the threshold amount at which unprotected, exposed personnel begin to manifest physical symptoms of exposure.

The cumulative exposure is estimated for each grid cell of the study domain. The combination of the cumulative exposure value with the number persons in each grid cell will be used to determine the total number of persons exposed above the reference values LCt_{50}, ICt_{50} and FNE.

3.   Case study

The developed methodology was applied in the Lisbon city centre, to the area of Entrecampos. The meteorological conditions of a typical weekday in Lisbon (1st of March 2000), with hourly values of wind velocity and direction, were considered in the simulation. A terrorist attack scenario was simulated through the release of 100 kg of Sulphur Mustard Agent HD, during 10s, in Entrecampos Square, at 8:00 (Figure 2). It is assumed that at the referred hour, the risk of exposure is higher in case of a terrorist attack, since a larger number of persons are present in the study domain. The place chosen for the release of the toxic gas was determined based on the area with higher population density during the day.

For this exercise it was considered that no emergency response measures were activated during the release, such as, evacuation or shelter-in-place. Moreover, it was considered that the population was unprotected

against the exposure to HD agent. The exposure time of the population is defined by the time interval of the output concentration files. It is assumed that during each time interval, the population present in the areas affected by the concentration plume is exposed to the HD agent.

3.1. STUDY AREA CHARACTERISATION

The selected study area, located in Lisbon city centre, is mainly a commercial and administrative zone, highly frequented by people walking on the streets or passing by car or public transports (FCT/UNL, 2005).

The study domain has an area of 1000 m^2, which was divided in cells of 25×25 m^2, each one allocated to a microenvironment (Figure 2).
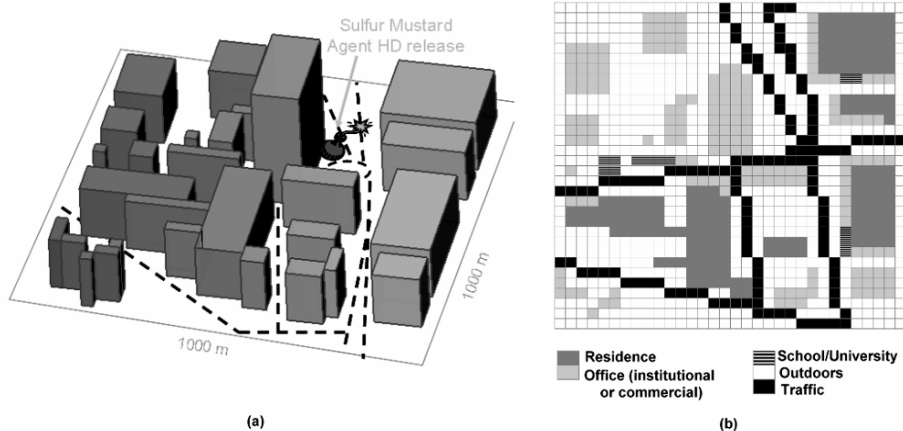
Figure 2. Study domain (a) 3-D view; (b) Microenvironments distribution.

Data from the year 2001 National Census were gathered, namely for resident population by age groups, employed population, number of schools and universities, number of students, for each one of the three sub-municipality regions ("Freguesias") included in the study region. The available data was analysed and used to estimate the hourly average number of persons in each indoor and outdoor microenvironment. Additional data on traffic counting, including buses and private cars, was also required to estimate the number of persons inside vehicles (Borrego et al., 2004a).

Figure 3 presents, for each microenvironment, the daily number of persons, as well as the time-activity pattern of the population, generated with one-hour time resolution. During the day, the total number of persons present in the study area almost triplicates due to the high density of offices

and commercial buildings (Borrego et al., 2004a). In a weekday, from 8:00 to 21:00, the average number of persons per hour in the study domain, including all microenvironments, is 12 000.

Occupation of schools was estimated considering their capacity, and the number of 0-14 and 15-24 year-old residents. Time-activity patterns were estimated based on the studies performed by Kousa et al., (2002) and Jensen (1999) and was adapted to the Portuguese situation. The hourly average number of persons in traffic microenvironment was calculated taking into consideration the sum of fractions of time that people stay in the area. (e.g. one person is equivalent to 60 persons staying one minute in the area). An occupation of 1.4 persons per car and a variable daily occupation per bus were considered (Borrego et al., 2004a).
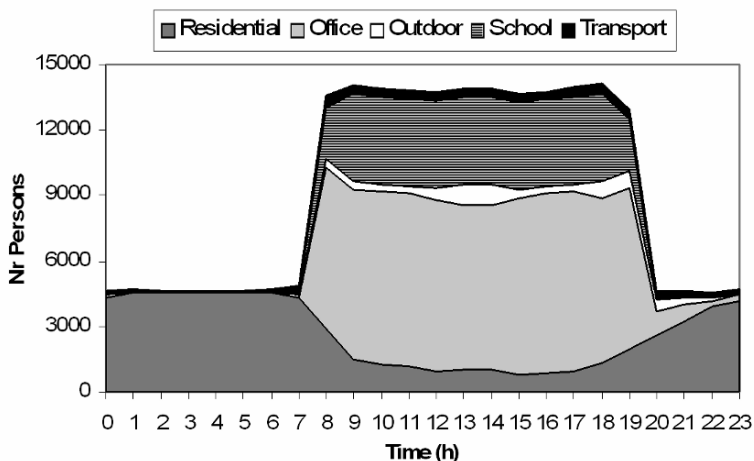
Figure 3. Number of persons per microenvironment in the study area.

3.2. RESULTS AND DISCUSSION

The flow and concentration fields of HD agent were determined for the 1st of March 2000, at 8:00, considering the release scenario of 100 kg Sulphur Mustard gas. With this approach it was possible to predict the air flow around this specific urban area, for the tested meteorological conditions. Moreover, it was possible to determine the evolution of the HD agent plume dispersion and the number of persons that are been affected if a chemical agent is released in an urban area.

Output concentration files of HD agent were generated with a time interval of 10s after the release. The last output file corresponds to a time interval of 200s. The cumulative exposure was determined for each cell of

the study domain, considering the concentration values at the same cell and the exposure time defined for the output concentration files. Cumulative exposure files were generated for the same time interval of the HD agent concentration files for the referred hours. The number of persons exposed above the limit values defined by LCt_{50}, ICt_{50} and FNE dosages was determined for each time interval, based on the cumulative exposure files.

Figure 4 presents the flow and dispersion fields of Sulphur Mustard Agent HD for the study area, at 8:00, for 10s, 60s and 100s, after the release in the area of Entrecampos Square (location signed in Figure 2).
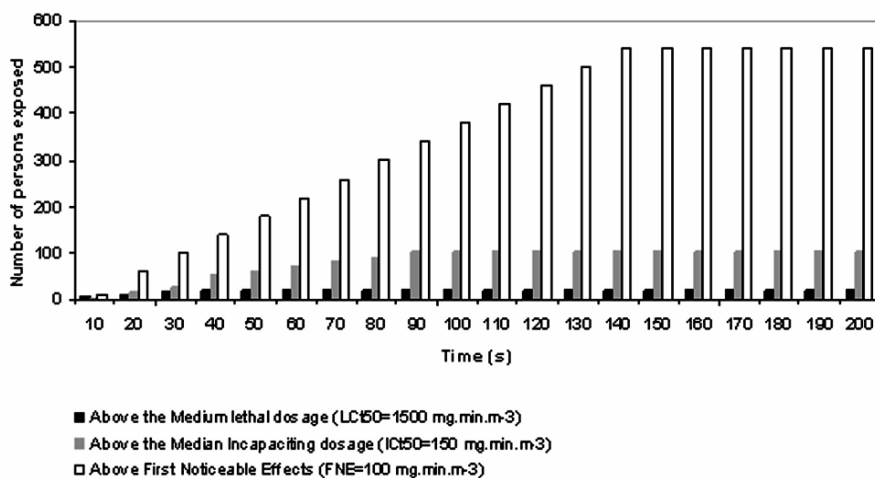
Figure 4. Flow and dispersion fields of Sulphur Mustard Agent HD, at 2m height, at 8:00, for 10s, 60s and 100s after the release.

10s after the release is possible to find concentration values of HD agent above 5000 mg.m^{-3} corresponding to dosage values above 850 mg.min.m^{-3}. Since the emission period of the toxic gas is of 10s, it is possible to notice for 60s and 100s after the release, a diminishing of the HD agent concentrations in the air and, also, a transportation of the gas mass due to the prevailing dispersion conditions.

For the same hour it is presented the number of persons exposed above the reference values LCt_{50}, ICt_{50} and FNE, for different exposure times (Figure 5).

The analysis of Figure 5 shows the number of persons that have been exposed above the LCt_{50}, ICt_{50} and FNE dosages values during the dispersion of Sulphur Mustard gas, at 8:00, for the meteorological conditions observed for the 1st of March 2001. The number of persons

exposed is cumulative and depends on the period of time after the release. 60s after the release, 220 unprotected persons, that were exposed to Sulphur Mustard concentrations, begin to manifest the first physical symptoms (FNE>100 mg.min.m^{-3}), that includes, burning blisters, wherever the gas contacted the skin; bleeding and blistering within the respiratory system; the eyes (if exposed) become sore and the eyelids swollen, possibly leading to conjunctivitis and blindness.
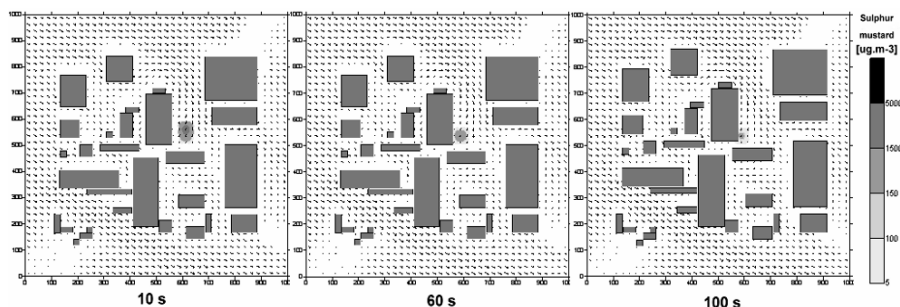
Figure 5. Number of persons exposed above the reference values LCt$_{50}$, ICt$_{50}$ and FNE, for different exposure times, at 8:00.

For the same period of time, 72 persons were exposed to dosage values higher than the ICt$_{50}$=150 mg.min.m^{-3}, meaning that 36 persons exposed will be disabled. Also, 10 persons will die exposed to dosage values higher than 1500 mg.min.m^{-3}. At 90s after the release, the concentrations of Sulphur Mustard gas in the ambient air will diminish and the dispersion of the plume will no longer affect areas were the population is located. This fact explains the constant values of the number of persons exposed found in Figure 5.

4.   Conclusions

The methodology developed in this study should be seen as a first approach to simulate the effect of a terrorist attack with Sulphur Mustard gas and its consequences in human health, through the estimation of the cumulative exposure and the number of persons affected above critical dosage values. The same methodology can be applied in case of an accidental release or to other C/B agents if outdoor/indoor relations are known.

The scenario defined for the Lisbon urban area has shown that for similar meteorological conditions of the 1st of March and to a release of 100kg of Sulphur Mustard gas in Entrecampos Square, at 8:00, 10 persons will die, 50 persons will be disable and 540 persons will start manifesting first noticeable effects. The definition of other possible scenarios by the national authorities, using the defined methodology, can help in the identification of areas with more risk of exposure and in the definition of an emergency response strategy to chemical and biological attacks that can include, for example, evacuation or shelter-in-place.

Mobilising the scientists to the protection of people and natural resources not from external threats coming from terrorist attacks can be considered a first step to achieve fruitful results.

Acknowledgements

References

Borrego, C., Tchepel, O., Costa, A.M., Martins, H., and Ferreira, J., 2004a, Urban population exposure to particulate air pollution induced by road transport, in: *27th Int. Tech. Meeting of NATO-CCMS on "Air Pollution Modelling and its Application", Banff, Alberta, Canada, 25–29 October 2004 - Air Pollution Modelling and its Application XVI,* Carlos Borrego and Ann-Lise Norman, eds., Kluwer Academic/ Plenum Publishers, New York, in press.

Borrego, C., Tchepel, O., Costa, A.M., Amorim, J.H., and Miranda, A.I., 2003, Emission and dispersion modelling of Lisbon air quality at local scale. *Atmospheric Environment* **37:** 5197–5205.

Borrego, C., Tchepel, O., Salmim, L, Amorim, J.H., Costa, A.M., and Janko, J., 2004b, Integrated modelling of road traffic emissions: application to Lisbon air quality management, *Cybern. and Syst.: An Int. Journal* **35:**535–548.

FCT/UNL, 2005, *Plans and Programs for the Improvement of Air Quality in the Lisbon and Tagus Valley Region,* Universidade Nova de Lisboa, p. 233.

Huber, A., Georgopoulos, P., and Gilliam, R., 2004, Modeling Air Pollution from the Collapse of the World Trade Center and Assessing the Potential Impacts on Human Exposures. EM – Homeland Security, February 2004, pp. 35–40.

Jensen S., 1999, *A Geographic Approach to Modelling Human Exposure to Traffic Air Pollution using GIS,* PhD Thesis, Ministry of Environment and Energy, National Environmental Research Institute, Denmark.

Kadlec, R. et al., 1997, Biological weapons control: prospects and implications for the future. *Journal of American Medical Association* **281(5):**351–6.

Kousa, A., Kukkonen, J., Karppinen, A., Aarnio, P., and Koskentalo, T., 2002, A model for evaluating the population exposure to ambient air pollution in an urban area, *Atmospheric Environment,* **36:**2109–2119.

Raber, E., Jin, A., Noonan, K., Mcguire, R., and Kirvel, R., 2001, *Int. Journal of Environmental Health Research*, **11:**128–148.

Shea, D., and Gottron, F., 2004, *Small-scale Terrorist Attacks Using Chemical and Biological Agents: An Assessment Framework and Preliminary Comparisons*, Congressional Research Service Report for Congress. The Library of Congress. RL32391.

URL1: http://www.ghasp.org/ (Galveston-Houston Association for Smog Prevention)

A MULTIPHASE MODEL TO ASSESS THE EFFECTIVENESS
OF EMISSION CONTROL SCENARIOS

GIOVANNA FINZI*, CLAUDIO CARNEVALE,
MARIALUISA VOLTA
*Department of Electronics for Automation,
University of Brescia,
Via Branze 38, 25123 Brescia, Italy*

Abstract. This paper presents the application of TCAM model to assess secondary pollution control policies. The work focuses on two emission scenarios: the current legislation one, related to the emission reduction established by the EU Directives, and the MFR one, referring to the emission reduction caused by the use of the most efficient available reduction technology for each emission sector. The results show that the impact of both scenarios on ozone mean concentration is limited, even as for AOT40, the reduction reaches the 50% with respect to the base case. The impact on PM10 is more significant, also in terms of mean and exceedance days. Therefore, the impact of both emission control strategies does not meet PM10 EU 2010 standards over the whole domain.

Keywords: secondary pollution control; multiphase model; scenario assessment.

1. Introduction

Multiphase models can simulate the physical-chemical processes involving secondary pollutants in the troposphere, allowing so to assess the effectiveness of sustainable emission control strategies. In this paper,

_____
   *To whom correspondence should be addressed. Giovanna Finzi, Department of Electronics for Automation, University of Brescia, Via Branze 38, 25123 Brescia, Italy; e-mail: finzi@ing.unibs.it

the chemical and transport model TCAM (Carnevale et al., 2005a) is introduced and applied, as a module of GAMES (Gas Aerosol Modelling Evaluation System) integrated modelling system (Volta and Finzi, 2005), also including the emission model POEM-PM (Carnevale et al., 2005b), the CALMET meteorological model (Scire et al., 1990), a pre-processor providing the initial and boundary conditions required by the model and the System Evaluation Tool (SET). The modelling system has been validated over a Northern Italy in the frame of national and international projects, and it has been used to asses the effectiveness of two different emission control strategies in the frame of CityDelta project (Thunis and Cuvelier, 2004). The first emission scenario is related to the emission reduction expected up to 2010 assuming the European Current Legislation (CLE). The second one is based on the Most Feasible emission Reduction (MFR) that could be obtained using the best available technology.

2.   TCAM model description

TCAM is an Eulerian multiphase three-dimensional model. The model solves the mass balance equation by means of a splitting operator technique. The horizontal advection module implements a finite difference scheme based on chapeau functions (Pepper et al., 1979) and the non linear Forester filter (Forester, 1977). The vertical transport is solved using either a semi-implicit or a fully implicit scheme on the basis of the value of vertical diffusivity (Yamartino et al., 1992). The dry deposition is treated using a resistance-based algorithm which takes into account pollutant properties, local meteorology and terrain features (Yamartino et al., 1992). The wet deposition module for gas and particles describes dissolution in droplets and precipitation scavenging (Seinfeld and Pandis, 1998). TCAM implements different chemical mechanism based both on lumped molecule and on lumped structure approaches. The gas phase chemistry is solved by the IEH (Sun et al., 1994) algorithm which separately treats the slow reacting species and the fast reacting ones. TCAM also includes and harmonizes a module describing aerosol dynamics by means of a fixed-moving approach. The aerosol module is coupled to COCOH97 chemical mechanism, an extended version of SAPRC97 (Carter et al., 1997), and it describes the dynamics of 21 chemical compounds (13 inorganics and 8 organics). The chemical compounds are split in 10 size bins. The inorganic thermodynamic module is derived by SCAPE2 (Kim et al., 1992). TCAM simulates the most relevant aerosol processes: the condensation, the evaporation, the nucleation of H_2SO_4 and the aqueous oxidation of SO_2 (Seinfeld and Pandis, 1998).

3. Case study

The model has been applied to a 300×300 km^2 domain in Northern Italy, centred on the Milan metropolitan area and including the whole Lombardia region. The site is characterized by complex terrain, high industrial and urban emission and a close road net. The domain has been horizontally divided into 5×5 km^2 grid cells and vertically in 11 varying levels ranging from 20 to 3900 meters above ground level. The 1999 year simulation has been performed. The boundary conditions have been estimated by a nesting procedure starting from the outputs of EMEP model (Simpson et al., 2003). Size characterization of aerosol species has been assumed processing PM measured patterns recorded during PIPAPO experimental campaign (Neftel et al., 2002). Meteorological fields have been computed by CALMET diagnostic meteorological model, merging ALADIN prognostic model output (Bubnova et al., 1993) and local measures, including 3-hourly series measured in 17 SYNOP stations, hourly series collected in 16 ground station of Lombardia, Piemonte and Emilia Romagna network and 3-hourly temperature and wind (speed and direction) vertical profiles, measured by a radio sounding in Milano Linate. The emission fields have been estimated merging the local inventory covering all the Lombardia region with a resolution of 5×5 km^2 and the EMEP European inventory at the 50×50 km^2 resolution. The profiles for temporal apportionment, VOC and PM10 chemical split and PM10 size distribution have been provided by EMEP.

Table 1 shows the total annual emission for each sector of the domain.

TABLE 1. Total yearly emission over the investigated domain.

Sector	NOx	VOC	CO	SOx	NH3	PM10
Energy production	97010	9743	22453	634035	0	8040
Domestic heating	18515	17164	323642	4731	0	20316
Combustion in manufacturing industry	34531	0	32656	18985	0	9940
Production processes	73730	40588	104918	51266	3263	12001
Extration of fossil fuel	0	51851	0	0	0	1
Solvent	0	210928	0	0	0	3633
Road transport	164153	303938	1237654	1470	3752	17640
Other mobile sources	68974	65875	74895	3760	0	9969
Waste treatment	7941	3684	12790	106	2524	1027
Agriculture	0	375	125222	0	162850	5796
Nature	1948	13943	55963	443	0	0
Total	466803	718087	1990194	714796	172389	176726

The assessment of the modelling system simulations both for gas and aerosol phase has been performed in the frame of CityDelta project (see for details (Angelino et al., 2005), (Carnevale et al., 2005a), (Carnevale, et al., 2005c).

4. Emission scenario impact assessment

The emission scenarios impact has been estimated processing the simulations provided by the modelling system assuming the base case meteorology and the 2010 expected emission and boundary condition fields. The two sustainable emission scenarios taken into account are described in the following.

4.1. CURRENT LEGISLATION SCENARIO

The Current LEgislation (CLE) scenario is related to the emission reduction obtained by the application of the EU control policies scheduled for the 2010.

Table 2 shows the % variation of emission with respect to the base case. The reductions are greater than 30% for all the pollutant with the exception of NH3. For all the other pollutants the most significant impact of the control strategies is on the transport sectors, with reductions higher than 45%.

TABLE 2. CLE emission variation (%) with respect to the base case (1999).

Sector	NOx	VOC	CO	SOx	NH3	PM10
Energy production	-31.60	-7.82	17.21	-82.35	0.00	-39.26
Domestic heating	6.16	-29.36	-22.46	-44.67	-	-37.55
Combustion in manufacturing industry	-27.75	-	-27.03	-46.49	-	-36.43
Production processes	-2.21	1.79	-5.34	-38.16	-10.56	-33.09
Extraction of fossil fuel	-	-22.25	-	-	-	-30.65
Solvent	-	-14.52	-	-	-	-34.71
Road transport	-53.94	-67.94	-56.25	-73.74	0.89	-46.69
Other mobile sources	-14.28	-30.81	-2.84	-4.93	-	-49.53
Waste treatment	0.71	0.01	0.00	-0.09	0.00	-37.19
Agriculture	-	-0.06	1.82	-	0.73	-31.80
Nature	0.00	0.00	0.00	0.00	0.00	0.00
Total	-29.79	-38.16	-39.16	-77.49	0.51	-39.65

4.2. MOST FEASIBLE REDUCTION SCENARIO

The Most Feasible Reduction scenario (MFR) takes into account the variation that could be obtained assuming for each pollutant the best available control technology. The main differences with respect the CLE scenario concern the NH3 emission, in particular in the waste treatment, road and transport and agriculture sectors (Table 3). The reduction of nitrogen oxides and sulphur dioxide are very close to the CLE ones, while the emissions of organic compounds, PM10 and CO are significantly lower.

TABLE 3. MFR emission variation (%) with respect to the base case (1999).

Sector	NOx	VOC	CO	SOx	NH3	PM10
Energy production	-31.60	-39.18	-38.03	-92.87	0.00	-84.35
Domestic heating	-21.80	-53.50	-58.02	-76.17	-	-74.78
Combustion in manufacturing industry	-47.09	-	-60.53	-78.13	-	-82.14
Production processes	-28.79	-33.06	-49.63	-74.97	-36.39	-80.52
Extraction of fossil fuel	-	-48.90	-	-	-	-100
Solvent	-	-44.07	-	-	-	-73.96
Road transport	-66.22	-78.93	-76.56	-89.29	-35.63	-72.05
Other mobile sources	-35.95	-54.39	-48.67	-22.28	-	-70.15
Waste treatment	-25.96	-34.32	-46.54	-59.39	-35.56	-68.38
Agriculture	-	-34.56	-45.81	-	-35.08	-91.73
Nature	0.00	0.00	0.00	0.00	0.00	0.00
Total	-44.50	-58.74	-66.10	-90.64	-35.12	-77.19

4.3. COMPARED IMPACT ASSESSMENT

Figure 1 (left) highlights the modest impact of CLE scenario on the ozone mean concentration (from -6 to 3 ppb). In high emission areas (typically VOC-limited, as urban areas) the reduction of NOx emission is higher than the VOC one, causing an increasing of ozone mean concentration.
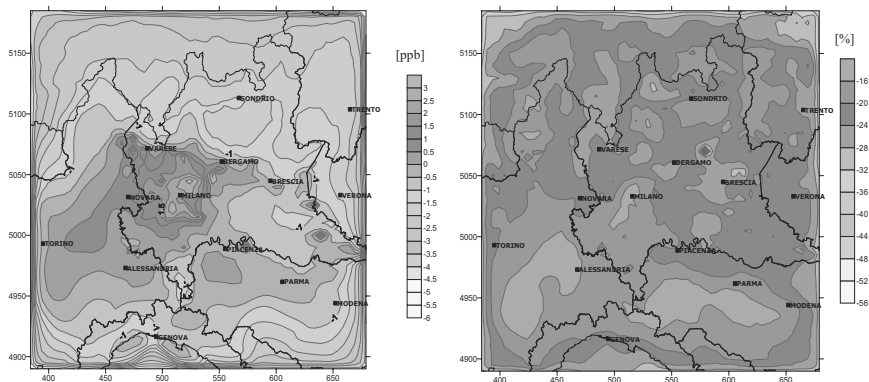
Figure 1. Impact (difference with respect to the base case) of CLE scenario: on O3 mean concentration (left) and AOT40 (right).

The impact on AOT40 indicator is more significant; the simulation estimates a reduction of AOT40 all over the domain and in particular on the centre-northern part of the valley where the highest concentration values are estimated in the base case (Figure 1, right). The reduction of PM10 concentrations due to the scenario application is noticeable all over the domain (Figure 2, left). In particular, the impact is greater in the centre part, reaching the 40 μg/m^3 in the Milan metropolitan area. The reduction is more intense during the winter, with peaks of 45 μg/m^3, where the primary PM10 fraction is higher. Although the scenario causes the reduction of exceedance days, it doesn't anyway allow the respect of 2010 legislation standards (7 days), mainly in the metropolitan areas located in the centre of the domain (Figure 2, right).
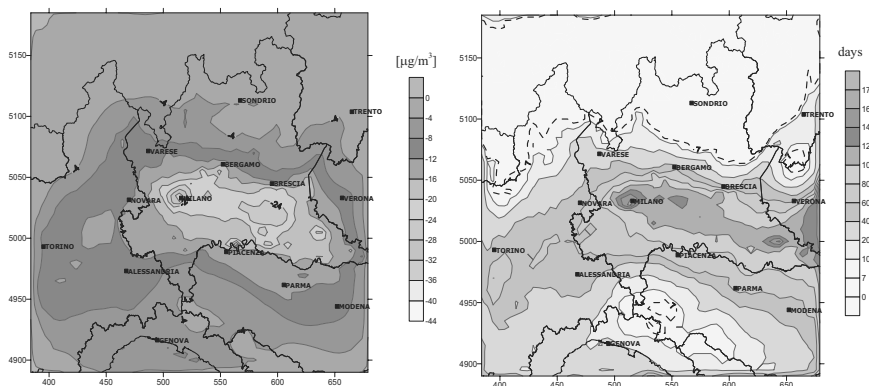
Figure 2. Impact of CLE scenario on PM10: mean concentration (difference with respect to the base case, left) and exceedance days (right).

As for the MFR scenario impact assessment, the ozone mean concentration variation is very similar to one simulated for the CLE scenario.
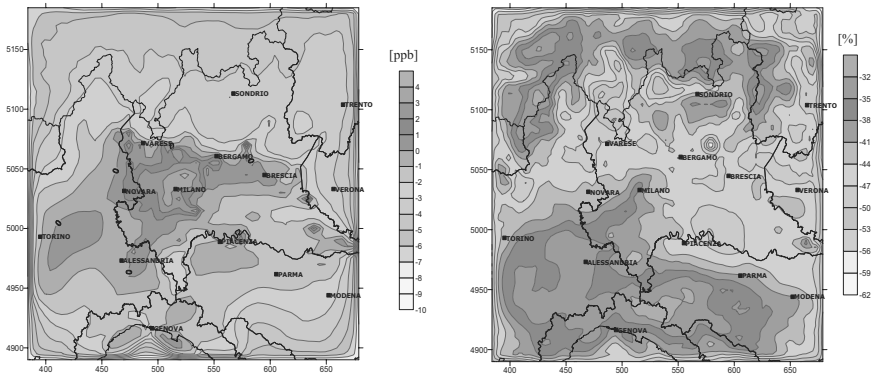
Figure 3. Impact (difference with respect to the base case) of MFR scenario: on ozone mean concentration (left) and AOT40 (right).

Also in this case, the impact is greater on AOT40 than on mean concentration, with reduction always higher than 30% (Figure 3, right). The rural area of Po Valley and the valleys in the centre north of the domain present considerable reduction. The MFR scenario, as the CLE one, highlights an high
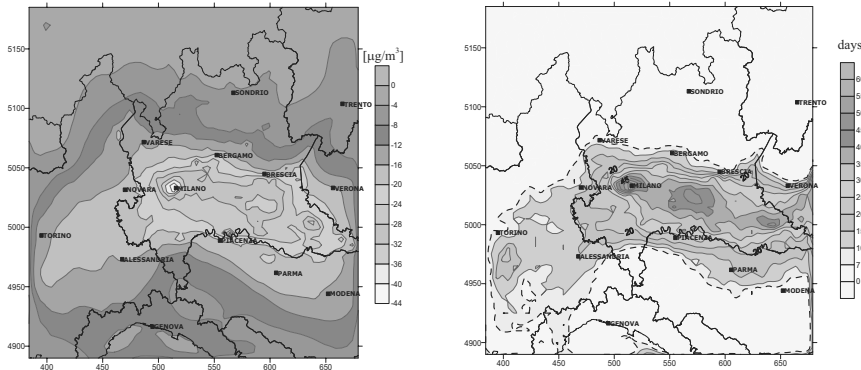
Figure 4. Impact of MFR scenario on PM10 mean concentration: (difference with respect to the base case, left) and exceedance days (right).

capability in limiting the ozone critical episodes occurring during the simulation period, in spite of the minor impact on the ozone mean concentration. The mean PM10 concentration reduction is significant all over the computational domain, in particular in the Milan metropolitan area, except for the low concentration areas in the north-west and north-east of the domain (Figure 4, left). Figure 4 (right) shows that, in spite of the emission reduction, a large part of the domain does not meet the EU directive up to 2010 regarding allowed exceedance days.

5.   Conclusions

The paper is focused on the TCAM model, used to assess secondary pollution control policies. The impact of two emission scenarios in Northern Italy is assessed: the current legislation (CLE) one, referred to the emission reduction established by the current EU directives, and the MFR one, obtained using for each emission sector the most efficient available reduction technology. The simulation results show that the application of both policies takes to a limited impact on O_3 summer mean concentration, but to a significant critical episodes reduction, as suggested by the reduction of AOT40 values. As for PM10, the results highlight a deep reduction both in mean values and exceedance days. Anyway, in both cases, the respect of EU 2010 standards is not met mostly in the urban and industrialized area of the domain.

References

Angelino, E., Bedogni, M., Carnevale, C., Finzi, G., Minguzzi, E., Peroni, E., Pertot, C., Pirovano, G., and Volta, M., 2005, PM10 chemical model simulations over the Milan area in the frame of CityDelta exercise, *Proc. of the 5th International Conference on Urban Air Quality*, Valencia (E).

Bubnova, R., Horanyi, A., and Malardel, S., 1993, International project ARPEGE/ALADIN. *EWGLAM Newsletter,* **22**: 117–130.

Carnevale, C., Finzi, G., Volta, M., 2005a, Design and validation of a multiphase 3D model to simulate tropospheric pollution. *Proc. 44th IEEE Conference on Decision and Control and European Control Conference*, CD-ROM, ISBN 0-7803-9568-9.

Carnevale C., Gabusi, V., and Volta, M., 2005b, POEM-PM: an emission modelling for secondary pollution control scenarios, *Environmental Modelling and Software*, doi:10.1016/j.envsoft.2004.11.003.

Carnevale, C., Finzi, G., and Volta, M., 2005c, Seasonal characterization of secondary aerosol in the Northern Italy using TCAM model, *Proc. of the 5th International conference on Urban Air Quality*, Valencia (E).

Carter, W., Luo, D., and Malkina, I., 1997, Environmental chamber studies for development of an updated photochemical mechanism for WOV reactivity assessment, *Tech. Rep., California Air Resource Board*, Sacramento, CA.

Forester, C.K., 1977, Higher order monotonic convection differences schemes, *Journal of Computational Physics*, **23**: 1–22.

Kim, Y.P., Seinfeld, J.H., Saxena, P., 1992, Atmospheric gas aerosol equilibrium, I: thermodynamic model. *Aerosol Science and Technology* **19**, 157–181.

Neftel, A., Spirig, C., Prévôt, A., Furger, M., Stuz, J., Vogel, B., and Hjorth, J., 2002, Sensitivity of photo-oxidant production in the Milan basin: an overview of results from a EUROTRAC-2 Limitation of Oxidant Production field experiment, *Journal of Geophysical Research* **107** (D22).

Pepper, D.W., Kern, C.D., and Long, P.E., 1979, Modelling the dispersion of atmospheric pollution using cubic splines and Chapeau functions, *Atmospheric Environment*, **13**: 223–237.

Scire, J., Insley, E., and Yamartino, R., 1990. Model formulation and user's guide for the CALMET meteorological model, *Tech. Rep. A025-1, California Air Resources Board*, Sacramento, CA.

Seinfeld, J.H., and Pandis, S.M., 1998, *Atmospheric Chemistry and Physics*. John Wiley & Sons.

Simpson, D., Fagerli, H., Jonson, J., Tsyro, S., and Wind, P., 2003. Transboundary, acidification, eutrophication and ground level ozone in Europe – Part I: Unified EMEP model description, *Tech. Rep. 1/2003, EMEP MSC-W*.

Sun, P., Chock, D.P., and Winkler, S.L., 1994, An Implicit-Explicit Hybrid Solver for a System of Stiff Kinetic Equations. *Proc. 87th Air & Waste Management Association Annual Meeting*.

Thunis, P., and Cuvelier, C., 2004, CITYDELTA: an European modelling inter-comparison to predict air quality in 2010, in *Air Pollution Modelling and its Application XVI,* Kluwer Academic/Plenum Publisher pp. 205–214.

Volta, M., and Finzi, G., 2005, GAMES, a comprehensive GAS Aerosol Modelling Evaluation System, *Environmental Modelling and Software*, doi: 10.1016/-j.envsoft.2004.06.012 .

Yamartino, R., Scire, J., Carmichael, G., and Chang, Y., 1992. The CALGRID mesoscale photochemical grid model – I. Model formulation. *Atmospheric Environment* **26A (8)**, 1493–1512.

ASSESSMENT OF LONG-RANGE TRANSPORT AND DEPOSITION FROM CU-NI SMELTERS IN RUSSIAN NORTH

ALEXANDER MAHURA*, ALEXANDER BAKLANOV,
JENS HAVSKOV SØRENSEN
*Danish Meteorological Institute, DMI, Lyngbyvej 100,
DK- 2100, Copenhagen, Denmark*

ANTON SVETLOV, VSEVOLOD KOSHKIN
*Institute of Northern Environmental Problems, INEP,
Kola Science Center, Fersman 14, 184200, Apatity,
Murmansk region, Russia*

Abstract. The main aim of this pilot study was an evaluation, from a probabilistic point of view, of possible temporal and spatial distribution of deposition patterns due to atmospheric transport from three smelters of the Kola Peninsula (Russia). These patterns with GIS integration can be used further for the estimation of possible short- and long-term consequences resulting from sources of continuous emissions for the environment and population on regional and Northern Hemispheric scales.

1. Introduction

Sources of continuous emissions may cause harmful impacts on population and environment due to the possibility of long-term effects and consequences. These depend on a number of factors among which are the

————
    *To whom correspondence should be addressed: Alexander Mahura, Research and Development Department, Danish Meteorological Institute, Lyngbyvej 100, DK-2100, Copenhagen, Denmark; e-mail: ama@dmi.dk.

types of harmful pollutants, their emission rates, heights of pollutants released, surrounding terrain and geographical location of sources, climatic conditions, vulnerability of surrounding flora and fauna, etc. All these are of importance for evaluation of possible both short- and long-term consequences.

In our pilot study, employing a methodology developed with the Arctic Risk project of the Nordic Arctic Research Programme, NARP (AR-NARP, 2003; Baklanov and Mahura, 2004; Baklanov et al., 2005), we evaluated the temporal and spatial variability of atmospheric transport and deposition patterns from sources of long-term anthropogenic pollution located on the Kola Peninsula, Russia. These sources are the two enterprises called the Pechenganickel (plants 1 and 2) and Severonickel situated in cities of Nickel-Zapolyarnyy and Monchegorsk, respectively. In total three geographical locations, i.e. plants/sites were selected. These enterprises (together with the Russian Norilsk Nickel enterprise) are the major producers of nickel, cupper, platinum, and other strategic metals for the related Russian and world industries. The production cycle resulted in significant emission of pollution into the atmosphere as well as a localized pollution of water and soil in the surroundings of these enterprises. Among the pollutants are heavy metals and gaseous substances. The study of atmospheric transport, dispersion, and deposition of pollution is one of the key aspects of the evaluation of possible consequences for population and environment on different scales ranging from local to regional, transboundary and large scales.

Here we focus, at first, on the simulation of long-term and large-scale concentration and deposition patterns resulting from the emission of these plants. Secondly, an estimation of monthly, seasonal, and annual variability of patterns was done for each of the locations. And thirdly, the boundaries of geographical territories/regions under influence of long-term continuous emissions from selected sources were evaluated.

2. Methodology

2.1. LONG-TERM DISPERSION MODELLING

The Danish Emergency Response Model for Atmosphere (DERMA) model developed at DMI was employed. It was used to simulate long-term atmospheric transport, dispersion, and deposition of pollutants from three locations of the Cu-Ni smelters. This model is a mathematical three-dimensional atmospheric dispersion model of Lagrangian type (Sørensen, 1998; Baklanov and Sørensen, 2001; Baklanov et al., 2005). It describes atmospheric transport, diffusion, and deposition in the range from local and

to global scales. In this study, we used the European Centre for Medium-Range Weather Forecast data (for the year of 2000) having a resolution of 1° latitude vs. longitude and 6 hour output time resolution.

For long-term simulations a set of assumptions was used. At first, every day the pollutants were released from the plants' locations at an arbitrary rate of 10^9 μg/s. The release of SO_4 was assumed to be continuous. For this the total amount of daily release was equal to 86.4 tons or 31.5 thousands tons per year (i.e. a mild scenario). However, note that in some years the total amount released was up to 200 thousands tons. Secondly, the simulations for three sites were performed for one year of 2000 on a daily basis where modelling during the first two weeks after release started at the sites. Thirdly, several variables were calculated: air concentration [μg/m^3]; time-integrated air concentration (TIAC) [μg•h/m^3]; dry deposition (DD) and wet deposition (WD) [μg/m^2].

Note, with respect to industrial smelters, the simulated fields of air concentrations and depositions can be interpreted in two ways. Firstly, it can be recognized as the long-term effects (accumulated or average contamination or depositions) from existing continuous emission sources. Secondly, it can be seen as probabilistic characteristics of industrial contamination of different territories/countries through atmospheric pathways.

2.2. SUMMARY AND AVERAGE DEPOSITION FIELDS

All calculated dispersion modelling results can be represented by 2D fields where values of the calculated variables (TIAC, DD, and WD) are given in the latitude vs. longitude grids of the model domain. The first approach considers the distribution of the total sum of daily continuous emissions from the sites. This type of field shows the most probable geographical distribution at the surface if the releases are occurring during a long-term period (see example in Fig. 1). The second approach is simply based on calculating the average value from the summary field. This type of field (summary field) shows the averaged spatial distribution of emissions occurring during any given average day of the period studied. Note, the scaling with similar magnitude isolines starting from 0.01 (see Figures 1-3) is used to simplify the interpretation and comparison of fields (also other scales can be selected and fields re-plotted based on the original archived data). More details regarding examples of nuclear risk sources can be found in Baklanov et al., (2005) and Mahura et al., (2005).

3. Results

3.1. GENERAL REMARKS

The focus of this study is the evaluation of long-term dispersion patterns from the smelters. Only the summary fields are discussed, although the average fields can also be used for the evaluation of consequences of short-term accidental releases of harmful pollutants at plants.

Several general remarks should be made. Firstly, using the average and summary fields it is possible to interpolate data to a particular geographical area of interest or for a particular geographical location (for example, a city). Secondly, the summary fields can be used to estimate potential consequences over a period (month, season, or year). These summary fields will be more representative for routine continuous emissions as they are generated by smelters. Thirdly, because all fields were calculated for a continuous release, it is possible to recalculate or rescale these fields for other releases of pollutants at different magnitude. Fourthly, we carried out simulations up to two weeks because we were interested in the evaluation of the long-term and long-range transport of emissions.

3.2. DEPOSITION PATTERNS

In this study, the evaluation of temporal and spatial variability of dry and wet deposition patterns resulting from continuous emissions of the Kola Peninsula

(a)   *(b)*   *(c)*
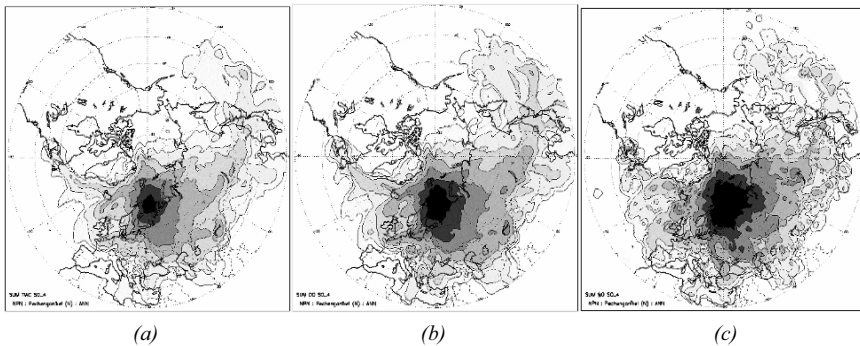
Figure 1. Annual summary (a) time integrated air concentration, (b) dry deposition, and (c) wet deposition fields of SO$_4$ resulting from continuous releases of atmospheric pollution of the Pechenganickel plant 1 (NPN, city of Nickel) /all isolines starting from the lowest value of 0.01.

smelters was performed on an annual, seasonal, and monthly basis. The annual summary fields for the TIAC, DD and WD patterns of SO4 are shown in Fig. 1 using the Pechenganickel plant 1 (located in city of Nickel) as an example.

Similar fields were also constructed and evaluated for two other plants. As seen on the large scale the TIAC field is more extended in the south-east sector from the Kola Peninsula than in all others. It even reaches the Central North Pacific region. Mostly, the North-West Russia, Scandinavian and Baltic Sea countries are within the zone of the highest potential impact from these plants. In general, the TIAC and DD have a similar structure compared with WD. Around the site both have a distribution which is closer to elliptical than circular; and moreover, the shape of these fields reflects the presence of dominating atmospheric transport patterns throughout the year. The WD field is less smooth and often has a cellular structure, because it reflects the irregularity of the rainfall patterns. Moreover, these fields have also different monthly spatial structures as shown in Fig. 2.

| | (a) | (b) |
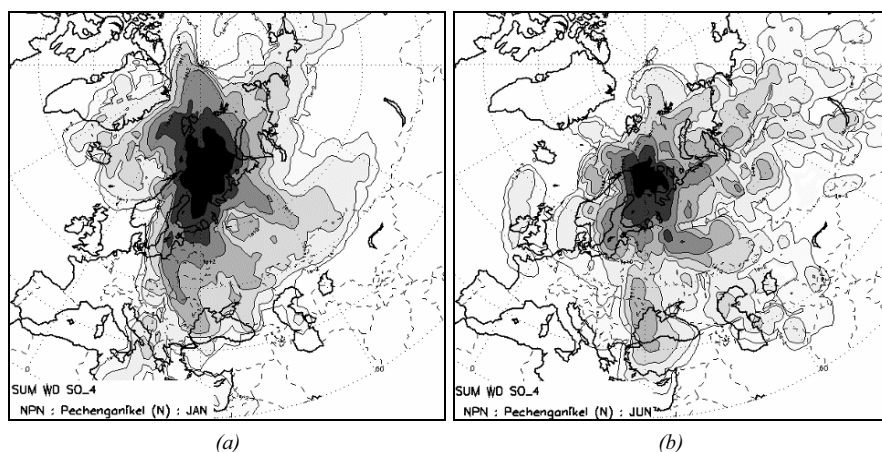
Figure 2. Monthly summary wet deposition fields of SO$_4$ resulting from simultaneous continuous releases of atmospheric pollution during (a) January and (b) June from Pechenganickel plant 1 (NPN, city of Nickel) /all isolines starting from the lowest value of 0.01.

The combined/added annual summary dry and wet deposition fields for all three sources of continuous emission are shown in Fig. 3. Obviously continuous emissions from plants of the Kola Peninsula have a significant influence not only on the regional, but also on large scales contributing to the Arctic haze pollution, transboundary exchange with the Northern European countries, and Central Russia pollution. Partially, its influence is seen even over territories of the North Pacific countries such as Japan, northern areas of China, and both Koreas. Moreover, for WD the total area

enclosed by the highest isoline is more than 2 times larger than for DD. Additionally, the WD pattern is also locally pronounced over the western shore of Canada and USA.

(a)   *(b)*
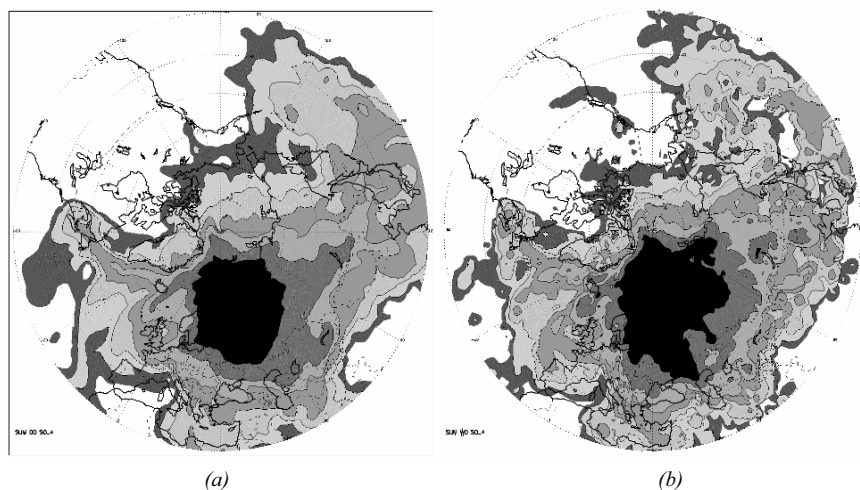
Figure 3. Annual summary (a) dry deposition and (b) wet deposition fields of SO4 resulting from simultaneous continuous releases of atmospheric pollution from three Cu-Ni plants of the Kola Peninsula /all izolines starting from the lowest value of 0.01.

For the Severonickel plant (city of Monchegorsk), the annual average daily DD value is 5.79 tons. The highest average DD (10.4) is in September, and the lowest – 2.9 tons – in March. The lowest values of maximum (6.9) and minimum (0.1) are observed in February and May, respectively. During July-November the standard deviations of DD are more than 5 tons (max of 9 tons in September) with the lowest of less than 2 tons during January-February. Although the annual average daily WD is 22.7 tons, a strong month-to-month variability is seen compared with DD patterns (Fig. 4b). The contribution of WD to the total deposition is quite similar to DD during July-September, and it is more than 10 times higher during January-March. The highest average WD (46.3) is in January, and the lowest – 5.5 tons – in July. The lower values of maxima (less than 3.5 tons) are observed during June-September, although for minima it is a more extended period – from May till November. The standard deviations of WD are also higher compared with DD, and especially during the colder months. Considering the amount deposited in total from daily releases (Fig. 5), the annual average is 32.9% ranging from 14.3 to 57.2% in July and January, respectively. The lowest maxima of around 40% are observed in June-July and the highest minimum of 28.9% - in February.
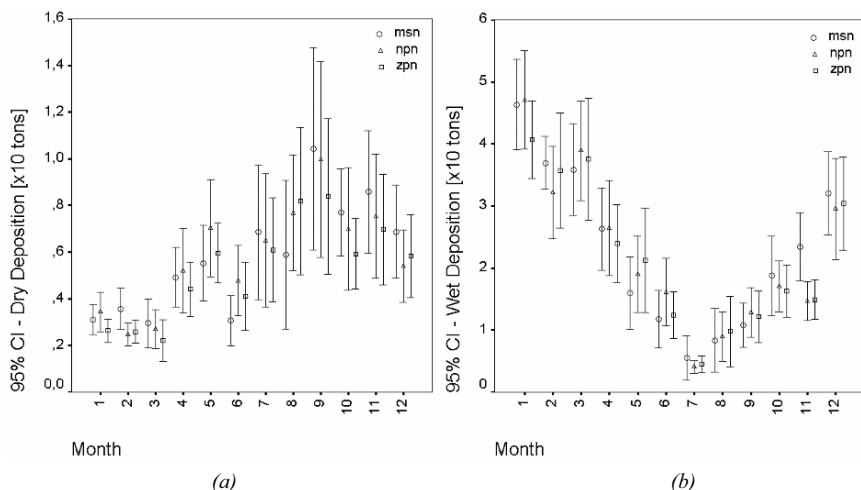
Figure 4. Monthly variability of (a) dry deposition and (b) wet deposition patterns [in tons] at 95% confidence interval during atmospheric transport and deposition from the Severonickel (Monchegorsk – msn) and Pechenganickel (Nickel – npn, Zapolyarnyy – zpn) plants.

For the Pechenganickel plant 1 (city of Nickel), the annual average daily DD value is 5.85 tons. The highest average DD (10) is in September, and the lowest – 2.5 tons – in February. The lowest values of maximum (3.9) and minimum (0.6) are observed in February and September, respectively. During September-November the standard deviations of DD are more than 7 tons (max of 8.7 tons in September) with the lowest of less than 2 tons during January-March. Although the annual average daily WD is 21.6 tons, a strong month-to-month variability is seen compared with DD patterns (Fig. 4b). The contribution of WD to the total deposition is almost similar to DD during July-September, and it is more than 13 times higher during January-March. The highest average WD (47.1) is in January, and the lowest – 4.1 tons – in July. The lower values of maxima and minima are observed during July-September (absolute lowest maximum and minimum of 7.9 and 0.5 tons, respectively, are in July). The standard deviations of WD are similar to DD during the same period, although they are higher during the colder months. Considering amount deposited in total from daily releases (Fig. 5), the annual average is 31.7% ranging from 12.2 to 58.5% in July and January, respectively. The lowest maximum of 29.6% is observed in July and the highest minimum of 20.7% - in February.

For the Pechenganickel plant 2 (city of Zapolyarnyy), the annual average daily DD value is 5.28 tons. The highest average DD (8.2) is in August-September, and the lowest – 2.2 tons – in March. The lowest values of maximum (4) and minimum (0.1) are observed in February and January, respectively. During September-November the standard deviations of

DD are more than 6 tons (max of 6.9 tons in September) with the lowest around 1 ton during January-March. Although the annual average daily WD is 21.6 tons, a strong month-to-month variability is seen compared with DD patterns (Fig. 4b). The contribution of WD to the total deposition is quite similar to DD during July-September, and it is more than 14 times higher during January-March. The highest average WD (40.7) is in January, and the lowest – 4.5 tons – in July. The lower values of maxima are observed during June-August and for minima during July-September (with absolute lowest maximum and minimum of 10.9 and 0.8 tons, respectively, are in July). The standard deviations of WD are similar to DD during summer months and higher during colder months. Considering the amount deposited in total from daily releases (Fig. 5), the annual average is 31.2% ranging from 12.3 to 50.1% in July and January, respectively. The lowest maximum of 24.5% is observed in July and the highest minimum of 19.3% - in February.
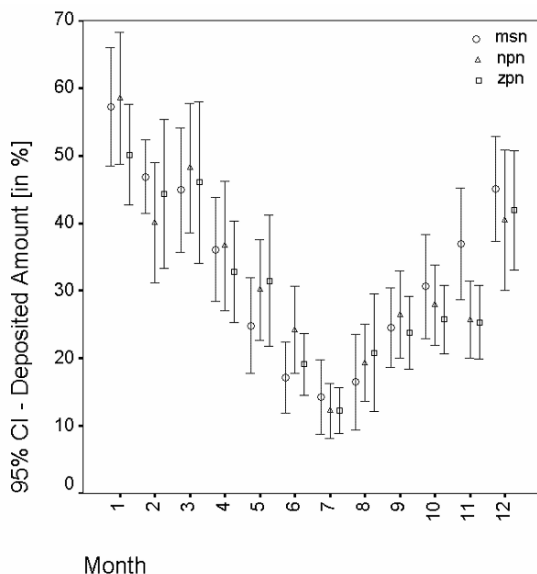
Figure 5. Monthly variability of deposited amount of pollution [in% from daily released] at 95% confidence interval during atmospheric transport and deposition from the Severonickel (Monchegorsk – msn) and Pechenganickel (Nickel – npn, Zapolyarnyy – zpn) plants.

Finally, note that in general the dry deposition monthly variability is relatively smooth and values remain approximately within the same order of magnitude. For wet deposition a strong month-to-month variability (by several orders of magnitude) was identified win contrast to the DD patterns. Moreover, since wet deposition dominates in the decrease/removal of

pollution during atmospheric transport, the total deposition also has a very similar pattern of variability.

4.   Conclusions

The main aim of this study was to combine atmospheric transport and dispersion modelling and statistical analyses to assess the temporal and spatial variability of continuous long-term emission from smelters in the Russian North. The DERMA model was employed to simulate long-term and long-range atmospheric transport, dispersion, and deposition of continuous emission (considering SO_4 particles) from the Severonickel and Pechenganickel enterprises of the Kola Peninsula. As input data the ECMWF meteorological gridded fields were utilized. For the considered mild scenario of continuous emissions from the plants (at a rate of 10^9 μg/s) in total approximately 32 thousands tons per year were released from each plant. The results of the probabilistic analysis of modelled dispersion for three locations were presented and analyzed with respect to dry and wet deposition patterns. To evaluate the temporal variability of these indicators, analyses were performed on an annual, seasonal, and monthly basis.

It was found that on average the daily dry deposition is the lowest (5.3 tons) for the Pechenganickel plant 2 located in Zapolyarnyy, and it is very similar (5.8 tons) for two other plants. In general, the value of dry deposition can be more than 10 times smaller, especially during colder months, compared to wet deposition. Moreover, it is of similar magnitude during July-September. The atmospheric transport in the western direction (toward the northern areas of the North Atlantic Ocean and surroundings) from both northerly situated Pechenganickel plants is more pronounced than from the Severonickel plant. The annual wet deposition is similar for both plants of the Pechenganickel enterprise, i.e. 21.6 tons, and it is slightly higher (22.7 tons) for the plant of the Severonickel enterprise. For all plants the total amount deposited during atmospheric transport was the highest in January, and lowest in July. On average the deposited amount was higher for the Severonickel than for the two other plants during October-February.

Furthermore, deposition patterns and their variability can be used for GIS-based approaches (Rigina and Baklanov, 2002) regarding the analysis of risk and vulnerability for population and environment.

References

AR-NARP, 2003, Atmospheric Transport Pathways, Vulnerability and Possible Accidental Consequences from the Nuclear Risk Sites in the European Arctic (Arctic Risk) of the NARP: Nordic Arctic Research Programme. DMI project; http://glwww.dmi.dk/-f+u/luft/eng/arctic-risk/main.html.

Baklanov, A., and Sørensen, J.H., 2001, Parameterization of radionuclide deposition in atmospheric dispersion models, *Phys. Chem. Earth (B)* **26**: 787–799.

Baklanov, A., Sørensen, J.H., and Mahura, A., 2005, Long-Term Dispersion Modelling: Methodology for Probabilistic Atmospheric Studies, *Environmental Modelling and Assessment*, In Review.

Baklanov, A., and Mahura, A., 2004, Assessment of possible airborne impact from risk sites: methodology for probabilistic atmospheric studies, *Atmospheric Chemistry and Physics*, **4**(2): 485–495.

Mahura, A., Baklanov, A., and Sørensen, J.H., 2005, Long-Term Dispersion Modelling: Assessment of Atmospheric Transport and Deposition Patterns from Nuclear Risk Sites in Euro-Arctic Region, *Journal of Computational Technolo*gy, **10**: 112–134.

Rigina, O., and Baklanov, A., 2002, Regional radiation risk and vulnerability assessment by integration of mathematical modelling and GIS-analysis, *Environment International*, **27**: 527–540.

Sørensen J.H., 1998, Sensitivity of the DERMA Long-Range Gaussian Dispersion Model to Meteorological Input and Diffusion Parameters, *Atmospheric Environment*, **32**: 4195–4206.

ASSESSMENT OF THE IMPACT OF INDUSTRIAL SOURCES ON URBAN AIR QUALITY IN TASHKENT

LUDMILA YU. SHARDAKOVA*, L.V. USMANOVA
Hydrometeorological Research Institute, 72, K. Makhsumov st., Tashkent, 700052, Uzbekistan

Abstract. Considerable changes have taken place in Tashkent for the last years – industrial activity schemes and scales have been modified, car traffic has increased. The analysis of the impact of stationary industrial emission sources on the state of urban air pollution was carried out by using a long-term Gaussian model. The modelling results have been compared with observations obtained with a monitoring system for air pollution.

Keywords: air pollution; modelling; Gaussian model; emissions; industrial sources

1. Introduction

Tashkent is the capital of the Republic of Uzbekistan and the biggest city in Central Asia. Its area is 337 km^2. The population is 2135400 people. There are many machinery engineering plants, chemical enterprises, plants producing construction materials and an aircraft manufacturing plant in Tashkent.

These ones and thermal power plants, Tashkent hydropower station, automobile, railway and airway transport are the main urban sources of pollution in the city. The power producing plants, machine works with foundry equipment usually are characterized by very hot emission sources.

During the last ten years the total emissions of pollutants from the stationary urban sources have significantly been reduced almost twice (Figure 1), and the emission scenario has changed.

---

*To whom correspondence should be addressed. L.Yu. Shardakova, Hydrometeorological Research Institute, 72, K.Makhsumov st., Tashkent, 700052, Uzbekistan; e-mail: lsh_wm@rambler.ru

The aim of this work is to assess the industrial sources impact of "classical" air pollution - sulphur dioxide, nitrogen dioxide, TSP- on the air pollution state. For this purpose a long-term Gaussian model of atmospheric dispersion was adapted, the database of industrial sources emissions was developed, and the climatic data assessment was carried out. The obtained model results were compared with observations from the stations of the air pollution monitoring system in Tashkent. It is the first attempt of integral assessment of the impact of industrial emission sources for the territory of Tashkent. The study is important for risk zone identification and evaluation of data provided by the monitoring system.

2. Methodology

2.1. MODEL DESCRIPTION

The formula of concentration calculation[1] for the big time periods (such as month, season, and year) is the basic equation of the model:

$$C(x,\theta) = \sum_{S}\sum_{N}\left\{\frac{2Qf(\theta,S,N)}{\sqrt{2\pi}\sigma_{2S}u_N(2\pi x/16)}\exp\left[-\frac{1}{2}\left(\frac{H_u}{\sigma_{2S}}\right)\right]\right\} ,$$

here:

$C(x, \theta)$ – air pollutant concentration at distance x in some sector with angular width θ from the continuous point source;

Q – average capacity of an emission source for the given time period;

$f(\theta,S,N)$ – long-term frequencies of wind direction and speed, Pasquill's stability classes;

u_N – a wind speed, in stability class N and in sector $2\pi x/r$ (r –directions number on which the wind is considered);

H_u – effective height of a plume, at a wind speed u;

σ_z – corresponds to σ_z –standard deviations of Gaussian distribution function at distance x for each stability class.

Members inside the braces are summarized over all wind speed and stability classes.

The ISC3 model recommendations[2] were used for the assessment of the effective height of a plume, for the calculation of wind speeds and standard deviations.

2.2. ANALYSIS OF INDUSTRIAL SOURCES EMISSIONS DATABASE

The database contains the characteristics of the emission sources: location, technical parameters, values of the total pollutant emissions and emissions by individual components. The enterprises annually submit their data on actual values of emissions to the city's environment protection committee. Information about more than 400 pollution sources is included in this data base. Their contribution to the total mass of industrial emissions in Tashkent is around 78% for TSP, 95% for nitrogen oxides and sulphur dioxide. An analysis of emission data was made and the enterprises owning the main pollution sources were chosen for calculations. The share of these emissions in the database is 90%.

Figure 1 presents the change of total emissions in Tashkent city for the last 10 years. As follows from Figure1 these changes have taken place due to a decrease of TSP mass, carbon oxide, nitrogen dioxide and volatile organic compounds (VOC). The amount of anthropogenic hydrocarbons emission increased almost four times in 2003 in comparison with 1992. In 1992 the share of CO was 38,9%, NO_x -21.1%, TSP -19.5%, SO_2 -3.4%, hydrocarbons - 1.5%, VOC - 15.2% of the total emissions. In 2003 the share CO was 35% of the total emissions, NO_x-21.7%, TSP – 8.2%, SO_2 – 12.5%, hydrocarbons – 17.6%, VOC-5.1%. During the last six years the contribution of the hydrocarbons to the total emissions has raised substantially because the urban traffic has increased.
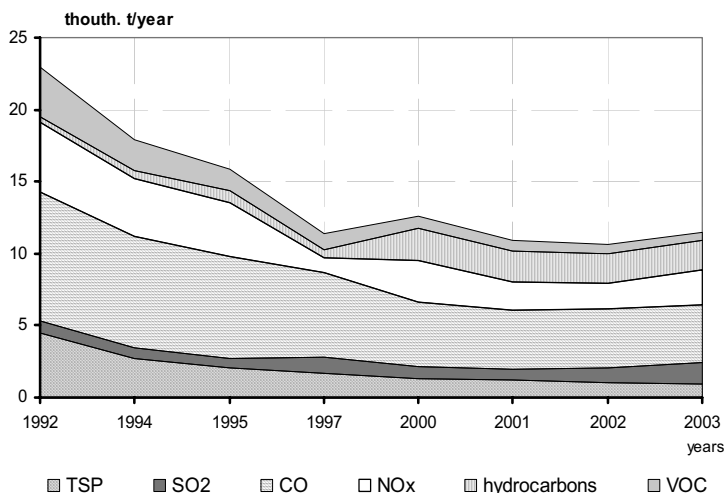
Figure 1. Changes and structure of industrial emissions from stationary sources for the period of 1992-2003 in Tashkent city.

Data analysis allowed the assessment of the spatial distribution of emissions all over the administrative districts of the city. As Figure 2 indicates:

- the districts N7 (Khamza) – 319 t/year, N11 (Yakkasaray) - 147t/year, N6 (Sergeli) -120.8 t/year show the strongest TSP emissions;
- districts N11(Yakkasaray) - 363 t/year, N4 (Mirzo-Ulugbek)-345t/year, N10 (Yunusabad) - 269 t/year show the strongest nitrogen oxide emissions;N2 (Bektemir) - 593 t/year, N4 (Mirzo-Ulugbek)-286 t/year, N10 (Yunusabad)-250 t/year show the strongest sulphur oxide emissions;
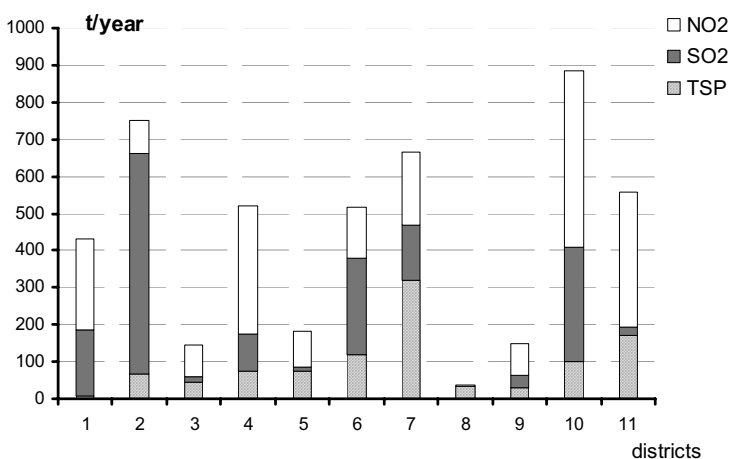
Figure 2. Structure and emission mass from stationary sources for administrative districts of Tashkent. The districts designation:

1-Akmal-Ikramovskiy	5- Sabir -Rakhimovskii	9- Sheykhantaur
2- Bektemir	6- Sergeli	10- Yunusabad
3- Mirabad	7- Khamza	11- Yakkasaray
4- Mirzo-Ulugbek	8- Chilanzar	

2.3. CLIMATIC DATA

The climatic characteristics were calculated based on the data measured at the stations "Tashkent Observatory", "Tashkent Airport", High-Altitude Meteorological Complex (HMC) "Tashkent" installed at the TV station tower. It is necessary to mention that the data of the high-altitude complex were processed for the first time for since the station started to operate. The differences in the wind roses for these stations (Figure 3) show:

- for "Tashkent Observatory" that eastern (24.2%) and north-western (17,3%) winds prevail and average wind speed is 1,2 m/sec,
- for "Tashkent Airport" that north-eastern winds prevail (23%)and the average wind speed is 2,7 m/sec,
- for HMC "Tashkent" that northern winds prevail (45%)and the average wind speed at the weather-vane level is 1,7 m/sec.
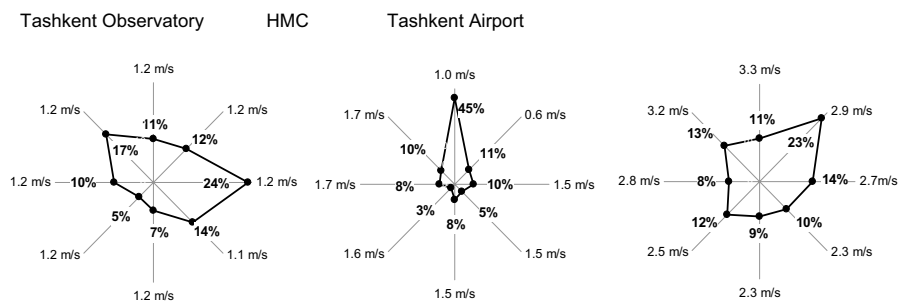
Figure 3. The annual average wind roses for meteorological stations of Tashkent city for 2003.

The frequent occurrence of weak winds (up to 70%) indicates the bad ventilation of the territory, especially at night time.

The climatic air pollution potential[3] is used for an estimation of climatic peculiarity of pollutant transfer and dispersion in the atmosphere. The statistical method is applied for calculation of the climatic air pollution potential. Frequency of ground inversions, air stagnation, fogs, and wind speeds of 0-1 m/s are meteorological factors necessary for its calculation. According to the conditional classification, the air pollution potential is divided into the classes: low (< 2.4), moderate (2.4-2.7), heightened (2.7-3.0), high (3.0-3.3) and very high (>3.3).

According to the results of previous aerological studies[4] the territory of Tashkent is attributed to the class of the very high air pollution potential (3.6–3.9). The mean daily value of the air pollution potential increases from 2.7 in the north-eastern city outskirts to 3.3 in the central part. It gradually increases in the south and south-east up to 3.7 and reaches 4 at night. The frequent occurrence of the surface temperature inversions (40–60%) impedes convective flows and dispersion of pollutants in the urban atmosphere. Often ground inversions with a very weak wind cause the air stagnation and accumulation of pollutants in the ground layer. The preliminary analysis of data measured at the High-Altitude Meteorological Complex "Tashkent" proves the existence of an uplifted inversion layer.

The classes of the atmospheric stability were selected in accordance with Pasquille's classification.

2.4. OBSERVATIONS OF THE AIR POLLUTION MONITORING SYSTEM

The air quality assessment is being carried out since 1966 using the observations data obtained by the monitoring system. At present such observations are conducted at 12 stationary points.

Maximum allowable concentrations[5] are used for air pollution assessment and control. Maximum allowable concentration is an ecological standard accepted within the CIS territory. MAC's are established for more than 400 substances and subdivided on a maximum single (averaged for 20 minutes) and daily average. The concentration measured for 20 minutes, is compared with the maximum single $MAC_{ms.}$ Monthly average and annual average concentrations are usually compared with the daily average MAC. MAC for TCP equals to 150 $\mu g/m^3$, sulphur dioxide –50 $\mu g/m^3$, nitrogen dioxide - 40 $\mu g/m^3$.

The database is developed based on the air pollution observations. The long-term mean monthly concentrations of the main pollutants are available for each measuring point. The level of urban air dust exceeds the MAC by a factor of 1.3-2 according to the mean long-term data. The level of the urban atmosphere pollution with the sulphur dioxide does not exceed the MAC and is within the range (0.2–0.34)xMAC. The mean concentrations of nitrogen dioxide in the city are at the level of 2.2 MAC.
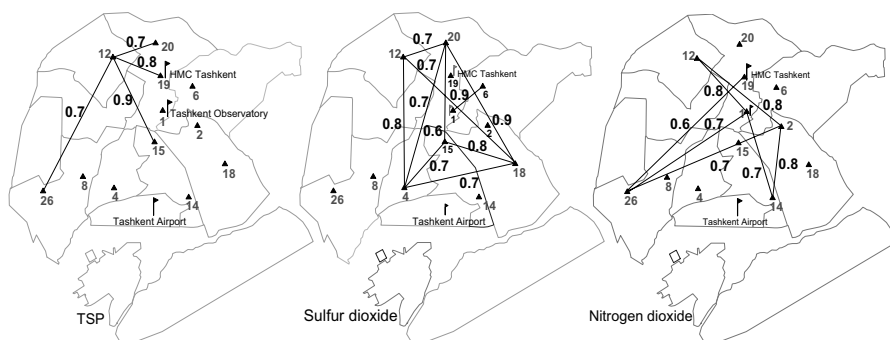
Figure 4. Values of correlation coefficients between monthly average pollutants concentrations measured on monitoring system points for 1996-2003.

▲ - the monitoring system points, __ - the districts borders

The correlation coefficients are calculated for different points using of mean monthly concentrations (Figure 4). The relationships between the pollutants concentrations measured at different points which prove the transfer of polluting substances along the prevailing wind directions is revealed.

3. Results

Model calculations were made for a period of one year with a 500 m step. The results are exhibited in Figures 5-6. Since the emission data are from 2003 to 2004, the model results are compared with the annual mean of TSP, sulphur dioxide and nitrogen dioxide concentrations which were observed at the monitoring stations during 2003.

TSP. The ground TSP concentrations in the city are generated by emissions from construction industry, TSP emitting machinery working plants and the manufacturing industry.

During the last years the TSP observations were only conducted at points N2, 4, 6, and 15. The highest TSP concentration is recorded at the point N4 -370 μg/m^3 (south part of the city). There is the largest transport nodal point in this area. Annual TSP concentrations at points N 2, N6, and N15 reached 95-114 μg/m^3.

The model results show, that the contribution of stationary sources to air pollution is not so significant. As follows from Fig. 5, two small zones with TSP concentration of about 130 μg/m^3 are observed; but they don't affect the monitoring data.

The cause of that discrepancy is as follows: the high natural background, the open building areas and highways generate the main contribution to the TSP concentration fields.

Sulphur dioxide: The surface field of the sulphur dioxide concentrations on the city territory is mainly affected by the thermal power stations (TPS), industrial boiler-houses and heat supplying lines which use natural gas with high sulphur content as fuel.

As follows from Table1 the measured concentrations were within 30-35 μg/m^3 for the most part.

The model results (Figure 5) reveal three pollution areas with the maximal annual concentration of 75-65 μg/m^3 (1.7-1.5 MAC) standing out against the background of the city territories. These zones are formed by large TPS and plant emissions.

The calculations lead to the conclusion, that air pollution by sulphur dioxide is mainly determined by stationary sources, but for calculations it is necessary to take into account seasonal changes of industrial activity.

Nitrogen dioxide: The ground field of nitrogen dioxide concentrations is formed by the emissions from TPS, heat supplying lines, mobile vehicles (traffic, railway and air transport) and foundries.

TABLE 1. Comparison of measured and calculated concentrations at 12 observation points of the Tashkent monitoring system.

N	1	2	4	6	8	12	14	15	18	19	20	26
sulphur dioxide ($\mu g/m^3$)												
Obs.	22	35	33	33	30	30	35	32	30	36	34	32
MR	60	60	40	50	40	50	40	60	60	75	40	30
nitrogen dioxide ($\mu g/m^3$)												
Obs.	20	102	45	50	86	94	117	196	77	104	71	112
MR	35	35	40	50	35	40	45	45	35	35	35	30

N – points numbers, Obs. –observation data, MR – modeling results
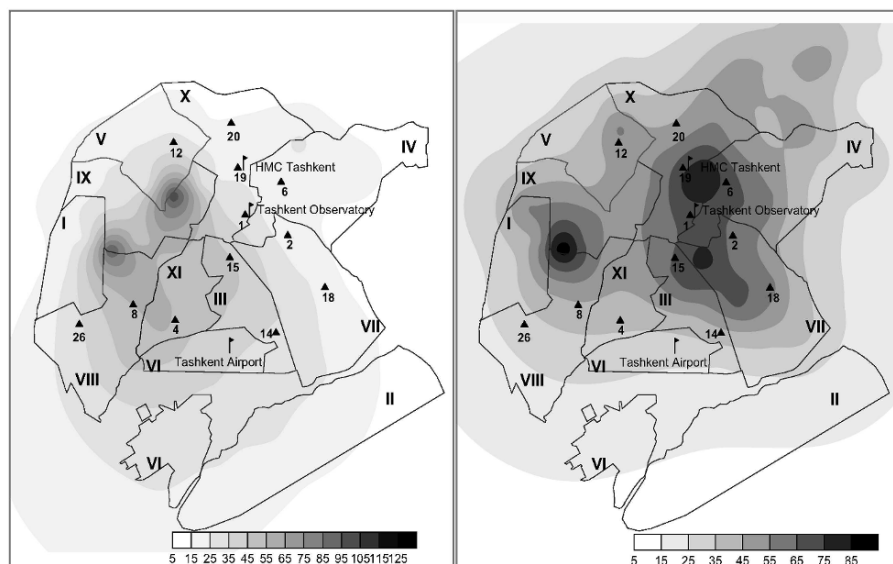
Figure 5. Annual average ground concentrations of TSP and sulphur dioxide ($\mu g/m^3$) in Tashkent. 2003.

▲ - monitoring system points, **II-** districts designation, ___ - districts borders

Maximum concentrations (196 μg/m³⁾) have been observed (Table 1) at the point N15 and large values of NO_2 at the points N14 (117 μg/m³), N19 - (104 μg/m³), N26 (112 μg/m³). It is necessary to note, that points NN 15, 19 are situated near arterial roads, N26 – near taxi station.

Maximum calculated concentrations (Figure 6) are found in the north-eastern outskirts of the city; they are equal to 60-75 μg/m³. This is caused by industrial emissions in this area.
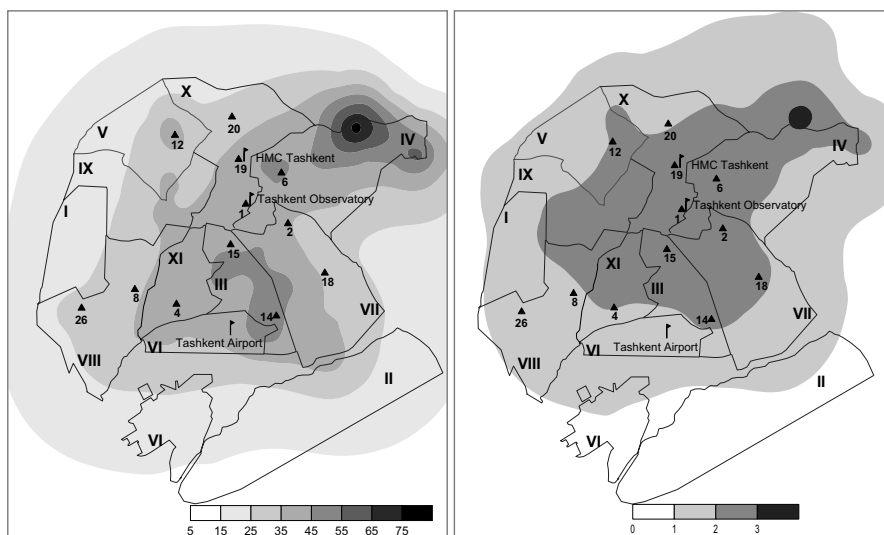
Figure 6. Annual average ground concentrations of nitrogen dioxide (μg/m³) and CAPI₃ values in Tashkent. 2003.

▲ - monitoring system points, **II** - districts designation, ___ - districts borders

The discrepancies observed and calculated values are explained by the following reasons:

- the calculations did not take into account the effect of traffic,
- the location of the monitoring system points does not properly reflect the peculiar features of emissions from some industrial enterprises.

Industrial sources of nitrogen are of particular importance in Tashkent. They account for about 40% for the nitrogen emissions.

The complex air pollution index[5] for three pollutants (CAPI₃) has been calculated on the basic of the model results. That parameter is used for total air pollution assessment of a number of pollutants

$$CAPI_m = \sum_{i=1}^{m} \left(\frac{C_i}{MAC_i} \right)^{c_i}$$

here:

C_i- annual average concentration *of* pollutant *i*;

MAC_i- daily average maximum allowable concentration *i*-pollutant;

c_i- the factor weighing the impact of the pollutant (0.85-1.5);

m – number of pollutants.

$CAPI_m$ indicates how many times the total level of air pollution exceeds the allowable value of the considered pollution set as a whole. There are four ranges of $CAPI_3$: $CAPI_3 < 3$ –allowable level, $3 < CAPI_3 < 5$ –increased level, $5 < CAPI_3 < 7$ - significant, $CAPI_3 > 7$ - high level of urban air pollution.

For the largest part of the city territory the indices are less than 3 (Figure 6). This means that air pollution caused by stationary industrial sources is within the limits of permissible load for the pollutants under consideration.

4. Conclusions

The model results are comparable to the observations of the monitoring system. In spite of the fact, that most $CAPI_3$ values are in the allowable range, zones of increased concentrations of nitrogen dioxide and sulphur dioxide have been identified in residential areas, where no monitoring stations have been established till now. For an estimation of risk in these zones comprehensive modeling is indispensable if reliable assessment of air pollution impact in such areas is sought.

References

1.   S. Calvert, H. Englund (Ed.) (1988) Handbook of air pollution technology, Metallurgy, Moscow (in Russian).
2.   EPA-454/B-95-003a. User's guide for the industrial source complex (ISC3) dispersion models. Volume I - User instructions: www.ess.co.at/AIRWARE/ISC3/isc3vol1.
     Volume II-Description of model algorithms:www.ess.co.at/AIRWARE/ISC3/-sc3vol2.
3.   E. Yu. Bezuglaya Meteorological potential and climatic peculiarities of urban air pollution, Gidrometeoizdat, Leningrad,1980.
4.   K.E. Zcerfas Climatic conditions of pollutant distribution in an atmosphere in territory of Uzbekistan, Gidrometeoizdat, Moscow, 1987.
5.   RD 52.04.186-89. Guide for air pollution control. - the State committee of the USSR on hydrometeorology. - Moscow, 1991.

DEVELOPING TECHNICAL APPROACHES TO MAN-CAUSED RISK ESTIMATION FOR THE KRASNOYARSK REGION

ALEXANDER TRIDVORNOV*
Institute of Computational Modelling SB R AS

VITALIY KOUROHTIN
 Siberian State Technological University

VLADIMIR MOSCVICHEV
Institute of Computational Modelling SB R AS

Abstract. On the Krasnoyarsk region territory more than 80 kinds of emergency situations are possible. The natural ones are floods and disastrous freshets, forest fires, storms, snowfalls etc. The technogenic ones are nuclear contamination, big industrial accidents and fires, including the accidents with release of dangerous chemicals. Statistical risk analysis of emergency situations in the Krasnoyarsk region shows that the risk, connected with technogenic emergency situations, is on the level 25 deaths of people per year. The individual risk of death is about $2 \cdot 10^{-5}$ men per year, the traumatism risk about $6 \cdot 10^{-5}$ men per year, the risk of life conditions disturbance about $5 \cdot 10^{-3}$ men per year. The death risk for men under emergency situations is considerably larger than the level of admissible risk specified in the European standards. It is one of the highest in the Eastern Siberia and in all Russia. This article gives a generalized approach to the estimation of industrial risk for the Krasnoyarsk region.

Keywords: Industrial risk assessment; large area; geo-information technologies

---

*To whom correspondence should be addressed. Alexander Tridvornov, Institute of computational modeling SB R AS

1. Introduction

We assume as a basic quantitative safety index the risks determined by the product of a dangerous (unfavourable) event (breakdown, catastrophe, emergency) occurrence probability and an average of damage distribution from this unfavorable event. The main index for analysis of man-caused risks R is the functional F_R in Eq. (1):

$$R = F_R\{U,P\} = \sum_i F_{R_i}(U_i, P_i) \tag{1}$$

where U is an average distribution of total damage from unfavourable events. P is the probability of occurrence of an unfavourable event; i characterizes different kinds of unfavourable events and processes leading to emergencies.

The calculation of man-caused risk from dangerous industrial enterprises is based upon the principle of superposition of the population damage probabilistic field in space and time and the spatial distribution of population. In this way an estimate of victims (for example, the number of inhabitants exposed to man-caused risk) is assigned to each grid point and the probability of damage with different degrees of severity is determined.
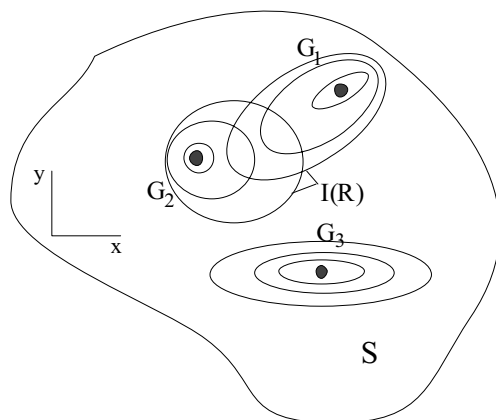
Figure 1. Visualization of complex risk estimation in a territory.

2. Methodology

While analyzing endangered territories it is necessary to consider complex threats distributed in the studied area. Let us assume that it is necessary to perform the risk analysis for an area S containing several danger sources G_k,

$k = 1, n$ (Figure 1). Then a "classical" complex risk analysis methodology can be carried out as follows:

An area S which requires risk analysis is shown on the territory map. Danger sources G_k are defined and the probabilities $P(t)$ (of intensity λ) of accidents, catastrophes, natural disasters are determined. Zones of damage and loss $U(x,y)$, as a function of losses from each considered danger source U_k, are calculated:

$$U(x, y) = U_1 \cap U_2 \cap U_3 ... \cap U_n \qquad (2)$$

The possibility of non-linear interference of losses is also considered.
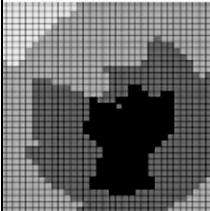
Isolines $I(R)$ of equal risk are determined for the territory. If there is no overlapping of risk zones, then the danger sources belong to non-interacting ones and their risks are considered to be non-complex ones. If the risk zones overlap then threat severity weight indices α are assigned to each danger source. If on the territory under study there are N man-caused danger sources whose damage zones may overlap, then as a first approximation the complex territorial risk $R_\Sigma(t)$ may be expressed as a sum (Eq. (3)) or product (Eq. (4)):

$$R_\Sigma(t) = \sum_{i=1}^{N} \alpha_i R_i(t) \qquad (3)$$

$$R_\Sigma(t) = \prod_{i=1}^{N} \left[R_i(t) \right]^{\alpha_i} \qquad (4)$$

Equation (3) may be used for simple summation of damage intensities. Multiplication is applicable in cases of mutually intensifying damage effects. In both cases the indices a_i reflect the "weight" of damage effects of each danger source. For calculation of the risk it is possible to use the methods listed in Table 1. Using GIS-technologies allows automating the most labour-consuming visualisation of risk isolines, sources and integrated losses.

TABLE 1. Methods used for risk assessment.

METHOD	Advantages	Disadvantages	Form of result	Spatial/land-use planning application
Rapid Risk Assessment (RRA)	The PRA method is quick and easy to conduct. It is powerful as a screening tool.	Too coarse, may be misleading due to potential for overestimation of result.	Estimation of casualties (individual and collective risk). Probability of death.	Not applicable
Quantitative Risk Assessment (QRA)	QRA is powerful method for risk assessment. It enables systematic hazard and consequence analysis. It provides trustful results for risk reduction policy development, inspection/auditing, emergency and land-use planning.	Complex, time consuming, extensive data requirement.	Probability of incident outcome. Impact area is presented with in whish certain consequences can be expected (overpressure thermal radiation, toxic release).	
Accidental Risk Assessment Methodology in the Seveso II Directive (ARAMIS)	ARAMIS risk Assessment methodology is trustworthy and straightforward. Is provides results useful in a licensing process and spatial/land-use planning. Intended for multiple users.	Requires familiarity with various risk assessment tools. Robust vulnerability analysis.	Probability of incident outcome. Impact area is presented in a form of Severity index and Vulnerability index – transformed into grid around hazardous installation.	

3.   Preliminary results

The described approach has been realized in a prototype of the automated system for territorial risk estimation which is being developed (Fig. 2). The calculation of after-effects of chemical accidents has been done using the

method "TOKSI"[2] integrated into an ArcMap with the help of modules specially designed in Visual Basic. The territory contamination forecast is carried out as a function of time from the occurrence of the accident, type and mass of released substances for given atmospheric conditions.

Set of databases according to the danger sources:
Dangerous processes and substances;
Dangerous substances properties;
Amounts of dangerous substances;
Accidents scripts;
Scripts frequencies.

Toxicological criteria

GIS INTERFACE
Analysis:
Selecting a danger source for risk estimation;
Calculating the accidents after-effects;
Calculating the number of fatal and affected victims;
Risks calculation.
Visualization:
Individual risks isolines;
Collective risks isolines;
Social risk.

Accidents after-effects Forecasting methods

Methods for accidents probabilities calculation

Tools:
1. Visual Basic;
2. ArcGIS Spatial;
3. ArcGIS Geostatistical;
4. ArcGIS 3D.

Area map

Danger sources

Data on the territory

Demographic data

Figure 2. Block diagram of GIS analysis of territorial risk.

The data generated by TOKSI are two-dimensional tables of toxic dose values at locations (x, y). These data are imported into GIS as a dot layer of toxic dose field. Then with the help of ArcGIS Spatial Analyst (employing the Spline Tension method) the dot-layer is interpolated for obtaining a raster layer of the toxic dose. As a result we get a map of the spreading chemical cloud where the value of the toxic dose is known for every point; and zones of lethal threshold and other effects are determined (Figure 3).
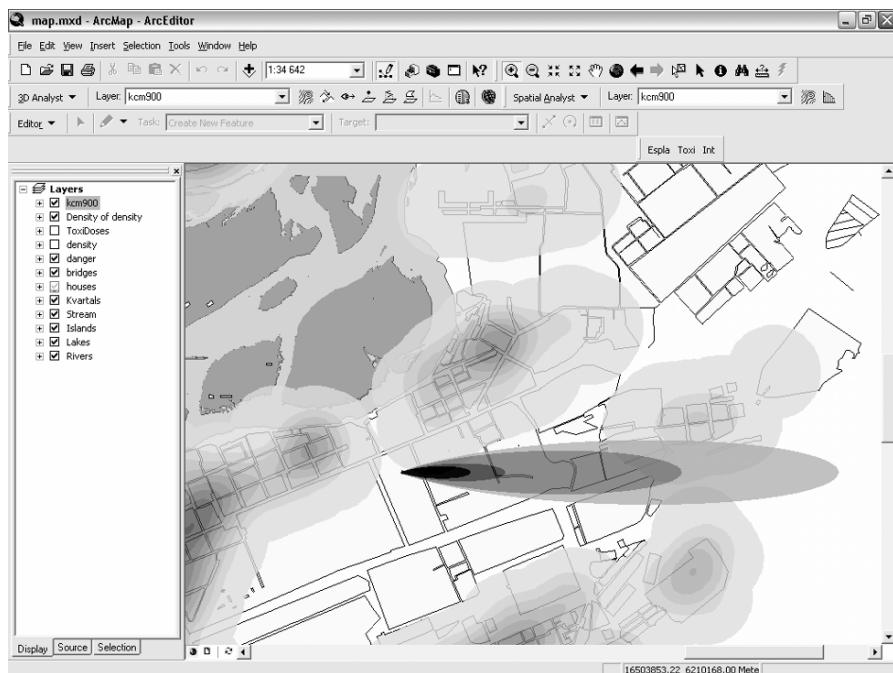
Figure 3. Results of calculation of the relative impact of a chemical accident (point source) using the TOKSI method; for Krasnoyarsk as an example.

References

1. N.A. Makhutov. Construction Strength, Life Time and Industrial Safety In 2 parts. / N.A. Makhutov. – Novosibirsk: Science, 2005 . – Part.2: Substantiation of Life Time and Safety. – 610 p.
2. Methods of estimation of chemical accidents consequences "TOKSI-2". Collection of documents. Series 27. Number 2/Group of authors – 2nd edition, corrected and completed.- M.: State Unitary Enterprise Scientific and Technical Center "Industrial safety", 2002. – 208 p.
3. Security of Russia. Legal, social and economical, scientific and technical aspects. Regional security problems. Krasnoyarsk region. – M.: "Znanije", 2001, 576 p.

MODELING AIR QUALITY AND DEPOSITION OF TRACE ELEMENTS IN THE VICINITY OF A CEMENT PLANT FOR HUMAN HEALTH RISK ASSESSMENT

HOCINE ALI-KHODJA*
Département de Chimie, Faculté des Sciences, Université Mentouri, Constantine 25017, Algeria

LEILA AOURAGH
Département d'Hygiène et Sécurité, Faculté des Sciences de l'Ingénieur, Université Hadj Lakhdar, Batna, Algeria

Abstract. No previous investigations of airborne particulate and trace metal levels have been undertaken in the area surrounding the cement plant located in the vicinity of the town of Didouche Mourad. The impact of this plant has been the subject of much controversy. Data related to suspended matter would therefore be very useful and informative. This town with a population of 36500 is located 550 meters above sea level and north of the city of Constantine. It has been suspected of having an air pollution problem originating from the cement plant situated 3 km south of it. Modeling of airborne concentrations and total deposition rates of trace metals originating from the cement plant through the use of ISCST3 software allowed the estimation of the average exposure of the population and thus quantification of the human health risks for the year 2003. University flats which are situated at the tip of east Didouche Mourad were used as a reference area for the assessment of health hazards.

Keywords: trace metals; TSP; deposition; airborne concentrations; health risks.

_____
 *To whom correspondence should be addressed. Hocine Ali-Khodja, Département de Chimie, Faculté des Sciences, Université Mentouri, Constantine 25017, Algeria

141

1. Experiment

1.1. DUST DEPOSITION MEASUREMENTS

A dust deposition gauge constructed according to the French standard AFNOR NF X43-006 with a 10 cm radius was collocated with a meteorological station. To sample dust deposition, the gauge is filled with 10 l of distilled water and left exposed to settling dust and rain for a period of 30 days. Rinsing of the internal surface of the sampler with distilled water is carried out after each sampling period to detach deposited particles. The sampling solution is then poured in a clean propylene container and then taken to the laboratory to perform the filter weighing.

1.2. MODELING METHODOLOGY

ISCST3 (Industrial Source Complex Model) is a steady-state Gaussian plume model used to assess pollutant concentrations from a wide variety of sources associated with an industrial complex. The ISCST3 software was put forth by the US Environmental Protection Agency and adapted by Lakes Environmental[1]. This model accounts for settling and dry deposition of particles, building downwash, flat and complex terrain. Hourly emission rates can be specified for one or more sources. Hourly meteorological data from separate surface and profile data files are used. The surface met data file is read into the model from a separate data file and contains observed and calculated surface variables, one record per hour.

1.3. INPUT DATA

1.3.1. *Meteorological data*

Meteorological data are pre-processed by a program called PCRAMMET[2]. The minimum input data requirements to PCRAMMET are the twice-daily mixing heights and hourly surface observations of wind speed, wind direction, dry bulb temperature, opaque cloud cover, and ceiling height. For dry deposition estimates, station pressure is recommended, and for wet deposition estimates, the precipitation type and the amount are required for those periods during which precipitation was observed.

1.3.2. *Emission source parameters*

The emission source considered in the modeling study is the kiln's stack from which the flue gas containing dust and metal constituents are discharged. A raw meal preheating system, utilizing the hot flue gases from the kiln directly to preheat the incoming feed, is used. According to the local maintenance staff of the cement plant, the average efficiency of the dust arrestment equipment is about 75%. The physical height and the diameter of the stack are 80 m and 4 m respectively. The stack gas exit velocity and temperature are 7.95 m s^{-1} and 413 K respectively. The emission factor for total suspended particulate matter for a preheater kiln with electrostatic precipitator is 0.13 kg Mg^{-1} of clinker[3]. On the basis of the above-mentioned dust abatement equipment, the emission factor would equal 32.5 kg Mg^{-1} of clinker since an emission factor of 130 kg Mg^{-1} is predicted by the EPA for a kiln preheater without any dust collection devices. Emission factors for trace elements have been derived accordingly[3]. Particle size distributions for emissions from dry process kilns are presented in Table 1[3]. Furthermore, actual clinker cooler emissions were neglected for they represent only a tiny fraction of what is emitted from the kiln's stack.

TABLE 1. Average particle size distribution for dry process cement kilns.

Particle size, μm	Cumulative Mass Percent Equal To Or Less Than Stated Size for Dry process
2.5	18
5	30
10	42
15	44
20	100

1.3.3. *Topographical data*

Digital Elevation Models (DEMs) that are arrays of elevations based on 100- by 100-meter data spacing with the Universal Transverse Mercator (UTM) projection have been produced manually by interpolating elevations from contours digitized from 1:25,000-scale topographic maps. The data are processed to produce a DEM with a 100-m sampling interval. The digitized area around the cement plant kiln's stack is equal to 10 km x 10 km. These data are used by ISC-AERMOD View to extract terrain elevations for the selected receptors.

1.3.4. *Human health risk assessment*

The exposure routes considered are inhalation of the metal elements and their ingestion as soil dust. We assume that all of these elements are attached to particles of inhalable size. Dietary intakes, ingestion of water and contribution from other exposure pathways have not been considered due to a lack of data. The uptake of contaminants from dermal contact accounts for only a tiny fraction of the administered dose and has not been taken into account. This study focuses on exposures of adults and 2-year old children to the trace elements Pb, Mn, Cr, Cu, Cd, As and Hg.

In order to assess chronic health hazard for non carcinogenic effects, screening tools such as RfDs and MRLs will be used, when available, to assess dose for chronic inhalation and/or oral exposure or minimum risk levels to metal elements that may pose risk to the exposed populations 4, 5. Minimum risk levels (MRLs) are derived using a modified version of the risk assessment methodology the US Environmental Protection Agency (EPA) provides to determine reference doses for lifetime exposure (RfDs)4. They provide valuable guidelines to protect public health but cannot be enforced by law. Carcinogenicity assessment for lifetime exposure from inhalation and/or oral exposure is based on air risk units.

2. Results

2.1. A SUMMARY OF THE ANALYSIS OF DATA

A summary of the results of modeling seven chemical species during the year 2003 are shown in Table 2. These values were modeled for a residential area comprising university flats in the newly urbanized area of the town of Didouche Mourad (Figure 1).

TABLE 2. Modeled metal concentrations (ng m^{-3}).and depositions (μg m^{-2}.day^{-1}).

Metallic element	Pb	Mn	Cr	Cu	Cd	As	Hg
Concentrations	76	43	0.72	550	0.9	1.4	23
Deposition rates	583	96	0.41	4219	6.8	10.4	192

2.2. DUST FALLOUT

The assessment of human health risks relies upon the on-site measurement of total dust fallout. The measured daily average dust fallout in the area of

university flats was 686 mg m^{-2}.day^{-1}. The latter exceeds the British "custom and practice" limit of 200 mg m^{-2}.day^{-1}, the Australian standard for "unacceptable reduction in air quality" of 333 mg m^{-2}.day^{-1}, and the German TA-Luft criteria[7] for "possible nuisance" of 350 mg m^{-2}.day^{-1}.
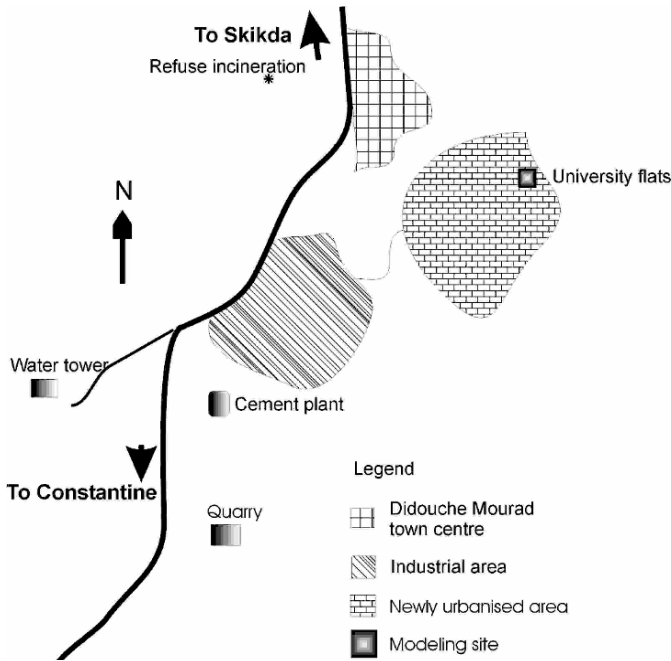
Figure 1. Location of the modeling site in a residential area of Didouche Mourad.

2.3. HEAVY METALS

The modeled average metal element concentrations and deposition fluxes are compared with the appropriate established standards. Daily ventilation rates of 20 m^3 day^{-1} for adults and 6 m^3 day^{-1} for 2-year old children are used in the human health risk characterization[5]. In all cases, we assume two exposure scenarios. The first one assumes that 20 mg day^{-1} of dirt is ingested by adults and 80 mg day^{-1} by children[8,9]. The second scenario assumes that the ingestion rates are 100 mg day^{-1} and 200 mg day^{-1} respectively[5]. The received doses are indicated in Table 3.

2.3.1. *Lead*

The modeled annual average Pb concentration was 76 ng m^{-3}. This value was lower than the annual standard[10] of 500 ng m^{-3} or the quarterly EPA standard[11] of 1.5 µg m^{-3}. However, the modeled Pb deposition was 583 µg m^{-2}.day^{-1} which is exceeds by a factor of 5.83 the German TA-Luft annual standard[12] of 100 µg m^{-2}.day^{-1}. Such dust is then an important Pb carrier for young children[13,14]. The average dust deposition through the period of study was 686 mg m^{-2}.day^{-1}. It follows that the average dust content of Pb was 850 µg g^{-1}. Assuming daily ventilation rates of 20 m^3 day^{-1} for adults and 6 m^3 day^{-1} for 2-year old children[5], the administered Pb dose originating from TSP for adults and children was 1.52 and 0.46 µg respectively. Furthermore, supposing that 20 mg day^{-1} of dirt is ingested by adults and 80 mg day^{-1} by children, the expected daily amounts of Pb ingested this way were 16.99 and 67.96 µg respectively. The total calculated intake of Pb was 18.51 and 68.42 µg respectively.

Dust represents the main source of Pb contamination. If the ingestion rates of soil dust are assumed to be 100 and 200 mg day^{-1} for adults and 2-year old children[5], then the daily dosages of lead are 84.94 and 169.89 µg day^{-1} respectively. The total calculated dosages of Pb would be 86.46 and 170.35 µg day^{-1} respectively (Table 3). These estimated values are minimal since Pb exposure from canned food and water contaminated from contact with plumbing has not been taken into account. Provisional maximum tolerable weekly intakes of Pb are 50 µg kg^{-1} body weight for adults and 25 µg kg^{-1} body weight for children[6] corresponding to 7.14 and 3.57 µg kg^{-1}.day^{-1} respectively. There exists a potential risk of exposure in both scenarios for children.

2.3.2. *Manganese*

The arithmetic mean during the year 2003 was 43 ng m^{-3}. This value is acceptable compared to the annual average guide value of 0.15 µg m^{-3} set by the WHO[12]. The average Mn fallout was 202 µg m^{-2}.day^{-1} which is lower[15] than the German TA luft standard of 250 µg m^{-2}.day^{-1}. The daily intake of Mn from ambient air is 0.019 µg kg^{-1}.day^{-1} for children. The latter exceeds the reference dose for chronic inhalation exposure (RfD) of 0.0114 µg kg^{-1}.day^{-1} set up by the US EPA[5]. The mass of Mn ingested from soil dust is 0.21 and 2.05 µg kg^{-1}.day^{-1} respectively which is less than the oral RfD of 10 µg kg^{-1}.day^{-1} according to the second scenario of dust ingestion[5] (Table 3).

2.3.3. *Chromium*

In the absence of better information, a conservative approach would assume Cr in the air is predominantly hexavalent. It should be noted that Cr concentration in air is often expressed as total Cr and not Cr (VI). The average ambient air concentration of Cr was 0.72 ng m^{-3} during the period of study. At an air concentration of Cr(VI) of 1 μg m^{-3}, the lifetime risk is estimated to be 4×10^{-2}. An excess lifetime risk of about 3: 100 000 can then be associated to the measured concentration. In terms of fallout to the ground, the deposition rate was 0.41 μg m^{-2}.day^{-1}. This value is in conformity with the German annual standard[15] of 250 μg m^{-2}.day^{-1}. The inhalation and ingestion intake doses of Cr by adults and children in Didouche Mourad are shown in Table 3. These results indicate that the maximum ingested Cr dose was 9 10^{-3} μg kg^{-1}.day^{-1} which is less than the oral RfD of 3 μg kg^{-1}.day^{-1} suggested by the USEPA[16]. The inhalation intake was negligible.

2.3.4. *Copper*

Modeled concentrations of Cu in the area of university flats over the period 1/1/2003-31/12/2003 averaged 550 ng m^{-3}. The latter exceeds the reference concentration[17] for inhalation of 20 ng m^{-3}. Cu deposition rate was estimated at 4220 μg m^{-2}.day^{-1}. It exceeds the German TA-Luft annual standard[15] of 250 μg m^{-2}.day^{-1}. An MRL of 20 μg kg^{-1}.day^{-1} has been derived for acute-duration oral exposure (1 – 14 days) to Cu and has also been adopted as the intermediate-duration oral MRL (14-365 days)[18]. The calculated intakes of Cu from soil dust are all well below the minimum risk level excepted in the case of both exposure scenario for children which amount to 36.4 and 90.65 μg kg^{-1}.day^{-1} (Table 3).

2.3.5. *Cadmium*

The mean level of modeled daily concentrations of Cd was 0.9 ng m^{-3}. It is less than the annual WHO guideline[10] of 5 ng m^{-3}. The deposition rate of this metal was 7 μg m^{-2}.day^{-1}. This value is 3.5-fold the German TA-Luft[12] annual standard of 2 μg m^{-2}.day^{-1}. The provisional tolerable weekly Cd intake of 400-500 μg for an adult should not be exceeded[19]. The intake values of 0.21 and 1 μg day^{-1} are in conformity with such a guideline. Moreover, an MRL of 0.2 μg Cd kg^{-1}.day^{-1} has been derived for chronic oral exposure (>365 days)[20]. Such a level was not exceeded for adults and children for both scenarios (Table 3).

2.3.6. *Arsenic*

Arsenic is a human carcinogen. When assuming a linear dose–response relation, a safe level for inhalation exposure cannot be recommended. At an air concentration of 1 µg/m^3 an estimate of lifetime risk[10] is 1.5 10^{-3}. The modeled average daily As concentration was 1.38 ng m^{-3} in the studied area. An excess lifetime risk of about 2: 10^6 can then be associated to the measured concentration. The amount of Ni deposition was 10.4 µg m^{-2}.day^{-1}. The reference dose for chronic oral exposure (RfD) to As[10] being equal to 0.3 µg kg^{-1} day^{-1}, there is no risk associated with chronic exposure to soil dust in the case of both scenarios for adults and 2- year old children Table 3).

2.3.7. *Mercury*

In this study, the mean modeled ambient air concentration of Hg was 23 ng m^{-3}. It is less than the New Zealand guideline value[21] of 330 ng m^{-3}. The modeled deposition rate of Hg was 192 µg m^{-2}.day^{-1}. A Joint FAO/WHO Expert Committee on Food Additives established a provisional tolerable weekly intake of 0.3 mg of total mercury per person[22]; this amount is equivalent to 3.15 and 0.6 µg per kg of body weight per day for children and adults respectively. These values are exceeded for children according to the second scenario.

3.   Conclusion

Ambient air concentrations of Pb, Mn, Cu, Cd and Hg were relatively small compared to the WHO guideline values, while those of Cu and carcinogenic element Cr and As pose a threat to health. Chronic inhalation of manganese may pose a threat to children's health. Furthermore, deposition of metal elements leads to concentrations in soil dust that present, in terms of non carcinogenic effects, a potential risk to children exposed via the oral route to Pb, Cu and Hg for both exposure scenarios considered. Quantification of the human health risks indicated that direct ingestion of contaminated particles represents a much more important pathway of exposure to trace metals than the inhalation route. The potential for adverse effects is greater for children than for adults.

TABLE 3. Daily intake of metal elements from TSP and soil dust.

Metal element	Media	Concentration	Adults (70 kg) intake μg day⁻¹	μg kg⁻¹ day⁻¹	2-year old children (13.6 kg) intake μg day⁻¹	μg kg⁻¹ day⁻¹	Standards	Ref.
Pb	Air (ng m⁻³)	76	1.52	0.02	0.46	0.03	Tolerable daily intakes = 7.14 and 3.57 µg kg⁻¹.day⁻¹ for adults/ and children respectively	[6]
	Soil dust (µg g⁻¹)	850	16.99 [a]	0.24 [a]	68 [a]	**5.00 [a]**		
			85 [b]	1.21 [b]	170 [b]	**12.49 [b]**		
Mn	Air (ng m⁻³)	43	0.85	0.012	0.25	**0.019**	RfD for chronic inhalation and oral exposures = 0.0114 and 10 µg kg⁻¹.day⁻¹ respectively	[5]
	Soil dust (µg g⁻¹)	139	2.78 [a]	0,04 [a]	11.13 [a]	0.82 [a]		
			13.92 [b]	0.20 [b]	27.84 [b]	2.04 [b]		
Cr	Air (ng m⁻³)	0.72	0.0144	$2.1\ 10^{-4}$	$4\ 10^{-3}$	$3\ 10^{-4}$	RfD for chronic oral exposure = 3 µ g kg⁻¹.day⁻¹	[16]
	Soil dust (µg g⁻¹)	77	0.012 [a]	$1.7\ 10^{-4}$ [a]	0.047 [a]	$3.5\ 10^{-3}$ [a]		
			0.06 [b]	$8.5\ 10^{-4}$ [b]	0.12 [b]	$8.6\ 10^{-3}$ [b]		
Cu	Air (ng m⁻³)	**550**	11	0.15	3.3	0.24	RfD for chronic oral exposure = 20 µ g kg⁻¹.day⁻¹	[18]
	Soil dust (µg g⁻¹)	50	123 [a]	1.75 [a]	492 [a]	**36.2 [a]**		
			615 [b]	8.8 [b]	1230 [b]	**90.4 [b]**		
Cd	Air (ng m⁻³)	0.89	0.017	$2.4\ 10^{-4}$	$5.3\ 10^{-3}$	$3.9\ 10^{-4}$	Tolerable weekly cadmium intake = 400-500 µg for an adult and chronic oral MRL (>365 days) = 0.2 µ g kg⁻¹.day⁻¹	[19, 20]
	Soil dust (µg g⁻¹)	9.9	0.2 [a]	$2.85\ 10^{-3}$ [a]	0.8 [a]	0.06 [a]		
			0.99 [b]	0.014 [b]	1.99 [b]	1.05 [b]		
As	Air (ng m⁻³)	1.4	0.02	$2.8\ 10^{-4}$	$8.2\ 10^{-3}$	$6\ 10^{-4}$	for chronic oral exposure (RfD) = 0.3 µg kg⁻¹.day⁻¹	[10]
	Soil dust (µg g⁻¹)	15.3	0.30 [a]	$4.2\ 10^{-3}$ [a]	1.23 [a]	0.09 [a]		
			1.51 [b]	0.02 [b]	3.06 [b]	0.22 [b]		
Hg	Air (ng m⁻³)	23	465	$6.6\ 10^{-3}$	139.6	$10.3\ 10^{-3}$	Provisional tolerable weekly intake = 3.15 and 0.6 µg kg⁻¹ day⁻¹ for children and adults respectively	[22]
	Soil dust (µg g⁻¹)	280	5.58 [a]	$7.9\ 10^{-2}$ [a]	22.35 [a]	**1.64 [a]**		
			27.9 [b]	0.39 [b]	55.9 [b]	**4.10 [b]**		

80 mg day   for children less than 2 years.

Scenario 2: Computed values are for an ingestion rate of 100 mg day⁻¹ for adults and 200 mg day⁻¹ for children less than 2 years.

Intakes exceeding the corresponding standards are emboldened.

Acknowledgements

References

1. Tesse, L.T., Cristiane, L.T. and Michael, A.J., Isc-Aermod View user's guide, Windows Interface for the U.S. EPA ISCST3, AERMOD, and ISC-PRIME Air Dispersion Models, Lakes Environmental Software, Waterloo, Ontario, Canada (2000).

2. Tesse, L.T., Cristiane, L.T. and Michael, A.J., Rammet View user's guide. Windows Interface for the U.S. EPA PCRAMMET Program, Lakes Environmental Software, Waterloo, Ontario, Canada (2000).

3. United States Environmental Protection Agency, Air Chief, Portland cement manufacturing, Emission Factor and Inventory Group EMAD/OAQPS, Version 9, EPA 454/C-01-003, pp. 9–15 (2001).

4. Barnes, D.G. and Dourson, M., Reference dose (RfD): Description and use in health risk assessments. *Regul Toxicol Pharmacol* **8**:471–486 (1998).

5. LaGrega, M.D., Buckingham, P.L. and Evans, J.C., Appendix B: Toxicological data. In: *Hazardous waste management*. McGraw-Hill, Singapore, pp. 1053–1077 (1994).

6. Organisation Mondiale de la Santé (OMS), *Rapport de la 30ᵉ réunion du Comité mixte FAO/OMS d'experts des additifs alimentaires*, Rome, 2–11 juin, 1986, Genève (1987).

7. Environment Agency, Air quality criteria. In: *Monitoring of Particulate Matter in Ambient Air around Waste Facilities*. Technical Guidance Document (Monitoring) M17, Environment Agency, Bristol, UK, pp. 23–32 (2003).

8. Binder, S., Sokal, D. and Maughan, M.A., Estimating soil ingestion: the use of trace elements in estimating the amount of soil ingested by young children. *Arch. Environ. Health*, **41**: 341, (1986).

9. Clausing, P., Brunekreef, B. and van Wijnen, J.H., A method for estimating soil ingestion by children. *Int. Arch. Occup. Environ. Health*, **59**: 73, (1987).

10. WHO, Inorganic pollutants. In: *Air Quality Guidelines for Europe*, Second Edition, Regional Office for Europe, WHO Regional Publications, European Series, No. 91, Copenhagen (2000).

11. Agency for Toxic Substances and Disease Registry (ATSDR), Public Health Statement. In: *Toxicological profile for lead*, U.S. Department of Health and Human Services, Public Health Service Atlanta, GA, pp. 13–17 (1999).

12. TA-Luft, *Erste Allgemeine Verwaltungsvorschrift zum Bundes-Immissionsschutzgesetz* (Technische Anleitung zur Reinhaltung der Luft **Vom** 24. Juli 2002). In: *GMBI*. 95 (2002).

13. U.S. Environmental Protection Agency, *Air quality criteria for lead*. Report N° EPA-600/8-83/028F (1986).

14. Drill S., Konz J., Mahar H. and Morse M., *The environmental lead problem: an assessment of lead in drinking water from a multimedia perspective*. Report N° EPA-570/9-79‑003, U.S. Environmental Protection Agency, (1979).

15. TA-Luft, *Erste allgemeine Verwaltungsvorschrift zum Bundes-Immissionsschutzgesetz* (Technische Anleitung zur Reinhaltung der Luft vom 27.2.1986). In: *GMBI*. 95, (1986).

16. Agency for Toxic Substances and Disease Registry (ATSDR), Regulations and advisories. In: *Toxicological profile for chromium,* U.S. Department of Health and Human Services, Public Health Service, Atlanta, GA, pp. 328–332 (2000).
17. California Environmental Protection Agency, *Determination of Chronic Toxicity Reference Exposure Levels*, (Draft), CalEPA, (1997).
18. Agency for Toxic Substances and Disease Registry (ATSDR), Appendix A. ATSDR minimal risk levels and worksheets. In: *Toxicological profile for copper - draft for public comment,* U.S. Department of Health and Human Services, Public Health Service, Atlanta, GA, pp. 3–4 (2002).
19. WHO, Cadmium. In: *Evaluation of certain food additives and contaminants*. Thirty-third Report of the Joint FAO/WHO Expert Committee on Food Additives, Technical Report Series No. 776, World Health Organization, Geneva, pp. 28–31 (1989).
20. Agency for Toxic Substances and Disease Registry (ATSDR), Appendix A. ATSDR minimal risk levels and worksheets. In: *Toxicological profile for cadmium,* U.S. Department of Health and Human Services, Public Health Service, Atlanta, GA, pp. 3–6 (1999).
21. Ministry for the Environment, *Ambient Air Quality Guidelines*, Air Quality Report No 32, PO Box 10–362, Wellington, New Zealand ISBN: 0-478-24064-3 (2002).
22. World Health Organization, Environmental health criteria 1, Mercury, International programme on chemical safety, Geneva, ISBN 92 4 154061 3.

SOURCE RECONSTRUCTION FOR ACCIDENTAL RELEASES OF RADIONUCLIDES

MONIKA KRYSTA, MARC BOCQUET*, NIS QUÉLO
CEREA, Research and Teaching Centre in Atmospheric Environment, Joint laboratory École Nationale des Ponts et Chaussées (ENPC)/EDF R&D, 6-8, avenue Blaise Pascal, 77455 Champs sur Marne, France. CLIME, Joint project INRIA/ENPC

Abstract. This report gives a short account on recent advances in the regional scale reconstruction of an accidental release of radionuclides. Variational techniques are used in conjunction with the Eulerian dispersion model Polair3D to determine the source of the release. New objective functions that better incorporate prior information on the source are designed and tested using observing system simulation experiment.

Keywords: source reconstruction; maximum of entropy; radionuclide dispersion

1. Motivation

Risk is interwoven with each human activity. Such a vital occupation like energy production is most often accompanied with continuous emission of substances that harm human health and alter their environment. The characteristics of environmental impact vary from one type of energy source to another. Nuclear energy contribution to persistent air pollution or greenhouse gas concentration is very limited. Nevertheless, although very unlikely, accidents may occur resulting in sizeable releases of radioactivity

_____
   *To whom correspondence should be addressed. Marc Bocquet, CEREA, Research and Teaching Centre in Atmospheric Environment, Joint laboratory École Nationale des Ponts et Chaussées (ENPC)/EDF R&D, 6-8, avenue Blaise Pascal, 77455 Champs sur Marne, France. CLIME, Joint project INRIA/ENPC; e-mail: bocquet@cerea.enpc.fr

to the atmosphere. Regional scale impact of an accident is driven by volatile fission products since refractory radio nuclides are likely to be deposited in the vicinity of a contaminating site.

Risks associated with a leak of radioactivity can only be evaluated if the amount of the rejected material is known. To a large extent, it is the case for a monitored release via a filtered stack. If, however, radioactivity is released to the atmosphere due to percolation through containment or worse its collapse or even its lack, the amount of emitted species would not be known. In these circumstances radioactivity measurements provide valuable, although indirect, information on the source. Mathematical techniques of data assimilation allow to couple measurement information with a model of physical phenomena and, further on, to reconstruct the source at origin of contamination. At regional scale source reconstruction means telling its location, the amount of released radioactivity and the temporal profile of emission. Variational data assimilation has been used to solve this problem in case of ETEX-I data (Robertson and Langner, 1997, 1998). This contribution illustrates an application of a recently introduced technique of inversion (Bocquet, 2005a, 2005b, 2005c), the maximum entropy method, to a reconstruction of a hypothetical source of radioactivity.

This report begins with the description of a hypothetical accident (section (2)). Next, the maximum entropy method is recalled in section (3). Section (4) illustrates the application of the method to the fictive release described in section (2).

2.   Hypothetical accident

Let us imagine a severe accident taking place at one of the European nuclear facilities. The Bulgarian power station in Kozloduy which hosts 4 functioning Soviet-type reactors (situation in 2005) has been chosen for this study. Despite numerous upgrades that have been made on them, the European Commission demands a shut-down of units 3 and 4, VVER-440/230 design, regarding them as posing significant safety and environmental risks because of inherent design deficiencies, notably low pressure containment of poor leak tightness.

The accident is hypothesised to result in a release of a large amount of activity, $2.3 \cdot 10^{17}$ Bq, due to a leak of ^{131}I, an abundant fission product. The release starts at 0900 UTC on 3rd May, 2001 and lasts for 12 hours. The temporal profile of the source has two equally long steps, the first one accounting for 75% of the released activity and the second one for the remaining 25% (see Fig. 2). Such a shape reflects features of an accidental release characterised by emission rate decreasing in time.

Accident consequences, namely radioactivity concentrations in the air, have been simulated with the chemistry transport model [CTM] Polair3D (Boutahar et al., 2004). The simulation period spreads from 0000 UTC 2nd May to 0000 UTC 9th May, 2001 and covers the release interval. The half-life time of ^{131}I, 8 days, is of the same order of magnitude as the simulated period and its daughter element, ^{131}Xe, is stable. Hence, radioactive decay contributes significantly to depletion of the radioactive cloud. As a consequence this phenomenon must be taken into account by the model along with the remaining depletion processes like dry deposition and wet scavenging (Brandt et al., 2002).

Beforehand, 50 monitoring stations were selected among all the ones constituting the European Radioactivity Environmental Monitoring network. They collect measurements during the entire period of simulation. Radioactivity concentrations are averaged over 3-hour intervals and taken with 3-hour frequency. The measurements are obtained by adding fictive observational noise to model outputs. The noise could represent up to 10% of the output value. Among all the measurements 896 have been randomly selected for further studies.

The remaining part of this paper presents the reconstruction of this accident performed on the basis of radioactivity measurements.

3. Maximum entropy method

Even before inversion has been performed, one may have some information on the source $\sigma \in R^{N}$. Statistical description of prior knowledge is encoded in the probability density function $\nu(\sigma)$. Information supplied by the measurements $\mu \in R^{p}$ increases the knowledge on the source and hence leads to an improved posterior probability density function $p(\sigma)$.

Transition from the prior pdf to the posterior one is achieved by maximising entropy function under the constraints imposed by measurements. The posterior pdf is the one that optimises the following functional:

$$L = \sum_{\sigma} p(\sigma) \ln \left[\frac{p(\sigma)}{\nu(\sigma)} \right] + \sum_{\varepsilon} q(\varepsilon) \ln \left[\frac{q(\varepsilon)}{\zeta(\varepsilon)} \right] + \beta^T \left[\mu - \sum_{\sigma} p(\sigma) H \sigma - \sum_{\varepsilon} q(\varepsilon) \varepsilon \right]. \quad (1)$$

Since neither model nor measurements are perfect, errors ε must be accounted for in the inversion procedure. Hence, prior, $\zeta(\varepsilon)$ and posterior, $q(\varepsilon)$ pdfs appear in the above formula. The sums run over all possible source and error configurations.

Advantage can be taken of the information contained in the measurements only if a connection between them and the source has been established. Physical modelling of dispersion, Eq. (2) and of measuring process, Eq. (3), both provide this link.

3.1. ADJOINT MODEL

An Eulerian model of atmospheric dispersion can be written in a general discrete form

$$c_{n+1} = c_n + \Delta t \, A_n \cdot c_n + \Delta t \, \sigma_n, \quad (2)$$

where A_n is the spatial operator and the index n runs over time. In case of radionuclide dispersion the model acts as a linear operator on the source σ.

Once the solution c has been computed, the measurement μ_i is given by

$$\mu_i = \sum_k \Delta t \pi_{i,k} c_k + \varepsilon_i, \quad (3)$$

where k runs over all spatial grid cells at all time steps and $\pi_{i,k}$ is the ith measurement sampling function at the kth grid cell.

The two equations embody the explicit dependence between the source and the measurements denoted H in Eq. (1). The matrix representation of operator H has N columns and p rows. One could compute H by employing successively all the base vectors of the source space R^N (the so-called *brute force* method). Solutions obtained in this way would be projected at each measurement point with the help of Eq. (3).

Another way of obtaining H is to proceed row by row. In this case each measurement sampling function π_i is at origin of a contribution to the operator H. The contribution c_i^* is the solution to the adjoint model:

$$c_{i,n-1}^* = c_{i,n}^* + \Delta t \, A_{n-1}^T \cdot c_{i,n}^* + \Delta t \, \pi_{i,n}. \quad (4)$$

The latter possibility has been used to solve atmospheric dispersion problems (Marchuk, 1995; Pudykiewicz, 1998; Kaminski et al., 1999; Issartel and Baverel, 2003) for some time already. It has also been chosen

in this study. It is preferred despite the fact that the adjoint model runs slower than the direct one. The advantage of this choice is the necessity to compute only a relatively small number p of solutions while the former approach would require as many as N solutions to the direct model, with N>>p. Moreover, to obtain the adjoint of Polair3D we resort to the automatic differentiation software O∂yssée (Faure and Papegay, 1998).

3.2. ENTROPY IN OBSERVATION SPACE

Optimisation of L in Eq. (1) boils down to minimisation of

$$\Psi = \ln Z_\sigma(\beta) + \ln Z_\varepsilon(\beta) - \beta^T \mu, \qquad (5)$$

which is a function of a vector of Lagrange coefficients $\beta \in R^p$. Here again one profits from a relatively small size p of the observation space in comparison to the dimension of the source space, N. Functional minimisation in the former space being obviously much faster.

The particular form of the partition functions

$$Z_\sigma(\beta) = \sum_\sigma v(\sigma) \exp(\beta^T H \sigma) \quad and \quad Z_\varepsilon(\beta) = \sum_\varepsilon \zeta(\varepsilon) \exp(\beta^T \varepsilon) \quad (6)$$

depends on prior information on the source and errors. It is very likely that in case of an accidental release, emission takes place in a single grid cell. Hence, it is stipulated in $v(\sigma)$, and consequently in $Z_\sigma(\beta)$, that if an accident takes place at some spatial grid cell it cannot take place at any other. For a given spatial grid cell it can however be spread over time. Encoding this information in a mathematical formula for $Z_\sigma(\beta)$ leads to a sum of spatial grid cell contributions, $l = 1, \ldots, N_s$. For a given spatial grid cell, factorisation of temporal contributions, $n = 1, \ldots, N_t$, expresses their independence.

For the sake of simplicity it is supposed here that for a given grid cell only one of the two states is possible - the cell either emits, mass m, or it does not. Bernoulli prior is well designed to describe such a situation. It associates probability $\gamma_k \in [0,1]$ to emission and $1 - \gamma_k$ to no emission from the kth cell. Consequently, $Z_\sigma(\beta)$ takes the form

$$Z_\sigma(\beta) = \sum_{l=1}^{N_s} \frac{1}{N_S} \prod_{n=1}^{N_t} \left(1 - \gamma_k + \gamma_k \exp\left(m\left[\beta^T H\right]_k\right)\right), \qquad (7)$$

where $k = (l-1) \cdot N_t + n$ runs over all grid cells in space and time.

Assumption that measurement errors are Gaussian of variance Δ_i but also independent one from another gives

$$Z_\varepsilon(\beta) = \prod_i \exp\left(\frac{1}{2}\Delta_i \beta_i^2\right). \tag{8}$$

3.3. SOURCE ESTIMATOR

Once $Z(\beta)$ have been computed and β which minimises Ψ, Eq. (5), found, $p(\sigma)$ can be determined as a function of $v(\sigma)$. The last step of the procedure consists in defining an estimator of the source. In general it is computed according to $\overline{\sigma} = \sum p(\sigma)\sigma$. In particular, for an accidental release, the reconstructed activity in the $k_0^{th} = (l_0 - 1)\cdot N_t + n_0$ grid cell takes the form

$$\overline{\sigma}_{k_0} = \frac{m\gamma_{k_0}\exp\left(m[\beta^T H]_{k_0}\right)}{1 - \gamma_{k_0} + \gamma_{k_0}\exp\left(m[\beta^T H]_{k_0}\right)} \cdot \frac{\prod_{n=1}^{N_t}\left(1 - \gamma_k + \gamma_k \exp\left(m[\beta^T H]_k\right)\right)}{\sum_\sigma v(\sigma)\exp\left(\beta^T H\sigma\right)} \tag{9}$$

and $k = (l_0 - 1)\cdot N_t + n$.
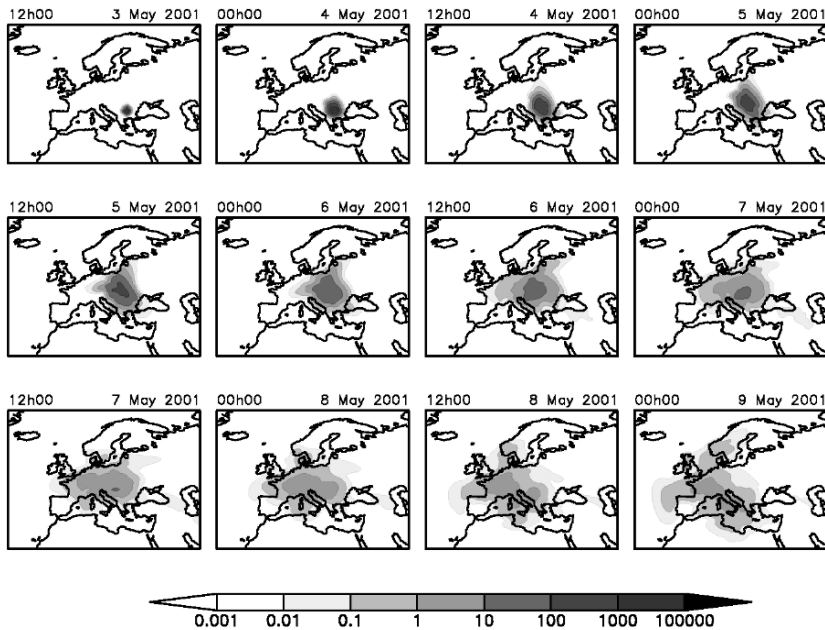
Figure 1. Contaminated cloud activity (in Bq m^{-3}) resulting from an accidental release of ^{131}I from a nuclear power station in Kozloduy, Bulgaria.

3.4. SCORE

The reconstructed source depends on many factors contributing to the inversion procedure. In order to tell the skills of reconstructions in given circumstances an objective indicator is used. It is a generalisation of the usual root mean square and it takes the form of the ratio of entropies. Thus, it reads (Bocquet, 2005a) $\rho = \Psi / \Psi_t$ where Ψ is the entropy of the reconstructed source and errors computed with respect to the entropy of the true source and true errors Ψ_t. The score takes values in [0,1] interval, with 0 corresponding to a failed reconstruction and 1 to a perfect one.

4. Examples of source retrieval

This section shows the reconstruction of the source described in section (2) carried out with the maximum entropy method presented in section (3). First, the shape of the contaminated cloud that results from the hypothetical accident is shown in Fig. 1. The first panel of the figure shows the form of the cloud three hours after the beginning of the release. The next ones illustrate its shape every twelve hours until the end of the simulation.

The results of source reconstruction follow. Only the grid cells containing nuclear facilities have been inverted. The underlying mesh has brought their number down to 134 since a grid cell counts as 1 no matter the number of nuclear installations it contains. Several reconstructions have been carried out on different subsets of the original set of 896 measurements. Each subset contains the previous one and 56 supplementary measurements, one for each of the 3-hour measurement periods. The inverted time interval has been reduced from 168 to 150 hours. The time resolution of inversion is 1 hour.

The changes in reconstruction quality with an increasing number of measurements are illustrated in Fig. 2(a). The reconstructed activity in Kozloduy, the total reconstructed activity and, in the smaller box, the score are shown as a function of the number of measurements. Despite employing noisy measurements, 56 of them are enough for the algorithm to clearly point the site of Kozloduy as the only candidate for the source location (Fig. 2(b)). The score value attached to this partial reconstruction is 0.57. Although not monotone, the curve of the score grows with a rising number of measurements and reflects the increasing quality of reconstruction, Fig. 2(c). Once the number of measurements rises above 600, the algorithm renders the particular two-step shape of the source profile, Fig. 2(d).

5.   Conclusions

The maximum entropy method which operates in observation space of a relatively small dimension has been used to invert a hypothetical nuclear accident accompanied by a sizeable release of ^{131}I to the atmosphere. Precise location, time and quantity of the released material allow to simulate the resulting averaged radioactivity concentrations. Noisy measurements are in turn used to infer information about the source. The list of the possible sources has been restricted to nuclear facilities scattered over the European continent. All the suspected sources have been reconstructed and among them also the true source.

For the particular accident shown here several tens of observations are needed to discriminate the reconstructed source in Kozloduy from the other reconstructed sources. With observational error of up to 10% of the measured activities, 600 or more measurements are needed so that the reconstructed source in Kozloduy reflects the 2-step shape of the true source.
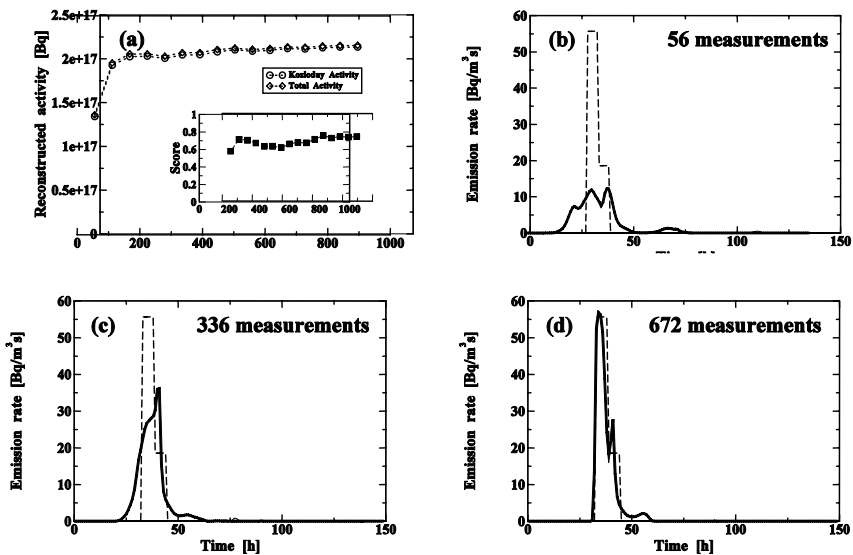
Figure 2. Source reconstruction for an accident in Kozloduy. Score (squares), reconstructed activity in Kozloduy (circles) and total reconstructed activity (diamonds) are presented in graph (a). Three examples of source reconstructions are illustrated in graphs (b), (c) and (d). The true source is drawn with a dashed line and the reconstructed sources with solid lines. The thick solid line represents the reconstructed source in Kozloduy. Other sources' contributions are barely visible.

Acknowledgements

References

Bocquet, M., 2005a, Grid resolution dependence in the reconstruction of an atmospheric tracer source, *Nonlinear Proc. in Geophys.* **12**, 219–234.

Bocquet, M., 2005b, Reconstruction of an atmospheric tracer source using the principle of maximum entropy. I: Theory, *Q.J.R.Meteorol.Soc.* **131**, 2191–2208.

Bocquet, M., 2005c, Reconstruction of an atmospheric tracer source using the principle of maximum entropy. II: Applications, *Q.J.R.Meteorol.Soc.* **131**, 2209–2224.

Boutahar, J., Lacour, S., Mallet, V., Musson-Genon, L., Quélo, D., Roustan, Y., and Sportisse, B., 2004, Development and validation of a fully modular platform for the numerical modeling of Air Pollution: POLAIR, *Int. J. of Environment and Pollution* **22**, 17–28.

Brandt, J., Christensen, J.H., Frohn, L.M., 2002, Modelling transport and deposition of caesium and iodine from the Chernobyl accident using the DREAM model, *Atmos. Chem. Phys.* **2**, 397–417.

Faure, C. and Papegay, Y., 1998, O∂yssée user's guide. Version 1.7. Technical Report RT-0224, INRIA.

Issartel, J.-P. and Baverel, J., 2003, Inverse transport for the verification of the Comprehensive Nuclear Test Ban Treaty, *Atmos. Chem. Phys.* **3**, 475–486.

Kaminski, T., Heinmann, M., and Giering, R., 1999, A coarse grid three-dimensional global inverse model of the atmospheric transport: I adjoint model and Jacobian matrix, *J. Geophys. Res.,* **104,** 18535–18553.

Marchuk, G.I., 1995, Adjoint equations and Analysis of Complex Systems, *Mathematics and its Applications*, Hazewinkel (Ed), Kluwer Academic Publisher, 295.

Pudykiewicz, J.A., 1998, Application of adjoint transport tracer equations for evaluating source parameters, *Atmos. Environ.* **32**, 3039–3050.

Robertson, L. and Langner, J., 1997, Variational assimilation of ETEX-I data, *Proceedings of the ETEX Symposium on long-range atmospheric transport, model verification and emergency response*, Vienna, Austria, Nodop, K. Editor.

Robertson, L., and Langner, J., 1998, Source function estimate by means of adjoint variational data assimilation applied to the ETEX-I tracer experiment, *Atmos. Environ.* **32**, No.24, 4219–4225.

ATMOSPHERIC CONVECTION OVER COMPLEX TERRAIN AND URBAN CANOPY: NON-LOCAL VENTILATION MECHANISMS AND APPLICATION TO POLLUTION-DISPERSION AND AIR-QUALITY PROBLEMS

SERGEJ S. ZILITINKEVICH*
*Division of Atmospheric Sciences, Department of Physical Sciences, University of Helsinki, Finland and
Nansen Environmental and Remote Sensing Centre / Bjerknes Centre for Climate Research, Bergen, Norway*

J. C. R. HUNT
Department of Space & Climate Physics and Earth Sciences, University College London, UK

A. A. GRACHEV
University of Colorado CIRES/NOAA ETL, USA / A. M. Obukhov Institute of Atmospheric Physics, Russia

I. N. ESAU
Division of Atmospheric Sciences, Department of Physical Sciences, University of Helsinki, Finland and

D. P. LALAS
National Observatory of Athens, Greece

E. AKYLAS, M. TOMBROU
Department of Physics, University of Athens, Greece

C. W. FAIRALL
NOAA Environmental Technology Laboratory, 325 Broadway, R/ET7, Boulder, CO 80305-3328, USA

H. J. S. FERNANDO
Environmental Fluid Dynamics Program, Arizona State University Tempe, AZ 85284-9809, USA

---

*To whom correspondence should be addressed. Sergej S. Zilitinkevich, Finnish Meteorological Institute (FMI), Vuorikatu 15 A, P.O. Box 503, 00101 Helsinki, Finland; e-mail: Sergej.Zilitinkevich@fmi.fi

A. BAKLANOV
Danish Meteorological Institute, Copenhagen, Denmark

S. M. JOFFRE
Finnish Meteorological Institute, Helsinki, Finland

Abstract. In modern atmosphere-hydrosphere-biosphere model chains, convective boundary-layer models and parameterization packages represent the most important coupling agents, which essentially control the overall quality of predictions from coupled models. This paper focuses on the enhancement of turbulent mixing due to large-scale semi-organized eddies and interactions between large eddies and surface roughness elements up to very high obstacles such as buildings, rocks and hills. Large-scale structures in the shear-free convective boundary layers consist of strong plumes and wider but weaker downdraughts. Close to the surface they cause local "convective winds" blowing towards the plume axes. The latter generate turbulence, in addition to its generation by the buoyancy forces, and strongly contribute to the turbulent fluxes of heat and other scalars. This mechanism is especially important over very rough surfaces. The proposed model is validated against data from measurements over different sites and also through large-eddy simulation (LES) of convective boundary layers (CBLs) over a range of surfaces from very smooth to extremely rough. Excellent correspondence between model results, field observations and large-eddy simulations is achieved. The obtained resistance and heat/mass transfer laws are recommended for practical use inmeso-scale, weather-prediction, climate and other environmental models.

The full text of this paper is to appear in *Quarterly Journal of the Royal Meteorological Society*, 2006, under the title "The influence of large convective eddies on the surface layer turbulence".

FACTOR SEPARATION IN ATMOSPHIC

MODELLING A REVIEW

T. SHOLOKHMAN, P. ALPERT*
Dept. Geophysics & Planetary Sciences
Tel-Aviv University, Tel-Aviv, 69978, Israel

Abstract. This paper presents a review of the factor separation (FS) technique and its fractional approach. The work focuses on two points. First, the FS methodology is applied to some fundamental mathematical functions. For each function we define the constrains for the factor values, by investigating the function under three different synergy states: synergy term equals zero; is opposite in its sign to the factors' contributions, or is dominant. Second, the application of the method is demonstrated with a simplified atmospheric problem with an analytical solution, i.e., the Haurwitz sea-breeze (SB) model. The FS method also assists in analyzing the effects of the dominant and secondary factors in given physical models that have analytical solutions. Study of factors with the FS methodology allows a better understanding of the various mechanisms and particularly the role of their interactions-synergies in atmospheric dynamics.

Keywords: Factor separation; synergy states; atmospheric dynamics

1. What is the factor separation method?

More then ten years have passed since the publication of "Factor separation in Numerical Simulation" (FS below) by Stein and Alpert (1993) and today this method provides a powerful tool for atmospheric research. A relatively

_____
*To whom correspondence should be addressed. P. Alpert, Dept. Geophysics & Planetary Sciences, Tel-Aviv University, Tel-Aviv, 69978, Israel; e-mail: pinhas@post.tau.ac.il

large number of studies have been devoted to the method of factor separation or, more accurate, to the application of this method in atmospheric research.

How does the method work or what do we need it for? Chapter 3 provides a brief mathematical description of the method, in which we suggest some basic intuitive explanation. The starting point is that we investigate the problem that includes several factors that are assumed to influence a final result. Important note is that both physical and geophysical values used in the model are often approximated or they may change sometimes very fast as function of the chosen factors. For example, the albedo of the surface depends on the structure of the surface and may change rapidly with the weather.

Other considerations are that the temporal variation is very important for modeling the problem, but it adds complexity by including the additional factors. The FS method identifies the most important factors and their combinations- the synergisms. Additional problem that the FS method is addressed to solve is the stability of the chosen factor in the problem. This means, how the result reacts to small changes in the factors' values. The FS standard method works on the principle of "on-off", in other words the factors are one-by-one switched off (zeroed) and the intermediate result is investigated independently for every case. The case where all of the chosen factors are switched off is the basic case, which obviously does not depend on the factors' and their combinations' influences. The opposite case, with all of the factors "on", is the "control" or "full" result, initially suggested by the model and that includes all the factors and their synergic contributions. The FS method provides the methodology to distinguish between the pure influence of each and every factor as well as their mutual influence commonly referred to as synergies, which are due to several factors "switched on" together. The understanding of which factor, or what combination of factors is most significant for the final result, is very important in atmospheric studies. Since, discovering the most dominant factors in a specific problem guides us to the important physical mechanisms and which improvement in the model formulations may be required.

2.   The philosophy of synergy

What does synergism really mean? Let us take, for example, the following process in life. A worker needs to push a cargo up to X meters. Let us assume that it will last time T. This time is not equal to the time that two workers need to push the same cargo to double the distance. If the workers are in good coordination (positive synergy) they will push the cargo to a larger distance then 2*X meters during the same time. But if they do not coordinate well (negative synergy) it will be less then 2*X meters.

In this case, every worker is considered as a factor and the investigated resulting value is the distance per specific time. Another example of a negative synergism for the above workers could be the case, when the total distance is limited to 1.5*X meters. Even if the two workers coordinate very well, the synergism must be negative by at least 0.5*X. This is the case of saturation. In the atmosphere, for example, it can be seen as humidity saturation for rainfall. In other words, processes in our life are not linear. The same is even more so in the atmosphere. There are nearly no factors in the real atmosphere that are not correlated at all. And this infinite chain of factors' interactions is intended to be explained by the scientists, involving a finite number of assumptions.

The FS method in atmospheric research became in recent decades an important tool for understanding how various factors or processes affect a certain phenomenon or development.

3. Generalization of the method for n factors:

Let the field f depend on n factors ψ_i where i=1, 2…n. Each factor is multiplied by a coefficient c_i , where

$$f = f(c_1, c_2, c_3, .., c_n) \tag{3.1}$$

In this paper full explanation of the final formula is not introduced, it can be found in Stein and Alpert (1993).The general form of the final formula is:

$$\hat{f}_{i_1 i_2 i_3 .. i_l} = \sum_{m=0}^{l} (-1)^{l-m} \left[\sum_{\substack{j_1, j_2, j_3 \cdots j_m = i_1, i_2, i_3, .. i_m}}^{i_{l-m+1}, i_{l-m+2}, \ldots, i_l} f_{j_1 j_2 j_3 \cdots j_m} \right] \tag{3.2}$$

where the sum $\displaystyle\sum_{\substack{j_1, j_2, j_3, \cdots j_m = i_1, i_2, i_3, .. i_m}}^{i_{l-m+1}, i_{l-m+2}, .. i_l}$ is over all groups of m

sorted indices chosen from l indices $i_1, i_2, i_3, .., i_l$ where $0 \leq l \leq n$. In the case of three factors, (3.2) yields eight equations:

The case: 3 factors

$$\hat{f}_0 = f_0 \tag{3.3}$$

$$\hat{f}_1 = f_1 - f_0 \tag{3.4}$$

$$\hat{f}_2 = f_2 - f_0 \tag{3.5}$$

$$\hat{f}_3 = f_3 - f_0 \tag{3.6}$$

$$\hat{f}_{12} = f_{12} - (f_1 + f_2) + f_0 \tag{3.7}$$

$$\hat{f}_{13} = f_{13} - (f_1 + f_3) + f_0 \tag{3.8}$$

$$\hat{f}_{23} = f_{23} - (f_2 + f_3) + f_0 \tag{3.9}$$

$$\hat{f}_{123} = f_{123} - (f_{12} + f_{13} + f_{23}) + (f_1 + f_2 + f_3) - f_0 \tag{3.10}$$

The result would then be not only the separation of the factors for $\hat{f}_1, \hat{f}_2, \hat{f}_3$, but also all the possible combinations of these factors, i.e. $\hat{f}_{12}, \hat{f}_{23}, \hat{f}_{13}$ and $\hat{f}_{123}$. The factor $\hat{f}_{123}$, for instance, is the contribution due to the triple interaction among the three factors under evaluation.

4. Earlier applications of the FS:

In the following table some examples from FS studies are summarized.

Article Ref.	Chosen factors	Analyzed field	Grid interval (km)
U. Stein and P. Alpert (1993)	Topography and surface flaxes	Rainfall	80
P. Alpert, U. Stein, M. Tsidulko and B.U. Neeman	Topography, surface latent heat flux, surface sensible heat flux and heat release	Rainfall	80

(1993 not published)	Topography and surface flaxes	Mountain winds	5
	Rotation and helicity of the flow	Turbulence decay	100m to 1 km
	Cloud reduction and ice cap elimination	Zero-dimensional global climate modeling	Theoretical model
P. Alpert, U. Stein, M. Tsidulko (1995)	Topography, latent heat flux, sensible heat flux and laten heat release	Lee cycloge-nesis; sea-le-vel-pressure (SLP)	80
P. Alpert, U. Stein, M. Tsidulko and S. Krichak (1995)	Topography, latent heat flux, sensible heat flux and laten heat release	Lee cyclogenesis SLP	80
P. Alpert, S.O. Krichak, T.N. Krishnamurti, U. Stein, M. Tsidulko (1996)	Lateral boundaries, initial fields and topography	Lee cyclogenesis; SLP	180 80 60 40
S. Krichak and P. Alpert (2002)	Sensible heat flux and latent heat flux	Trough development	210
A. Berger, M. Laussen and Ci. Kubatzki (2005)	Atmosphere, ocean vegetation	Temperature, precipitations	Paleoclimate model
R. Romero (2001)	Atlas mountains orography and latent heat exchange	Precipitation and low level circulation	~50
P. Alpert, D. Niyogi, R.A. Pielke, Sr. and J.L. Eastman, Y.K. Xue and S. Raman (2006)	Soil moisture under non-limiting conditions and doubling of CO2 concentrations	CO2	~50
Global Planetary Change, LULUC Special issue	Land-used effect, the radiative effect of CO2 and biophysical effect of CO2	Minimum surface temperature	50

	Clouds and green-house gases	Averaged surface temperature	~400
S. Guan and G.W. Reuter (1995)	Waste heat, vapor, and cloud condensation nuclei	Rainfall	
R. Romero, C. Ramis, S. Alonso, C.A. Doswell III, D.J. Stensrud (1998)	Orography and water vapor flux	Rainfall	~50
C.R. Rozoff and W. R. Cotton (2003)	Topography, urban energy flux and urban momentum flux	Moist convection	1.5 7.5 37.5

As it can clearly be seen, the FS methodology is often used being an helpful tool for attaining the results. However, except two of the mentioned works, no other study examined the method itself.

5. FS method and Synergism for some fundamental functions

In spite of wide use of the FS method for complex functions, to investigate the FS method analytically, we start with only a few examples of mathematical functions chosen from a great variety of functions. In other words, firstly, the method of Factor Separation is checked on simple mathematical functions that build up a base to meteorological or, in general, physical fields.

A bivariate polynomial $f(x_1, x_2) = ax_1 + bx_2 + kx_1x_2 + d$.

Let the factors x_i be multiplied by a varying coefficient c_i

$$f(c_1, c_2) = ac_1x_1 + bc_2x_2 + kc_1c_2x_1x_2 + d \qquad (5.1)$$

It is probably preferred to write the unction $f(x_1, x_2)$ as $f(c_1x_1, c_2x_2)$, but here we focus on the variable c_i (just simplified writing).

It can easily be seen that the value of f and $\hat{f}$ in the different simulations are related through:

$$f_0 = d$$
$$f_1 = ax_1 + d$$
$$f_2 = bx_2 + d \qquad (5.2)$$
$$f_{12} = ax_1 + bx_2 + kx_1x_2 + d$$

$$\hat{f}_0 = d$$
$$\hat{f}_1 = ax_1$$
$$\hat{f}_2 = bx_2 \qquad (5.3)$$
$$\hat{f}_{12} = kx_1x_2$$

5.1. THE SYNERGISM IS ZERO

We can see from equation 5.3. that synergism equals to zero by definition when k=0, or in the series of the points when one of coordinates, i.e. x_1, x_2 is zero.

5.2. THE OPPOSED INFLUENCE OF THE SYNERGISM

Here, the synergism works in the opposite direction to that the resulting field; that means:

$$\text{either} \begin{cases} f_{12} > 0 \\ \hat{f}_{12} < 0 \end{cases} \qquad \text{or} \qquad \begin{cases} f_{12} < 0 \\ \hat{f}_{12} > 0 \end{cases} \qquad (5.4)$$

Substituting the relevant functions from (5.3) into (5.4); this yield,

$$\text{either} \begin{cases} ax_1 + bx_2 + kx_1x_2 + d > 0 \\ kx_1x_2 < 0 \end{cases}$$

$$\text{or} \begin{cases} ax_1 + bx_2 + kx_1x_2 + d < 0 \\ kx_1x_2 > 0 \end{cases} \qquad (5.5)$$

There are many points that solve the inequalities of equation (5.5). These points denominate the field in which separately every factor works "for" final result and together they work "against". It is important statement for the physical analysis of functions.

5.3. THE DOMINANT SYNERGISM

This is the case when the synergism term is larger than any of the factors separately:

$$\begin{cases} f_{12} > 0 \\ \hat{f}_{12} > \hat{f}_1 \\ \hat{f}_{12} > \hat{f}_2 \end{cases} \quad \text{or} \quad \begin{cases} f_{12} < 0 \\ \hat{f}_{12} < \hat{f}_1 \\ \hat{f}_{12} < \hat{f}_2 \end{cases} \tag{5.6}$$

Substituting (5.3) into (5.6) yields,

$$\begin{cases} ax_1 + bx_2 + kx_1x_2 + d > 0 \\ kx_1x_2 > ax_1 \\ kx_1x_2 > bx_2 \end{cases} \quad \text{or}$$

$$\begin{cases} ax_1 + bx_2 + kx_1x_2 + d < 0 \\ kx_1x_2 < ax_1 \\ kx_1x_2 < bx_2 \end{cases} \tag{5.7}$$

Transposition from right side to left in (5.7) leads to

$$\begin{cases} ax_1 + bx_2 + kx_1x_2 + d > 0 \\ -ax_1 + kx_1x_2 > 0 \\ -bx_2 + kx_1x_2 > 0 \end{cases} \quad \text{or}$$

$$\begin{cases} ax_1 + bx_2 + kx_1x_2 + d < 0 \\ -ax_1 + kx_1x_2 < 0 \\ -bx_2 + kx_1x_2 < 0 \end{cases} \tag{5.8}$$

Addition all of three inequalities, additions of first inequality with second inequality and with third inequality separately results

$$\begin{cases} kx_1x_2 > -\dfrac{d}{3} \\ kx_1x_2 > ax_1 \\ kx_1x_2 > bx_2 \end{cases} \quad \text{or} \quad \begin{cases} kx_1x_2 < -\dfrac{d}{3} \\ kx_1x_2 < ax_1 \\ kx_1x_2 < bx_2 \end{cases} \tag{5.9}$$

Over the last two systems, the synergism controls the final result in some specific cases. With a given example, in this way, it is possible to see a range where the factors contribute only a small percent from the result while their combination is much more important and valid.

The graphic application in simple cases could be good tool to see behaviouristic characteristics of the functions.

6. FS method applied to Haurwitz sea breeze (SB) model

The example of FS methodology is the dynamic model of the sea breeze suggested by B. Haurwitz (1947).

6.1. THE HAURWITZ SB MODEL

In large-scale atmospheric motions it can often be assumed that at every instant the wind velocity is adjusted to the forces governing the motion. The geostrophic and gradient-wind motions are examples of such a balance. In the case of the sea-breeze circulation, this balance cannot exist. Haurwitz argued that the local derivatives and the Coriolis terms must be included in a realistic dynamic theory of the sea breeze. He set up a simple model in which spatial changes and changes in air compressibility were ignored. The equations of motion were as follows:

$$\frac{du}{dt} - fv + k_f u = P_x - F(t), \quad \frac{dv}{dt} + fu + k_f v = P_y \qquad (6.1)$$

where u and v are the x and y components of the surface horizontal wind, x is the horizontal axis positive from land to water, i.e. from west to east, y is the horizontal axis parallel to the shore from south to north, P_x and P_y are the components of large scale pressure gradient force, $F(t)$ is a periodic function representing the pressure gradient between land and water that is caused by the diurnal variation of the temperature differences, $f = 2\Omega \sin \phi$ is the Coriolis parameter and k_f is the friction coefficient. The general pressure gradient has the following components:

$$P_x = -\frac{1}{\rho}\frac{\partial p}{\partial x} = -fv_{gs}, \quad P_y = \frac{1}{\rho}\frac{\partial p}{\partial y} = fu_{gs} \qquad (6.2)$$

where u_{gs} and v_{gs} are the x and y components of the geostrophic wind. $F(t)$ was chosen to be:

$$F(t) = A\Big/ \pi + \frac{1}{2} A \cos \omega t \qquad (6.3)$$

where $\qquad A = \frac{1}{\rho}\frac{\partial p_0}{\partial x} = \frac{gz}{T}\frac{\partial T}{\partial x} \qquad (6.4)$

A - represents the relationship between horizontal temperature and pressure gradients, p_0 is the surface pressure.

The solution of equations (7.1) is:

$$w = \frac{P_z - A/\pi}{if + k_f} - \frac{A\Omega}{2} \frac{\sin\Omega t + (if + k_f)\cos\Omega t}{(if + k_f)^2 + \Omega^2} + Ce^{-(if + k_f)t} \qquad (6.5)$$

where w and P_z are complex numbers.

The first term on the right-hand side of (6.5) represents the motion caused by the constant part of the pressure-gradient force. In the case of motion without friction, the term would be reduced to an expression for geostrophic motion. The second and third terms represent the effect of the pressure gradient which is due to the temperature difference between land and water. In the fourth term, C is an arbitrary integration constant. Since the velocity w should vanish if both parts of the pressure-gradient force are zero, namely, $P_z = 0$ and $A = 0$, it follows that $C = 0$.

To obtain the velocity components, equation (6.5) must be separated into the real and imaginary parts. Thus, after some rearrangement the real part is:

$$u = \frac{k_f P_x + f P_y}{f^2 + k_f^2} - \frac{A}{\pi} \frac{k_f}{f^2 + k_f^2}$$
$$- \frac{A}{2} \frac{(k_f^2 + \Omega^2 - f^2)\Omega\sin\Omega t + (k_f^2 + \Omega^2 + f^2)k_f\cos\Omega t}{\left(k_f^2 + \Omega^2 - f^2\right)^2 + 4k_f^2 f^2} \qquad (6.6)$$

and the imaginary part is:

$$v = -\frac{f P_x - k_f P_y}{f^2 + k_f^2} + \frac{A}{\pi} \frac{1}{f^2 + k_f^2}$$
$$- \frac{A}{2} \frac{(\Omega^2 - f^2 - k_f^2)f\cos\Omega t - 2fk\Omega\sin\Omega t}{(k_f^2 + \Omega^2 - f^2)^2 + 4f^2 k_f^2} \qquad (6.7)$$

By substituting (6.2) in (6.6) and (6.7) one can obtain:

$$u = \frac{-k_f f}{f^2 + k_f^2} v_{gs} + \frac{f^2}{f^2 + k_f^2} u_{gs} - \frac{A}{\pi} \frac{k_f}{f^2 + k_f^2}$$
$$- \frac{A}{2} \frac{(k_f^2 + \Omega^2 - f^2)\Omega\sin\Omega t + (k_f^2 + \Omega^2 + f^2)k_f\cos\Omega t}{\left(k_f^2 + \Omega^2 - f^2\right)^2 + 4k_f^2 f^2} \qquad (6.8)$$

$$v = \frac{f^2}{f^2 + k_f^2} v_{gs} + \frac{k_f f}{f^2 + k_f^2} u_{gs} + \frac{A}{\pi} \frac{1}{f^2 + k_f^2}$$

$$- \frac{A}{2} \frac{(\Omega^2 - f^2 - k_f^2) f \cos \Omega t - 2 f k \Omega \sin \Omega t}{(k_f^2 + \Omega^2 - f^2)^2 + 4 f^2 k_f^2}$$

$$(6.9)$$

Haurwitz himself admitted that the equations for u and v are difficult to discuss in general terms because of the auxiliary constants. He proceeded by taking a numerical example in which:

$$A = 0.048 cm \sec^{-1}$$

$$\Omega = 0.73 * 10^{-4} s^{-1}$$

The Coriolis parameter is $f = 10^{-4} s^{-1}$ matches the latitude of 43^0. Also Haurwitz assumed that coefficient of friction has the value of $k_f = 0.58 * 10^{-4} s^{-1}$.

6.2. FACTORS CHOSEN FOR THE MODEL

Suppose that the effects of two factors are investigated: the friction and the Coriolis force. The Coriolis force is a fictitious force exerted on a body when it moves in a rotating reference frame. It is called a fictitious force because it is a by-product of measuring coordinates with respect to a rotating coordinate system as opposed to a real force. The Earth rotates about its axis from west to east once every 24 hours. Consequently, an object moving above the Earth in a generally northerly or southerly direction, and with a constant speed relative to space, will be deflected in relation to the rotation of the Earth. This deflection is clockwise, or to the right, in the Northern Hemisphere and anticlockwise, or to the left, in the Southern Hemisphere.

In physics, friction is the resistive force that occurs when two surfaces move along each other when forced together. The surface of the Earth exerts a frictional drag on the air blowing just above it. This friction can act to change the wind direction and slow it down – keeping it from blowing as fast as the wind aloft. Actually, the difference in terrain conditions directly affects how much friction is exerted. For example, a calm ocean surface is pretty smooth, so the wind blowing over it does not move up, down, and around any features. By contrast, hills and forests force the wind to slow down and/or change direction much more. Hence, exert larger friction forces.

The two factors described above – the friction and the Coriolis force, were chosen for the model. There are a number of studies about sea breeze that ignore both of the chosen factors (classical paper by Jeffreys 1922).

The FS method shows that these two factors have a great impact on the circulation of the sea breeze and therefore can not be disregarded.

The FS method allows examining the fluctuations of the intensity and the direction of the wind close to the coast. These fluctuations are caused by the different latitude of the location and by different choices of the value of the friction term.

6.3. A FRACTIONAL APPROACH TO HAURWITZ SEA BREEZE SOLUTION

In this paper we do not analyze the basic case of FS method due to the fact that theories of the sea breeze without Coriolis force and friction were thoroughly discussed before. The starting point of Haurwitz model was with a positive friction and rotation of the earth.

Our function with two factors is from (6.8) and (6.9):

$$u(k_f, f) = \frac{-k_f f}{f^2 + k_f^2} v_{gs} + \frac{f^2}{f^2 + k_f^2} u_{gs} - \frac{A}{\pi} \frac{k_f}{f^2 + k_f^2}$$

$$- \frac{A}{2} \frac{(k_f^2 + \Omega^2 - f^2)\Omega \sin \Omega t + (k_f^2 + \Omega^2 + f^2)k_f \cos \Omega t}{(k_f^2 + \Omega^2 - f^2)^2 + 4k_f^2 f^2}$$

$$v(k_f, f) = \frac{f^2}{f^2 + k_f^2} v_{gs} + \frac{k_f f}{f^2 + k_f^2} u_{gs} + \frac{A}{\pi} \frac{1}{f^2 + k_f^2}$$

$$- \frac{A}{2} \frac{(\Omega^2 - f^2 - k_f^2)f \cos \Omega t - 2 f k \Omega \sin \Omega t}{(k_f^2 + \Omega^2 - f^2)^2 + 4 f^2 k_f^2}$$

Recall that zero position is

$$k_f = 0.58 * 10^{-4} s^{-1}$$
$$f = 10^{-4} s^{-1}$$

(6.10)

and, at first, we examine the case with:

$$k_f = 10^{-4} s^{-1}$$
$$f = 0.77 * 10^{-4} s^{-1}$$

(6.11)

The first factor is the friction and the second is the Coriolis parameter. The case is without the geostrophic wind at t=0. After substituting Eqs. (6.10)

and (6.11) into (6.8) and (6.9) the contribution functions are (the winds in cm/s   consistently to values in the Eqs. (6.8)-(6.11)) :

$$\begin{cases} u_0 = u(0.58*10^{-4},10^{-4}) = -257.2623 \\ v_0 = v(0.58*10^{-4},10^{-4}) = 255.8436 \end{cases} \qquad \begin{cases} \hat{u}_0 = -257.2623 \\ \hat{v}_0 = 255.8436 \end{cases}$$

$$\begin{cases} u_1 = u(10^{-4},10^{-4}) = -218.2941 \\ v_1 = v(10^{-4},10^{-4}) = 158.5851 \end{cases} \qquad \begin{cases} \hat{u}_1 = 38.9682 \\ \hat{v}_1 = -97.2585 \end{cases}$$

$$\begin{cases} u_2 = u(0.58*10^{-4},0.77*10^{-4}) = -328.1865 \\ v_2 = v(0.58*10^{-4},0.77*10^{-4}) = 210.3937 \end{cases} \begin{cases} \hat{u}_2 = -70.9242 \\ \hat{v}_2 = -45.4499 \end{cases} \quad (6.12)$$

$$\begin{cases} u_{12} = u(10^{-4},0.77*10^{-4}) = -252.65 \\ v_{12} = v(10^{-4},0.77*10^{-4}) = 134.0343 \end{cases} \begin{cases} \hat{u}_{12} = 36.5683 \\ \hat{v}_{12} = 20.8991 \end{cases}$$

The contribution functions show that the increase of the friction results in a positive u component of the sea breeze and a negatively v component. The decrease of the Coriolis coefficient results in both negative components. However, the synergism is positive. The joint work of the two factors results in an increase of the wind.

At t=12 we have (the winds in cm/s also):

$$\begin{cases} u_0 = 124.4256 \\ v_0 = -28.9669 \end{cases} \qquad \begin{cases} \hat{u}_0 = 124.4256 \\ \hat{v}_0 = -28.9669 \end{cases}$$

$$\begin{cases} u_1 = 65.7568 \\ v_1 = -6.7726 \end{cases} \qquad \begin{cases} \hat{u}_1 = -58.8669 \\ \hat{v}_1 = 22.1943 \end{cases}$$

$$\begin{cases} u_2 = 138.1161 \\ v_2 = 40.6585 \end{cases} \qquad \begin{cases} \hat{u}_2 = 13.6905 \\ \hat{v}_2 = 69.6254 \end{cases} \qquad (6.13)$$

$$\begin{cases} u_{12} = 61.4089 \\ v_{12} = 12.6895 \end{cases} \qquad \begin{cases} \hat{u}_{12} = -18.0384 \\ \hat{v}_{12} = -50.1633 \end{cases}$$

Greater friction produces a weaker wind, while a weaker Coriolis force produces a stronger wind. The synergism in this case is negative for two components.
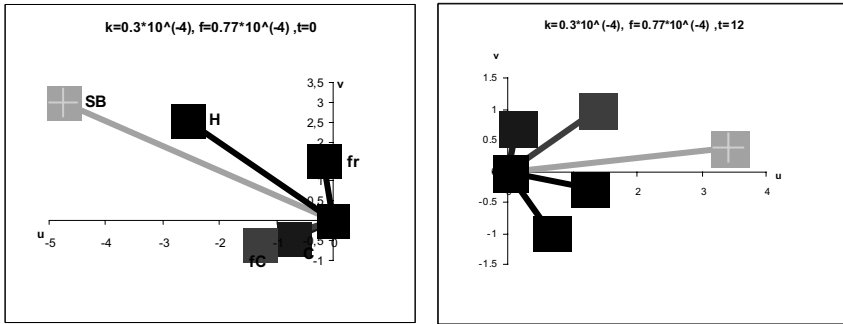
Figure 1. Graphs of sea-breeze for t=0 (mid-day) and t=12 for case with friction coefficient $0.3 * 10^{-4} s^{-1}$ and Coriolis parameter $0.77 * 10^{-4} s^{-1}$ (see Tab.7 decreased friction, increased Coriolis). Factor-separated wind vectors are the initial choice of Haurwitz (H), friction (fr), Coriolis force (C), synergic vector (FC) and sea-breeze in final choices as is noted in the title of the graph (SB). The wind velocity is in ms-1. The four contribution vectors sum up to the control wind vector – SB. In all cases land lies to the left and water to the right of the N-S line. Vectors of wind start in point (0,0).

Friction $\Downarrow$, Coriolis $\Downarrow$

7. Summary

We provide a short review of the Factor Separation method introduced over a decade ago by Stein and Alpert (1993). The method was used since by many groups worldwide for a variety of atmospheric studies; some are summarized in a table presented here.

An interesting feature of this method is that it allows the investigation of non-linear synergic terms directly. In this paper we first present some examples from simple analytical functions and explore cases of no-synergy, high-synergy or opposite-synergy to the primary factors contributions. Also we investigate the synergy with a simple sea-breeze theoretical early study by Haurwitz (1947). The synergic contribution due to the Coriolis/Friction terms is found important and its characteristics are exemplified in two cases.

References

Ackerman S.A., Knox J., 2002, *Meteorology: Understanding the Atmosphere*, Brooks/Cole. Publishing Co.

Alpert, P., Krichak , S. O., Krishnamurti, T. N., Stein, U., and Tsidulko, M., 1996, The Relative Roles of Lateral Boundaries, Initial Conditions and Topography in Mesoscale Simulations of Lee Cyclogenesis, *J. Appl. Meteor.* **35:**1091–1099, 1996.

Alpert, P., D. Niyogi, R.A. Pielke Sr., and J.L. Eastman, 2006, First evidence for carbon dioxide and moisture synergies from the leaf cell to global scale - Implications to human-caused climate change", *J. Global Planetary Change* (in press).

Alpert. P., U. Stein and M. Tsidulko, 1995, Role of sea fluxes and topography in eastern Mediterranean cyclogenesis, *The Global Atmosphere-Ocean System* **3:** 55–79.

Alpert. P., U. Stein, M. Tsidulko and B.U. Neeman, 1993, *Synergism in Weather and climate*, unpublished.

Alpert, P., and M. Tsidulko, 1994, Project WIND-numerical simulations with Tel-Aviv PSU/NCAR model at Tel-Aviv University 1994, Mesoscale Modeling of the Atmosphere, in: *Meteor. Monogr., No.25*, Amer. Meteor. Soc., pp. 81–95.

Alpert, P., M. Tsidulko and U. Stein, 1995: Can sensitivity studies yield absolute comparisons for the effects of several processes?, J. Atmos. Sci., 52, pp. 597–601.

Alpert. P. , M. Tzidulko and D. Izigsohn, 1999: A shallow short- lived meso-beta cyclone over the gulf of Antalya, eastern Mediterranean, Tellus, 51A, pp. 249–262.

Alpert. P. , M. Tzidulko, S. Krichak and U. Stein1996: A multi-stage evolution of an ALPEX cyclone, Tellus, 48A, pp. 209–220.

Berger A., ,1998, The role of CO2, sea level and vegetation during the Milankovitch-forced glacial-interglacial cycles, in: *Geosphere-Biosphere Interactions and Climate,* L. Bengtsson and C.U. Hammer (eds.), Geosphere-Biosphere Interactions and Climate. New-York, Cambridge University Press.

Berger A., Claussen M. and Kubatzki Ci., 2005, Identifying the individual contribution of climatic factors and of their synergism, *submitted.*

Doswell, C. A. III, C. Ramis, R. Romero, and S. Alonso, 1998: A diagnostic study of three heavy precipitation episodes in the western Mediterranean region, Wea. Forecasting, 13, pp. 102–124.

Guan S. and G. W. Reuter, 1996: Numerical simulation of an industrial cumulus affected by heat, moisture and CCN released from an oil refinery, J. Applied Meteor., 35, 1257–1264.

Haurwitz, B., 1947, Comments on the sea-breeze circulation, J. Meteorol. 4, 1–8.

Homar, V., C. Ramis, R. Romero, S. Alonso, J. A. Garcia-Moya and M. Alarcon, 1999: A case of convection development over the western Mediterranean sea: A study through numerical simulations, Meteorol. Atmos. Phys., 71, 169–188.

Khain A.P., D. Rosenfeld, and I. Sednev, 1993: Coastal effects in the E. Mediterranean as seen from Experiments using a cloud ensemble model with Detailed Description of Warm and Ice Microphysical Processes, Atmos. Reserch, 30, 295–319.

Krichak S. and P. Alpert, 2002: A fractional approach to the factor separation method, *J. Atmos. Sci.* **59:**2243–2252.

Krichak. S., P. Alpert and T.N. Krishnamurti, 1997: Red Sea trough/cyclone development numerical investigation, Meteor. Atmos. Phys. 63, pp. 159–170.

Krichak. S., and P. Alpert, 1998: Role of the Large-Scale Moist Dynamics in Nov 1–5 1994 hazardous Mediterranean Weather, J. Geophy. Res., Vol. 103, No. D16, pp. 19453–19468.

Levy G. and M. Ek, 2001: The simulated response of the marine atmospheric boundary layer in the western Pacific warm pool region to surface flux forcing, J. Geophys. Res., 106, pp. 7229–7241.

Lindzen, R.S., 1990: Dynamics in atmospheric physics, Cambridge Univ. Press, p. 310.

Morgenstern O., 1998: Alpine Southside Precipitation Events: Model Studies and Physical Concepts, PhD thesis, ETH Switzerland No. 12421.

Pielke R.A. : "Mesoscale Meteorological Modeling", Academic Press, Orlando, 1984.

Ramis. C., R. Romero, 1995: A first numerical simulation of the development and structure of the sea breeze in the Island of Mallorca, Ann. Geophysicae, Vol. 13, pp. 981–994.

Ramis, R., R. Romero, V. Homar, S. Alonso, and M. Alarcon, 1998: Diagnosis and numerical simulation of a torrential precipitation event in Catalonia (Spain), Meteorol. Atmos. Phys., 69, pp. 1–21.

Romero, R: "Numerical simulation of mesoscale processes in the western Mediterranean: Environmental impact and natural hazards", Ph. D. Thesis, Universitat de les Illes Balears, p. 164, 1998.

R. Romero, C. A. Doswell III and C. Ramis: " Mesoscale Numerical Study of Two Cases of Long-lived Quasistationary Convective Systems over Eastern Spain", Mon. Wea. Rev. , vol. 128, no. 11, pp. 3731–3751, 2000.

Romero, R., C. Ramis, and S. Alonso, 1997: Numerical simulation of an extreme rainfall event in Catalonia: Role of orography and evaporation from the sea, Quart. J. Roy. Meteor. Soc., 123, pp. 537–559.

Romero, R., Ramis, C., Alonso, S., Doswell III, C. A., Stensrud, D. J., 1998, Mesoscale Model Simulations of Three Heavy Precipitation Events in the Western Mediterranean Region, *Mon. Wea. Rev.* **126:**1859–1881.

Rozoff, C.R., and Cotton, W. R., 2003, Simulation of St. Louis, Missouri, Land Use Impacts on Thunderstorms, *J. Appl. Meteor.* **42:**6,716–738.

Stein, U., and Alpert, P., 1993, Factor separation in numerical simulations, *J. Atmos. Sci.* **50:**2107–2115.

Tsidulko, M., and Alpert, P., 2001, Synergism of upper-level potential vorticity and mountains in Genoa lee cyclogenesis - A numerical study, *Meteor. Atmos. Phys.* **78:**261–285.

MATHEMATICAL MODELLING OF DYNAMICAL AND ECOLOGICAL PROCESSES IN THE SYSTEM SEA-LAND-ATMOSPHERE

AVTANDIL KORDZADZE

M. Nodia Institute of Geophysics, Georgian Academy of Sciences, 1, Alexidze Str., 0193 Tbilisi, e-mail: avtokor@ig.acnet.ge

Abstract. Basic questions concerning the statement of hydro-thermodynamic problem of the system sea-land-atmosphere, which should become the basis for studying of geophysical and ecological processes in the natural environment of the Black Sea region, are considered. The basis of a coupled regional model is full systems of the ocean and atmosphere hydro-thermodynamic equations, equations of molecular heat conductivity in the soil active layer and heat balance of the underlying surface (water, land). The model consists of separate blocks, each of them represents mathematical model describing hydro-thermodynamic processes in separate objects of the environment. Statements of ecological problems, connected to distribution of polluting substances from known sources and definition of a probable location of a source in water medium on known pollution concentrations in the upper layers, are discussed.

1. Introduction

Black Sea - the richest source of natural resources, it has great influence on social and economic condition of the Black Sea-shore states. Making uniform hydro-thermodynamic system with the atmosphere, the Black Sea plays an important role in formation of weather and regional climate. Ecologically safe and rational use of natural resources of the Black Sea

substantially depends on reception of operative information on possible changes of the Black Sea and atmosphere states. Therefore, nowadays creation of monitoring and forecasting system of the sea and atmosphere states is very actual for the Black Sea region. The realization of this system will enable to observe continuously the temperature, salinity of the sea, currents, zones of contamination, their intensity and other parameters, that describe current and future states of the Black Sea and atmosphere.

Interest of forecasting Black Sea and atmosphere conditions considerably grows because the region of the Black Sea is located in the central zone of the transport corridor connecting Europe with Asia. In conditions of intensive transportation of power resources danger of occurrence of man-caused failures has considerably increased.

The monitoring and forecasting system should be based on the coupled hydro-thermodynamic regional model of the sea-land-atmosphere, adequately describing physical processes in the environment. It is necessary to note, that nowadays the majority of models of the ocean and atmosphere dynamics are considered separately from each other.[1-13]

In spite of the fact that nowadays high resolution global coupled ocean-atmosphere models are created using the variable grid step for separate regions, nevertheless creation of a regional hydro-thermodynamic model in view of the Black Sea-atmosphere interaction is rather actual and important problem for more detailed description of regional features and use the obtained results in operative forecast service. Therefore, the interest of modelling regional processes in view of interaction between the Black Sea and the atmosphere has considerably increased. The regional coupled model will be considered for extended area enveloping the basins of the Black, Caspian seas and some part of the Mediterranean sea.

2. Regional coupled model

2.1. STRUCTURE OF THE MODEL, EQUATIONS

The coupled model consists of separate blocks, each of them represents mathematical model describing hydro-thermodynamic processes in separate objects of the environment (sea, atmosphere, active layer of the soil).

The vertical structure of the model comprises the following layers: 1. Troposphere; 2. the surface layer; 3.active layer of the soil; 4. active layer of the sea; 5. lower layer of the sea.

In each layer for description of physical processes the following differential equation systems are considered:

I. *In the troposphere* the full system of atmospheric hydro-thermodynamic equations;

II. *In the lower turbulent layer of the atmosphere* simplified one-dimensional equation system of atmospheric boundary layer;

III. *In the active layer of the seas* two variants of models are offered. The first variant, based on the three-dimensional equations of ocean hydro-thermodynamics allows considering processes of horizontal transport more completely, but such approach requires significant computer resources. The second one is based on the one-dimensional equations of ocean hydro-thermodynamics and allows the use of high vertical resolution that is very important for correct descriptions of vertical hydrological structure in this layer;[14,15]

IV. *In the active layer of the soil* we have the equation of heat conductivity.

2.2. BOUNDARY CONDITINS

These equations are connected with one another with boundary conditions on a vertical which basically express continuity of solutions and their first derivatives at transition from one layer to another. As one of boundary conditions on the underground surface (water, land) the equation of heat balance is considered.

It is much more difficult to write adequate boundary conditions on the interface sea – air, where the sea surface is exposed to permanent changes in time depending on atmospheric conditions. On formation of momentum, heat and water vapour turbulent fluxes near the sea surface major influence renders a state of the sea surface. Dependence of these fluxes from the state of the sea surface is possible to take into account with the help of semi-empirical BULK formulas.

It is well-known, that at solving of the equation system of the atmosphere for the limited territory there are the difficulties connected to statement of lateral boundary conditions. Difficulties are connected to absence of meteorological information on lateral boundaries. In this case it is necessary to use such boundary conditions that practically will not deform the solution. For such conditions it is possible to apply fixed boundary conditions, equality to zero derivatives on a normal to lateral boundaries of meteorological values, etc. Such approach is expedient to use in that case when the coupled model is realized for the term of several model days. With the purpose of examination of a climate change, when the model is realized on more long-range term, it is necessary to use on lateral boundaries results of calculations on global models of general circulation of the atmosphere or ocean-atmosphere.

2.5. METHOD OF SOLUTION

The resolvability of separate mathematical problems included in the coupled model is established in.[16,17]

   With the purpose of numerical solution of problems included in the coupled model, well-known splitting methods are used, which were suggested by G. I. Marchuk for the first time for solution of problems of dynamics of the atmosphere and ocean.[18,19]
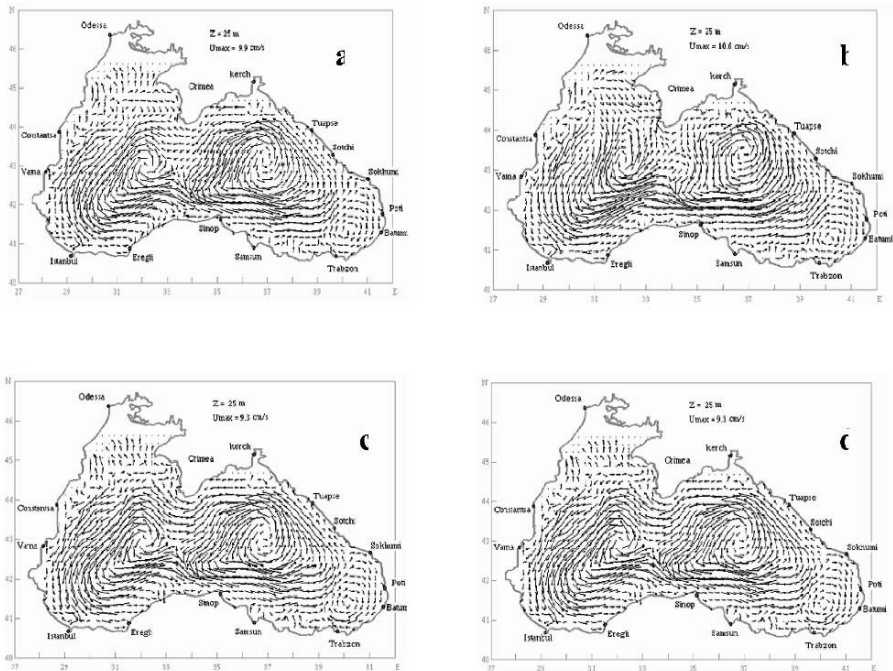
Figure 1. Calculated current fields of the Black Sea on depth of 25 m in July at different time moments: (a) – 4486h, (b) – 4502 h, (c) – 4550 h, (d) – 4554 h (time is counted since 1st January of the 3 modeling year).

3. Models of the Black Sea and atmosphere dynamics

At present the separate blocks of the coupled model – the Black Sea and the atmosphere dynamics models are realized.

3.1. THE BLACK SEA DYNAMICS MODEL

The model of the Black Sea dynamics[9,10] is based on the complete system of the ocean hydro-thermodynamic equations, which is written in the Cartesian coordinate system for deviations of thermodynamical values from their standard vertical distributions. The model takes into account: water exchange with the Mediterranean Sea, Danube River inflow, atmospheric forcing, quasi-realistic bottom relief, the absorption of short-wave radiation by surface layer of the sea, space-temporal variability of horizontal and vertical exchange. Atmospheric forcing on hydrophysical processes is taken into account by boundary conditions on the sea surface considered as a rigid surface, where the stress wind components, temperature (or heat fluxes) and salinity (or evaporation and precipitation) are given as known functions. On the sea bottom the velocity components, heat and salt fluxes are equal to zero. On the lateral surfaces, limiting the domain of solution, two following kinds of boundary conditions are considered: a) On the rigid boundaries, sharing sea from land, components of current velocity, gradients of temperature and salinity normal to the boundary surface are equal to zero; b) On the liquid boundaries, connecting the sea with Bosporian Strait and Danube River – values of discharges, temperature and salinity are given on the basis of experimental data.

Figure 1 illustrates calculated sea currents on depth of 25 m in July when above the Black Sea alternation of different types of atmospheric circulation, characteristic for the Black Sea basin, took place. Integration started on the 1st of January by 5 km horizontal spacing and as initial conditions annual mean climatic fields of current, temperature, and salinity were used, which were obtained by the same model on annual mean input climatic data. Results of numerical experiment were analyzed on the third model year when quasi-periodical regime was established.

In Figure 1 basic features of the Black Sea circulation known from observations,[4,7,8] such as the general cyclonic character of current, cyclonic circulations in east and western parts of the basin, an anticyclonic vortex in the southwest part (Batumi anticyclone) are well visible.

3.2. ATMOSPHERE DYNAMICS MODEL

The evolution of the meteorological values (the wind velocity components, temperature, pressure, water vapor and atmospheric water) in atmosphere is described by a 3-D non-stationary, non-adiabatic system of atmospheric hydro-thermodynamics equations in the hydrostatic approximation.[13]

In order to obtain realistic boundary conditions on the interface levels of the soil-atmosphere and sea water-atmosphere 1-D equations of heat diffusion and infiltration of soil water in the active layers of sea water and soil are solved, respectively.

On the tropopause the fluxes of momentum, heat, water vapor and cloud water are absent. The deviation of the pressure is determined by using the condition of continuity pressure on this level. On the top of the surface layer the turbulent flux of water is equal to zero, the turbulent fluxes of the momentum, heat, and water vapor are known values and they are determined by wide using parameterization formulas. At the lateral boundaries of the area the horizontal gradients of wind velocity and deviations of the meteorological elements from their background values are equal to zero. At the start the distribution of meteorological values corresponded to the background unperturbed state of the atmosphere.
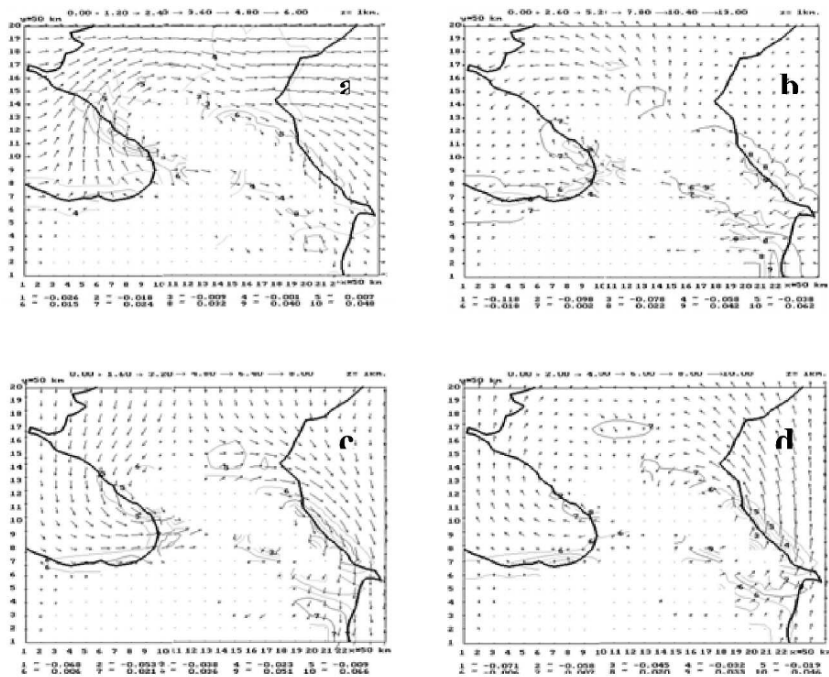
Figure 2. Fields of wind velocity (m/s) and isolines of vertical velocity W (m/s) in cases: (a) ~ western; (b) ~ eastern; (c) ~ north; (d) ~ south winds on height z = 1 km at t = 5 h.

As an example in Figure 2 results of calculations for the Caucasian region are given. From this figure it is visible, that the relief of the Caucasian region substantially defines spatial structure of a wind field. In case of western and northern background wind well-known from

observations anticyclonic and cyclonic vortexes are received in vicinities of the Kolkhida valley and Mugan steppe.

4. Spreading of polluting substances in the Black Sea

Among problems connected to marine ecology, calculation and the forecast of distribution of different impurities in the sea and atmosphere are very actual. It is known, that in change of concentration of any impurity, besides of physical, chemical and biological factors, hydrodynamic factors play a major role connected with transport of an impurity by currents and its dispersion by turbulent vortexes. Therefore, circulating characteristics obtained on the basis of sea dynamics models are directly used in problems of distribution of an impurity.

4.1. A 3-D MODEL

A 3-D model of spreading of non-conservative admixture in a sea basin[20] is based on a transfer - diffusion equation

$$\frac{\partial \varphi}{\partial t} + \frac{\partial u \varphi}{\partial x} + \frac{\partial v \varphi}{\partial y} + \frac{\partial w \varphi}{\partial z} + \sigma \varphi = \nabla \mu_\varphi \nabla \varphi + \frac{\partial}{\partial z} v_\varphi \frac{\partial \varphi}{\partial z} + f$$

,

where

$$\nabla \mu_\varphi \nabla \varphi = \frac{\partial}{\partial x} \mu_\varphi \frac{\partial \varphi}{\partial x} + \frac{\partial}{\partial y} \mu_\varphi \frac{\partial \varphi}{\partial y} .$$

Here φ is the volume concentration of a polluting substance; u, v and w are the components of the flow velocity along axes x, y and z (x is directed eastward, y – northward, z - from a sea surface vertically downward), which satisfy the continuity equation and velocity vector's normal component to the surfaces limited the area of integration is equal to zero; μ_φ and v_φ are the horizontal and vertical turbulent diffusion coefficients; $\sigma = \ln 2 / T_0$ is the parameter of non-conservativity, which in case of a radioactive contamination describes reduction of concentration because of radioactive decay (T_0 - the decay period); f is the function describing distribution of pollution sources. We simulated the spatial distribution of a non-conservative impurity (on an example of a radioactive isotope strontium - 90), continuously allocated in the sea environment from a deep hypothetical source by power 2000 Ci per year (depth of an arrangement of sources - 805, 1205 and 2205 m). As boundary conditions the homogeneous Neumann conditions on all boundaries of 3-D area were used and at the initial moment pollution of a sea basin was absent.

1 ~2.315 2 ~2.557 3 ~2.799 4 ~3.040 5 ~3.282
6 ~3.524 7 ~3.766 8 ~4.007 9 ~4.249 10 ~4.491

1 ~1.968 2 ~2.053 3 ~2.139 4 ~2.225 5 ~2.311
6 ~2.397 7 ~2.482 8 ~2.568 9 ~2.654 10 ~2.740
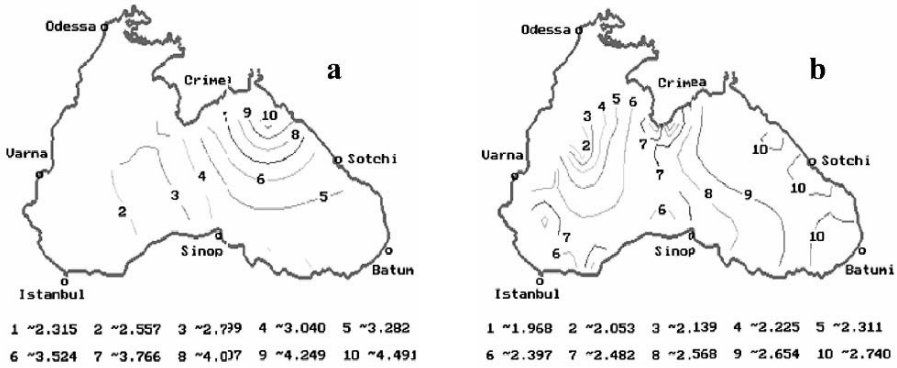
Figure 3. Isolines of polution concentrations (in units of Bq/m^3) on horizons:

(a) - 705 м; (b) - 85 м.

1 ~1.635 2 ~1.892 3 ~2.150 4 ~2.407 5 ~2.665
6 ~2.923 7 ~3.180 8 ~3.438 9 ~3.695 10 ~3.953

1 ~1.603 2 ~2.106 3 ~2.609 4 ~3.113 5 ~3.616
6 ~4.119 7 ~4.622 8 ~5.125 9 ~5.629 10 ~6.132
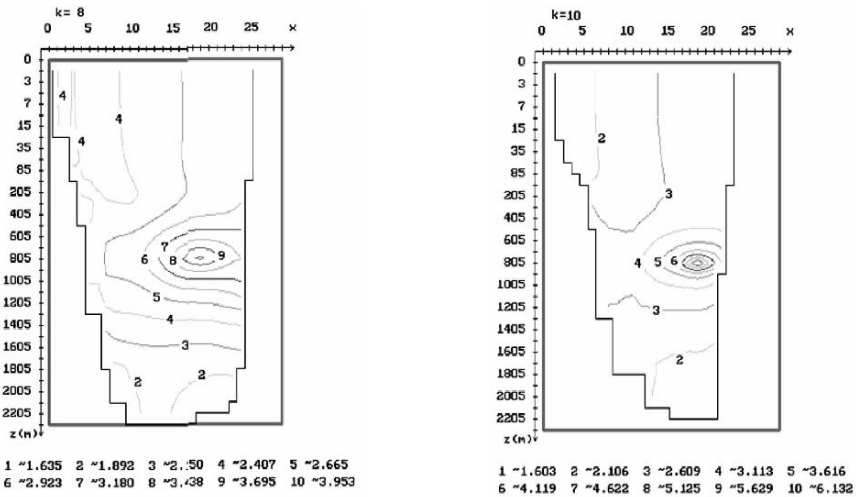
Figure 4. Isolines of pollution concentrations (in units of Bq/m^3) on vertical sections zx.

In Figures 3 and 4 after 39 modelling years concentrations of an impurity on horizons 705 m and 85 m and in some vertical sections, when dynamic balance was achieved, are shown (the source was located at depth of 805 m).

.

4.2. A 2-D OIL DISPERSION MODEL

A 2-D version of pollution dispersion model was realized for simulation of oil spreading on the Black Sea surface in case of emergency emission of oil into the open part of the Black Sea.[21] The numerical experiments were carried out at different locations of a point source. In one of these experiments the oil in the amount of 100000 t was falling into the sea basin at a point: $44^o11`N$ and $31^o02`E$. This point was located in north-western branch of the main Black Sea current, where the flow was directed to south-west. Figure 5 illustrates the process of space-temporal distribution of oil pollution in this case.

5.   Determination of a source location in a sea basin

Important environmental problem is finding of the probable location of a pollution source in water basin on known concentrations of polluting
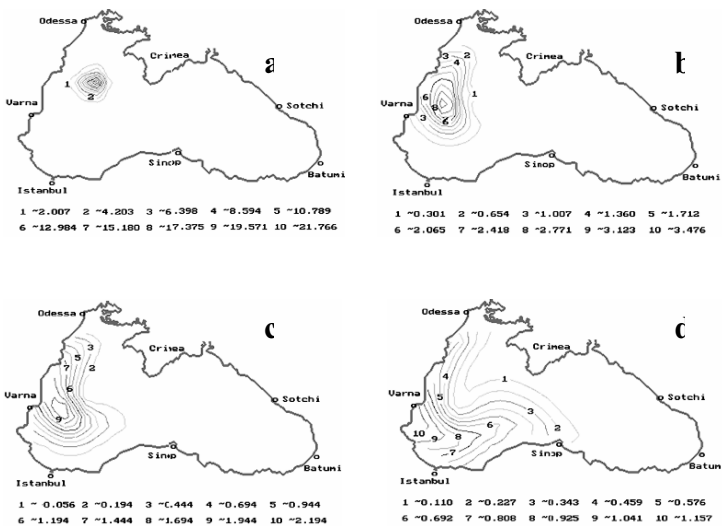
Figure 5. Isolines of oil concentrations (in units of mg/l) at different moments after accidental oil emission: (a) – 2 days, (b) – 10 days, (c) – 15 days, (d) – 30 days.

substance in some points of the upper layer. It is well-known that sometimes highly toxic substances used to be dump in the Black Sea (as well as some interior seas). Such burial places in deep layers of the sea are "bombs of a slow operation". In some cases locations of such burials are not known. The finding of such sources with the purpose of their neutralization is connected to realization of the expensive experimental works.

In[22] the conjugate transfer-diffusion equation was used for decision of an important ecological problem of optimum accommodation of the industrial enterprises. This theory can be also used for determination of the location of a pollution source in water basin on known concentrations of an polluting substance in some points of the basin.[23,24] The method is based on solving of conjugate transfer-diffusion equation and the principle of duality of corresponding functionals.
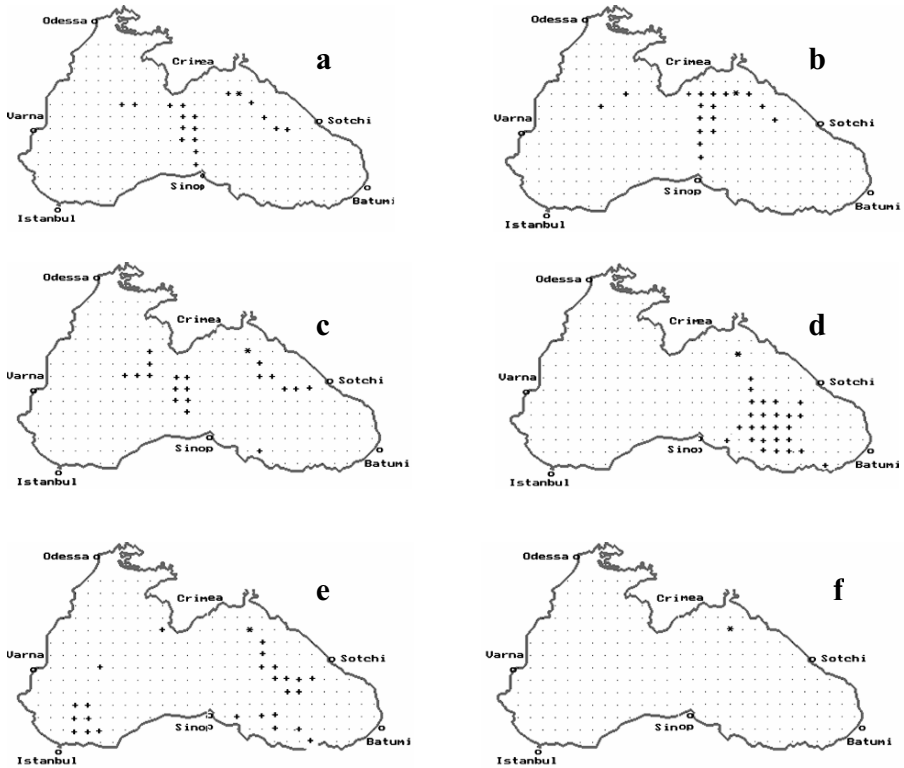
Figure 6. Subsets of possible points of the source location on the horizon z=805 m . See text for explanations.

5.1. DESCRIPTION OF THE THEORETICAL METHOD

We will assume, that concentration field in a water area Ω is generated as a result of action of a stationary point source by power Q in deep layers, and as a result of experimental measurements the pollution concentrations are known in some points $\vec{\xi}_i \in \Omega$ (*i=1,2,...,N*) in the upper layer of the sea.

Our problem consists in determination of the domain $\omega \subset \Omega$, where the source is located. For the solution of this problem N quantity of the conjugate transfer-diffusion equations with a corresponding right part P_i is considered. P_i by means of delta-function can be defined as $P_i = \delta \left(\vec{r} - \vec{\xi}_i \right)$. The conjugate problem is solved with decreasing t in the interval $T \geq t \geq 0$ for every selected point in the upper layer of the sea.

At the solution of each conjugate problem corresponding functional

$$J_{p_i} = Q \int_0^T \varphi_i^* \left(\vec{r}_0, t \right) dt \ \ (i=1,2,...,N)$$

is calculated, where - φ_i^* is the solution of the conjugate problem. After that, on the basis of the use of property of a duality of functionals subsets $\omega_i \subset \Omega$, which contain possible points of location of the source, are defined. The area of the location of the source is defined as intersection of subsets ω_i.[23,24]

With the purpose of approbation of the suggested method test numerical experiments are carried out for the Black Sea basin. They consist in the following: as a result of solution of the direct problem of transfer - diffusion in the time interval (0, T) on known source power Q and its location we receive the calculated field of pollution concentrations on the whole basin. After that we "forget" coordinates of location of a source and our purpose is to define the location of the source on above described method.

5.2. APPROBATION OF THE METHOD FOR THE BLACK SEA BASIN

The method has been approved in two cases: 1. The source was in deep layers of the sea. 2. The source was on a surface of the sea. Fig. 6 illustrates this method in that case when the source was located on depth of 805 m. In this figure subsets a, b, c, d, e, corresponding to ω_i (i = 1,2,...,5), are shown, which correspond to points, lying at the level of 15 m. In this case the intersection ω of these subsets contains only one point (see Figure 6f). It is the point of a source location and thus, the location of the source is defined with ideal accuracy.

References

1. G. I. Marchuk, V. B. Zalesny, and V. N. Lykosov, Modeling of Winter Climate of the World Ocean. Preprint, Moscow, OVM AN SSSR, 1982, p. 42 (in Russian).
2. G. I Marchuk and A. A. Kordzadze, in: *Numerical Modeling of Climate of the World Ocean/Numerical Modeling of the Sea Dynamics on the Basis of the Splitting Method* (OVM SSSR, Moscow,1986), pp. 151–163 (in Russian).

3. F. Blumberg and G. L. Mellor, in: *Three Dimensional Shelf Models, Coastal Estuarine Sci./A Description of a 3-D Coastal Ocean Model*. (AGU, Washington, 1987, v. 5), pp. 1–16.

4. E. V. Stanev, D. I. Truhchev, and V. M. Roussenov, *The Black Sea Water Circulation and Numerical Modeling of Currents* (Kliment Ohridski University Press, Sofia, 1988) (in Russian).

5. A Kordzadze, *Mathematical modeling of the sea current dynamics (theory, algorithms, numerical experiments*) (OVM AN SSSR, Moscow, 1989) (in Russian).

6. Ch. Mooers and H. S. Kang, in: *Proceed. of the PICES Workshop on the Sea of Okhotsk and Adjacent Areas/Preliminary Results from a Sea of Japan Numerical Circulation Mode.,* PICES Scientific Report No 6, 1996, pp. 202–214.

7. T. Oguz, P. Malanotte-Rizzoli., and D. Aubrey. Wind and thermohaline circulation of the Black Sea driven by yearly mean climatological forcing. *J. Geophys. Research.* 100(c4), 6845–6863 (1995).

8. S. G. Demyshev and G. K. Korotaev, Numerical modeling of synoptic variability of the Black Sea with consideration for seasonal boundary conditions, *Izv. Acad. Sci. Russia, Atmospheric and Oceanic Physics,* v.32, No 1, 108–116 (1996) (in Russian).

9. A. Kordzadze., K. Bilashvili, and D. Demetrashvili, in: *Proceed. of the Second Inter. Conf.: "Oceanography of the Eastern Mediterranean and Black Sea: Similarities and Differences of Two Interconnected Basins"/Numerical Modeling of Hydrological Rregime in the Black Sea with Taking into Account of Water Exchange with the Mediterranean Sea.* (Ankara/Turkey, 2003), pp. 888–896.

10. A. Kordzadze and D. Demetrashvili, in: *Proceed. of the Intern. Conference: "A year after Johanesburg-Ocean Governance and Sustainable Development: Ocean and Coasts – a Glimpse into the Future"/Numerical Modeling of Inner-annual Variability of the Hydrological Regime of the Black Sea with Taking into Account of Alternation of Different Types of the Wind above its Surface.* (Kiev/Ukraine, 2003), pp. 495–505.

11. K. A. Korotenko, R. M Mamedov, and C. N. K. Mooers, Prediction of the Transport and Dispersal of Oil in the South Caspian Sea Resulting from Blowouts, *Environmental Fluid Mechanics.* v. 1, 383–414 (2002).

12. G. P. Kurbatkin, in: *Achivments in Hydrometeorology and Monitoring of Natural Environment/Hydrodynamical Operative Weather Predictions*. (Gidrometeoizdat, Leningrad/Russia, 1987), pp. 10–33.

13. A. Kordzadze and A. Surmava A non-adiabatic model of the development of the middle-scale atmosphere process above the Caucasian region. *J. Georgian. Geophys. Soc.*, v.6b, 33–40 (2001).

14. A. Kordzadze and D. Demetrashvili, On main structure of a coupled hydrodynamical model "sea-atmosphere" and possible ways of its construction. *Transactions of the Institute of Hydrometeorology*, Tbilisi, v. 101, 28–38 (1998) (in Georgian).

15. A. Kordzadze and D. Demetrashvili, in: *Contemporary Change of Climate of Georgia. Correlation and Variability of the Weather Elements. Proceed. of V. Bagrationi Institute of Geography /A Regional Hydrodynamic Model of Climatic System Sea-Land-Atmosphere* (Tbilisi/Georgia, 2003), v.21, pp. 16–30 (in Georgian).

16. V. I. Sukhonosov, In: *The Mechanics of the Heterogeneous Continuous Medium./On the general correctness of 3-D problem of the ocean dynamics* (Comp. Center of Siberian Branch of AS USSR, Novosibirsk/Russia, 1979) v. 52, pp. 37–53.

17. A. Kordzadze, A. Mathematical problems of solution of the ocean dynamics tasks (Comp. Center of Siberian Branch of AS USSR, Novosibirsk , 1982) (in Russian).

18. G. I. Marchuk, Numerical methods in the weather prediction (Gidrometeoizdat, Leningrad, 1967).

19. G. I. Marchuk, Numerical solution of problems of the atmosphere and the ocean dynamics (Gidrometeoizdat, Leningrad, 1974).
20. A. Kordzadze and D. Demetrashvili, A 3D numerical model of distribution of non-conservative admixture in the Black Sea. *J. Georgian Geophys. Soc.*, v. 5b, 3–11 (2000).
21. D. Demetrashvili and A. Kordzadze, Numerical modeling of distribution of pollution substances in the Black Sea. *Reports of enlarged sessions of the seminar of I. Vekua Institute of applied mathematics*. v. 17, No 3, 44–57 (2002).
22. G. I. Marchuk, Mathematical modelling in the environmental problem. (Science, Moscow, 1982).
23. A. Kordzadze and D. Demetrashvili, Numerical experiments on the determination of the pollution source location in the Black Sea. 3D problem. *J. Georgian Soc.*, v.6b, 3–12 (2001).
24. A. Kordzadze and D. Demetrashvili, Numerical experiments on the determination of the pollution source location in the Black Sea. 2D problem. *J. Georgian Geophys Soc.*, v.6b, 13–22 (2001).

MATHEMATICAL MODELLING AND NUMERICAL SOLUTION OF SOME PROBLEMS OF WATER AND ATMOSPHERE POLLUTION

DAVID GORDEZIANI*
I. Vekua Institute of Applied Mathematics, Iv. Javakhishvili Tbilisi State Universit,2 University St., 0143, Tbilisi, Georgia

EKATERINE GORDEZIANI
Iv. Javakhishvili Tbilisi State University, 2 University St., 0145, Tbilisi, Georgia

Abstract. In the current work there are shortly described several methods and prospective directions of mathematical and numerical modelling, that seem very promising and efficient for further application and investigation of problems of water and air quality control in water bodies and the atmosphere, respectively. Namely, for certain linear non-classical problems issues of existence and uniqueness, finite-difference are investigated and decomposition methods are developed for their solution.

Keywords: Water pollution models; classical and non-classical boundary conditions; non-local problems; finite-difference methods; decomposition algorithms: parallel count

_____

*To whom correspondence should be addressed. D. Gordeziani, I. Vekua Institute of Applied Mathematics, Iv. Javakhishvili Tbilisi State Universit, 2 University St., 0143, Tbilisi, Georgia; e-mail: gord@viam.hepi.edu.ge

1. Introduction

Having improved in various fields of science and technology and liberalizing the mankind, using environment resources and more deeply interfering in the outer world, upsets the existing balance of nature. The earth ecosystem is being destroyed and research of the ways of its rehabilitation is one of the most important tasks of the contemporary world. The water and atmosphere are necessary items for life, pure drinking water and clean air are required for healthy existence.

Mathematical modelling and application of numerical analysis enables us to forecast these or those parameters of water/atmosphere quality via computer simulation and thus becomes possible to control and manage the current processes. This is cost-effective and preserves expenses that would be needed for the arrangement and conduction of experiments, and sometimes it appears to be the only way of studying relevant phenomena. Thus, mathematical modelling of diffusion processes in the environment and investigation of pollution problems is one of the most actual and interesting challenges of applied and computational mathematics. Therefore, all stages of mathematical modelling of that kind of problems are being constantly improved, refined and in some cases even simplified.

Actually, a big variety of non-linear mathematical models describing pollution processes exist, but in the current work we only focus on linear mathematical models describing pollution transfer or, more generally, solution diffusion processes in water streams. Similar issues are considered for the processes of admixture transfer in the atmosphere. For the purpose of clarity, the stated problems are examined for the first case, i.e. when the object of the study is water environment. The results obtained for water bodies can obviously be transferred and applied to the similar processes taking place in the atmosphere.

The literature concerning the research of problems and questions of mathematical modelling on the basis of classical equations of mathematical physics with classical initial-boundary conditions is rather rich and vast (e.g.[1-10]).

In some works concerning mathematical modelling of admixture diffusion processes in various environments, the authors have encountered a specific type of equations that until recently were not used to describe the above mentioned processes[11]. Such equations are known under the name of "pluri-parabolic" equations[12-17]. Theoretical issues and algorithms of numerical solution of these types of equations with classical initial-boundary conditions are poorly studied yet. Thus, the investigation of the mentioned problems has very substantial theoretical and practical value.

It is also important to emphasize that in some cases during the process of mathematical modelling of pollution problems we deal with initial-boundary value problems with non-classical boundary conditions. Naturally the question of investigation of mathematical problems comes up that are based on classical equations of mathematical physics with non-classical (e.g. non-local) initial-boundary conditions. This problem has been addressed by many authors[12-31]. However, it should be noted that very few studies are devoted to the numerical solution of such problems.

Finally, we would like to present mathematical models with non-classical equations and non-classical boundary conditions (conditions of Cannon, Bitsadze-Samarskii, etc.[26-31]. Only a few papers deal with theoretical analysis and numerical solution of such models.

In the present work we consider some of the mathematical models of the mentioned type, carry out their analysis and for some of them and suggest and study respective difference methods.

1.   Mathematical models

Aiming at mathematical modelling of contamination processes in the water/atmosphere environment we usually obtain the following kinds of problems written in mathematical terms:

(i)   Classical equation (second order linear partial differential equation of parabolic, elliptic type) with classical initial-boundary condition (Dirichlet, Neumann, mixed);

(ii) Classical equation with non-classical initial-boundary conditions (Bitsadze-Samarskii, Integral);

(iii) Non-classical equation with classical boundary conditions;

(iv) Non-classical equation with non-classical conditions.

Comprehensive and deep theoretical knowledge and flexible tools of solution exist for classical problems (see e.g.[1-10]) and so, there is no need to concentrate on them. We will mainly focus our attention to the latter three cases, i.e. (ii) - (iv).

The process of pollution diffusion in water flows could be described more or less precisely, as was mentioned above, via diffusive mathematical models. Let us very shortly take a look on these models.

The linear partial differential equation describing the diffusion of matter in the water is (see [1,11])

$$\frac{\partial S}{\partial t} = \frac{\partial}{\partial x}\left(K_x\frac{\partial S}{\partial x}\right) + \frac{\partial}{\partial y}\left(K_y\frac{\partial S}{\partial y}\right) + \frac{\partial}{\partial z}\left(K_z\frac{\partial S}{\partial z}\right) - \qquad (1)$$

$$- v_x\frac{\partial S}{\partial x} - v_y\frac{\partial S}{\partial y} - v_z\frac{\partial S}{\partial z} - u_y\frac{\partial S}{\partial y} + F,$$

$$(x,y,z)\in G, \ t\in(0,T),$$

where x, y, z are spatial coordinates; t - time; $S \equiv S(x,y,z,t)$ - concentration of polluting substance; K_x, K_y, K_z - coefficients of turbulent diffusion along the Ox, Oy, Oz axes; v_x, v_y, v_z - components of the water flow velocity vector along the Ox, Oy, Oz axes; u_y - hydraulic size of particle.

To formulate the initial and initial-boundary conditions it is necessary to determine the area where the water flow is considered. Assume that (x,y,z) is a Cartesian system of coordinates the water flow occupies area G with the boundaries $\Gamma = \Gamma_1 \cup \cdots \cup \Gamma_6$; Γ_1 - surface of upper cross section; Γ_2 and Γ_4 - side surfaces, Γ_5 - bottom surface; Γ_6 - free surface; Γ_3 - surface of lower cross section of the river; Γ_0 - orthogonal cross section between the upper and lower surfaces.

Equation (1) with initial-boundary conditions represents the mathematical model of the considered process. Thus, the following initial and boundary conditions are used to determine the concentration of a polluting substance during the time period $[0,T]$ $(T = const > 0)$ in the area G by solving Eq. (1):

$$S(x,y,z,0) = S_0(x,y,z), \ (x,y,z)\in G, \qquad (2)$$

$$S(x,y,z,t) = \varphi_1(x,y,z,t), \ (x,y,z)\in\Gamma_1, \ t\in[0,T], \qquad (3)$$

$$\frac{\partial S}{\partial v} + \alpha S = \varphi_2, \ (x,y,z)\in\Gamma_2\cup\Gamma_4\cup\Gamma_5\cup\Gamma_6, \ t\in[0,T], \qquad (4)$$

$$\frac{\partial S}{\partial v} = 0, \ (x,y,z)\in\Gamma_3, \ t\in[0,T], \qquad (5)$$

where S_0, φ_1, φ_2, α are prescribed functions, $\vec{n}$ - external normal to Γ,

$$\frac{\partial S}{\partial v} = K_x\frac{\partial S}{\partial x}\cos(Ox,\vec{n}) + K_y\frac{\partial S}{\partial y}\cos(Oy,n) + K_z\frac{\partial S}{\partial z}\cos(Oz,\vec{n}).$$

The mathematical model (1)-(5) belongs to the classical group (i), that is, when the equations describing the process of diffusion and initial-boundary conditions are classical from mathematical point of view.

Due to some properties and various peculiarities of the water flow more simplified models are being considered instead of model (1)-(5). For example, the model (1)-(5) was substituted for the purpose of practical calculations by the models where $v_x = v_{1cp}$ (averaged velocity) was sufficiently large, and the transport of the substance along x was much faster than diffusion, $v_{1cp} = const > 0$ (see[1]). In this case Eq. (1) takes the form:

$$v_{1cp}\frac{\partial S}{\partial x} = \frac{\partial}{\partial y}\left(K_y\frac{\partial S}{\partial y}\right) + \frac{\partial}{\partial z}\left(K_z\frac{\partial S}{\partial z}\right) - v_y\frac{\partial S}{\partial y} - v_z\frac{\partial S}{\partial z} - u_y\frac{\partial S}{\partial y} + F, \quad (6)$$

$$(x, y, z) \in G,$$

which again represents an equation of parabolic type.

Using the self-purification property we naturally obtain a mathematical model where condition (5) is replaced by the following one:

$$S(x, y, z, t) = q(x, y, z, t)S(x^*, y^*, z^*, t) + \varphi_3, \quad (5')$$

$$(x, y, z) \in \Gamma_3, \ (x^*, y^*, z^*) \in \Gamma_0, \ t \in [0, T],$$

where q is the coefficient of self-purification ($0 \le q \le 1$), φ_3 is a known function, $\Gamma_0 = I(\Gamma_3)$, $I(\cdot)$ is diffeomorfism between Γ_0 and Γ_3. Thus, the problem (1)-(4), (5') is already a non-classical problem from group (ii).

In the non-stationary case Eq. (6) takes the form of

$$\frac{\partial S}{\partial t} + v_{1cp}\frac{\partial S}{\partial x} = \frac{\partial}{\partial y}\left(K_y\frac{\partial S}{\partial y}\right) + \frac{\partial}{\partial z}\left(K_z\frac{\partial S}{\partial z}\right) - v_y\frac{\partial S}{\partial y} - v_z\frac{\partial S}{\partial z} - u_y\frac{\partial S}{\partial y} + F, \quad (7)$$

$$(x, y, z) \in G, \ t \in (0, T).$$

and this latter equation appears to be complicated enough and unknown from the theoretical as well as from the numerical point of view.

Referring to[2], it makes sense to consider the following equation:

$$\frac{\partial S}{\partial t} + v_{1cp}\frac{\partial S}{\partial x} + v_{2cp}\frac{\partial S}{\partial y} = \frac{\partial}{\partial z}\left(K_z\frac{\partial S}{\partial z}\right) + F, \quad (8)$$

$$(x, y, z) \in G, \ t \in (0, T).$$

Equations (7) and (8) are pluri-parabolic and they belong to the non-classical group of equations. Thus consideration of them with conditions (2)-(5) will give us problems of type (iii).

Actually it is already very easy to understand what kind of problems should give us the models of group (iv), that is, when the equation describing the process is non-classical and the boundary conditions are non-classical as well.

The above stated mathematical models are linear diffusive models and their choice depends on hydro-dynamical characteristics of the water flow in the considered area. The initial-boundary conditions also depend on water characteristics.

After successful application of mathematical analysis to diffusion models describing displacement and immixture of polluting substances, it is necessary to find algorithms for their numerical solution.

2.　　　Mathematical statement of problems

In the present paragraph the following general problem is stated: one should find the function $u(x,t) \in C^{2,1}(D) \cap C^{1,0}(\overline{D})$, satisfying equation

$$P_t u(x,t) - L u(x,t) = f(x,t),\ (x,t) \in D, \tag{9}$$

and the following initial and initial-boundary conditions

$$u(x,0,t_2,...,t_m) = \varphi_{11}(x,t_2,...,t_m),\ x \in \overline{G},\ 0 \le t_i \le T_i, i = \overline{2,m}, \left.\begin{array}{l} \\ \\ \end{array}\right\}$$

$$\cdots \tag{10}$$

$$u(x,t_1,...,t_{m-1},0) = \varphi_{1m}(x,t_1,...,t_{m-1}),\ x \in \overline{G},\ 0 \le t_i \le T_i, i = \overline{1,m-1},$$

$$u(x,t) = \varphi_2(x,t),\ x \in \Gamma^+,\ 0 \le t_i \le T_i,\ i = \overline{1,m}, \tag{11}$$

$$\beta \frac{\partial u(x,t)}{\partial v} + \alpha u(x,t) = \sum_{i=0}^{P} \alpha_i u(x_{\Gamma_i},t) + \varphi(x,t), \tag{12}$$

$$x \in \Gamma^-,\ 0 \le t_i \le T_i,\ i = \overline{1,m},\ x_{\Gamma_i} \in \Gamma_i,\ i = \overline{0,P},$$

where

$$L \equiv \sum_{i,j=1}^{n} \frac{\partial}{\partial x_i}\left(a_{ij}(x,t)\frac{\partial}{\partial x_j}\right) + \sum_{i=1}^{n} b_i(x,t)\frac{\partial}{\partial x_i} + c(x,t)\ ,$$

$$P_t \equiv -\sum_{i=1}^{m} a_i(x)\frac{\partial}{\partial t_i}, \tag{13}$$

in the initial-boundary limitations (10)-(13) there is assumed that conditions of compatibility are fulfilled; α, β, α_i $(i = \overline{0,P})$ are given constants; $a_i \ge q = const > 0$, φ_{1i} $(i = \overline{1,m})$, $\varphi_2(x,t)$, $\varphi(x,t)$ and $f(x,t)$ are prescribed, sufficiently smooth functions defined on the corresponding areas of definition;

$$\frac{\partial u}{\partial v} = \sum_{j,i=1}^{n} a_{ij}\frac{\partial u}{\partial x_j}\cos(Ox_i,\vec{n}),$$

$\vec{n}$ is an external normal of Γ boundary, $(Ox_i,\vec{n})$ $(i = \overline{1,n})$ are the angles between Ox_i axis and $\vec{v}$ normal vector; D - $(n+m)$-dimensional area in R^{n+m} space, $D = G \times \Omega$, $(x,t) = (x_1,...,x_n,t_1,...,t_m) \in D$; $G \subset R^n$, Γ is sufficiently smooth boundary of $\overline{G} = G \times \Gamma$; in addition $\Gamma = \Gamma^+ \cup \Gamma^-$; in the G there are given Γ^i $(i = \overline{0,P})$ curves crossing the G without touching Γ^- and there exists diffeomorphism $I_i(\cdot)$ between Γ^i curves and Γ^- boundary, $I_i(\Gamma^i) = \Gamma$ $(i = \overline{0,P})$; $\Omega = (0,T_1) \times \cdots \times (0,T_m)$, where T_i $(i = \overline{0,m})$ are known constants. We also assume that everywhere farther the following conditions are satisfied:

(A) for any $(x,t) \in D$ point and real vector $\zeta = (\zeta_1,...,\zeta_n) \neq 0$ the

inequality $\underline{\alpha} \sum_{i=1}^{n} \zeta_i^2 \leq \sum_{i,j=1}^{n} a_{ij} \zeta_i \zeta_j \leq \overline{\alpha} \sum_{i=1}^{n} \zeta_i^2$ is true, where $\overline{\alpha}$, $\underline{\alpha}$ are

given positive numbers;

(B) the coefficients of L operator are continuous functions in $\overline{D}$;

(C) $c(x,t) \leq 0$ in $\overline{D}$.

For the pluri-parabolic operator the principle of maximum is proved. Practically it is the analogue of well-known principle of maximum for the parabolic operator.

Under the assumptions that $G = (0,l_1) \times \cdots \times (0,l_n)$, $l_i = const$, $i = \overline{1,n}$ and

$$L \equiv \sum_{i,j=1}^{n} \frac{\partial}{\partial x_i}\left(a_{ii}(x,t)\frac{\partial}{\partial x_i} \right) + c(x,t),$$

$$P_t \equiv \sum_{i=1}^{m} \frac{\partial}{\partial t_i},$$

$\alpha > 0$, $\beta > 0$, $a_{ii} \geq a_0 = const > 0$, $(i = \overline{1,n})$, $a_{ii} = a_{ii}(x_1,...,x_{i-1},x_{i+1},...,x_n,t)$,

the following problem is generated from the problem (9)-(13),:

$$\sum_{i=1}^{n} \frac{\partial}{\partial x_i}\left(a_{ii}(x,t)\frac{\partial u}{\partial x_i} \right) + c(x,t)u - \sum_{i=1}^{m} \frac{\partial u}{\partial t_i} = f(x,t), \ (x,t) \in D, \quad (14)$$

$$\left.\begin{array}{l}u(x,0,...,t_m) = \varphi_{11}(x,t_2,...,t_m), \ x \in \overline{G}, 0 \leq t_i \leq T_i, i = \overline{2,m}, \\ \cdots \\ u(x,t_1,...,t_{m-1},0) = \varphi_{1m}(x,t_1,...,t_{m-1}), \ x \in \overline{G}, 0 \leq t_i \leq T_i, i = \overline{1,m-1},\end{array}\right\} \quad (15)$$

$$\left.\begin{array}{l}u(0,...,x_n,t) = \varphi_{21}(x_2,...,x_n,t), \ t \in \overline{\Omega}, \ 0 \leq x_i \leq l_i, i = \overline{2,n}, \\ \cdots \\ u(x_1,...,x_{n-1},0,t) = \varphi_{2n}(x_1,...,x_{n-1},t), \ t \in \overline{\Omega}, \ 0 \leq x_i \leq l_i, i = \overline{1,n-1},\end{array}\right\} \quad (16)$$

$$\left.\begin{array}{l}u(x_1,l_2,...,x_n,t) = \varphi_{31}(x_3,...,x_n,t), \ t \in \overline{\Omega}, \ 0 \leq x_i \leq l_i, i = \overline{1,n}, \ i \neq 2, \\ \cdots \\ u(x_1,...,x_{n-1},l_n,t) = \varphi_{3n}(x_1,...,x_{n-1},t), \ t \in \overline{\Omega}, \ 0 \leq x_i \leq l_i, i = \overline{1,n-1}, i \neq n,\end{array}\right\} \quad (17)$$

$$\beta \frac{\partial u(l_1,x_2,...,t)}{\partial x_1} + \alpha u(l_1,x_2,...,t) =$$

$$= \sum_{i=1}^{P} \alpha_i u(\xi_i,x_2,...,t) + \int_0^{\xi_0} \rho(x_1)u(x,t)dx_1 + \varphi_{31}(x_2,...,t), \quad (18)$$

$$t \in \overline{\Omega}, \ 0 \leq x_i \leq l_i, i = \overline{2,n},$$

where φ_{2i}, φ_{3i}, $(i = \overline{1,n})$ are sufficiently smooth prescribed functions in the corresponding areas, $\{\xi_k\}_{k=0}^{P}$ are given points $0 < \xi_0 \leq \cdots \leq \xi_P < l_1$.

The existence issue is considered for the following problem: there has to be found a function

$$u(x,t) \in C^{2,1,1}\left((0,l_1) \times (0,T_1) \times (0,T_2)\right) \cap C^{1,0,0}\left([0,l_1] \times [0,T_1] \times [0,T_2]\right),$$

satisfying the equation

$$\frac{\partial u(x,t)}{\partial t_1} + \frac{\partial u(x,t)}{\partial t_2} - \frac{\partial^2 u(x,t)}{\partial x_1^2} - \frac{\partial^2 u(x,t)}{\partial x_2^2} = f(x,t), \qquad (19)$$

$$x \in (0,1), \ t_1 \in (0,T_1), \ t_2 \in (0,T_2),$$

initial conditions

$$\left.\begin{array}{l} u(x,0,t_2) = \varphi_{11}(x,t_2), \ 0 \le x \le 1, \ 0 \le t_2 \le T_2, \\ u(x,t_1,0,) = \varphi_{12}(x,t_1), \ 0 \le x \le 1, \ 0 \le t_1 \le T_1, \end{array}\right\} \qquad (20)$$

and classical boundary limitations

$$\left.\begin{array}{l} u(0,t_1,t_2) = \varphi_2(t_1,t_2), \ 0 \le t_1 \le T_1, \ 0 \le t_2 \le T_2, \\ u(1,t_1,t_2) = \varphi_3(t_1,t_2), \ 0 \le t_1 \le T_1, \ 0 \le t_2 \le T_2. \end{array}\right\} \qquad (21)$$

Finally, the finite-difference methods are developed for the next problem: there has to be found a function

$$u(x,t) \in \ C^{2,1,1}\left((0,1) \times (0,T_1) \times (0,T_2)\right) \cap \ C^{1,0,0}\left([0,1] \times [0,T_1] \times [0,T_2]\right)$$

satisfying the equation

$$\frac{\partial^2 u(x,t)}{\partial x^2} - \frac{\partial u(x,t)}{\partial t_1} - \frac{\partial u(x,t)}{\partial t_2} = f(x,t), \qquad (22)$$

$$x \in (0,1), \ t_1 \in (0,T_1), \ t_2 \in (0,T_2),$$

initial conditions,

$$\left.\begin{array}{l} u(x,0,t_2) = \varphi_{11}(x,t_2), \ 0 \le x \le l_1, \ 0 \le t_2 \le T_2, \\ u(x,t_1,0,) = \varphi_{12}(x,t_1), \ 0 \le x \le l_1, \ 0 \le t_1 \le T_1, \end{array}\right\} \qquad (23)$$

and classical boundary limitations,

$$\left.\begin{array}{l} u(0,t_1,t_2) = \varphi_2(t_1,t_2), \ 0 \le t_1 \le T_1, \ 0 \le t_2 \le T_2, \\ u(1,t_1,t_2) = \varphi_3(t_1,t_2), \ 0 \le t_1 \le T_1, \ 0 \le t_2 \le T_2. \end{array}\right\} \qquad (24)$$

3.   Existence and uniqueness issues

In the fourth paragraph the following theorems of uniqueness are proved:

THEOREM 1.

If $\rho(x_1) = 0$, $\beta = 0$, $\alpha \ne 0$, $\left| \sum_{i=1}^{m} \alpha_i \right| < |\alpha|$ in the condition (13) and there exists solution of the problem (9)-(13), then it is unique.

THEOREM 2.

If in non-local condition (18) one of the following two conditions are satisfied: a) $\rho(x_i) = 0, \alpha_i \geq 0$ $(i = 1, P)$, $\sum\limits_{i=1}^{P} \dfrac{\alpha_i}{\alpha} \leq 1$; or b) $\alpha_i \leq 0$ $(i = 0, P)$,

$\sum\limits_{i=1}^{P} \dfrac{|\alpha_i|}{\alpha} \leq 1$ and there exists the solution of the problem (14)-(18), then solution is unique.

Existence of problem (19)-(21) is stated in the next theorem:

THEOREM 3.
There exists solution of the problem (19)-(21), it is unique and could be presented in the form of the following series,

$$u(x,t) = \sum_{k=1}^{\infty} \sum_{m=1}^{\infty} B_{km}(t) \sin k\pi x_1 \sin m\pi x_2,$$

$$B_{km} = \begin{cases} \varphi_{11km}(x, t_2 - t_1) e^{-\lambda t_1}, t_2 \geq t_1, \\ \varphi_{12km}(x, t_1 - t_2) e^{-\lambda t_2}, t_1 \geq t_2, \end{cases}$$

where $\lambda = \sum\limits_{i=1}^{2} \lambda_{k_i}$ and λ_{k_i} are given values of parameter; φ_{11km} and φ_{12km} are Furrier coefficients corresponding to φ_{11} and φ_{12} functions.

It should be emphasized that having solution of classical problem (19)-(21) it is easy to construct the solution for the problem with non-local boundary condition.

4.   Methods of solution

For the resolution of the problem stated in paragraph one there is suggested the iteration process:

$$P_t u^{k+1}(x,t) - L u^{k+1}(x,t) = f(x,t), (x,t) \in D, \tag{25}$$

$$\left. \begin{aligned} u^{k+1}(x,0,t_2,...,t_m) &= \varphi_{11}(x,t_2,...,t_m), \ x \in \overline{G}, \ 0 \leq t_i \leq T_i, i = \overline{2,m}, \\ &\cdots\cdots\cdots\cdots\cdots\cdots\cdots\cdots\cdots\cdots\cdots\cdots\cdots\cdots\cdots\cdots\cdots\cdots\cdots \\ u^{k+1}(x,t_1,...,t_{m-1},0) &= \varphi_{1m}(x,t_1,...,t_{m-1}), \ x \in \overline{G}, \ 0 \leq t_i \leq T_i, i = \overline{1,m-1}, \end{aligned} \right\} \tag{26}$$

$$u^{k+1}(x,t) = \varphi_2(x,t), \ x \in \Gamma^+, \ 0 \leq t_i \leq T_i, \ i = \overline{1,m},$$

$$\beta \frac{\partial u^{k+1}(x,t)}{\partial \nu} + \alpha u^{k+1}(x,t) = \sum_{i=0}^{P} \alpha_i u^k(x_{\Gamma_i}, t) + \varphi_{31}(x,t), \tag{27}$$

$$x \in \Gamma^-, \ 0 \leq t_i \leq T_i, \ i = \overline{1,m}, \ x_{\Gamma_i} \in \Gamma_i, \ i = \overline{0,P},$$

$$k = 0,1,2,...$$

The following theorem is true for the above iteration:

THEOREM 4.

If in the condition (14) $\rho(x_1) = 0$, $\beta = 0$, $\left|\sum_{i=1}^{P} \alpha_i\right| < |\alpha|$ and there exists the unique solution of the problem (14)-(18), then the iteration process (25)-(27) converges to an exact solution of the problem (14)-(18) with the speed of geometrical progression.

For the regular grid
$$\overline{\omega}_{h\tau_1\tau_2} = \left\{(x_q, t_{1j}, t_{2k}): x_q = qh, t_{1j} = j\tau_1, t_{2k} = k\tau_2, \right.$$
$$\left. q = \overline{0, N}, \; j = \overline{0, N_1}, \; k = \overline{0, N_2}, \; h = 1/n, \; \tau_k = 1/N_k, k = 1,2 \right\}$$

there is constructed the following finite-difference problem corresponding to the differential problem (22)-(25): there has to be found $y_i^{j,k} = y(x_i, t_j, t_k)$ grid function, satisfying the following difference equation,

$$\theta_1 \frac{y_i^{j+1,k+1} - y_i^{j+1,k}}{\tau_2} + (1 - \theta_1) \frac{y_i^{j,k+1} - y_i^{j,k}}{\tau_2} + \theta_2 \frac{y_i^{j+1,k+1} - y_i^{j,k+1}}{\tau_1} + (1 - \theta_2) \frac{y_i^{j+1,k} - y_i^{j,k}}{\tau_1} =$$
$$= \theta_3 \theta_4 L_h y_i^{j+1,k+1} + \theta_3 (1 - \theta_4) L_h y_i^{j+1,k} + (1 - \theta_3) \theta_5 L_h y_i^{j,k+1} + (1 - \theta_3)(1 - \theta_5) L_h y_i^{j,k} + \quad (28)$$
$$+ F_i^{j,k},$$
$$i = \overline{1, N-1}, \; j = \overline{0, N_1 - 1}, \; k = \overline{0, N_2 - 1},$$

and the conditions

$$\left. \begin{array}{l} y_i^{0,k} = \varphi_{11i}^{0,k}, \; i = \overline{0, N}, \; k = \overline{0, N_2}, \\ y_i^{j,0} = \varphi_{12i}^{j,0}, \; i = \overline{0, N}, \; j = \overline{0, N_1}, \end{array} \right\} \quad (29)$$

$$\left. \begin{array}{l} y_0^{j,k} = \varphi_2^{j,k}, \; j = \overline{0, N_1}, \; k = \overline{0, N_2}, \\ y_N^{j,k} = \varphi_3^{j,k}, \; j = \overline{0, N_1}, \; k = \overline{0, N_2}, \end{array} \right\} \quad (30)$$

where $y_i^{j,k}$ function is the grid function defined on the $\omega_{h\tau_1\tau_2}$ discrete area corresponding to D, which corresponds to the $u(x, t_1, t_2)$ function, $0 \leq \theta_i \leq 1$ $\left(i = \overline{1,5}\right)$ are given parameters, $F_i^{j,k}$, $\varphi_{11i}^{0,k}$, $\varphi_2^{j,k}$ and $\varphi_3^{j,k}$ are respectively grid functions of $\left[-f(x,t)\right]$ and those used in the left side of initial and initial-boundary conditions (22)-(25), h, τ_1, τ_2 are steps of regular grid $\omega_{h\tau_1\tau_2}$ respectively for the arguments x, t_1 and t_2; $L_h y_i^{j,k} = \frac{y_{i+1}^{j,k} - 2y_i^{j,k} + y_{i-1}^{j,k}}{h^2}$.

The following theorem is true for the scheme (28)-(30):

THEOREM 5.

If the function $u(x,t)$ is sufficiently smooth, then the scheme (28)-(30) approximates the problem (22)-(24) with the precision of $O(\tau_1 + \tau_2 + h^2)$ order, if in the difference equation (28),

a) $\theta_1 = \theta_2 = \theta_3 = \dfrac{1}{2}$, $\theta_4 + \theta_5 = 1$, $F_i^{j,k} = -f_i^{j+\frac{1}{2},k+\frac{1}{2}} - \dfrac{h^2}{12}\dfrac{\partial^2 f}{\partial x^2}$, then

$\psi_i^{j,k} = O\big(\tau_1^2 + \tau_2^2 + h^2\big)$;

b) if $\theta_1 = \theta_2 = \dfrac{1}{2}$, $\theta_3 = \dfrac{1}{2} - \dfrac{h^2}{12\tau_1}$, $\theta_3\theta_4 - \theta_3\theta_5 + \theta_5 = \dfrac{1}{2} - \dfrac{h^2}{12\tau_2}$,

$F_i^{j,k} = -f_i^{j+\frac{1}{2},k+\frac{1}{2}} - \dfrac{h^2}{12}\dfrac{\partial^2 f}{\partial x^2}$, then $\psi_i^{j,k} = O\big(\tau_1^2 + \tau_2^2 + h^4\big)$,

where $\psi_i^{j,k}$ is an approximation error.

There are considered two explicit and two implicit schemes. They are obtained by selecting the concrete values for parameters θ_i $\big(i = \overline{1,5}\big)$ in the problem (28)-(30).

If $\theta_1 = \theta_2 = \dfrac{1}{2}$, $\theta_3 = \theta_5 = 0$, then difference equation (28) gets the form:

$$\dfrac{1}{2}\dfrac{y_i^{j+1,k+1} - y_i^{j+1,k}}{\tau_2} + \dfrac{1}{2}\dfrac{y_i^{j,k+1} - y_i^{j,k}}{\tau_2} + \dfrac{1}{2}\dfrac{y_i^{j+1,k+1} - y_i^{j,k+1}}{\tau_1} + \dfrac{1}{2}\dfrac{y_i^{j+1,k} - y_i^{j,k}}{\tau_1} = \quad (31)$$

$$= L_h y_i^{j,k} + F_i^{j,k}, \ i = \overline{1,N-1}, \ j = \overline{0,N_1-1}, \ k = \overline{0,N_2-1},$$

where there is assumed, that $\tau_1 = \tau_2 \equiv \tau$. Simulation of difference equation (31) consists of four grid points.

The following theorem is true:

THEOREM 6.

If $\tau \leq \dfrac{h^2}{2}$, the finite-difference scheme (31), (29), (30) is stable and its solution converges to the solution of the problem (22)-(24) in the sense of uniform norm.

When $\theta_1 = \theta_2 = 1$, $0 < \theta_3 < 1$, $\theta_4 = 0$, $\theta_5 = 1$, there is obtained the following scheme:

$$\dfrac{y_i^{j+1,k+1} - y_i^{j+1,k}}{\tau_2} + \dfrac{y_i^{j+1,k+1} - y_i^{j,k+1}}{\tau_1} = \theta_3 L_h y_i^{j+1,k} + (1-\theta_3)_h y_i^{j,k+1} + F_i^{j,k}, \quad (32)$$

$$i = \overline{1,N-1}, \ j = \overline{0,N_1-1}, \ k = \overline{0,N_2-1},$$

and the simulation of this scheme consists of seven grid points.

Stability and convergence issues are covered in the following theorem:

THEOREM 7.

If $\tau_1 \leq \dfrac{h^2}{2\theta_3}$, $\tau_2 \leq \dfrac{h^2}{2(1-\theta_3)}$, the scheme (32), (29), (30) is stable and its solution converges to the exact solution of the problem (22)-(24) with the sense of energetic norm.

Selecting the parameters in the following way: $\theta_1 = \theta_2 = \theta_3 = \theta_4 = 1$ will lead to the equation,

$$\frac{y_i^{j+1,k+1} - y_i^{j+1,k}}{\tau_2} + \frac{y_i^{j+1,k+1} - y_i^{j,k+1}}{\tau_1} = L_h y_i^{j+1,k+1} + F_i^{j,k}, \tag{33}$$

$$i = \overline{1, N-1}, \ j = \overline{0, N_1 - 1}, \ k = \overline{0, N_2 - 1},$$

with the simulation, which consists of five grid points.

THEOREM 8.

The scheme (33), (29), (30) is absolutely stable and the solution converges to the exact solution of the problem (22)-(24) in the sense of energetic norm.

When $\theta_1 = \theta_2 = \theta_3 = 1/2$, $\theta_4 = 1$ and $\theta_5 = 0$, there is obtained another implicit scheme:

$$\frac{1}{2}\frac{y_i^{j+1,k+1} - y_i^{j+1,k}}{\tau_2} + \frac{1}{2}\frac{y_i^{j,k+1} - y_i^{j,k}}{\tau_2} + \frac{1}{2}\frac{y_i^{j+1,k+1} - y_i^{j,k+1}}{\tau_1} + \frac{1}{2}\frac{y_i^{j+1,k} - y_i^{j,k}}{\tau_1} = \tag{34}$$

$$= \frac{1}{2}L_h y_i^{j+1,k+1} + \frac{1}{2}L_h y_i^{j,k} + F_i^{j,k}, \tau_1 = \tau_2 \equiv \tau,$$

$$i = \overline{1, N-1}, \ j = \overline{0, N_1 - 1}, \ k = \overline{0, N_2 - 1},$$

with simulation consisting of eight grid points.

THEOREM 9.

The scheme (34), (29), (30) is absolutely stable and its solution converges to the exact solution of the problem (22)-(24) in the sense of energetic norm.

For simplicity there is considered the problem (14)-(18), when $L \equiv \sum_{i=1}^{n} \frac{\partial^2}{\partial x_i^2}$, and $G = (0, l_1) \times \cdots \times (0, l_n)$. Initial problem is split and there is constructed the following semi-discrete decomposition algorithm of parallel count:

$$\left.\begin{array}{c} \sigma_1 \left(\sum_{i=1}^{m} y_{1t_i}^{k_1+1,\ldots,k_i,\ldots,k_m+1} \right) = \frac{\partial^2 y_1^{k_1+1,\ldots,k_m+1}}{\partial x_1^2} - f_1^{k_1+1,k_2+1,\ldots,k_m+1}(x,t), \\ \ldots\ldots\ldots\ldots\ldots\ldots\ldots\ldots\ldots\ldots\ldots\ldots\ldots\ldots\ldots\ldots \\ \sigma_n \left(\sum_{i=1}^{m} y_{nt_i}^{k_1+1,\ldots,k_i,\ldots,k_m+1} \right) = \frac{\partial^2 y_n^{k_1+1,\ldots,k_m+1}}{\partial x_n^2} - f_n^{k_1+1,k_2+1,\ldots,k_m+1}(x,t), \end{array}\right\} \tag{35}$$

$$\sum_{i=1}^{n} \sigma_i = 1, \sigma_i \geq 0 \ t_{k_i} \in \omega_{\tau_i}, \left(k_i = \overline{0, N_i - 1} \right) j = \overline{1, m},$$

$$\left.\begin{array}{l} y_1^{k_1,k_2+1,\ldots,k_m+1} = y_2^{k_1,k_2+1,\ldots,k_m+1} = \cdots = y_n^{k_1,k_2+1,\ldots,k_m+1} = v^{k_1k_2+1,\ldots,k_m+1}, k_1 = \overline{1,N_1}, \\[2mm] v^{k_1,k_2+1,\ldots,k_m+1} = \sum_{i=1}^{n} \sigma_i y_i^{k_1,k_2+1,\ldots,k_m+1}, v^{0,k_2+1,\ldots,k_m+1} = \varphi_{11}^{0,k_2+1,\ldots,k_m+1}, \\[2mm] \cdots \\[2mm] y_1^{k_1+1,k_2+1,\ldots,k_m} = y_2^{k_1+1,k_2+1,\ldots,k_m} = \cdots = y_n^{k_1+1,k_2+1,\ldots,k_m} = v^{k_1+1,k_2+1,\ldots,k_m}, k_m = \overline{1,N_m}, \\[2mm] v^{k_1+1,k_2+1,\ldots,k_m} = \sum_{i=1}^{n} \sigma_i y_i^{k_1+1,k_2+1,\ldots,k_m}, v^{k_1+1,k_2+1,\ldots,0} = \varphi_{1m}^{k_1+1,k_2+1,\ldots,0} \end{array}\right\} \quad (36)$$

$$\left.\begin{array}{l} y_1^{k_1+1,k_2+1,\ldots,k_m+1}(0,x_2,\ldots,t_{k+1}) = \varphi_{21}(x_2,\ldots,t_{k+1}), 0 \le x_i \le l_i, \left(i=\overline{2,n}\right), \\[2mm] \dfrac{\partial y_1^{k_1+1,k_2+1,\ldots,k_m+1}}{\partial x_1}(l_1,x_2,\ldots,t_{k+1}) + \alpha\, y_1^{k_1+1,k_2+1,\ldots,k_m+1}(l_1,x_2,\ldots,t_{k+1}) = \\[3mm] = \sum_{i=0}^{m} \alpha_i y_1^{k_1+1,k_2+1,\ldots,k_m+1}(\xi_i,x_2,\ldots,t_{k+1}) + \varphi_{31}(x_2,\ldots,t_{k+1}), \\[2mm] 0 \le x_i \le l_i, \left(i=\overline{1,n}, i \ne 1\right), k_i = \overline{0,N_i-1}, \end{array}\right\} \quad (37)$$

$$\left.\begin{array}{l} y_2^{k_1+1,k_2+1,\ldots,k_m+1}(x_1,0,x_3,\ldots,t_{k+1}) = \varphi_{22}^{k_1+1,k_2+1,\ldots,k_m+1}(x_1,0,x_3,\ldots,t_{k+1}), \\[2mm] y_2^{k_1+1,k_2+1,\ldots,k_m+1}(x_1,l_2,x_3,\ldots,t_{k+1}) = \varphi_{32}^{k_1+1,k_2+1,\ldots,k_m+1}(x_1,l_2,x_3,\ldots,t_{k+1}) \\[2mm] 0 \le x_i \le l_i, \left(i=\overline{1,n}, i \ne 2\right), k_i = \overline{0,N_i-1}, \end{array}\right\}$$

$$\cdots$$

$$\left.\begin{array}{l} y_n^{k_1+1,k_2+1,\ldots,k_m+1}(x_1,\ldots,x_{n-1},0,t_{k+1}) = \varphi_{2n}^{k_1+1,k_2+1,\ldots,k_m+1}(x_1,\ldots,x_{n-1},0,t_{k+1}), \\[2mm] y_n^{k_1+1,k_2+1,\ldots,k_m+1}(x_1,l_2,x_3,\ldots,t_{k+1}) = \varphi_{3n}^{k_1+1,k_2+1,\ldots,k_m+1}(x_1,\ldots,x_{n-1},0,t_{k+1}) \\[2mm] 0 \le x_i \le l_i, \left(i=\overline{1,n}, i \ne n\right), k = \overline{0,N-1}, \end{array}\right\} \quad (38)$$

where

$$\omega_{\tau_i} = \left\{ t_{k_i} : t_{k_i} = k_i \tau_i, k_i = \overline{0,N_i}, N_i \tau_i = T_i \right\},$$

$$t_{k+1} = \left(t_{k_1+1},\ldots,t_{k_m+1}\right), y_i^{k_1+1,k_2+1,\ldots,k_m+1} = y_i(x,t_{k+1}), \; i=\overline{1,n}, \; k = \overline{0,N},$$

$$f_i^{k_1+1,k_2+1,\ldots,k_m+1} = f_i(x,t_{k+1}), \; i=\overline{1,n}, \; k_i = \overline{0,N_i};$$

$$y_{jt_i}^{k_1+1,\ldots,k_i,\ldots,k_m+1} = \frac{1}{\tau_i}\left[y_i^{k_1+1,\ldots,k_i+1,\ldots,k_m+1} - v^{k_1+1,\ldots,k_i,\ldots,k_m+1} \right], \; \left(j=\overline{1,n}\right);$$

φ_{1i}, $\left(i=\overline{1,m}\right)$, φ_{2i}, $\left(i=\overline{1,n}\right)$ and φ_{3i}, $\left(i=\overline{1,n}\right)$ are given functions. The following theorem is true:

THEOREM 10.

If in non-local condition (19) one of the two following conditions are satisfied: a) $\alpha_i \ge 0$ $\left(i=\overline{0,m}\right)$, $\sum_{i=0}^{m} \dfrac{\alpha_i}{\alpha} \le 1$ or b) $\alpha_i \le 0$, $\sum_{i=0}^{m} \dfrac{|\alpha_i|}{\alpha} \le 1$ $\left(i=\overline{0,m}\right)$,

then (35)-(38) algorithm of parallel count is stable with respect to initial conditions and right hand function and converges to the exact solution of the initial problem with the speed of $O(\tau^{1/2})$.

5.   Conclusion

It is out of question that numerical realization of the derived algorithms should be carried out for real conditions, and it will be interesting to compare the obtained results with the outcome of known classical models. We suggest that such simplifications or, vice versa, complexity would result in efficient methods.

Obviously, the development of new and refinement of old mathematical models describing contamination processes in water and air, the construction and elaboration of more flexible and efficient algorithms for their solution, reasonably using old and contemporary computer techniques, could lead to more precise risk assessment through more precise predictions of the polluted state of the media.

References

1.   A.V.B. Karaushev, River Hydraulic, *Hydro-meteorological Edition*, Leningrad, 1969, p. 415.
2.   G.I. Marchuk, Mathematical Modelling in Environmental Problem, *M.J. Nauka,* 1982, p. 319.
3.   A.M. Nikanorov, N.M. Trunov, Internal Processes in Reservoirs and Quality Control of Natural Waters, *Under the Edition of A.I. Bedritskii, Sankt-Peterburg*, GIDROMETEOIZDAT, 1999, p. 155.
4.   A.A. Samarskii, Introduction to Theory of Finite Difference Schemes, *Naukam* 1971.
5.   A.A. Samarskii, Theory of Finite Difference Schemes, Moskva, *Nauka,* 1977.
6.   A. Fridman, Partial Differential Equations of Parabolic Type, *Edition Mir*, 1968, p. 420.
7.   A.N. Tikhonov, A.A. Samarskii, Equations of Mathematical Physics, *Edit. "Nauka",* Main Edition of Physical-Mathematical Literature, Moscw, 1977.
8.   A.A. Samarskii, On One Economic Difference Method of Solution of Multi-Dimensional Parabolic Equation in Arbitrary Area, *JAM and MPh*, 1962, vol. 2, №5, pp. 787–811.
9.   B. Samarskyi and A. Gulin, Numerical Methods,-Moscow, *Nauka,* 1989, p. 430.
10. J. Brandt, I. Dimov, K. Georgiev, I.Uzia, Z. Zlatev, Numerical Algorithms for Three-dimensional Version of the Danish Eulerian Model, *Regional Modelling of Air pollution in Europe Proceedings of the first REMAPE Workshop,* Copenhagen, Denmark, 1996, pp. 250–262.
11. A.V. Karaushev, Hydraulic of Rivers and Water Reservoirs, *River Transport Edition*, Leningrad, 1955.

12. E. Gordeziani, On numerical methods for the resolution of one non-classical problem with pluri-parabolic equation, Proceedings of I. Vekua Institute of Applied Mathematics, Tbilisi State University Press, 50–51, 2000–2001, pp. 38–47.
13. E. Gordeziani, D. Gordeziani, Difference schemes for pluriparabolic equations, Bulletin of TICMI, Tbilisi University Press, Vol. 4, 2000, pp. 41–46.
14. J.R. Cannon, The solution of the heat equation subject to the specification of energy, Quart. Applied Mathematics 21, 1963, pp. 155–160.
15. R. Dautray, J.-L. Lions. Analyse mathématique et calcul numérique pour les science et les techniques. Vol. 7, Évolution: Fourier, Laplace, MASSON, Paris, Milan, Barcelona, Mexico, 1988, pp. 187–200.
16. N.D. Gordeziani, On the Resolution of Non-local Boundary-value Problems for Elliptic Equations, *Seminar of Vekua Institute of Applied Mathematics, Reports,* vol. 23, 1997, pp. 26–35.
17. D. Gordeziani, N. Gordeziani, G. Avalishvili, On One Class of Non-local Problems for Partial Differential Equations, Reports of Enlarged Session of the Seminar of Vekua Institute of Applied Mathematics, vol. 10, #3, 1995, pp. 13–16.
18. D. Gordeziani, N. Gordeziani, G. Avalishvili, Non-local Boundary-value Problems for Some Partial Differential Equations, Bulletin of the Georgian Academy of Sciences, 157, #1, 1998, pp. 365–369.
19. E. Gordeziani, N. Gordeziani, On Some Generalization of Non-local Boundary Value Problems for Elliptic Equations, Bulletin of TICMI, *Tbilisi University Press,* Vol. 2, 1998, pp. 34–36.
20. E. Gordeziani, D. Gordeziani, On Investigation of Difference Schemes for Some Pluriparabolic Equations, Reports of enlarged sessions of the seminars of I. Vekua Instutute of Applied Mathematics, Tbilisi University Press, Vol. 14, # 3, 1999, pp. 53–57.
21. E.D. Gordeziani, H.V. Meladze, On Investigation of One Non-classical Initial Boundary Value Problem, Third International Conference Finite Difference Schemes (FDS), September 1–4. 2000, Palanga, Lithunia, Abstracts, p. 18.
22. E.D. Gordeziani, H.V. Meladze, F.C. Torralba, On Mathematical Modelling and Numerical Resolution of Pollution Diffusion in Rivers, Proceedings of the third international conference on advances of computer methods in geotechnical and geoenvironmental engineering, Geoecology and Computers, Edited by Sergey A. Yufin, Center of Underground and Special Engineering, Moscow State University of Civil Engineering, Moscow/Russia/1–4 February, A.A. Balkema/Rotterdam/-Prookfield/2000, pp. 509–511.
23. E. Gordeziani, On Investigation of Non-local Problem for Certain Elliptic Equation, Proceedings of I.Vekua Institute of Applied Mathematics, Tbilisi State University Press, 50–51, 2000–2001, pp. 48–57.
24. N. Gordeziani, Non-local in Time Problems in the Theory of Elasticity, Reports of Enlarged Session of the Seminar of Vekua Institute of Applied Mathematics, vol.14, #3, 1999, pp. 16–20.
25. D. Gordeziani, N. Gordeziani, G. Avalishvili, Non-local Boundary-value Problems in Mathematical Physics. Abstract, Differential Equations and Mathematical Physics, International Symposium dedicated to the 90-th Birthday Anniversary of Academician I. Vekua, Tbilisi, 1997, pp. 127–128.
26. N. Gordeziani, On Some Non-local Problems of the theory of elasticity. Tbilisi International Centre of Mathematics and Informatics, BULLETIN of TICMI, Volume 4, 2000, pp. 43–47.

27. D.G. Gordeziani, On resolution of non-local by time problems for some equations of mathematical physics, ICM-94, Abstracts, Short communication, 1994, p. 240.

28. A.V. Bitsadze., A.A. Samarskii, On Some Generalization of Linear Elliptic Equations, DAN SSSR, 1969, vol. 185, #4, pp. 739–740.

29. A. M. Il'in, On a certain class of ultraparabolic equations, DAN SSSR. 159, No. 6, 1964, pp. 1214–1217.

30. D. Gordeziani, N. Gordeziani, G. Avalishvili, On the Investigation and Resolution of Non-local Boundary and Initial-boundary Value Problems, Reports of Enlarged Session of the Seminar of Vekua Institute of Applied Mathematics, vol. 12, #3, 1997, pp. 20–23.

31. A. Bouziani, Strong solution for a mixed problem with non-local condition for certain pluriparabolic equations Hiroshima Math. J., 1997, vol. 27, pp. 373–390.

APPLICATION OF INTEGRAL INDICES TO THE ASSESSMENT OF ECOLOGICAL RISKS AND DAMAGES

IRYNA BASHMAKOVA*
Odessa State Environmental University, Odessa 65016, Ukraine

SEMEN LEVIKOV
HYDROMOD Scientific Consulting, Wedel, Holstein, Germany

Keywords: water quality; ecological health; integral ecological indices; ecological risks and damages; Danube River

1. Introduction

Human activities such as industry, agriculture and sewage water discharge have considerable impact on water ecosystems and lead to their degradation. Quantitative evaluation of the environmental status of ecosystems with regard to various types of pollutants is an important factor in the river system management. Among various parameters, trace metal concentrations in water and in water organisms and sediments are widely used for environmental monitoring (Van der Oost et al., 1997; Sokal and Rohlf, 2000). The following problems are relevant to the management of complex natural systems: the level of pollution, probabilities of extreme pollution events, risks for human health, etc. (Levikov and Baumert, 2002). Here, integral ecological indices (henceforth referred to as "eco-indices") represent a convenient tool. In this paper we demonstrate applications of eco-indices using measurements in the Danube River in 1995-1996. We distinguish between eco-indices characterising (i) variations of microbiological and hydro-chemical conditions in different parts of a water basin (Bashmakova, 1997, 2001, 2002, 2004; Muller et al., 2000); and (ii) hydro-chemical or ecological state of a region or the whole basin (Levikov and Baumert, 2002).

―――――
*To whom correspondence should be addressed. Iryna Bashmakova, Odessa State Environmental University, Odessa 65016, Ukraine; e-mail: zilitinkevich@elisanet.fi

B(6) trophicity index, Danube River 1995 - 1996
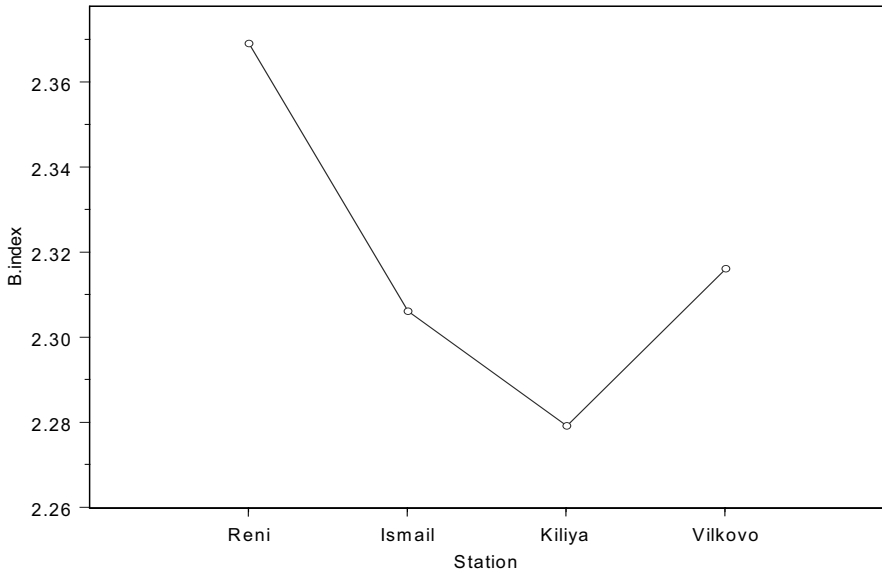
Figure 1. The trofic index B(6) at four stations in the Ukrainian part of Danube River during 1995-1996.

2. Eco-index

We consider a water basin covered with M measurement stations $s = 1,2,...,M$. Each station s provides measurements of N parameters: $P_{sj}, j = 1,2,...,N$. The dimensionless concentration of each parameter at the station s is $C_{sj} = P_{sj}/L_j$, where L_j is the maximum acceptable concentration (MAC) of the parameter P_j in the water basin. To characterize the station s, we determine the index

$$B_s = \sum_{j=1}^{N} \alpha_j C_{sj} ,$$

where α_j are weight coefficients satisfying the condition

$$\sum\nolimits_{j=1}^{N} \alpha_j = 1 .$$

Their concrete values should be chosen from ecological / hydro-biological expertise to reflect relative importance of each parameter for the ecological "health". The mean value of this index, namely

$$\overline{B} = \sum\nolimits_{s=1}^{M} B_s ,$$

characterises the whole basin over the period of field measurements.

B(6)
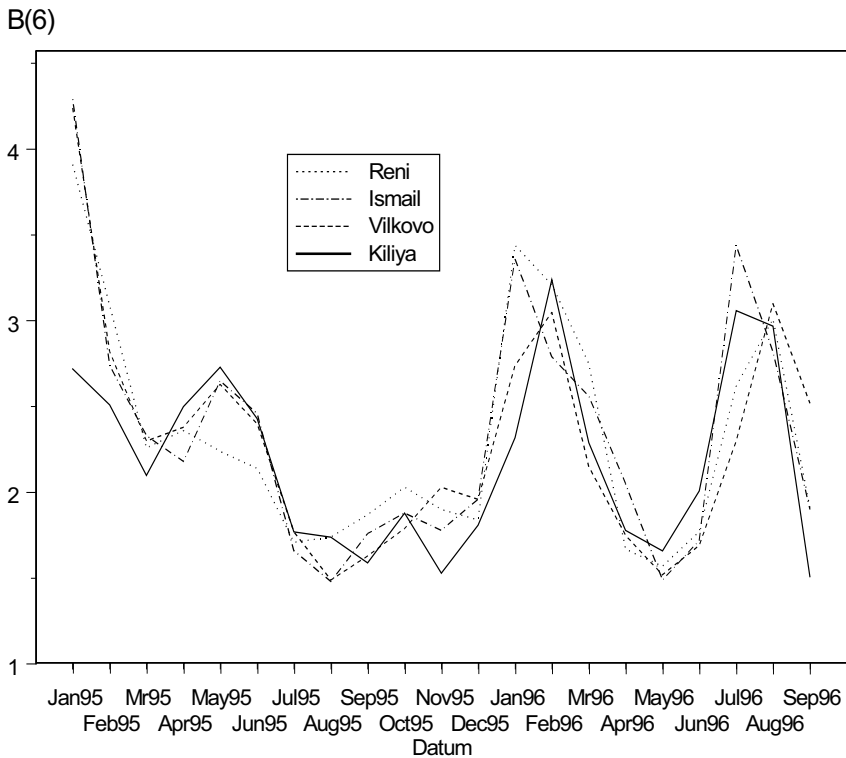
Figure 2. Time variation of the trophic index B(6) based on 22-months measurements from 1995 to 1996.

As examples we show in Figures 1 and 2 the trophic index B_s for the Ukrainian part of the Danube River in 1995-1996 calculated using N=6 measured parameters: $P_{sj} = NH_4,\ NO_2,\ NO_3\ P,\ O_2,\ BOC$ (biological oxygen

demand) with the following MACs: $L_j = 0.51, 0.011, 0.51, 0.051, 4.1, 1.5,$ and taking equal weight coefficients: $\alpha_J = 1/6$. As is seen from Figures 1 and 2, because of the economical crises in the country in the mid nineties, the ecological state of the Ukrainian part of the Danube River was determined basically by hydrological factors. These were, first of all, seasonal variations of the river drainage (winter and spring-summer floods) and water exchange with near-Danube water reservoirs characterised by high concentrations of nutrients and phytoplankton, with maximum values in the winter and summer periods. At that time, no considerable anthropogenic impacts were observed. Local increase of the trophic index in the upper portion of the Kilia Delta (in surroundings of the town Vilkovo) was probably caused by periodic discharges from rise plantations
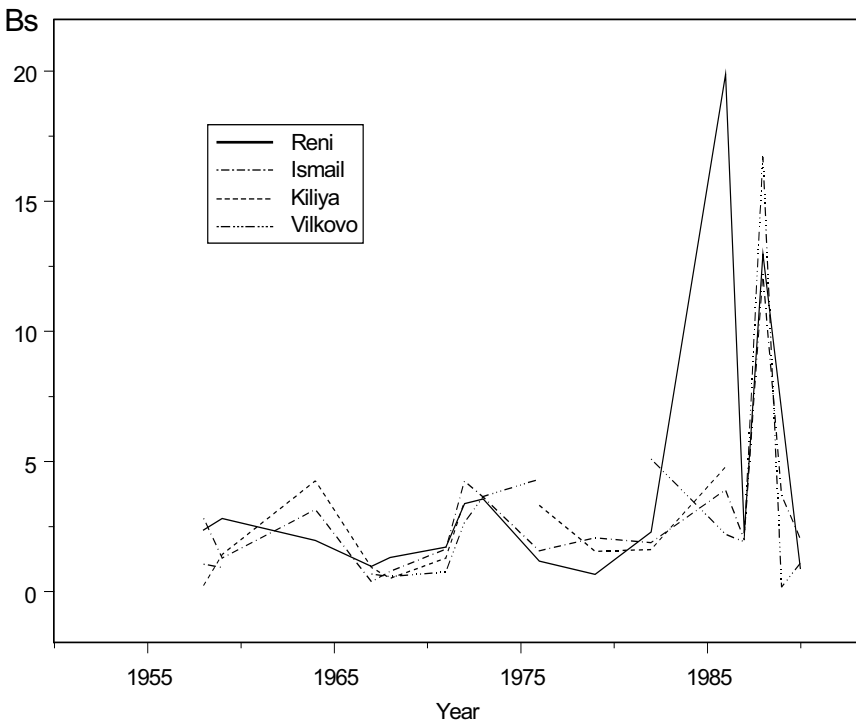
Figure 3. Time variation of the sanitary-bacteriological index based on four parameters for four stations in the Ukrainian part of the Danube River from 1958-1990.

located downstream of the town Kilia. In Figure 3 we show the sanitary-bacteriological index calculated similarly using the following microbiological parameters: the general number of bacteria in water, the bacterial biomass, the number of saprophyte bacteria and the number of bacteria of the Coli-group.

3. Concluding remarks

Analysis of data over the period 1958-1990 shows pronounced worsening of the ecological state (evaluated after sanitary-bacteriological parameters) in the second half of the eighties, especially at the Ukrainian-Romanian border in surroundings of the town Reni. Comprehensive explanation of this fact needs additional data including detailed information from sanitary-epidemiological services. In the early nineties the situation has been stabilised. Maximum values of the trophic and sanitary-bacteriological indices are observed near Reni. This allows concluding that the lower quality waters came here from the upper part of the Danube River to its Ukrainian part. Thus the use of the proposed indices allows to efficiently and reasonably accurately characterising the ecological state and its changes in different portions of the Danube River.

References

Bashmakova I., 1997, Use of microbiological parameters for estimation of water quality and functioning of estuaries of big rivers, *Ukrainian Hydroecological Society*, **1**: 100–106.

Bashmakova I., 2001, Modern state of biodiversity and structure/functioning characteristic of bacterioplankton of the Danube Delta, *Ukrainian Hydroecological Society*, **4**: 68–73.

Bashmakova I., 2002, Eco-index for hydrobiological monitoring and water quality assessment with application to the Kilia Delta of River Danube, in: *34th International Conference IAD*, Tulcea, Romania, 27–30 August 2002, 463–469.

Bashmakova I., 2004, Ecological indexes for estimation of ecological state and water quality in estuarine zones of big rivers, *Hydrobiol. J.*, **40**, No. 2: 17–21.

Mueller, D., Bashmakova I. Kh., Ljashenko, A.V., 2000, Assessment of ecological risk from the heavy metals and organic contamination for vital activity of hydrobionts and self-purification processes in the estuarine zones of big rivers, by the example of the River Danube delta, INTAS-Publication, 176 p.

Sokal, R.R. and Rohlf, F.J., 2000, *Biometry: The Principles and Practice of Statistics in Biological Research*, W. H. Freeman and Co., N. Y., 887 p.

Van der Oost, R., Vindimian, E., van den Brink, P.J., Satumalay, K., Heida, H., and Vermeulen, N.P.E., 1997, Biomonitoring aquatic pollution with feral eel (*Anguilla anguilla*), III: Statistical analysis of relationships between contaminant exposure and biomarkers, *Aquatic Toxicology*, **39**: 46–75.

Levikov, S. and Baumert, H., 2002, Statistical analysis of fish parameters, in: *North Sea*, 1999–2000, Vol. 10. PCA models "fish residues–fish biomarkers" and "fish residues–fish parasitological index", HYDROMOD Scientific Consulting, Wedel, Holstein, Germany.

USE OF BENTHIC INVERTEBRATES AS INDICATORS OF POLLUTION ORIGIN IN AGRICULTURAL AND URBAN AREAS

KAREN JENDEREDJIAN
Ministry of Nature Protection, Government Bidg.3, Republic Sq., Yerevan, 375010, Armenia

SUASANNA HAKOBYAN
National Academy of Science 24, Marshall Baghramian Avenue, room 908-909, Yerevan 375019 Armenia

ARPINE JENDEREDJIAN*
Yerevan State University, Faculty of Biology, 8 Byron St., apt 5, Yerevan 375009, Armenia

Abstract. The benthos is one of the most important elements of the continental water ecosystems, which can be used as indicator of water pollution, as it reacts quickly to minor environmental changes. The distribution of benthic animals depends on substratum, quantity and composition of organic matter in sediments. The results of long-term studies of the qualitative and quantitative development of the benthos animals in Lake Sevan and its tributaries, as well as in the outlet River Hrazdan, show that using benthos as an indicator of water pollution of different origin gives workable data. Due to pollution, the species composition in some areas was changed. The organisms that preferred clean water (Trichoptera, Plecoptera) were replaced by organisms that are resistant to water pollution (Tubificidae, Chironomidae).

————
*To whom correspondence should be addressed. Jenderedjian Arpine, Yerevan State University, Faculty of Biology, 8 Byron St., apt 5, Yerevan 375009, Armenia; e-mail: arpinej@yahoo.com

217

1.   General aspects

The benthos is one of the most important elements of the continental water ecosystems. Unfortunately, there is lack of information about it. Bottom invertebrates and their communities are very sensitive indicators of organic and toxic pollution. Using benthos as an indicator of water pollution has become very popular.

Using chemical, as well as biological indicators can improve water quality management with higher sensitivity to environmental changes. Quantity and composition of benthic organisms are the only hydrobiological index for bottom and near-bottom water pollution. Not all animals and plants react in the same way to changes of environmental conditions. Some of them are very resistant; others vanish upon minor changes. The capability of organisms for reacting in different ways to environmental changes underlies the bases of biological valuation of water quality. Such kinds of organisms occur among plants, animals and microorganisms of the rivers and lakes. One can use these organisms as indicators of water pollution, which react quickly to environmental changes; they are known as biological indicators. Their quantity can abruptly increase or decrease, very sensitive ones can totally disappear. Benthic invertebrates that have long life cycles are most suitable as biological indicators.

On the base of the above mentioned information models were developed for water quality assessment. The distribution of benthic animals depends on hydrological regime, substratum and, above all on quantity and composition of organic matter in sediments. Pronounced preferences of some species of bottom invertebrates (especially Oligochaeta) to different types of organic matter (Fomenko, 1972) is a unique opportunity for use of quantitative and qualitative development of benthos as a cheap and effective method of indication of the origin of organic pollution in agricultural and urban areas. Many models were developed for risk assessment in rivers, but these models are not sufficient for lakes and ponds. Big mountain lakes, to which Lake Sevan belongs, have their specificity and require special methods for risk assessment regarding anthropogenic influence. For long-term observation, we developed model using Oligochaetes as biological indicator.

2.   Lake Sevan studies

In Lake Sevan, the largest lake of the Transcaucasus Region, eight main substrata are distinguished: river sediment, macrophyte zone, stones, sand, oozy sand, yellow and black silt.

Oligochaetes of 26 species inhabit different biotopes and depths in Lake Sevan (Jenderedjian and Poddubnaya, 1987). The *Naididae* comprise all oligochaete fauna on stones covered by periphyton. *Limnodrilus hoffmeisteri* and Tubifex tubifex prefer anthropogenic organic matter. *L. hoffmeisteri* is the dominant species in river sediments polluted mainly by sewage waste and *T. tubifex* in river sediments polluted mainly by agricultural fertilizers. *Rhyacodtilus coccineus* prefers organic matter of plant origin, such as stonewort (*Chara* spp.) and moss *(Fontinalis antipiretica* L.) and dominates in the macrophyte zone. *Trichodrilus sp*. is found exclusively on the bare stone bottom. *Potamothrix alatus paravanicus* prefers planktonogenous organic matter and its greatest biomass occurs in the deeper zone where sedimentation rate of remains of plankton is most significant. *P. a. paravanicus* is the dominant species on pure and oozy sand, yellow and black silt (Jenderedjian, 1994).

The results of long-term studies of the qualitative and quantitative development of the benthic animals in Lake Sevan and its tributaries, as well as in the outlet River Hrazdan, show that using benthos as an indicator of water pollution of different origin gives workable data, which are very effective and cheap. According to this data, most polluted river in Lake Sevan basin is the down-stream of river Gavaraget and most clean one is river Lichk. In the down-stream of river Gavaraget large quantities of L. hoffmeisteri and T. tubifex were found (total 130g/m2), which formed big red fields. This part of the river is strongly polluted with sewage from urban and agronomical areas. Zoobenthos of river Lichk is present mostly with animals that require high concentration of oxygen (Hakobyan, 1998). The organisms that prefer clean water (*Trichoptera, Plecoptera*), were replaced by organisms that are resistant to water pollution (*Tubificidae, Chironomidae*).

Studies of zoobenthos in Lake Sevan tributaries with a similar hydrobiological regime, but with different levels of pollution from agricultural and urban sewages give the possibility of comparison between pollution level and benthos composition. This gives also possibility to predict possible changes in the ecosystem in case of growing pollution. Our studies allow not only risk assessment for organic and toxic pollution of Lake Sevan, but also the valuation of consequences of abrupt water level increase and decrease.

References

Fomenko, N.V., 1972, Ecological groups of oligochaeta in the Dnieper Basin. In: *Aquatic oligochaete worms: taxonomy, ecology, and faunistic studies in the USSR*, G.M. Belyaev, ed., Nauka Publishers, Moscow, Russia. pp. 105–118.

Hakobyan, 1998, Draft Management Plan for Lake Arpi, RIZA, 26 p.

Jenderedjian, K., 1994, Influence of environmental factors on the production of *Potamothrix alatus paravanicus* Poddubnaya & Pataridze (Tubificidae) in different areas of Lake Sevan, *Hydrobiologia* **278:** 287–290.

Jenderedjian, K., and Poddubnaya, 1987, Population dynamics of *Potamothrix alatus paravanicus* Poddubnaya & Pataridze (Tubificidae) in different areas of Lake Sevan, *Hydrobiologia* **278:** 281–286.

ANALYTICAL AND NUMERICAL MODELING OF PHYSICAL AND CHEMICAL PROCESSES IN THE VADOSE ZONE

JIRKA ŠIMŮNEK
Department of Environmental Sciences, University of California Riverside, Riverside, CA 92521, USA

Abstract. A large number of models for simulating water flow and solute transport in the unsaturated zone are now used for a wide range of applications in research, management, and risk assessment of subsurface systems. Many models of varying degree of complexity and dimensionality have been developed during the past several decades to quantify the basic physical and chemical processes affecting water flow and contaminant transport in the unsaturated zone. Modeling approaches range from relatively simple analytical and semi-analytical solutions, to complex numerical codes. In this paper a brief overview of more widely used analytical and numerical models is given. Some typical problems in which the numerical codes have been applied are also identified.

1. Introduction

A large number of models for simulating water flow and solute transport in the unsaturated zone are now used for a wide range of applications in research, management, and risk assessment of subsurface systems. Many models of varying degree of complexity and dimensionality have been developed during the past several decades to quantify the basic physical and chemical processes affecting water flow and contaminant transport in the unsaturated zone. Modeling approaches range from relatively simple

221

analytical and semi-analytical solutions, to complex numerical codes. While analytical and semi-analytical solutions are still popular for some applications, the ever-increasing power of personal computers and the development of more accurate and numerically stable solution techniques have motivated the much wider use of numerical codes in recent decades. The wide use of numerical models is also significantly enhanced by their availability in both the public and commercial domains, and by the development of sophisticated graphics-based interfaces that can tremendously simplify their use.

2. Analytical models

While under certain conditions (i.e., for linear sorption, a concentration independent sink term, and a steady-state flow field) solute and heat transport equations are linear equations, water flow equations are generally a highly nonlinear because of the nonlinearity of the soil hydraulic properties. Consequently, many **analytical solutions** have been derived in the past for solute transport equations and these analytical solutions are now widely used for analyzing solute transport under steady-state conditions. Many of these analytical solutions were compiled in STANMOD (STudio of ANalytical MODels, www.hydrus2d.com) (Šimůnek et al., 1999b), a public domain Windows based computer software package for evaluating solute transport in porous media using analytical solutions of the
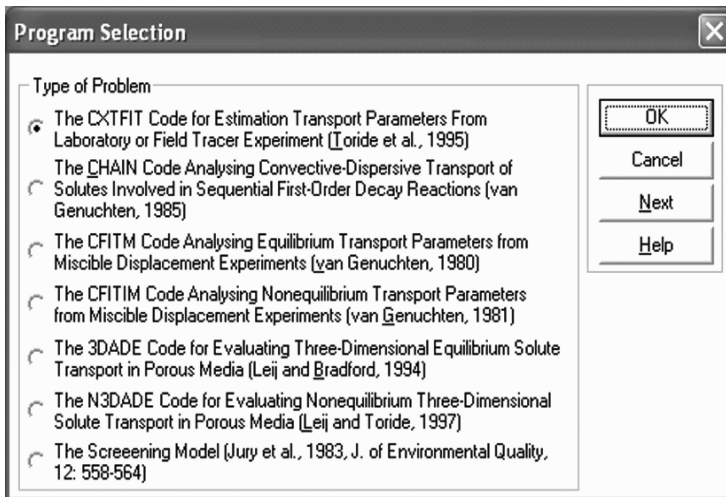
Figure 1. The "Program Selection" dialog window in the STANMOD software package.

convection-dispersion solute transport equation. It includes at present the following one-dimensional models: CFITM (van Genuchten, 1980), CFITIM (van Genuchten, 1981), CHAIN (van Genuchten, 1985), CXTFIT (Toride et al., 1995), and SCREEN (Jury et al., 1983), and two- and three-dimensional models: 3DADE (Leij and Bradford, 1994) and N3DADE (Leij and Toride, 1997).

2.1. ONE-DIMENSIONAL ANALYTICAL MODELS

An updated version of the **CFITM** code of van Genuchten (1980) that is included into STANMOD is intended for analyzing observed column effluent data using analytical solutions of the one-dimensional **equilibrium** convective-dispersive transport equations. The code considers analytical solutions for both semi-finite and finite columns. The model provides an easy to use, efficient and accurate means of determining various transport parameters by optimizing observed column effluent data.

An updated version of the **CFITIM** code of van Genuchten (1981) can be used for analyzing observed column effluent data using analytical solutions of the one-dimensional equilibrium and **nonequilibrium** convective-dispersive transport equations. The code includes analytical solutions for semi-finite columns. The nonequilibrium solutions consider the two-region dual-porosity (bi-continuum) flow model for physical nonequilibrium and the one-site or two-site sorption models for chemical nonequilibrium. CFITM and CFITIM represent simple alternatives to the much more comprehensive, but also more complex, CXTFIT model.

A modified and updated **CHAIN** code of van Genuchten (1985) analyzes the convective-dispersive transport of solutes involved in sequential **first-order decay reactions**. Examples are the migration of radionuclides in which the chain members form first-order decay reactions, and the simultaneous movement of various interacting nitrogen or organic species.

A modified and updated version of the **CXTFIT** code of Toride et al., (1995) that is included in STANMOD is intended for estimating solute transport parameters using a nonlinear least-squares parameter optimization method. This code may be used to solve the inverse problem by fitting a variety of mathematical solutions of theoretical transport models, based upon the one-dimensional convection-dispersion (or advection-dispersion) equation (CDE), to experimental results. The program may also be used to solve the direct or forward problem to determine concentrations as a function of time and/or position. Three different one-dimensional transport models are considered: **(i) the conventional CDE**; **(ii) the chemical and physical nonequilibrium CDEs**; and **(iii) a stochastic stream tube model** based upon the local-scale equilibrium or nonequilibrium CDE.

Finally, the screening model of Jury et al., (1983), **SCREEN**, for behavior assessment of trace organics in soils is included. This model is intended to classify and screen organic chemicals for their relative susceptibility to different loss pathways (volatilization, leaching, and degradation in the soil and air). The model considers the following processes: gaseous diffusion, liquid dispersion, liquid convection, volatilization, sorption, and first-order degradation processes.
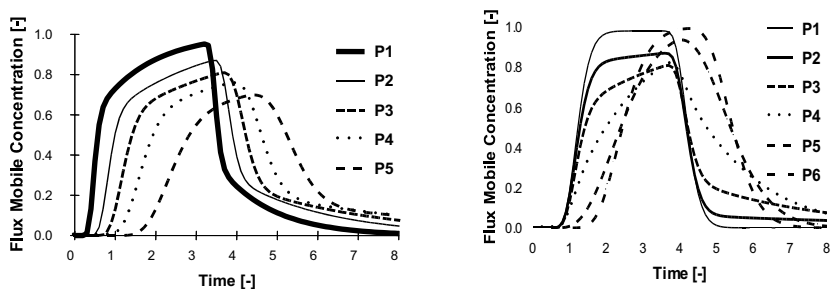

Figure 2. Examples of breakthrough curves at the end of the soil column (40 cm long) demonstrating the effect of the retardation factor (R=1, 1.75, 2.5, 3.5, and 5) and the mass transfer coefficient (ω=0.02, 0.2, 0.5, 1.5, 7.5, and 1000) in the two region model. Calculations were carried out using CXTFIT2 in STANMOD.

2.2. TWO- AND THREE-DIMENSIONAL ANALYTICAL MODELS

STANMOD also includes the **3DADE** code of Leij and Bradford (1994) for evaluating analytical solutions for **three-dimensional equilibrium** solute transport in the subsurface. The analytical solutions pertain to selected cases of three-dimensional solute transport during steady unidirectional water flow in porous media having uniform flow and transport properties. The transport equation contains terms accounting for solute movement by convection and dispersion, as well as for solute retardation, first-order decay, and zero-order production. The 3DADE code can be used to solve the direct problem, i.e., the concentration is calculated as a function of time and space for specified model parameters, and the indirect (inverse) problem in which the program estimates selected parameters by fitting one of the analytical solutions to specified experimental data.

Finally, STANMOD incorporates the **N3DADE** code of Leij and Toride (1997) for evaluating analytical solutions for a **three-dimensional non-equilibrium** solute transport in porous media. The analytical solutions pertain to three-dimensional solute transport during steady unidirectional water flow in porous media in systems of semi-infinite length in the

longitudinal direction, and of infinite length in the transverse direction. The solutions can be applied also to one- and two-dimensional problems. The flow and transport properties of the medium are again assumed to be macroscopically uniform. Nonequilibrium solute transfer can occur between two domains in either the liquid or the absorbed phase. The transport equation contains terms accounting for solute movement by advection and dispersion, as well as for solute retardation, first-order decay, and zero-order production.
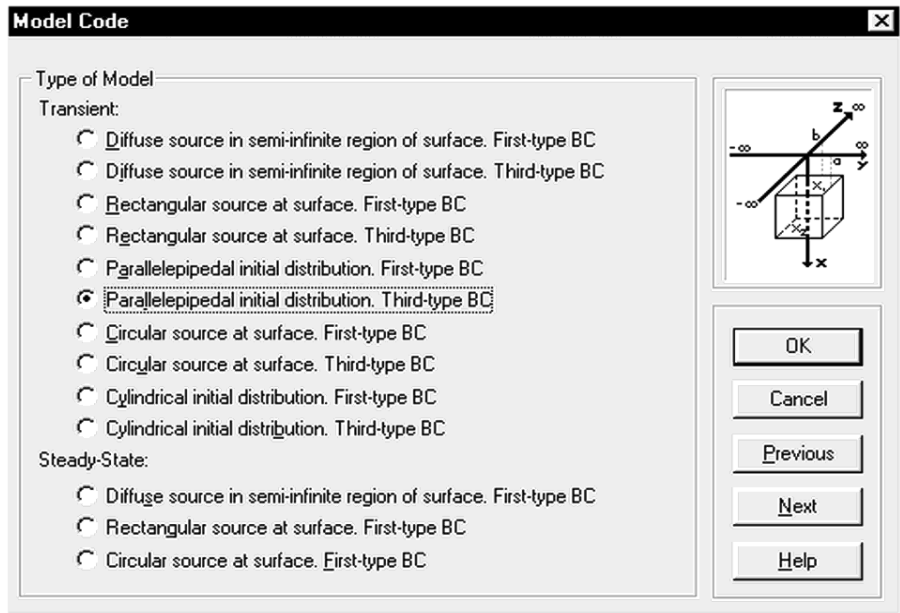
Figure 3. The "Model Code" dialog window for the 3DADE model in the STANMOD software package.

3.   Numerical models

Although a large number of analytical solutions also exist for water flow equation, they can generally be applied only to drastically simplified problems. The majority of applications for water flow in the vadose zone require a numerical solution of the Richards equation.

   Numerical methods are in general superior to analytical methods in terms of being able to solve much more practical problems. They allow users to design complicated geometries that reflect complex natural geologic and hydrologic conditions, control parameters in space and time,

prescribe realistic initial and boundary conditions, and implement nonlinear constitutive relationships. Numerical methods usually subdivide the time and spatial coordinates into smaller pieces, such as finite differences, finite elements, and/or finite volumes, and reformulate the continuous form of governing partial differential equations in terms of a system of algebraic equations. In order to obtain solutions at certain times, numerical methods generally require intermediate simulations (time-stepping) between the initial condition and the points in time for which the solution is needed.

There is a large number of **numerical models** that are available for evaluating variably-saturated water flow and solute transport in the subsurface. Some of these models are in the public domain, such as MACRO (Jarvis, 1994), SWAP (van Dam et al., 1997), UNSATH (Fayer, 2000), VS2DI (Healy, 1990), and HYDRUS-1D (Šimůnek et al., 1998; www.hydrus2d.com), while others are in the commercial domain, such as HYDRUS-2D (Šimůnek et al., 1999a) and MODFLOW-SURFACT (HydroGeoLogic, 1996). These models vary widely in terms of their complexity, sophistication, and ease of use. Although some models are still being run under the DOS operating system, with associated difficulties of preparing input files and interpreting tabulated outputs, many others, especially those in the commercial domain, are supported by sophisticated graphics-based interfaces that tremendously simplify their use (e.g., Šimůnek et al., 1998; 1999a).

Models have recently become increasingly sophisticated in terms of the type and **complexity of solute transport processes** that can be simulated. Transport models are no longer being limited to solutes undergoing relatively simple chemical reactions such as linear sorption and first-order decay, but now consider also a variety of nonlinear sorption and exchange processes, physical and chemical nonequilibrium transport, volatilization, gas diffusion, colloid attachment/detachment, decay chain reactions, and many other processes. For example, the general formulation of the transport equations in the HYDRUS codes allows one to simulate not only non-adsorbing or linearly sorbing chemicals, but also a variety of other contaminants, such a viruses (Schijven and Šimůnek, 2001), colloids (Bradford et al., 2002), cadmium (Seuntjens et al., 2001), and hormones (Casey et al., 2003, 2004), or chemicals involved in the sequential biodegradation of chlorinated aliphatic hydrocarbons (Schaerlaekens et al., 1999; Casey and Šimůnek, 2001).

A substantial amount of research has been recently devoted to developing methods for describing **preferential/nonequilibrium flow** in structured media (macroporous soils). A variety of dual-porosity, dual-permeability, multi-porosity, and/or multi-permeability models (e.g., Gerke and van Genuchten, 1993; Jarvis, 1994; Šimůnek et al., 2003) has been developed to describe preferential flow. Dual-porosity and

dual-permeability models both assume that the porous medium consists of two interacting regions, one associated with the inter-aggregate, macropore, or fracture system, and the other one comprising micropores (or intra-aggregate pores) inside soil aggregates or the rock matrix. While dual-porosity models assume that water in the matrix is stagnant, dual-permeability models allow for water flow in the matrix as well. For a recent comprehensive review of various modeling approaches used to simulate preferential flow see Šimůnek et al., (2003).

Several of the dual-porosity and dual-permeability features were recently included in the HYDRUS software packages (Šimůnek et al., 2003, 2005). Examples of their application to a range of laboratory and field data involving transient flow and solute transport are given by Šimůnek et al., (2001), Zhang et al., (2004), Köhne et al., (2004, 2006), Kodešová et al., (2005), Haws et al., (2005), and Pot et al., (2005), among others.

Numerical models are, however, still lacking that would fully describe colloid transport and **colloid-facilitated solute transport** in a complex subsurface environment. This complex process requires knowledge of variably saturated water flow, colloid transport, dissolved contaminant transport, and colloid-facilitated contaminant transport. Colloids are inorganic and/or organic constituents that are generally chemically reactive. Inorganic colloids are primarily fine-sized mineral soil constituents, while organic colloids are organic matter-based. Transport equations must be formulated for both colloids and contaminants, in all its forms. Equations therefore must be written for the total contaminant, for contaminant sorbed kinetically or instantaneously to the solid phase, and for contaminant sorbed to mobile colloids, to colloids attached to the soil solid phase, and to colloids accumulating at the air-water interface. Some of these processes were recently incorporated in the HYDRUS software package (van Genuchten and Šimůnek, 2004). A complete description of the colloid-facilitated transport can be, for example, found in Hornberger et al., (1992) and Šimůnek et al., (2006a).

4. Biogeochemical models

Significant efforts have recently been carried out to couple physical flow and transport models with **geochemical models** to simulate even more complex reactions, such as surface complexation, precipitation/dissolution, cation exchange, and/or biological reactions. Geochemical models can be divided into two major groups: those with specific chemistry and general models (Šimůnek and Valocchi, 2002). Models with specific chemistry are limited in the number of species they can handle and their application is quite restricted to problems having a prescribed chemical system. They are, however, much easier to use and can be more computationally efficient than

general models. Typical examples of models with specified chemistry are models simulating the transport of major ions, such as LEACHM (Wagenet and Hutson, 1987) UNSATCHEM (Šimůnek and Suarez, 1994; Šimůnek et al., 1996), and HYDRUS-1D (Šimůnek et al., 2005) and various reclamation models (Šimůnek and Valocchi, 2002). These models typically consider transport of major ions and their mutual reactions such as complexation, cation exchange, and precipitation/dissolution. A recent application of HYDRUS-1D and its major ion chemistry module is given by Gonçalves et al., (2006) who simulated solute transport in three lysimeters irrigated with different quality waters over a time period of three years. HYDRUS-1D successfully described field measurements of not only the overall salinity, but also of individual soluble cations as well as SAR (Sodium Adsorption Ratio) and ESP (Gonçalves et al., 2006).

Also models simulating carbon and nitrogen cycles are becoming a standard feature of many environmental models, such as COUP (Jansson and Karlberg, 2001) or HYDRUS-2D coupled with CW2D (Langergraber and Šimůnek, 2005). These models typically distribute organic matter, carbon, and organic and mineral nitrogen over multiple computational pools, while allowing organic matter to be decomposed by multiple microbial biomass populations. They can account for most of the major reaction pathways, such as inter-pool transfer of carbon and nitrogen, nitrification (ammonium to nitrate-N), denitrification (leading to the production of N_2 and N_2O), volatilization losses of ammonia (NH_3), and microbial biomass growth and death. HYDRUS-2D coupled with CW2D (Langergraber and Šimůnek, 2005) was specifically developed to describe processes in constructed wetlands.

Models with generalized chemistry provide users with much more freedom in designing their particular chemical systems; possible applications of these models are also much wider. Users can either select species and reactions from large geochemical databases, or are able to define their own species with particular chemical properties and reactions. Most codes with general geochemistry are limited to fully saturated porous media with constant water contents and velocities, and evaluate only solute transport and biogeochemical reactions (e.g., PHREEQC, Parkhurst and Appelo (1999)). Only few models allow the velocity field to be calculated internally. Several codes for transient unsaturated flow have also been coupled to general biogeochemistry models. These include, for example, 3DHYDROGEOCHEM (Yeh and Cheng, 1999) and HP1 (Jacques and Šimůnek, 2005).

The HP1 program (Jacques and Šimůnek, 2005) resulted from coupling HYDRUS-1D (Šimůnek et al., 1998) with the PHREEQC geochemical code (Parkhurst and Appelo, 1999). This new, very powerful code contains modules simulating (1) transient water flow in variably-saturated media, (2)

the transport of multiple components, (3) mixed equilibrium/kinetic biogeochemical reactions, and (4) heat transport. HP1 is a significant expansion of the individual HYDRUS-1D and PHREEQC programs by preserving and combining most of their original features and capabilities. The code still uses the Richards equation for simulating variably-saturated water flow and advection-dispersion type equations for heat and solute transport. However, the HP1 program can now simulate also a broad range of instantaneous and kinetic low-temperature biogeochemical reactions in water, the vadose zone and in ground water systems, including interactions with minerals, gases, exchangers and sorption surfaces based on thermodynamic equilibrium, kinetic, or mixed equilibrium-kinetic reactions. HP1 uses the operator-splitting approach with no iterations during one time step (non-iterative sequential approach). The accuracy of this operator-splitting approach for (a) a kinetic reaction network (i.e., sequential and parallel kinetic degradation reactions) by comparing HP1 with an analytical solution for TCE-degradation and (b) for mixed equilibrium and kinetic reactions for different flow conditions (steady-state and transient) has been evaluated by Jacques et al., (2006). HP1 is available on request from www.sckcen.be/hp1.

Jacques et al., (2003, 2005, 2006), Jacques and Šimůnek (2005), and Šimůnek et al., (2006b) demonstrated the versatility of HP1 on several examples such as a) the transport of heavy metals (Zn^{2+}, Pb^{2+}, and Cd^{2+}) subject to multiple cation exchange reactions, b) transport with mineral dissolution of amorphous SiO_2 and gibbsite ($Al(OH)_3$), c) heavy metal transport in a medium with a pH-dependent cation exchange complex, d) infiltration of a hyperalkaline solution in a clay sample (this example considers kinetic precipitation-dissolution of kaolinite, illite, quartz, calcite, dolomite, gypsum, hydrotalcite, and sepiolite), e) long-term transient flow and transport of major cations (Na^+, K^+, Ca^{2+}, and Mg^{2+}) and heavy metals (Cd^{2+}, Zn^{2+}, and Pb^{2+}) in a soil profile, f) cadmium leaching in acid sandy soils, g) radionuclide transport, h) long term uranium migration in agricultural field soils following mineral P-fertilization, and i) fate and subsurface transport of explosives.

There is an increasing concern about the presence of explosives and energetics in the subsurface environment. Such chemicals are the result of the manufacture, distribution, testing and/or unsafe disposal of ammunition, but can also be released into the environment during a terrorist attack. Šimůnek et al., (2006b) showed an application of HP1, in which they simulated the transport of the major explosive (the parent product TNT, 2,4,6-trinitrotoluene), and its various metabolites (the daughter products) 2ADNT, 4ADNT, and TAT, as they are being created sequentionally by degradation of the parent compounds. HP1 further allows the parent and daughter compounds to have different mobilities in the subsurface as

dictated by their specific dissolution, sorption and transport properties. In its most general case, the model permits contaminants to reside in all three phases, i.e., the liquid, solid (precipitated and sorbed), and gaseous phases. This example indicated that ground water may be more vulnerable to leaching of TNT daughter products (notably TAT) than of the parent compound itself, and that monitoring for the daughter products may provide an early warning of possible TNT leaching.

These various examples demonstrate that the coupling of HYDRUS-1D and PHREEQC leads to a potentially very powerful tool for simulating a broad range of interacting physical, chemical and biological processes affecting transport of contaminants in soils.

Acknowledgment

References

Bradford, S. A., Yates, S. R., Bettehar, M. and Šimůnek, J., 2002, Physical factors affecting the transport and fate of colloids in saturated porous media. *Water Resources Research,* **38**(12):1327, doi:10.1029/2002WR001340, 63.1–63.12.

Casey, F. X. M. and Šimůnek, J., 2001, Inverse analyses of the transport of chlorinated hydrocarbons subject to sequential transformation reactions. *Journal of Environmental Quality*, **30**(4):1354–1360.

Casey, F. X. M., Larsen, G. L., Hakk, H. and Šimůnek, J., 2003, Fate and transport of 17β-Estradiol in soil-water systems. *Environ. Sci. Technol.*, **37**(11):2400–2409.

Casey, F. X. M., Larsen, G. L., Hakk, H., and Šimůnek, J., 2004, Fate and transport of testosterone in agriculturally significant soils. *Environ. Sci. Technol.*, **38**(3):790–798.

Gerke, H. H., and van Genuchten, M. Th., 1993, A dual-porosity model for simulating the preferential movement of water and solutes in structured porous media. *Water Resour. Res*. **29**:305–319.

Gonçalves, M. C., Šimůnek, J., Ramos, T. B., Martins, J. C., Neves, M. J. and Pires, F. P., 2006. Multicomponent solute transport in soil lysimeters irrigated with waters of different quality, Water Resour. Res., **42**, W08401, doi:10.1029/2006WR004802, p. 17.

Fayer, M. J., 2000, UNSAT-H Version 3.0: Unsaturated Soil Water and Heat Flow Model. Theory, User Manual, and Examples. *Pacific Northwest National Laboratory* 13249.

Haws, N. W., Rao, P. S. C., and Šimůnek, J., 2005, Single-porosity and dual-porosity modeling of water flow and solute transport in subsurface-drained fields using effective field-scale parameters*, J. of Hydrology*, **313**(3–4):257–273.

Healy, R. W., 1990, Simulation of solute transport in variably saturated porous media with supplemental information on modifications to the U.S. Geological Survey's computer program VS2D. U.S. Geological Survey, *Water-Resources Investigation Report* 90–4025:125.

Hornberger, G. M., Mills, A. L., and Herman, J. S., 1992, Bacterial transport in porous media: Evaluation of a model using laboratory observations. *Water Resour. Res*. **28**:915–938.

HydroGeoLogic, Inc., 1996, MODFLOW-SURFACT, A Comprehensive MODFLOW-Based Flow and Transport Simulator, Version 2.1, HydroGeoLogic, Inc.

Jacques, D., Šimůnek, J., Mallants, D., and van Genuchten, M. Th., 2003. The HYDRUS-PHREEQC multicomponent transport model for variably-saturated porous media: Code verification and application, MODFLOW and More 2003: Understanding through Modeling, Conference Proceedings, ed. E. Poeter, Ch. Zheng, M. Hill, and J. Doherty, Int. Ground Water Modeling Center, Colorado School of Mines, 23–27.

Jacques, D., and Šimůnek, J. 2005, Multicomponent - Variable Saturated Transport Model, Description, Manual, Verification and Examples, Waste and Disposal, SCK•CEN, *BLG-998*, Mol, Belgium.

Jacques, D., Šimůnek, J., Mallants, D., and van Genuchten, M. Th., 2005. Long term uranium migration in agricultural field soils following mineral P-fertilization, Proc. Of "The 10th Int. Conf. on Environ. Remediation and Radioactive Waste Management, Sept. 4–8, 2005, Scottish Exhibition & Conference Center, Glasgow, Scotland, UK.

Jacques, D., Šimůnek, J., Mallants, D., and van Genuchten, M. Th., 2006. HP1: A coupled numerical code for variably saturated water flow, solute transport, and biogeochemistry in soil systems, *J. Contam. Hydrology*, (in press).

Jansson, P.-E., and Karlberg, L. 2001, Coupled heat and mass transfer model for soil-plant-atmosphere systems. Royal Institute of Technology, Dept of Civil and Environmental Engineering, Stockholm 325 p.

Jarvis, N. J., 1994, The MACRO model (Version 3.1), Technical description and sample simulations, *Reports and Dissertations 19*. Dept. Soil Sci., Swedish Univ. Agric. Sci., Uppsala, Sweden, 51 p.

Jury, W. A., Spencer, W. F., and Farmer, W. J., 1983, Behavior assessment model for trace organics in soil: I. Model description, *J. Environ. Qual.* **12**(4):558–564.

Kodešová, R., Kozák, J., Šimůnek, J., and Vacek, O., 2005. Field and numerical study of chlorotoluron transport in the soil profile: Comparison of single and dual-permeability model, *Plant, Soil and Environment*, **51**(7):310–315.

Köhne, J. M., Köhne, S., Mohanty, B. P. and Šimůnek, 2004, J., Inverse mobile-immobile modeling of transport during transient flow: Effect of between-domain transfer and initial water content, *Vadose Zone J.*, **3**(4):1309–1321.

Köhne, S., Lennartz, B., Köhne, J. M., and Šimůnek, J., 2006, Bromide transport at a tile-drained field site: experiment, one- and two-dimensional equilibrium and non-equilibrium numerical modeling, *J. Hydrology*, **321**(1–4):390–408.

Langergraber, G. and Šimůnek, J., 2005, Modeling Variably-Saturated Water Flow and Multi-Component Reactive Transport in Constructed Wetlands, *Vadose Zone Journal*, **4**:924–938.

Leij, F. J., and Bradford, S. A., 1994, 3DADE: A computer program for evaluating three-dimensional equilibrium solute transport in porous media, *Research Report No. 134*, U. S. Salinity Laboratory, USDA, ARS, Riverside, CA.

Leij, F. J., and Toride, N. 1997, N3DADE: A computer program for evaluating nonequilibrium three-dimensional equilibrium solute transport in porous media, *Research Report No. 143*, U. S. Salinity Laboratory, USDA, ARS, Riverside, CA.

Parkhurst, D. L., and Appelo, C. A. J., 1999, User's guide to PHREEQC (version 2) – A computer program for speciation, batch-reaction, one-dimensional transport, and inverse geochemical calculations. Water Resources Investigation, *Report 99–4259*, Denver, Co, USA, 312 p.

Pot, V., J. Šimůnek, P. Benoit, Y. Coquet, A. Yra and M.-J. Martínez-Cordón, 2005, Impact of rainfall intensity on the transport of two herbicides in undisturbed grassed filter strip soil cores. *J. of Contaminant Hydrology*, **81**:63–88.

Schaerlaekens, J., Mallants, D., Šimůnek, J., van Genuchten, M. Th. and Feyen, J., 1999, Numerical simulation of transport and sequential biodegradation of chlorinated aliphatic hydrocarbons using CHAIN_2D. *Journal of Hydrological Processes*, **13**(17):2847–2859.

Schijven, J. and Šimůnek, J., 2002, Kinetic modeling of virus transport at field scale. *Journal of Contaminant Hydrology*, **55**(1–2):113–135.

Seuntjens, P., Tirez, K., Šimůnek, J., van Genuchten, M. Th., Cornelis, C., and Geuzens, P., 2001, Aging effects on cadmium transport in undisturbed contaminated sandy soil columns. *Journal of Environmental Quality,* **30**:1040–1050.

Šimůnek, J., and D. L. Suarez, 1994, Two-dimensional transport model for variably saturated porous media with major ion chemistry. *Water Resour. Res*. **30**(4):1115–1133.

Šimůnek, J., Suarez, D. L., and Šejna, M., 1996, The UNSATCHEM software package for simulating one-dimensional variably saturated water flow, heat transport, carbon dioxide production and transport, and multicomponent solute transport with major ion equilibrium and kinetic chemistry. Version 2.0. *Research Report No. 141*, U.S. Salinity Laboratory, USDA, ARS, Riverside, California, 186 p.

Šimůnek, J., Šejna, M., and van Genuchten, M. Th., 1998, The HYDRUS-1D software package for simulating the one-dimensional movement of water, heat, and multiple solutes in variably-saturated media. Version 2.0, *IGWMC - TPS - 70,* International Ground Water Modeling Center, Colorado School of Mines, Golden, Colorado, 202 p.

Šimůnek, J., Šejna, M., and van Genuchten, M. Th., 1999a, The HYDRUS-2D software package for simulating two-dimensional movement of water, heat, and multiple solutes in variably saturated media. Version 2.0, *IGWMC - TPS - 53,* International Ground Water Modeling Center, Colorado School of Mines, Golden, Colorado, 251 p.

Šimůnek, J., van Genuchten, M. Th., Šejna, M., Toride, N., and Leij, F. J., 1999b, The STANMOD computer software for evaluating solute transport in porous media using analytical solutions of convection-dispersion equation. Versions 1.0 and 2.0, *IGWMC - TPS - 71,* International Ground Water Modeling Center, Colorado School of Mines, Golden, Colorado, 32 p.

Šimůnek, J., Wendroth, O., Wypler, N., and van Genuchten, M. Th., 2001, Nonequilibrium water flow characterized from an upward infiltration experiment, *European J. of Soil Sci.*, **52**(1):13–24.

Šimůnek, J. and Valocchi, A. J., 2002, Geochemical Transport, In: *Methods of Soil Analysis*, Part 1, Physical Methods, Chapter 6.9, Eds. J. H. Dane and G. C. Topp, Third edition, SSSA, Madison, WI, 1511–1536.

Šimůnek, J., Jarvis, N. J., van Genuchten, M. Th., and Gärdenäs, A., 2003, Nonequilibrium and preferential flow and transport in the vadose zone: Review and case study. *J. Hydrol*. **272**:14–35.

Šimůnek, J., van Genuchten, M. Th., and Šejna, M., 2005. The HYDRUS-1D software package for simulating the one-dimensional movement of water, heat, and multiple solutes in variably-saturated media. Version 3.0, *HYDRUS Software Series 1*, Department of Environmental Sciences, University of California Riverside, Riverside, CA, 270 p.

Šimůnek, J., He, Changming J., Pang, L., and Bradford, S. A., 2006a. Colloid-facilitated transport in variably-saturated porous media: Numerical model and experimental verification, *Vadose Zone Journal*, *5*, 1035–1047, 2006.

Šimůnek, J., Jacques, D., van Genuchten, M. Th., and Mallants, D., 2006b. Multicomponent geochemical transport modeling using the HYDRUS computer software packages, *J. Am. Water Resour. Assoc.*, (in press).

Toride, N., Leij, F. J., and van Genuchten, M. Th., 1995, The CXTFIT code for estimating transport parameters from laboratory or field tracer experiments. Version 2.0, *Research Report No. 137*, U. S. Salinity Laboratory, USDA, ARS, Riverside, CA.

van Dam, J. C., Huygen, J., Wesseling, J. G., Feddes, R. A., Kabat, P., van Valsum, P. E. V., Groenendijk, P., and van Diepen, C. A., 1997, Theory of SWAP, version 2.0. Simulation of water flow, solute transport and plant growth in the Soil- Water- Atmosphere- Plant environment. Dept. Water Resources, WAU, *Report 71*, DLO Winand Staring Centre, Wageningen, Technical Document 45.

van Genuchten, M. Th., 1980, Determining transport parameters from solute displacement experiments, *Research Report No. 118*, U. S. Salinity Laboratory, USDA, ARS, Riverside, CA.

van Genuchten, M. Th., 1981, Non-equilibrium transport parameters from miscible displacement experiments, *Research Report No. 119*, U. S. Salinity Laboratory, USDA, ARS, Riverside, CA.

van Genuchten, M. Th., 1985, Convective-dispersive transport of solutes involved in sequential first-order decay reactions, *Computers & Geosciences,* **11**(2):129–147.

van Genuchen, M. Th., and Šimůnek, J., 2004, Integrated modeling of vadose zone flow and transport processes, *In* "Unsaturated Zone Modelling: Progress, Challenges and Applications" (R. A. Feddes, G. H. de Rooij, and J. C. van Dam, Eds.), Wageningen, The Netherlands, October 3–5, 2004, pp. 37–69.

Wagenet, R. J., and Hutson, J. L., 1987, LEACHM: Leaching Estimation And CHemistry Model, A process-based model of water and solute movement, transformations, plant uptake and chemical reactions in the unsaturated zone. *Continuum 2*. Water Resour. Inst., Cornell University, Ithaca, New York.

Yeh, G.-T., and Cheng, H.-P., 1999, 3DHYDROGEOCHEM: A 3-dimensional model of density-dependent subsurface flow and thermal multispecies-multicomponent HYDROGEOCHEMi-cal transport. EPA/600/R-98/159, 150 p.

Zhang, P., Šimůnek, J., and Bowman, R. S., 2004, Nonideal transport of solute and colloidal tracers through reactive zeolite/iron pellets, *Water Resour. Res.,* **40**, doi:10.1029/2003WR002445.

INTERPOLATION AND UPDATE IN DYNAMIC DATA-DRIVEN APPLICATION SIMULATIONS

CRAIG C. DOUGLAS
University of Kentucky, Department of Computer Science, 325 McVey Hall, Lexington, KY 405061 and Yale University, Department of Computer Science, P.O. Box 208285, New Haven, CT, 06520

YALCHIN EFENDIEV*, RICHARD EWING, RAYTCHO LAZAROV
Department of Mathematics and Institute for Scientific Computation, Texas A&M University, College Station, TX 77843

MARTIN J. COLE, GREG JONES, CHRIS R. JOHNSON
Scientific Computing and Imaging, University of Utah, Salt Lake City, UT 84112-9205

Abstract. In this paper we discuss numerical techniques involved in dynamic data driven application simulations (DDDAS). We present an interpolation technique and update procedures. A multiscale interpolation technique is designed to map the sensor data into the solution space. In particular we show that frequent updating of the sensor data in the simulations can significantly improve the prediction results and thus important for applications. The frequency of sensor data updating in the simulations is related to streaming capabilities and addressed within DDDAS framework (Douglas et al., 2003). We discuss the update of permeability and initial data.

Keywords: dynamic data driven application; porous media; update; multiscale

———
*To whom correspondence should be addressed. Yalchin Efendiev, Department of Mathematics and Institute for Scientific Computation, Texas A&M University, College Station, TX 77843

1. Introduction

Dynamic data driven simulations are important for many practical applications. Consider an extreme example of a disaster scenario in which a major waste spill occurs in a subsurface near clean water aquifer. Sensors can now be used to measure where the contamination is, where the contaminant is going to go, and to monitor the environmental impact of the spill. One of the objectives of dynamic data driven simulations is to incorporate the sensor data into the real time simulations. A number of important issues are involved in DDDAS and they are described in Douglas et al., 2003.

Sensors and data generating devices may take many forms including other running computational simulations. The intent of this paper is to discuss several DDDAS enabling technologies in the context of a specific application area in order to provide techniques and tools to effectively demonstrate the potential of dynamic data driven simulations for other areas. Our primary application is contaminant tracking, which in groundwater reservoirs is modeled by strongly coupled systems of convection-reaction-diffusion equations. The solution process of such systems becomes more complicated when modeling remediation and clean-up technologies since they exhibit strong nonlinearities and local behavior. Many of these applications are essentially computer models that solve nonlinear, unsteady, coupled, partial differential equations. All require consistent initial conditions, adequate forcing fields, and boundary conditions to advance the solution in time. Collectively these fields represent the input data necessary to run the models. The input data can originate from observations, e.g., sensor based telemetry, can be internally generated from ensemble type simulations, or can be externally generated (e.g., providing boundary conditions for very high resolution regional models). The skill of these models to adequately represent realistic conditions is intimately tied to the quality, spatial and temporal coverage, and intelligent use of their input data sets. These applications in turn generate large amounts of output data that must be either analyzed or passed on to other more specialized subcomponents.

One of difficulties arisen in DDDAS is due to multiscale features of the underlying problem. Subsurface formations typically exhibit heterogeneities over a wide range of length scales while the sensors are usually located at sparse locations and sparse data from these discrete points in a domain is broadcasted. Since the sensor data usually contains noise it can be imposed both as a hard constraint as well as a soft manner. To incorporate the sensor data into the simulations in a multiscale environment we introduce multiscale interpolation operator. This is done in the context of general nonlinear parabolic operators that include many subsurface processes. The main idea of this interpolation is that we do not alter the

heterogeneities of the multiscale field that drives the contaminant. Rather based on the sensor data we rescale the solution in a manner that it preserves the heterogeneities. The main idea of this rescaling is follows some previous findings and use the solutions of local problems. This interpolation technique fits nicely with new multiscale framework for solving nonlinear partial differential equations. The combination of both the interpolation and multiscale framework provides robust and fast simulation techniques.

The errors in the simulations will persist if one does not change the input parameters. As new data are obtained from sensors measurements, the initial data needs to be updated. This update reduces the computational errors associated with incorrect initial data and improves the predictions. To address parameter update, we consider linear subsurface flows involving convection and diffusion. The proposed approaches can be easily extended to non-linear problems.

Initial data is sought in a finite dimensional space. Using the first set of measurements, the approximation of the initial data is recovered. As new data are incorporated into the simulator, we update the initial data using an objective function. We note that the formulated problem is ill-posed. Two facts can be attributed to this ill-posedness. First, the data gathered from the sensor measurements always contain some defects that come from factors such as human errors and inherent factory errors of the sensors. Secondly, the numbers of sensors that can be installed are limited, and in general are much fewer than the finite dimensional space describing the initial data. For the latter, we can regularize the problem by using the prior information about the initial data. This prior information is the updated initial data. The penalization constants depend on time of update and can be associated with the relative difference between simulated and measured values. Using multiscale basis functions, one can reduce the size of the finite dimensional space representing the initial condition. This renders efficient computation for initial data recovery. One can consider this problem in a Bayesian framework also. We briefly describe this procedure.

In the paper, we also address the update of the permeability field. This problem is more difficult compared to the update of the initial data. Typically, the dimension of the parameter space describing the permeability field is very large, while the obtained data only represents the integrated response. We propose a solution technique using Markov Chain Monte Carlo (MCMC) methods (Robert and Casella, 1999).

2. Data driven simulations Interpolation

Our goal in this section is to discuss the mapping of the sensor data to the finite dimensional space where the solution is calculated. This procedure is

nontrivial in general, because the solution space usually has high dimension, while the sensors are located only at few locations. To illustrate this in Figure 1 we schematically plot gray scale image of a heterogeneous field. The sensors in this Figure marked by X. Due to uncertainties in the data the random fields used for the simulations and the true field can differ significantly. Thus, one has to be able to reconcile the streamed data from the sensors with that produced by our simulations.

Our simplified approach presented in this paper consists of passing the sensor data to the simulations and its use for the next time step simulations. Since the sensor data represents the solution only at few coarse locations one has to modify the solution conditioned to this data. This step we call multiscale interpolation which consists of mapping the sensor data to the solution space. At each time step the sensor data is received by the simulator. There are two options to handle the data. We can treat it as hard data or as soft data. The latter means that the data contains some noise and not needed to be imposed exactly. In this paper the first approach, "hard constraint", will be considered. At the beginning of each time step the sensor data needs to be mapped to the discrete solution space. This is performed using DDDAS mapping operator,
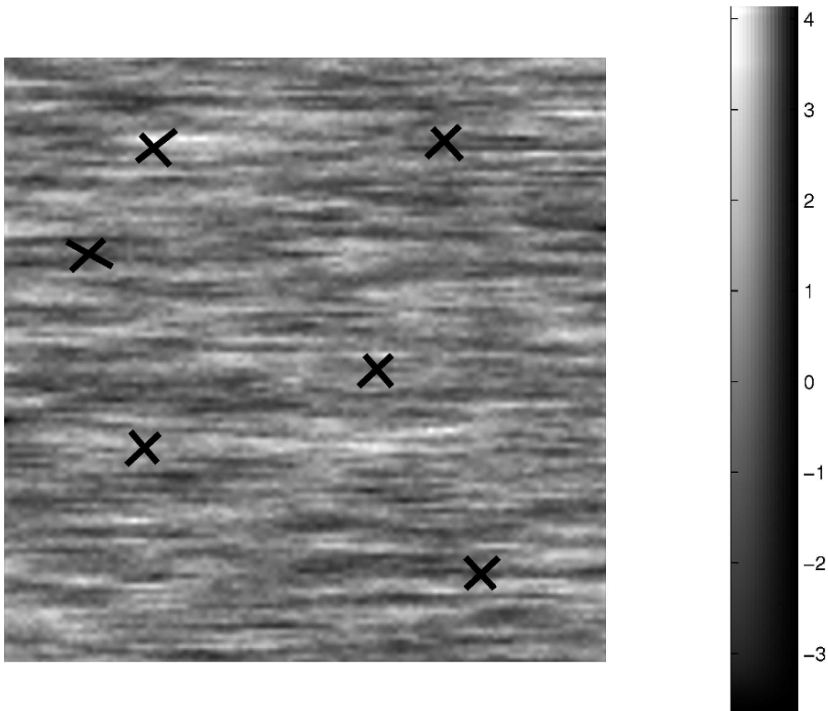
Figure 1. A heterogeneous log-permeability field. The locations of the sensors marked.

the main feature of which is *not* to alter the heterogeneous field. Another words, each time we will update the data and will not seek the error source.

The proposed mapping for the sensor data is very general and applicable to various classes of equations. To demonstrate this we consider general nonlinear parabolic equations

$$D_t u_\varepsilon = div(a_\varepsilon(x,t,u_\varepsilon,D_x u_\varepsilon)) + a_{0,\varepsilon}(x,t,u_\varepsilon,D_x u_\varepsilon), \text{in} Q_0 \times [0,T], \quad (1)$$

where ε indicates the presence of the small scales, heterogeneities and Q_0 is the spatial domain. This equation includes various physical processes that occur in subsurface. Assume the domain is divided into the coarse grid such that the sensor points are the nodal points of the coarse grid. This can be always accomplished. Note that we do not require all nodal points to be sensor locations. Further denote by S^h the space of piecewise linear functions on this partition,

$$S_h = \{v_h \in C^0(\overline{Q_0}) : \text{the restriction} v_h \text{is linear for each triangle} K \in \Pi_h\}.$$

Our objective now is to map the function defined on S^h to the fine grid that represents the heterogeneities. This grid is obtained from *apriori* information about the field using geostatistical packages (Deutsch and Journel, 1998). Denote by the operator E the mapping from the coarse dimensional space into the fine grid,

$$E : S^h \to V_\varepsilon^h,$$

which is constructed as follows. For each element in $u_h \in S^h$ at a given time t_n we construct space time function $u_{\varepsilon,h}(x,t)$ in $K \times [t_n,t_{n+1}]$ such that it satisfies

$$D_t u_{\varepsilon,h}(x,t) = div(a_\varepsilon(x,t,\eta,D_x u_{\varepsilon,h})) \quad (2)$$

in each coarse element K, where η is the average of u_h. $u_{\varepsilon,h}(x,t)$ is calculated by solving (2) on the fine grid, and thus it is a fine scale function. To complete the construction of E we need to set boundary and initial conditions for (2). One can set different boundary and initial conditions and this will give rise to different maps. These maps will differ from each other slightly. The main underlying property of our map is that it is constructed as a solution of local problems. The latter guarantees, that the solution is consistent with prescribed heterogeneities. In our numerical simulations we have taken the boundary and initial condition for the local problems to be linear with prescribed nodal values. The nodal values are obtained from the sensor data, if available. If the sensor data is not available at some location

we use the values obtained from the simulations at previous time. Note that one can not impose the values of the solutions directly at some locations. The latter can cause artificial discontinuities in the solution. Mathematical aspects of this interpolation operator, such as convergence and etc, are described in Efendiev and Pankov, 2004.

Once the solution at time $t = t_n$ is computed its values with sensor data at the sensor locations are compared. After changing the values of the solution we interpolate it to the fine grid and use it for the next time step. At the last step we use multiscale approach which is computationally efficient. In particular, the solution at the next time step is calculated based on

$$
\int_{Q_0} (u_h(x,t_{n+1}) - u_h(x,t_n))v_h dx + \sum_K \int_{t_n}^{t_{n+1}} \int_K ((a_\varepsilon(x,t,\eta,D_x u_{\varepsilon,h}), D_x v_h) +
$$

$$
a_{0,\varepsilon}(x,t,\eta,D_x u_{\varepsilon,h})v_h)dxdt = \int_{t_n}^{t_{n+1}} \int_{Q_0} fdxdt.
$$

$$(3)$$

Here Q_0 refers to the spatial domain and K are the coarse elements. This approach combined with interpolation technique has great CPU advantages over the fine scale calculations (cf. Efendiev and Pankov, 2004).

For linear problems, the approach based on the interpolation technique reduces to multiscale finite element method (Hou and Wu, 1997). In this approach, the multiscale nodal basis functions are constructed, and the solution is sought in the coarse dimensional space spanned by the multiscale basis functions. The permeability values at sensor locations are incorporated using the approaches discussed in the next sections. The update of the solution value involves the update of the nodal value of the coarse-scale solution, while the basis functions are kept the same. Basis functions are changed only if the heterogeneities change. The latter is the case for nonlinear problems, or when the sharp dynamic fronts alter the heterogeneities.

We have performed a number of numerical examples which demonstrated the efficiency and robustness of our interpolation technique. We have considered both linear equations in the form of $D_t u = div(a_\varepsilon(x)D_x u)$, where $a_\varepsilon(x) = \exp(\alpha_\varepsilon(x))$, and $\alpha_\varepsilon(x)$ is a realization of the random field with prescribed covariance structure as well as nonlinear equations in the form of $D_t u_\varepsilon = div(a_\varepsilon(x,u_\varepsilon)D_x u_\varepsilon)$, where $a_\varepsilon(x,\eta) = k_\varepsilon(x)/(1+\eta)^{\alpha_\varepsilon(x)}$. $k_\varepsilon(x) = \exp(\beta_\varepsilon(x))$ is chosen such that $\beta_\varepsilon(x)$ is a realization of a random field with prescribed covariance structure. $\alpha_\varepsilon(x)$ is chosen such that $\alpha_\varepsilon(x) = k_\varepsilon(x) + const$ with the spatial average of 2. True and simulated random fields are taken to be

linear combinations of independent realizations of a random field with different scaling and linear coefficients. The sensors are placed in a few points in the domain, and the values of true solution are fed into the simulations. Objective of these numerical results is to demonstrate how frequency of updating sensor data in the simulations improves the accuracy of the method. Simulation results with more frequent update show that the frequent updating improve by several fold the accuracy of the predictions and thus important for DDDAS. We observe this consistently in various numerical examples for both linear and nonlinear equations which we have tested (see Douglas et al., 2004a, 2004b).

2. The update of initial data and permeability

We will demonstrate the update of the initial data and permeability data on the example of linear convection diffusion equation. However, the proposed approaches can be extended to nonlinear problems. The model that we consider is

$$D_t C + v \cdot D_x C - div\left(d\, D_x C\right) = 0 \quad \text{in} \quad Q_0 \tag{4}$$

where by Darcy's Law, $v = -k D_x p$, with the pressure p satisfies $-div\left(k\, D_x p\right) = 0$.

Here k, as before, is a generated permeability with certain statistical variogram and correlation structure, and d is the diffusion coefficient. As we mentioned before, our goal is the estimation of the initial condition $C^0(x)$ given a set of spatially sparse concentration measurements at certain times.

Let N_s be the number of sensors installed in various points in the porous medium and $\{x_j\}_{j=1}^{N_s}$ denote be such points. Let N_t be the number of how many times the concentration is measured in time and $\{t_k\}_{k=1}^{N_t}$ denote such times. Furthermore let $\gamma_j(t_k)$ denotes the measured concentration at sensor located in x_j and at time t_k. We set

$$M(\gamma) = \{\gamma_j(t_k), j = 1, \cdots, N_s, k = 1, \cdots, N_t\}. \tag{5}$$

Suppose we have a set of N_c possible initial conditions $\{\tilde{C}_i^0(x)\}_{i=1}^{N_c}$, where $\tilde{C}_i^0(x)$ are basis functions with support determined a priori, or $\tilde{C}_i^0(x)$ can be functions of certain form determined a priori. Furthermore, we designate $\tilde{C}_i(x,t)$ the solution of (4) using an initial condition $\tilde{C}_i^0(x)$. Let $\alpha = (\alpha_1, \alpha_2, \cdots, \alpha_{N_c})$ be a vector of real numbers, and write

$$\tilde{C}^0(x,t) = \sum_{i=1}^{N_c} \alpha_i \tilde{C}_i^0(x). \qquad (6)$$

Then the solution of (4) with initial condition (6) has the following form

$$\tilde{C}(x,t) = \sum_{i=1}^{N_c} \alpha_i \tilde{C}_i(x,t) \qquad \text{Next, we introduce a target function}$$

$$F(\alpha) = \sum_{k=1}^{N_t} \sum_{j=1}^{N_s} \left(\sum_{i=1}^{N_c} \alpha_i \tilde{C}_i(x_j,t_k) - \gamma_j(t_k) \right)^2 + \kappa \sum_{i=1}^{N_c} (\alpha_i - \beta_i)^2, \qquad (7)$$

where κ is the penalty coefficient for an a priori vector $\beta = (\beta_1, \beta_2, \cdots, \beta_{N_c})$. The first approach, which is appropriate for linear problems, is to minimize the target function over α. Minimization of the target function (7) is done by setting

$$\frac{\partial F(\alpha)}{\partial \alpha_m} = 0, \quad m = 1, \cdots, N_c, \qquad (8)$$

which gives the linear system $A\alpha = R$, where $A_{mn} = \sum_{j=1}^{N_s} \tilde{C}_m(x_j,t)\tilde{C}_n(x_j,t) + \delta_{mn}\kappa_m$, $m,n = 1, \cdots, N_c$ with $\delta_{mn} = 1$ if $m = n$ and zero otherwise, and $R_m = \sum_{j=1}^{N_s} \tilde{C}_m(x_j,t)\gamma_j(t) + \kappa_m\beta_m$, $m = 1, \cdots, N_c$. We would like to note that one can use multiscale basis functions to reduce the dimension of the parameter space. The research along this direction is currently under way.

Another, more general way, looking at this problem is the following. Due to measurement errors, the data obtained from the sensors will not be necessarily imposed exactly and one needs to use the error covariance matrix. Hence, the general idea is to draw sample of initial condition from its posterior distribution, which we denote by $P(\tilde{C}^0(x) | M(\gamma))$. From Bayes' theorem we have

$$P(\tilde{C}^0(x) | M(\gamma)) \propto P(M(\gamma) | \tilde{C}^0(x))P(\tilde{C}^0(x)), \qquad (9)$$

where $P(M(\gamma) \mid \tilde{C}^0(x))$ is the likelihood probability distribution, and $P(\tilde{C}^0(x))$ is the prior probability distribution. Using the formulation described above, (9) may be expressed as

$$P(\alpha \mid M(\gamma)) \propto P(M(\gamma) \mid \alpha) P(\alpha). \qquad (10)$$

In other words, we may transform the task of estimating the initial condition of (4) into a problem of finding the "best" α such that $\tilde{C}^0(x) \approx C^0(x)$.

Using this target function, the posterior probability can be written as a zero-mean Gaussian distribution:

$$P(\alpha \mid M(\gamma)) = \exp\left(-\frac{F(\alpha)}{2\sigma^2}\right), \qquad (11)$$

where σ^2 is the variance of the distribution. In general, one can derive an error covariance function to describe the error statistics more accurately.

To draw a sample from the posterior distribution, Markov Chain Monte Carlo (MCMC) approach with Metropolis-Hasting rule is used. MCMC scheme can be carried out by updating α using the Metropolis-Hasting algorithm. In the single step of this algorithm, α^* is generated from a pre-specified proposal distribution $q(\alpha^* \mid \alpha)$ for a given α. Then the proposed α^* is accepted with probability of acceptance

$$P_r = \min\left\{1, \frac{P(\alpha^* \mid M(\gamma))}{P(\alpha \mid M(\gamma))} \frac{q(\alpha \mid \alpha^*)}{q(\alpha^* \mid \alpha)}\right\}. \qquad (12)$$

We note that for linear problems the likelihood probability can be determined using the pre-computed $\tilde{C}(x,t)$ prior to MCMC simulation. MCMC approaches can be applied to nonlinear problems (such as NAPL infiltration) and this approach can give some advantage since it avoids solving linear system for the minimization.

One of the drawbacks of MCMC approaches in subsurface applications is that the acceptance rate can be small. For the linear problems, we follow the idea presented in Oliver et al., 1997, to increase the acceptance rate. In particular, using the minimization problem one achieves the acceptance probability to be one. We would like to note that this is only true for linear problems, and does not work for nonlinear problems. Next, we will discuss the algorithm where the acceptance probability is one for linear problems. The main idea of this algorithm is to generate samples that have high acceptance probability. We will sample γ and β from some distribution and use them to explore the space of uncertainties. The algorithm is as follows:

1.   Propose $\tilde{\gamma}$ and $\tilde{\beta}$ from the following distribution:

$$f(\tilde{\gamma}, \tilde{\beta}) \propto \exp\left(-\frac{1}{2\sigma^2}\left[\sum_{k=1}^{N_t}\sum_{j=1}^{N_s}\left(\gamma_j(t_k) - \gamma_j(t_k)\right)^2 + \kappa \sum_{i=1}^{N_c}\left(\beta_i - \beta_i\right)^2\right]\right) \quad (13)$$

2.   Minimize $F(\alpha)$ in (7) where $\tilde{\gamma}$ and $\tilde{\beta}$ are used replacing γ and β, respectively.

In this algorithm, we do not need to implement the acceptance step, since the acceptance probability is 1, (Oliver et al., 1997). We have tested the algorithm and observed the significant improvement of the initial data, reduction of the uncertainty after each update, and better predictions. In particular, we have observed an improvement of the initial data after each update. The use of the updated initial data provides better predictions for DDDAS. We would like to stress again that the initial data does not necessarily represent the data at time zero, but it can be the data at some previous time steps.

One of the main error sources is due to incorrect permeability field. Thus, it is necessary to update the permeability field as we gain new data. The update of the permeability is a difficult task since the permeability field is represented on the large number of grid blocks. To reduce the dimension of the parameter space, we use Karhunen-Loeve expansion (Loeve, 1977) to express the permeability field in terms of an optimal basis. In particular, expressing the permeability field, $k = \exp(Y)$, as $Y = \sum_i \theta_i \phi_i(x)$, we truncate the expansion using eigenvalues that are less than five percent of the largest eigenvalue. To impose the hard constraint (the values of the permeability at prescribed locations) we will find a linear subspace of our parameter space (a hyperplane) which yields the corresponding values of the permeability field.

In our simulations, we consider log-normal Gaussian fields with prescribed correlation lengths and variance as a prior distribution. We first determine eigenvalues numerically and obtain the eigenpairs $\{\lambda_k, \phi_k\}$. Further, the permeability expansion is truncated (typically to 20 eigenvalues). In the simulation, we first generate true (reference) permeability field using all eigenvectors and compute corresponding measurement data. To propose permeability fields from prior distribution, we assume that at 7 distinct points (sensor locations), the permeability field is known. This condition is imposed by setting

$$\sum_{k=1}^{20} \sqrt{\lambda_k} \theta_k \phi_k(x_j) = \alpha_j, \quad (14)$$

where α_j ($j = 1, ..., 7$) are prescribed constants. In our simulations we propose 13 θ_i and calculate the rest of θ_i from (14).

Next we state Metropolis-Hasting MCMC for permeability sampling using the notations defined above. From Bayes' theorem we have

$$P(k(x)\,|\,M(\gamma)) \propto P(M(\gamma)\,|\,k(x))P(k(x)).$$

This relation can be written in terms of θ_i, because the permeability field can be represented in terms of θ_i. The prior distribution, which is based on experimental prior knowledge, is taken to be Gaussian with correlation lengths $L_1 = 0.4$, $L_2 = 0.1$ and $\sigma^2 = 2$ and with permeability values fixed at sensor locations. The values of the permeability field are known at the sensor locations.
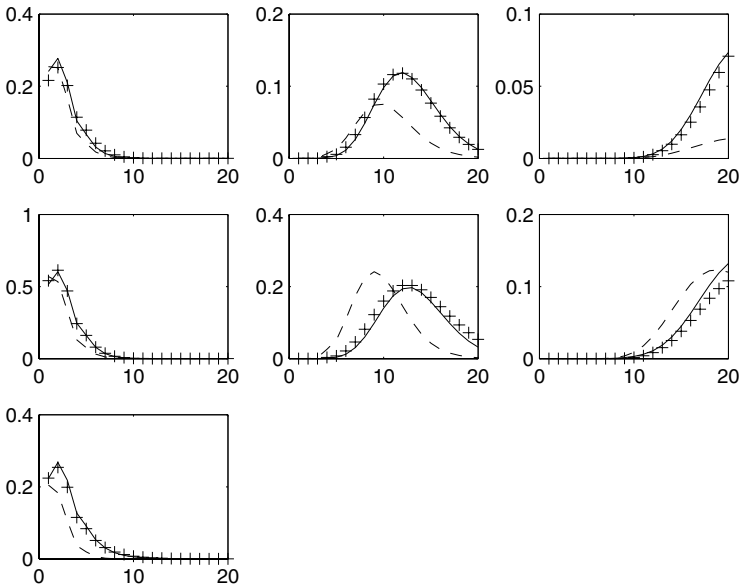
Figure 2. Concentration at different time instants - the solid line designates the observed concentration, the dashed line designates the first match, and the data marked with '+' designates the concentration after the measurement information is incorporated into the simulations.

As for the likelihood, we take the L_2 norm of the difference between the sensor information obtained by solving the equations (4) and the observed sensor information. This relationship is strongly nonlinear. We take the measurement precision to have Gaussian error covariance with variance 0.0007. The random walk sampler is used as a proposal. This typically allows higher acceptance rate. In Figure 2, we plot the measurements at each sensor location as a function of time instants. Solid line designates the observed values of the concentration at the sensor

locations, dashed line designates the initial predictions of the concentration at the sensor locations, and the lines marked with + designates the concentration after 10000 MCMC iterations at these locations. As we see from this figure, using MCMC approach, we can obtain adequate permeability samples which provide us with accurate predictions.

Acknowledgement

References

Deutsch, C.V. and Journel, A.G., 1998, *GSLIB: Geostatistical software library and user's guide,* 2nd ed.*,* Oxford University Press, New York.

Douglas, C.C., Efendiev, Y., Ewing, R, Lazarov, R., Cole, M.R., Johnson, C.R. and Jones, G., 2003, Virtual telemetry middleware for DDDAS, in: *Computational Sciences - ICCS,* edited by P. M. A. Sllot, D. Abramson, J. J. Dongarra, A. Y. Zomaya, and Yu. E. Gorbachev.

Douglas, C.C., Shannon, C., Efendiev, Y, Ewing, R., Ginting, V., Lazarov, R., Cole, M.R., Jones, G., Johnson, C.R., and Simpson, J., 2004a, Telemetry-Driven Application Simulations, in: *Computational Sciences , ICCS 2004,* M. Bubak, G. D. van Albada, P. M. A. Sloot, and J. J. Dongarra, eds., **3**, pp. 701–708.

Douglas, C.C., Shannon C., Efendiev, Y., Ewing, R., Ginting, V., Lazarov, R., Cole, M., Jones, G., Johnson, C.R., and Simpson, J., 2004b, A note on data-driven contaminant simulation, *Lecture Notes in Computer Science*, Springer-Verlag, 3038, pp. 701–708.

Efendiev Y., and Pankov, A., 2004, Numerical homogenization of nonlinear random parabolic operators. *SIAM Multiscale Modeling and Simulation*, **2(2),** 237–268.

Hou T.Y., and Wu, X.H., 1997, A multiscale finite element method for elliptic problems incomposite materials and porous media, *Journal of Computational Physics*, **134,** pp. 169–189.

Loeve, M., 1977, *Probability Theory,* 4th ed., Springer, Berlin

Oliver, D., Cunha, L., and Reynolds, A., 1997, Markov Chain Monte Carlo methods for conditioning a permeability field to pressure data, *Mathematical Geology*, **29.**

Robert, C., and Casella, G.,1999, *Monte Carlo Statistical Methods*, Springer-Verlag, New-York.

OIL INFILTRATION INTO SOIL: PROBLEMS

OF THE GEORGIAN SECTION OF TRACECA

AND THEIR NUMERICAL TREATMENT

TEIMURAZ DAVITASHVILI
I.Vekua Institute of Applied Mathematics of Tbilisi State University, 2 University St., 0143, Tbilisi, Georgia. E-mail: tedav@viam.hepi.edu.ge

Abstract. Spreading of spilled oil in soil is investigated regarding accidents on railway routes and damage of pipelines along the Georgian section of the Transport Corridor Europe-Caucasus-Asia (TRACECA). Processes controlling the penetration of oil into soil are studied applying analytical and numerical models of oil infiltration. Some analytical solutions are given and analyzed. Results of numerical calculations for conditions found along TRACECA are presented.

Keywords: oil infiltration into soils; analytical models; numerical models; TRACECA; oil pipeline

1. Introduction

It is well known that the Caspian Sea region has abundant reserves of oil and gas, but limited accessible markets for the products. On the other hand, Georgia with limited own fossil energy resources provides a large internal market for oil on the Black Sea coast. Because of its geopolitical position the European Union (EU) considers Georgia as an important partner for the development of transport networks between the Black Sea and Central Asia. The Transport Corridor Europe-Caucasus-Asia (TRACECA) is seen by the EU as a mechanism of inter-state and inter-regional collaboration contributing to peace and stability in the region. Using railways, highways and oil-gas-pipelines, strategic row materials like oil, gas, coal, cotton and non-ferrous metals will be conveyed across Georgia from central Asia and

Azerbaijan to other countries. According to current estimates the reserves of oil in the Caspian Sea area appear to be twice more than the earlier estimates[1,2]. Therefore the capacity of freightage in the Georgian transport corridor will be increased, big oil and gas reservoirs will be built.

At present the following routes of oil and gas transportation via the territory of Georgia exist: the Baku(Azerbaijan)-Supsa(Georgia) pipeline; the Western Export Pipeline (WEP); the Tengiz deposit (Kazakhstan)-Baku-Batumi(Georgia) railway route (TBB); the Baku-Poti(Georgia) railway route (BaP); Baku-Kulevi(Georgia) railway route(BK); the Vladikavkaz (Russia)-Erevan(Armenia) (VE) gas pipeline; the Baku-Tbilisi(Georgia) –Ceyhan(Turkey) oil pipeline (BTC, will transport up to 50 million tons of fresh oil from an expanded Sangachal terminal near Baku through Georgia to Turkey[1-3]. Also a new pipeline system - the South Caucasus pipeline (SCP) - is under construction and will convey 7.3 billion cubic meters of gas per year from Sangachal to Turkey via Georgia [1-4].

2. Short review of environmental aspects regarding TRACECA on the territory of Georgia

According to the experience of European transit countries the transit of raw materials causes great losses regarding the ecological situation besides the intended political and economical benefits. In addition to ordinary pollution of the environment it is possible that non-ordinary situations like pipeline and railway accidents will arise. As foreign experience with pipelines shows, the main reasons of crashes and spillages (and fires as a consequence) are the destruction of pipes as a result of corrosion, defects of welding and natural phenomena. Also terrorist attacks and sabotage may occur. The probability of crashes for oil pipeline transport rises with the age of the pipelines in service, and with the extent of their network. For example, 250 ruptures, which are accompanied by spillages of the transferred products, occurred every year from 1973 to 1983 in the US pipeline network with a total length of about 250,000 km. In West Europe it has been found that 10–15 leakages happen every year in a pipeline network of around 16,000 km length, resulting in a loss of 0.001% of transferred products[3-4]. Now a short review of environmental conditions on the territory of Georgia is given focusing on the routes of the WEP pipeline, TBB railway and BTC pipeline as examples.

2.1. WESTERN EXPORT PIPELINE ROUTE

From 1991 to 1993 the WEP pipeline was almost destroyed on the territory of Georgia (caused by terrorism and sabotage). Almost all transported oil (pipeline with diameter 580 mm.) was spilled on the ground and into the rivers. From 1998 to 2000 about 80% of the WEP pipeline was restored and 20% was reconstructed all over again[3]. Unfortunately, there were accidents at WEP after the year 2000, too. For instance, recently (28. 09. 2005) there was an accident of the WEP near the village Norio and 25 tons of oil were spilled on the ground and further into the river Norio.

2.2. TENGIZ DEPOSIT-BAKU-BATUMI RAILWAY ROUTE

During one day about 4 oil trains cross the territory of Georgia on the TBB route. Each of them is transporting about 3500 tons of oil. According to official data of the Georgian Railway Department there were 6 big oil train accidents on the territory of Georgia from 1979 to 2000. About 610 tons of the oil were spilled into the Black Sea and rivers. Besides the above cases, there were about 11 smaller accidents spilling about 13 tons of oil into the Black Sea[2-4]. Data on accidents, received from the Georgian Railway Department, allows us to derive some statistical characteristics of the space-time distribution of these phenomena. The frequency of small accidents with losses of 10 tons or less and the frequency of large events with more than 1000 tons are almost equal. The largest probability of crashes is found for middle-size spills between 100-500 tons. The amount of transported oil increased from 1998 (2.5 million ton) till 2004 (5.5 million ton) by a factor of about 2 indicating a considerable growth of risk of accidents on the TBB route[4].

2.3. BAKU-TBILISI-CEYHAN PIPELINE ROUTE

The proposed pipeline route crosses a large number of rivers and ditches. Six major rivers crossings are found along the route on the territory of Georgia. It is necessary to carry out additional protective measures for the places, where the oil-pipeline crosses the rivers. Therefore the BTC pipeline is buried deeper in the ground (3-4 meters instead of nominal 2.2 meters) under the rivers. But the mountain rivers are characterized by frequent floods. Namely, in Georgia there are many cases, where flooded rivers undermine the bridge fundaments and sometimes even destroy the bridges. Eventually, erosion of the soil may take place decreasing the protective

layer of soil to a minimum, damaging the protective coverage of the pipeline by rocks transpoeted by the flooded river. This may finally cause corrosion of pipes and leakage of oil. In addition, one should take into account, that Georgia is placed in a seismically active zone. (Observations of the last 80 years show that 13% of all earthquakes occuring in the Caucasus are destructive). Unfortunately, the largest zones of the seismic activity are observed in the vicinity of the TRACECA and BTC routes[3,4]. Therefore the possibility of oil spills into rivers generated by natural disasters is not negligible.

Ground water along the route is also abundant and generally of high quality. Namely, the central part of the route is characterized by drinking water used as the main source of water supply by the local population. The western part of the route crosses the reservoir of therapeutic water for which the Borjomi springs are famous. Thus, if ecologically protective mechanisms would not be developed and implemented in time, the frequency of crashes and fires generated by them could be high. Therefore it is very important and pressing to develop reliable methods for the assessment, prediction and management of possible environmental impacts. For solving this problem there exist different methods and approaches. Among them the mathematical simulation of environmental processes is a very promising and important way. The investigation and assessment of possible environmental damage along the TRACECA route is one of the most urgent tasks of the present days for environmental research.

3. Formulation of the problem and mathematical model of oil infiltration into soil

3.1. METHODS OF MODELLING

In order to study spilled oil transformation, infiltration and diffraction processes in soils along the Georgian section of TRACECA (with a pretty complicated orography) we investigate the following scenarios:
I) Suppose that a big amount of oil with the mass M is spilled on flat ground. This may happen through accidents at the TBB, BaP and BK railway routs or at the WEP route.
II) Suppose that a big amount of oil with the mass M is spilled on sloping terrain, which is originating from a bank of a river or flat terrain (see Fig. 3.1a).
III) We consider the case when a big amount of oil with the mass M is spilled into a concave structure (see Fig. 3.1b).
IV) As BTC pipeline trenches are excavated to a normal depth of 2,2m. (a minimum depth is 1 m in soil and 9,6 m in rock) we suppose that leaks occur through damage of the pipeline in the ground under high pressure

(see Fig 3.1c). In this case we consider the following types of leakage: a) point source; b) line source; c) area source.
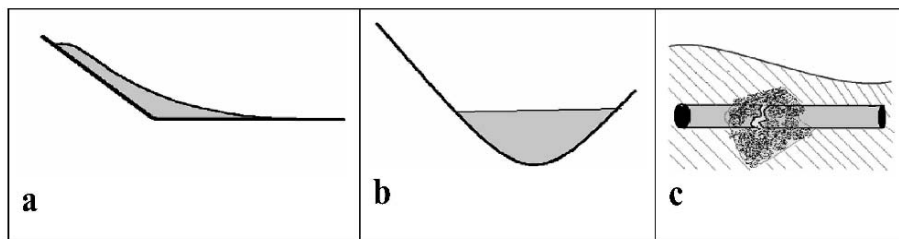
Figure 3.1. Types of spills.

Remark: We have studied the above mentioned variants I) – IV) for different kinds of oil and oil products accounting for different intensities of evaporation of oil in different seasons. The calculations have been performed for four main types of soil.

3.2.   MATHEMATICAL MODEL OF OIL INFILTRATION INTO SOILS WITH FLAT SURFACE

The investigation of water, oil and soil mixtures is a difficult problem. Processes like infiltration of water and oil products, exchange of mass between solutions and the interaction of different phases in soil is controlled by about 40 factors. It is necessary to take into account the composition of soil, and the existence of electrical, magnetic and thermal forces in soils among other features. This makes the design of a mathematical model, which takes into account all processes happening in soil in a realistic way, practically impossible.

As known, soil contains two kinds of pores – capillary and non-capillary ones-which differ with respect to size and ability of oil-water infiltration[5-7]. Capillary pores are able to keep water and oil, whereas non-capillary pores contribute to quick seepage of liquid in soil. As we mainly are interested in the subject of liquid infiltration into soil, we will limit ourselves to the case, when only non-capillary pores exist in the soil. For this case we consider the equation of saturation of soil by a liquid. The process of oil product spreading in soil can be described by the following equation[5-8]:

$$\frac{\partial W}{\partial t} = \frac{\partial}{\partial x}\left(\frac{K(W)}{\gamma}\frac{\partial P}{\partial W}\frac{\partial W}{\partial x}\right) + \frac{\partial}{\partial y}\left(\frac{K(W)}{\gamma}\frac{\partial P}{\partial W}\frac{\partial W}{\partial y}\right)$$
$$+ \frac{\partial}{\partial z}\left(\frac{K(W)}{\gamma}\frac{\partial P}{\partial W}\frac{\partial W}{\partial z}\right) + \frac{\partial K(W)}{\partial z} + Q,$$

(3.2.1)

where W is the relative content of oil in soil, i.e., the ratio of the mass of oil in a volume to the total mass of soil in the same volume ; t is time; axis Ox is directed along the earth surface; axis Oz is directed vertically downward; $K(W)$ is the hydraulic conductivity of oil in soil resulting from Darcy's law; P is pressure and $\gamma = g\rho$ with ρ the density of the liquid and g gravitational acceleration; Q(x,y,z,t) is the normalized source term for infiltrating oil.

Averianov[5,8] has investigated the dependence of $K(W)$ on W, W_0, σ and obtained the following relationship[13]:

$$K(W) = K_1\left(\frac{W - W_0}{\sigma - W_0}\right)^n \cdot \frac{y_W}{y_{oil}},$$

(3.2.2)

where K_1 is the hydraulic conductivity of water in soil when the soil is saturated with water (experiments yield $n = 3.5$); W_0 is the ratio of the mass of water contained in soil to the total mass of soil in the same volume; σ is the porosity of soil; y_W, y_{oil} are the kinematic viscosity of water and oil, respectively. If we denote

$$D(W) = \frac{K(W)}{\gamma}\frac{\partial P}{\partial W},$$

(3.2.3)

where D(W) is the diffusivity of oil, then Eq. (3.2.1) can be rewritten in the following diffusive form:

$$\frac{\partial W}{\partial t} = \frac{\partial}{\partial x}\left(D(W)\frac{\partial W}{\partial x}\right) + \frac{\partial}{\partial y}\left(D(W)\frac{\partial W}{\partial y}\right)$$
$$+ \frac{\partial}{\partial z}\left(D(W)\frac{\partial W}{\partial z}\right) + \frac{\partial K(W)}{\partial z} + Q,$$

(3.2.4)

In the theory of fluids it is anticipated, that pressure is a given function of W. From Eqs. (3.2.1) and (3.2.3) it is evident, that we obtain different representations of Eq. (3.2.4) for different forms of $K(W)$ and $\frac{\partial P}{\partial W}$. There exist some experimental observations which have shown a direct relationship between pressure P and saturation W. Here the relationship between P and W is expressed in the following form according to Averianov8:

$$P = P_0 \left(\frac{W - W_0}{\sigma - W_0} \right)^{m+1}.$$ (3.2.5)

Here P_0 is the pressure of the liquid at full saturation, i.e. when $W = \sigma$, $m \in [-1, +\infty]$.

Taking into account Eq. (3.2.5), Eq. (3.2.3) becomes

$$D(W) = \frac{K(W) \cdot \alpha_1}{\gamma} \left(\frac{W - W_0}{\sigma - W_0} \right)^m,$$ (3.2.6)

where $\alpha_1 = \dfrac{P_0 y_W}{(\sigma - W_0) y_{oil}}$, and, after defining $S = W - W_0$, Eq. (3.2.4) can be rewritten in the following form[9-11]:

$$\frac{\partial S}{\partial t} + K_{11} \frac{\partial S^n}{\partial z} = D_{11} \frac{\partial^2 S^{n+m+1}}{\partial x^2} + D_{11} \frac{\partial^2 S^{n+m+1}}{\partial y^2}$$

$$+ D_{11} \frac{\partial^2 S^{n+m+1}}{\partial z^2} + Q,$$ (3.2.7)

where S is the saturation of the soil by oil and

$$K_{11} = \frac{-K_1}{(\sigma - W_0)^n} \cdot \frac{y_W}{y_{oil}}, \quad D_{11} = \frac{K_1 \alpha_1}{(n + m + 1)\gamma(\sigma - W_0)^m},$$ (3.2.8)

Analysis of equation (3.2.7) will be carried out later. Now we solve the practical problem I described above. Suppose a big amount of oil is spilled into a cavity of cylindrical form with basis Ω_1, height H_0 and volume $V = \Omega_1 * H_0$. We seek the solution of of Eq. (3.2.7) in the rectangular parallelepiped $G = \{0 \le x \le l_1, 0 \le y \le l_2, 0 \le z \le l_3\}$, fulfilling the following condition:

$$H(t) = H_0 - \int_0^t dt \iiint_G S dG, \quad H(t) \ge 0.$$ (3.2.9)

The problem is solved with the following initial conditions:
$S(O, x, y, z) = -W_0$ at $x, y, z \notin \Omega$; $S(O, x, y, z) = \sigma - W_0$ at $x, y, z \in \Omega$, and boundary conditions:
$S(x, y, O, t) = \sigma - W_0$ at $x, y \in \Omega$, $S(x, y, O, t) = -W_0$ at $x, y \notin \Omega$,

$\dfrac{\partial S}{\partial z} = 0$, at $z = l_3$, $\dfrac{\partial S}{\partial x} = 0$, at $x = l; x = 0;$ $\dfrac{\partial S}{\partial y} = 0$, at $y = 0, y = l_2$.

Equation (3.2.7) contains the parameters n and m, the values of which have to be determined before numerically solving Eqs. (3.2.7) - (3.2.9). For simplicity we limit the case to a one-dimensional problem, namely the problem of oil infiltration in the vertical direction. For this case Eqs. (3.2.7) - (3.2.9) can be written in the following form:

$$\frac{\partial S}{\partial t} + K_{11}\frac{\partial S^n}{\partial z} = D_{11}\frac{\partial^2 S^{n+m+1}}{\partial z^2} + Q, \qquad (3.2.10)$$

where K_{11} and D_{11} are determined by Eq. (3.2.8).

For solving Eqs. (3.2.7) - (3.2.9) numerically, we use the difference scheme of Adams-Beshfort (this is a scheme of second order accuracy with respect to time) for time integration of Eq. (3.2.7). For integration in space the Schumann scheme is employed, which also is of second order accuracy[10]. Later we have also used the implicit finite difference scheme for the integration of the multidimensional parabolic equation (3.2.7) with a simple unified algorithm[12].

4. Numerical investigation of oil penetration in soils with flat surfaces along the TRACECA route (numerical experiments and results of calculation)

There are 10 types of soil found along the Georgian section of the TRACECA route. The main types are meadow-alluvial, sandy and sub-sandy (MAS); meadow-marshy (MM); brown-black, peat (BBP); grey-brown salty (GBS).

We have carried out numerical experiments for these four types of soil along the TRACECA route employing the infiltration Eq. (3.2.7). Numerical integration was carried out for $t = 240$ days for the MAS soils, $t = 265$ days for the MM soils, $t = 424$ days for the BBP soils and $t = 270$ days for the GBS soils. Some of the results are presented in Figs. 4.1 and 4.2.
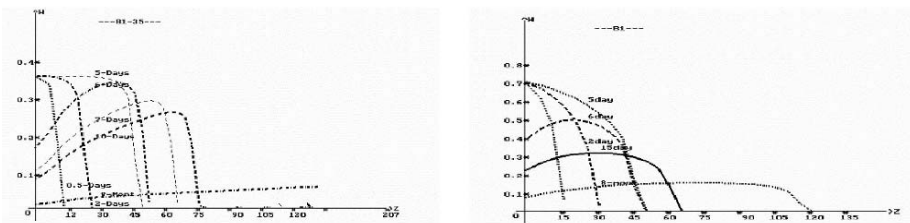
Figure 4.1 (left). Distribution of the concentrations $W(z)$ of oil (vertical axis) at $t=0.5$ 2, 5, 6, 15, and 265 days for meadow-alluvial and sandy soils. Horizontal axis: depth z in m.

Figure 4.2 (right). The same as Fig. 4.1 for meadow-marshy soils.

The numerical calculations show that the process of oil infiltration is qualitatively equal in all considered soils. It is possible to distinguish a

phase of absorption of oil in the soil and a phase of spreading of oil in horizontal and vertical direction[9-13]. In our case the phase of oil absorption lasts about 5 days in all types of soils (with the exception of the grey-brown and salty soils with about 6.3 days). In this time, an oil spillage with 5 cm thickness is fully absorbed by the surface layer of soil. During this phase the oil concentration W (for the meadow-alluvial, sandy and sub-sandy type of soils) is maximal at the soil surface, and it quickly decreases with depth. In the depth of 62 cm W is minimal and the oil distributed over a wider volume. The front of contamination at $t = 0.5, 2, 5$ and 10 days is found at a depth of $9, 27, 48$ and 75 cm, respectively. During the second stage of infiltration the concentration W of oil at the surface gradually decreases (see Fig. 4.1).

Infiltration into brown-black peat soils is most intensive, and the maximal values of concentration at $t = 5$ and 10 days reaches a depth $z = 26$ and 50 cm, respectively. The process of infiltration into the grey-brown and salty soils is the least intensive one. The maximal concentration at $t = 5$ and 10 days reaches a depth of 12 and 21 cm, respectively. The front of oil at $t = 5$ and 10 days is found at 25 and 37 cm depth, respectively. Infiltration into the meadow-alluvial, sandy and sub-sandy soils is qualitatively equal to that in brown-black peat soils, though less intensive (front at $t = 5$ and 10 days at a depth of 153 and 203 cm, respectively; maximal concentration at $t = 5$ and 10 days at a depth of 24 and 45 cm, respectively). The front of oil pollution at $t = 1, 2$ and 5 days reaches a depth of 15, 30 and 48 cm, respectively, and the maximal concentration at $t = 15$ and 265 days is found in a depth of 63 and 120 cm, respectively (see Fig. 4.2).

5. Spreading of spilled oil on sloping terrain (methods of modelling)

The aim is to develop a methodology which allows precise and useful assessment of spreading of oil spilled on sloping or moulded terrain for any kind of occasion. Application to heavy accidents and assessment of risks is intended. For this purpose model runs were performed for the TRACECA route employing the digital relief model of the TRACECA corridor (with average width of 2 km) using the estimated amount of leaked petroleum[1]. In the model the following variables were applied: time of leaking, permeability of soil, evaporation of oil and topography of the route (created by means of the geographic information system). A resolution of 100 m has been used to simulate spreading of petroleum from a leak on sloping terrain[1,3].

After determining the lowest spot towards which the leaked petroleum is flowing, the mass petroleum is calculated which is reduced by the petroleum taken up by the soil at the extent admitted by its conductivity and through evaporation. After adopting the amount of spilled oil the infiltration into the soil is calculated applying Eqs. (3.2.7) - (3.2.9) with the assumption that the thickness of the layer of spilled oil is 0.5 cm. When the cavity is

filled with oil in the model the accumulated amount is calculated (Fig. 3.1b). After reaching the lowest height of the mould rim the oil will continue to flow further down slope (Fig. 3.1a) till it reaches a water surface. The model provides rather conservative results in the sense that it only takes into account the most probable direction of the flow and does not provide estimates of the travel time of the spilled oil to lakes or rivers.

6. Numerical investigation of oil propagation in soils under high pressure

In the presence of high pressure in soils it is necessary to take into account the change of porosity by compression of soil applying the following expression[7,15]:

$$m = m_0 + \beta p (P - P_0) \tag{6.1}$$

where P is pressure, m is porosity of soil under high pressure;, m_0 and P_0 are porosity and pressure, respectively, under normal conditions (i.e., $m_0 = \sigma$, see Eq. 3.2.2). $\beta p = \beta_0 / P$ where β_0 is kept constant. Its value is $\beta_0 = 1.5 * 10^{-5}$. With Eq. (6,1), Eq. (3.2.1) will take the following form:

$$\beta_0 \frac{\partial P}{\partial t} = \frac{\partial}{\partial x} \left(\frac{K(m)}{\mu} \frac{\partial P}{\partial x} \right) + \frac{\partial}{\partial y} \left(\frac{K(m)}{\mu} \frac{\partial P}{\partial y} \right)$$
$$+ \frac{\partial}{\partial z} \left(\frac{K(m)}{\mu} \left(\frac{\partial P}{\partial z} - \rho g \right) \right) - \frac{\partial K(m)}{\partial z} + Q \tag{6.2}$$

Using Eq. (6.2) we have carried out some numerical experiments dealing with problem IV of Section 3 (oil spilled after damage of a pipeline in deeper layers under high pressure; see Fig. 3.1c). Problem IV was simplified by neglecting the presence of a pipe in the soil. We have investigated the following types of leakage of oil under high pressure: a) a point source; b) a line source; c) an area source. For the sake of brevity we are only discussing results of numerical calculations obtained for a point source. The solutions show a complex behaviour. Some of them are presented in Figs. 6.1 and 6.2. As it can be seen in the figures the vertical distribution of oil usually exhibits a single maximum of concentration, but there are also cases where two or several maximal of the concentration are found. In particular, this happens after leaking from the point source has been stopped (see Fig. 6.2).
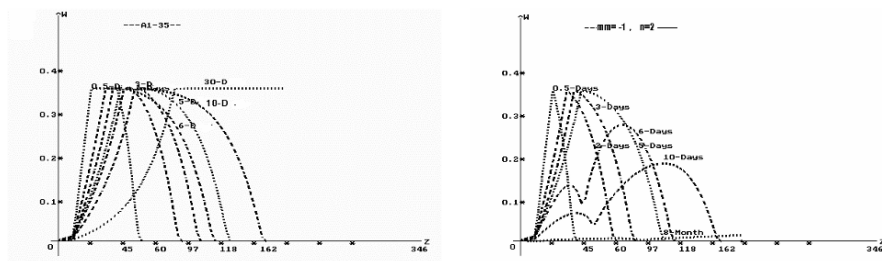
Figure 6.1 (left). Distribution of the concentrations $W(z)$ of oil (vertical axis) at different times (see labels for MAS soils. Horizontal axis: depth z in m, vertical axis W(z).

Figure 6.2 (right). The same as Fig. 6.1 for GBS soils.

The numerical calculations show that the features of oil infiltration into soils under high pressure are qualitatively similar for all considered soils. Absorption of oil in the soil is much more intensive than penetration of oil to deeper layers and lateral spreading. Oil infiltration into BBP soils was found to be most intensive, whereas it was least intensive in GBS soils.

7.   Conclusions

It is evident that environmental problems can arise from oil spillage along the TRACECA route as discussed for the territory of Georgia, in particular. Numerical calculations of oil penetration into soils in flat and sloping terrain were investigated and selected results are presented in this paper**.** Furthermore, numerical calculations of oil propagation in soil under high pressure have been investigated and discussed.

References

1.   Environmental and Social Impact Assessment Baku-Tbilisi-Ceyhan, Georgia, Non-technical Executive Summary, April 2002.
2.   Investigation of Ecological Safety for the pump station PS-15 of Baku-Supsa Pipeline Rout, Report of Hydrometeorological Institute of Georgian Academy of Sciences with GPC-Georgian Pipeline Company, Tbilisi, 2002.
3.   EIA for the Western Route Export Pipeline, RSK, 1996.
4.   Report on Preliminary Estimation of the Oil and Oil-Products Impact on the Environment in the Region of the River Khobi's Outfall. Zenith Gamma Consultory, Vol. 1 and 2, Tbilisi, 2001.
5.   P. Polubarinova-Kochina, *Theory of Flow of Ground Water.* (Nauka, Moscow, 1977).

6. K. Aziz and A. Settarri, *Mathematical Modelling of Plast Layer Systems*(Nedra, Moscow, 1982).
7. H. P. Leibenson, *A Manual on OilField Mechanics*, *Part 2* (Novost, 1934).
8. S. Averianov, Dependence of Water Permeability of Soil from the Air Maintenance in the Soil, Reports of AS pf USSR. 69, No. 2, pp. 141–144.
9. T. Davitashvili, Numerical and Theoretical Investigation of Spreading Oil Filtration in Soils for the Caucasus Region, Geography and Natural Resources, Novosibirsk, Russia, 2004, pp. 215–226.
10. D. Gordeziani, T. Davitashvili and Z. Khvedelidze, On the mathematical model of the Georgian transport corridor pollution,*Bulletin of the Georgian Academy of Sciences*, *Vol. 162, No. 1,* 73–76 (2000).
11. T. Davitashvili, A. Khantadze and I. Samkharadze, Environmental And Social–Economical Baseline Of The Georgian Section Of The Baku-Tbilisi-Ceyhan Pipeline, Proceedings of the Odlar Yurdu University, 2004, Baku, Azerbaijan, pp. 110–119.
12. T. Davitashvili, N. Dikhaminjia, G. Gunava and O. Komurjishvili, Polutants transfer in environment with one new three-dimensional numerical scheme, *Reports of the Seminar of the I. Vekua Institute of Applied Mathematics, Vol. 28,* 25–30 (2002).
13. A. Surmava, Numerical investigation of the spreading of spilling oil and oil-products along a territorial strip of the Poti-Kulevi Railvay. *Reports of VIAM, Vol. 17, No. 3*, 123–130 (2002).
14. A. Khantadze and T. Davitashvili, On the non-linear theory of oil filtration in soils, Proceedings of the Odlar Yurdu University, 2004, Baku, Azerbaijan, pp. 70–73.
15. V. Georgievskii, Unified *Algorithms for Determination of Parameters of Filtration* (Kiev, 1971).

MODELLING OF DAM-BREAK SEDIMENT FLOWS

JOSE MATOS SILVA

CEHIDRO, Instituto Superior Tecnico, 1049-001 Lisbon, Portugal, email: jmsilva@civil.ist.utl.pt

Abstract. Dam-break sediment flow is an especially rapid unsteady flow, important in terms of risk assessment, mainly observed in flow-type landslides and dam breaks. The paper presents MUDEP, a computational model under development in IST, Lisbon, Portugal, to model such flows, using the l-D explicit differential TVD MacCormack scheme to solve the adapted St-Venant equations. The function calculating the friction slope varies according to the rheological model. In order to verify the results, experiments were performed in a tilting flume, using a highly viscous oil to simulate the expected laminar behaviour of such flows. The fluid was suddenly released down a slope by the removal of a gate. The comparisons of the computational and experimental results demonstrate the validity of the developed model.

Keywords: fluvial processes; sediment flow; dam break; St-Venant equations; TVD MacCormack method; MUDEP

1. Introduction

Most studies on flood propagation have been purely hydraulic in character. Real problems, however, are seldom so. Actually, flows can be grouped into three types: 1) *Clear Water* - to be analysed with the classical hydraulic methods, based on the governing equations, first developed by St-Venant in 1871. 2) *Water with sediment* - to be analysed by the traditional two-phase flow model (St-Venant-Exner equations). For closure, two additional equations are required (e.g., Vanoni, 1977). 3) *Sediment flow* - the sediment

and water mixture forms a pseudo-one-phase fluid, and sediment can no longer be considered as material carried by the water.

The purpose of this research was to model dam-break sediment flows.

2. Physical observations

2.1. DAM BREAK AND SEDIMENTS

There is an increasing awareness in engineering practice of the need to predict magnitude, shape, duration and impacts of the outflow hydrograph resulting from dam failures. As part of the risk analysis, those predictions are currently produced via modelling of the dam-break flood wave propagation through the river valley.

According to their sediment production source, dam-break sediment flows may be classified into three categories: *Reservoir Sediment*, *Dam Material*, and *Downstream Bed*.

When a dam fails, the *bottom sediment of the reservoir* tends to be carried away downstream by the corresponding wavy flow. The characteristics of this flow will depend on the characteristics of that sediment, which, in turn, are related to the supply conditions of sediment in the watershed.

In the cases of instantaneous natural dam failure, that mainly occur with concrete dams, the resulting sediment flow has comparatively short duration and it is strongly attenuated as it runs down the stream valley. In the case of an earthfill dam, a huge debris flow may occur due to either: 1) instantaneous release of dammed up water behind the deposit, or 2) piping of seepage water through the dam. These processes can be classified into three types (Takahashi, 1991): a) overtopping, b) abrupt sliding collapse, and c) progressive failure.

Fluvial processes associated with dam-break flows are usually characterized by great and rapid processes of aggradation or degradation of the *downstream bed*. The morphological change of the river pattern during the passage of such a flood can be significant, and it affects the sediment transport in turn.

2.2. SEDIMENT TRANSPORT PROCESSES

To maintain the movement of solid grains in the flow, a force is needed to balance their submerged weight and prevent them from depositing. According to origins of these forces, solid particles carried by a flow can be classified as *bed load*, *suspended load* and *neutrally buoyant load*. They may occur independently or simultaneously.

The flow is considered *hyperconcentrated* when the sediment concentration is very high, so that sediment and water mixture forms together a pseudo-one-phase fluid. *Debris flow* differs from an ordinary hyperconcentrated flow mainly in its catastrophic nature and high competency in carrying solid material. *Mudflows* are the more fluid forms of mass movements.

2.3. RHEOLOGICAL PROPERTIES OF SEDIMENT FLOWS

Water with low concentration of sediment remains Newtonian fluid, but the viscosity increases with increasing concentration. This may lead to a laminar flow. As sediment concentration exceeds a certain value, the water-sediment mixture behaves no longer as a Newtonian fluid. The critical concentration varies with mineral composition of the sediment and water quality.

The rheograms of some typical time-independent fluids (or fluids without memory effect) are plotted in Figure 2.1. The general rheologic equation is

$$\tau = \tau_B + K(\frac{du}{dy})^m \tag{2.1}$$

(du/dy) is the shear rate of the moving fluid, K is the coefficient of consistency or rigidity and *m* the plastic index.

1 Pseudoplastic (m<1)
2 Newtonian (m=1, K=μ, τ_B=0)
3 Dilatant (m>1)
4 Bingham (m=1, K=μ, τ_B=Bingham yield stress)
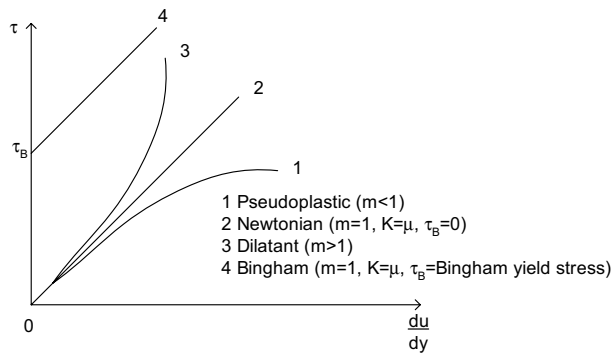
Figure 2.1. Some typical rheograms.

3.   Numerical modeling of dam-break sediment flows

3.1. UNSTEADY FLOW GOVERNING EQUATIONS

The one-dimensional St-Venant equations for a rectangular section, obtained by derivation of the continuity and the dynamic equations are:

$$\frac{\partial h}{\partial t} + \frac{\partial (Uh)}{\partial x} = 0 \tag{3.1}$$

$$\frac{\partial (hU)}{\partial t} + \frac{\partial (hU^2)}{\partial x} + gh\frac{\partial h}{\partial x} = gh(S_0 - S_f) \tag{3.2}$$

in which U is the mean velocity, h the flow height, S_0 the channel bed slope, S_f the friction slope, t the time, and x the distance.

The following assumptions were made: 1) the flow is one-dimensional (1-D), 2) S_o is small, 3) the pressure distribution is hydrostatic, 4) the channel is straight, 5) the hydraulic variables are continuous and derivable, 6) the bed and the banks are fixed and impermeable, 7) the liquid is incompressible and homogeneous (one-phase flow), and 8) the friction losses for a transient-state may be computed using formulas for steady-state flow.

Expanding the differential terms, rearranging the continuity equation and dividing by h, Eq. (3.2) yields:

$$\frac{\partial U}{\partial t} + U\frac{\partial U}{\partial x} + g\frac{\partial h}{\partial x} = g(S_0 - S_f) \tag{3.3}$$

Bragard (1997) derived different expressions for the friction slope, S_f, in Eq. (3.3), considering several rheological models [respectively, Highly viscous, Turbulent, Dilatant, Bingham, General Quadratic model (O'Brien and Julien, 1993), and Generalised Viscoplastic Fluid (GVF) model (Chen, 1988)].

3.2. THE MAC-CORMACK RESOLUTION SCHEME

3.2.1. *Introduction*

The developed model (Bragard, 1997) uses the explicit-MacCormack scheme (Chaudry and Hussaini, 1983) for the numerical integration of the St-Venant hyperbolic equations system. This method has the advantage of reducing the effects of numerical diffusion usually present in first-order schemes, reproducing better the shock waves with steep fronts, and it is more efficient regarding computational costs than first-order schemes or finite element methods for 1-D problems.

The MacCormack resolution scheme is a second-order finite explicit difference method, in time and space, consisting in the calculation sequence of two predictor-corrector steps in the time interval Δt. In each of the predictor-corrector steps, one-sided finite difference approximations are used. Depending upon the way these difference approximations are used, two alternatives are possible: 1) forward predictor and backward corrector approximation, 2) backward predictor and forward corrector approximation. Herein, these alternatives were used in sequence, i.e., the first alternative at one time step, the second alternative in the next time step, and so on.

The St-Venant equations can be written in the conservative-law form:

$$\frac{\partial F}{\partial t} + \frac{\partial G(F)}{\partial x} = S(F) \tag{3.4}$$

The assumptions made for the derivation of the St-Venant equations fail in the proximity of the wave-front. But, these equations, written in the conservative form (Chaudry, 1987), permit the simulation of shock waves without the need of additional equations. F, $G(F)$ and $S(F)$ are two-component vectors:

$$F = \begin{pmatrix} h \\ hU \end{pmatrix}, \ G(F) = \begin{pmatrix} hU \\ \beta hU^2 + (1/2)gh^2 \end{pmatrix}, \ S(F) = \begin{pmatrix} 0 \\ gh(S_0 - S_f) \end{pmatrix} \tag{3.5}$$

In this form, F corresponds to the local variation, G to the flux through the boundaries of the calculation grid, and S to the perturbation source.

3.2.2. *Initial Conditions*

It is assumed that, at time $t=0-$ (until gate removal), the fluid behind the dam is still and the downstream bed is dry (Figure 3.1). The depth before breakage is given by

$$h(x,0) = \begin{cases} \dfrac{h_{dam}}{(x_D - x_{FE})}(x - x_{FE}) & \text{for} \quad x < x_D \\[4mm] 0 & \text{for} \quad x > x_D \end{cases} \tag{3.6}$$

where x_D is the abscissa of the dam section, x_{FE} the abscissa of the fictitious reservoir end[*], and the velocity is (Figure 3.1):

---

[*] the actual experimental flume under study has not a reservoir long enough to present a real reservoir end, except for $S_o=0.1$ and above.
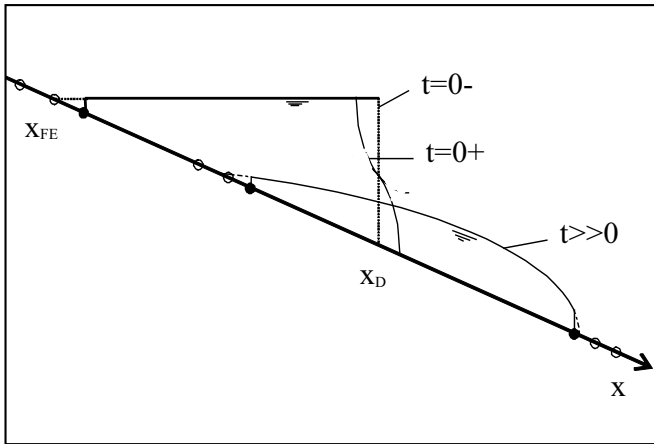
Figure 3.1. Sketch of the initial conditions and the considered grid nodes.

$$U(x,0) = 0 \qquad (3.7)$$

At time *t=0*, the vertical flat gate is removed instantaneously. The discontinuity in the water depth is overcome by assuming Ritter solution (Franco, 1996) for the first time step of flow initiation:

$$\begin{cases} h(x_D,0) = \dfrac{4}{9} h_{dam} \\[4mm] U(x_D,0) = \dfrac{2}{3}\sqrt{gh_{dam}} \end{cases} \qquad (3.8)$$

3.2.3. *Boundary Conditions*

This model does not need any downstream boundary condition since it is a wave front progressing on a dry bed, once the flow reaches the end of the flume, the simulation stops. On the other hand, depending on the flume slope, the mixture retained before the dam-break simulation, can be or not be in contact with the upstream wall (Figure 3.2).

upstream boundary condition needed   no boundary condition needed
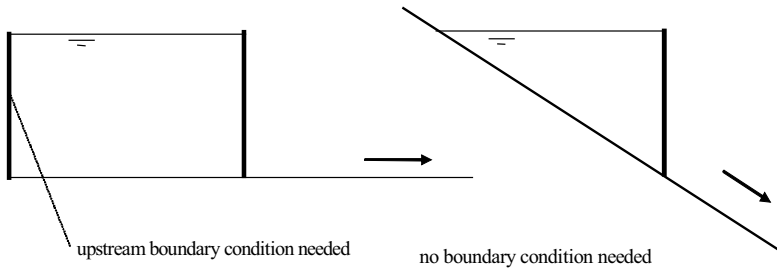
Figure 3.2. Definition of the upstream boundary conditions.

3.2.4. *Stability and Convergence*

MacCormack explicit scheme insures stability if and only if the time interval Δt verifies the Courant-Friedrichs-Lewys' (CFL) criterion, established by the three authors in 1928:

$$\Delta t = C \frac{\Delta x}{\max\left(\sqrt{gh} + |U|\right)} \tag{3.9}$$

where, necessarily, the *Courant number*, $C \leq 1$. The best results in the numerical experiments were obtained for a value of $C = 0.8$.

In order to suppress oscillations and computational difficulties due to very small or even negative depths at the boundaries of the flow field (wave-front and wave-tail), computed depths are accepted if they are larger than a minimum value, of the order of $0.01\ h_{dam}$; otherwise, they are set equal to zero. It is also understood that when the height $h = 0$, the velocity $U = 0$.

The space grid Δx is chosen arbitrarily, but some comparison has to be done in order to determine its influence. It has been shown that very little effect is noticed on the main part of the profile, while the diminution of Δx in the front wave region makes the profile smoother and the front steeper.

For the purpose of facilitating computational effort, the computational field at any given moment is considered to include two more grid nodes, with zero depth flow, on each side of the actual flow field (see Figure 3.1).

3.2.5. *Flood Propagation on Dry Areas*

In order to avoid divergence, the method presented by Aguirre et al., (1994) is used: 1) at the wave front (two first nodes), only the friction slope due to bed roughness is considered. If the height is smaller than a tolerance, it is

set equal to zero; 2) Inside the flow, if depths are smaller than this tolerance, they are set equal to the tolerance. Besides: 3) if the depth is smaller than a certain value, it is set equal to zero; 4) if a negative velocity appears at the wave front, it is set equal to zero.

3.3. TVD SCHEME

The nonlinearity of the governing St-Venant equations may give rise, in their numerical solution, to the possibility of discontinuous unrealistic solutions. For some methods, it is possible to demonstrate that the total variation of the solution does not grow with the simulation in time. These methods are called "Total Variation Diminishing Methods" (TVD) and have characteristics of High-Resolution Methods. The TVD method used in this model (Garcia-Navarro et al., 1993) assumes an equivalence between the MacCormack and the Lax-Wendroff resolution schemes (in fact, this is guaranteed only for linear equations). Some ameliorated techniques are now used (Franco, 1996).

3.4. PROGRAM MUDEP

The developed numerical model (Bragard, 1997), *MUDEP*, was performed for Manning-Strickler's coefficient*, n = 0.02*, and kinematic viscosity, $v = 0.0008 \ m^2 \ s^{-1}$. The following values were used in the computational discretization: $\Delta x = 0.04 \ m$, *C = 0.8*, and *height tolerance = 0.001 h_{dam}*.

4.   Experimental verification

4.1. EXPERIMENTAL FACILITY, MATERIALS AND EXPERIMENTS

A *perspex* flume 8.0 m long, 0.1 m wide and 0.2 m high was built in Instituto Superior Técnico, Portugal, with slope varying from 0 to 10%. At a distance of 2.0 m from the upstream end of the flume, the channel can be closed by a gate to simulate the dam. The measurements were done using a video camera, with 12 pictures per second. Along the flume transparent walls, rulers marks were placed every 10 cm. The filmed experiments permit to distinguish depth differences of 2 mm. Video recording by following the flow was used for determination of the wave front propagation.

    First, fifteen water experiments were performed to calibrate the model. Then, thirty oil experiments were performed, with initial height 0.195 m and 0.11 m, and bed slopes of 0.02% and 0.08%. In order to respect the laminar nature of these experiments, a highly viscous mineral oil

(ν = 0.0008 m^{2}s^{-1}, at 20ºC) was used. Laminar regimen was observed throughout all the experiments. Experiments proved the validity of the 1-D approximation of the flow.

A peculiar phenomenon occurred at higher velocities. Some oil drops, with order of magnitude of 1 cm in diameter, are pushed violently further away from the wave front. They "slide" ahead with a higher velocity then decelerate until they are caught up by the wave front. No conclusion was reached yet for this phenomenon, that also occurs in nature.

4.2. EXPERIMENTAL VERSUS NUMERICAL RESULTS

The following comparisons were done: 1) the variation in a fixed section (*punctual evolution*); 2) the overall shape of the flow over the entire flume (*shape evolution*[†]); 3) the *wave front propagation*.

Figure 4.1 shows the *punctual evolution*, for the initial conditions: S_0 = 0.08, h$_{dam}$ = 0.11 m. Figure 4.2 shows the *shape evolution*, for the same initial conditions (Bragard, 1997).

Water experiments confirm the validity of the developed model, *MUDEP*. The time lag between experiment and numerical modelling for the wave front can be decreased by adjusting Manning's friction coefficient.
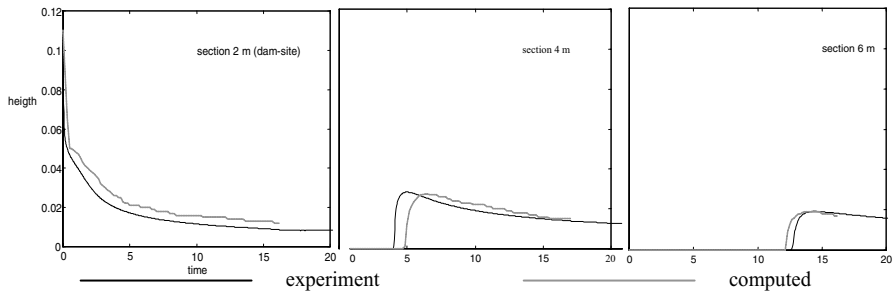
Figure 4.1. Height as a function of time at several sections.

[†] Note that the bed is shown horizontally in these graphs, in order to improve visual resolution; since the x- and y-axis scales are different, curvature is not conserved.

Oil experiments demonstrated that the implemented scheme seems adequate to treat such laminar behaviour. The agreement between numerical model and experiment improves for decreasing heights. Initially, the computation overestimates the wave-front velocity but, finally, it tends to underestimate it.
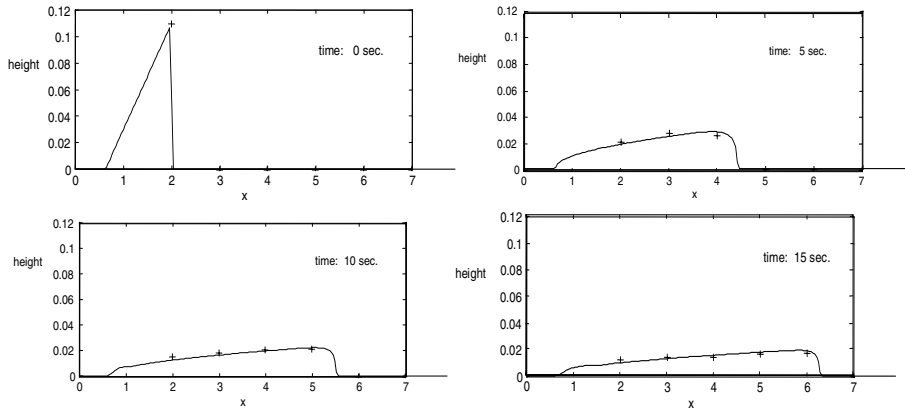
Figure 4.2. Height as a function of distance at several instants.

References

Aguirre-Pe, J. et al., 1994, Modelo numérico unidimensional de una onda viscosa en un canal de alta pendiente", *Solución de problemas en Ingeniería con Métodos Numéricos*, M. Cerrolaza y A. Guillen (Editores), p. MF1-MF10.

Bragard, C. 1997, *Modelling of Dam-Break Flows with High Concentrations of Sediments*, Final Project in Civil Engineering, IST, Lisbon, Portugal, and Université Catholique de Louvain-la-Neuve, Belgium.

Chaudry, M.H., 1987, Transient flows in open channels, *Applied hydraulic transients*, 2nd ed., Von Nostrand Reinhold Company, 382–414.

Chaudry, M.H. and Hussaini, M.Y., 1983, Second-order explicit finite-difference methods for transient-flow analysis, *Journal of Fluids Engineering*, **107**: 523–529.

Chen, C.I., 1988a, Generalized viscoplastic modeling of debris flow, *ASCE Journal of Hydraulic Engineering*, **114**(3): 237–258.

Chen, C.I., 1988b, Generalized viscoplastic modeling of debris flow, *ASCE Journal of Hydraulic Engineering*, **114**(3): 259–282.

Franco, A.B., 1996, Modelação computacional e experimental de escoamentos provocados por roturas de barragens, *Tese de Doutoramento em Engenharia Civil*, IST, UTL.

O'Brien, J.S. and Julien, P.Y., 1993, Two-dimensional water flood and mudflow simulation, *J. of Hydraulic Engineering*, ASCE, **119**(2): 244–261.
Takahashi, T., 1991, *Debris Flow*, IAHR Monograph Series, Balkema, Rotterdam.
Vanoni, V.A., 1977, "Sediment Engineering", *ASCE Manuals and Reports on Engineering Practice*.

IDENTIFYING CHANGES IN SOIL QUALITY: CONTAMINATION AND ORGANIC MATTER DECLINE

PAT H. BELLAMY*, R.J.A. JONES
*National Soil Resources Institute,Cranfield University,
Silsoe,Bedfordshire MK45 4DT*

Abstract. Soil is increasingly affected by applied agrochemicals, atmospheric pollutants, sewage sludge, and manures which can have adverse impacts on soil quality. The European Commission has embarked recently on a Thematic Strategy for Soil Protection that identifies eight threats to soil in Europe of which contamination and decline in organic matter are accorded high priority. To identify changes in soil quality it is important to have some baseline against which to measure that change. In the UK, a National Soil Inventory was made to provide an unbiased inventory of soil resources in Great Britain. Soil samples were taken on a national UTM grid and analysed for a range of physical and chemical properties. About 40% of the grid points in England and Wales were resampled providing an ideal data set from which to identify changes in soil properties, an essential requirement for 'monitoring'. Geostatistics have been used to estimate the temporal change in several metal concentrations and in soil organic carbon (OC), the major constituent of soil organic matter. In almost all cases, a normally distributed random variable with outliers is shown to be a suitable statistical model to study the change in metal concentrations. A map of change in lead concentration, identifying 'hotspots', shows how these methodologies can be applied. It is also shown that the variation of the change in organic carbon is not spatially structured but that the rate of change depends on the initial OC level in the soil. Very large estimates of OC decline over a 15 year period were revealed and this decline has serious implications for carbon sequestration and climate

––––––––
   *To whom correspondence should be addressed. P.H. Bellamy, National Soil Resources Institute,Cranfield University, Silsoe, Bedfordshire MK45 4DT; e-mail: p.bellamy@Cranfield.ac.uk

change. The geostatistical procedures used in this study have wide applicability across Europe.

Keywords: Organic Carbon; Soil; Quality; Heavy Metals; Contamination; Geostatistics

1.   Introduction

Soils may be characterized in terms of the properties they inherit from the underlying rock (the parent material) and the properties resulting from alteration of the original parent material by soil forming 'pedogenic' processes namely climate, vegetation, time and human activity. Pedogenic processes operate mainly in the surface and subsurface horizons normally found in the upper 2m. Human activities are increasingly contaminating soil and ground water through applied agrochemicals, deposition of atmospheric pollutants, spreading of sewage sludge and manures and these can have adverse impacts on the ability of soil to perform its vital functions (Blum, 1993).

The industrial revolution in Great Britain transformed human life in the 18th and 19th centuries resulting in higher levels of soil contamination than in other parts of Europe, which were only industrialized in the early 20th century. This contamination, particularly by heavy metals, has been exacerbated by the high population density associated with the development of heavy industries based on coal. Following the unprecedented expansion and intensification of agriculture during the 20th century, there is clear evidence of a consequent decline in the organic carbon (OC) contents in many soils. This decline in OC contents has important implications for agricultural production systems, as well as ecosystems, because OC is a major component of soil organic matter.

Recently the European Commission issued an official Soil Communication (EC, 2002) 'Towards a Thematic Strategy for Soil Protection' identifying eight threats to soil quality in Europe of which contamination and decline in organic matter are accorded high priority. Detecting change in soil properties *reliably* is a significant technical challenge since relatively small changes, which might nevertheless be important in themselves or as precursors of greater change, must be measured against a background of considerable spatial uncertainty as well as analytical variability.

2.   Data sources

To identify changes in soil quality it is important to have some baseline against which to measure that change. This requires a detailed inventory.

2.1. NATIONAL SOIL INVENTORY

A National Soil Inventory (NSI) was set up 25 years ago to provide an unbiased inventory of soil resources in Great Britain. Soil samples were taken at the 5km intersections of a national UTM grid across the whole of England and Wales, and at 10km intervals on the same grid in Scotland, and these samples were analyzed for a range of physical and chemical properties including organic carbon and a range of heavy metals (McGrath and Loveland, 1992). Between 1995 and 2003, a proportion (about 40%) of the sites in England and Wales were resampled providing an ideal dataset from which to identify changes in soil properties.

The agricultural soils, resampled 1995-6, were analyzed for the same soil properties as the original samples. The non-agricultural samples were analyzed for pH and organic carbon only. The data from the agricultural soils consisted of 1624 points resampled from an original 4157 points. These data were used to identify hotspots of change in metal contamination. The data for the whole of England and Wales, which consisted of 2179 points resampled from the original 5662, were used to investigate the change in organic carbon over the period 1978-2003.

3. Methodology

3.1. ROBUST STATISTICS

Change variables, the difference in soil properties from one time to another, seem to contain a significant number of outliers. These can have a marked effect on statistics such as the standard deviation or the coefficient of skew. In the latter case the fact that data values are cubed to generate the statistic makes the coefficient of skew adversely affected by rogue values. This is a serious problem. If the data are drawn from a markedly non-Gaussian distribution then we would usually transform them, but we do not want to transform our data because of the disproportionate effects of a few outliers. For this reason we made use of some robust statistics that are designed to be as resistant as possible to unusual values.

The following robust statistics were used:

Median. A robust location estimator

A robust estimator of the standard deviation. Rousseeuw and Croux (1992, 1993) proposed Q_n, an *L*-estimator, so called because it is based on linear combinations of the order statistics of the *n* data $X_1, X_2, \ldots X_n$.

A robust measure of skew. The octile skew (*OS*), recommended by Brys et al., (2004), as being robust to outliers and of reasonable efficiency, was

used. A value of *OS* greater than 0.2 suggests that the underlying data are not symmetrically distributed (c.f. conventional skew greater than 1).

A significant number of outliers will also effect the estimation of spatial statistics such as the variogram. The conventional standard estimator due to Matheron and three estimators which are resistant to outliers: those due to Cressie and Hawkins, Dowd and Genton (Lark, 2000), were used to describe the spatial structure in the change variables. These models were then tested by cross-validation whereby each datum is estimated from the others by kriging. This provides an estimate at location x_j where we know the true value $z(x_i)$. It also provides an estimate of the variance of the kriging error, $\sigma_K^2(x_i)$ the kriging variance.

We define $\theta(x_i)$ as the ratio of the squared estimation error at site x_i to the kriging variance at this site:

$$\theta(x_i) = \frac{\left\{z(x_i) - \hat{Z}(x_i)\right\}^2}{\sigma_K^2(x_i)} \tag{1}$$

The median of $\theta(x_i)$ over all sites, $\widetilde{\theta}$,was used as a cross validation statistic, Lark (2000). This statistic only assumes normality of the kriging errors where these are unaffected by outliers, and that fewer than half of the errors are so affected – the breakdown point of the median. Under these assumptions $E[\widetilde{\theta}] = 0.455$ if the kriging variance is unbiased.

3.1.1. *Detecting outlying values*

If the variogram analysis and cross-validation support the hypothesis that the change variables are contaminated normal random variables, the spatial characteristics of the contaminating process might be important both for understanding the mechanisms which generate it and implications for sampling. Note that we use the term 'contaminating' in a statistical sense. Processes of diffuse soil pollution may be represented by the normal process estimated by the robust statistical tools.

Lark (2002) presented a method for identifying outliers from data which conform to a contaminated normal model and defined a test statistic O(x), which is a standard normal variable of mean zero under a null hypothesis that the datum $z(x_i)$ belongs to the underlying normal process and not the contaminating process.

3.1.2. *Disjunctive kriging*

Disjunctive kriging (DK) is a non-linear kriging technique. It is based on an initial transformation of the data using Hermite polynomials, to obtain a

normally distributed variable. The output of the DK includes local estimates of the original variable and estimates of the conditional probability (conditioned on the data) that the true value at a particular site falls below some threshold. Details of the method are provided by Webster and Oliver (1989), Lark and Ferguson (2004).
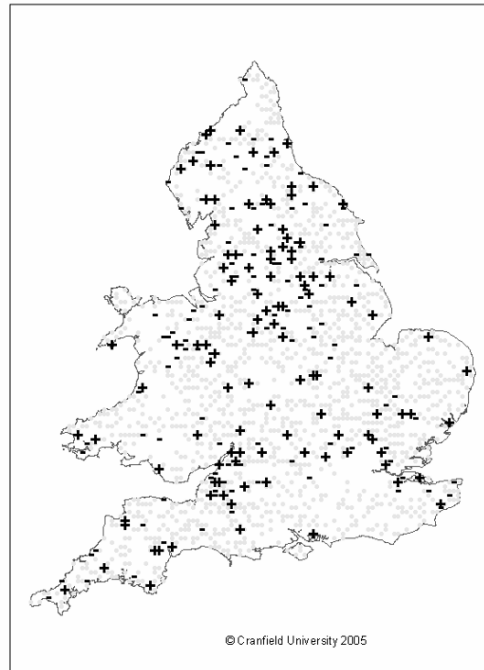
Figure 1. O(x) statistic for cross-validated changes in Lead. '+' symbols indicate the increase in Pb at the resampling date appears to be a distinct process from the robustly modelled background (grey). '−' symbols indicate a reduction in Pb which appears distinctive.

3.2. T ALTERNATIVE METHODOLOGY

Investigation of the change in organic carbon in the soil identified that an alternative to the methodology already outlined was required. It was found that the baseline carbon content may be a good predictor of carbon loss. A random subsample of the data was selected and a linear regression fitted, specifying an exponential variogram for the residuals using REML, see Bellamy et al. (2005).

4.   Results and discussion

4.1.   CHANGE IN METAL CONTAMINATION

The spatial variation identified in the study of the baseline data (Scholz et al., 1999) was attributable, at least in part, to coarse-scale factors such as geology which are stable over time. The spatial variability of the change in a soil variable over time will not necessarily be attributable to these coarse scale factors and could be completely different.

Looking at the changes in lead, nickel and copper, the distributions were more symmetric than was implied by the conventional statistics. The values of $\tilde{\theta}$ for cross-validations with variograms based on Matheron's estimator were all substantially smaller than the lower bound of the confidence interval so we could be confident that this estimator was over-estimating the variogram. This means that it is important to use robust methods for estimating the variogram as the effects of outliers will cause the conventional methods to underestimate the spatial dependence in the data.

The variogram analysis and cross-validation support the hypothesis that for lead nickel and copper the change variables are contaminated normal random variables. Hot spots were identified for lead (as an example) using the methodology described above. Figure 1 shows the $O(x)$ statistics obtained for the lead data, '+' symbols represent upper-tail outliers (a more positive change in the variable than expected), '−' symbols represent data where the change appears to be a lower-tail outlier (a more negative change than expected). The threshold used to define these categories is the 99% confidence limit of the standard normal distribution. For lead, nickel and copper, between 4% and 14% of the data were classed as outliers by this criterion. In most cases the upper- and lower-tail outliers were of similar frequency.

The mean distance between a sampled (upper-tail) outlier and its nearest neighbouring upper-tail outlier $\bar{\omega}$, was calculated for each variable (see Table 1).

TABLE 1.

Variable $\bar{\omega}$ /metres x 10^3	
Lead	20.9
Nickel	21.2
Copper	22.6

Confidence limits were computed for this statistic under a null hypothesis that the outliers are distributed entirely at random in space. In no case was there evidence to reject this null hypothesis. This is, however, a global test and should not be regarded as grounds for not looking further at what appear to be local clusters in the distribution of outliers.

4.2. CHANGE IN ORGANIC CARBON CONTENT

Exploratory analysis of the NSI data for the whole of England and Wales showed 6% of resampled sites had extreme values of change in organic carbon. No reason was found to believe that these outlier values reflect artefacts, so it was decided to analyse them using disjunctive kriging. The variogram estimates (see Figure 2) showed that there was little spatial structure in the change in organic carbon. This encouraged us to investigate alternative methods of estimating the organic carbon at those sites not resampled.
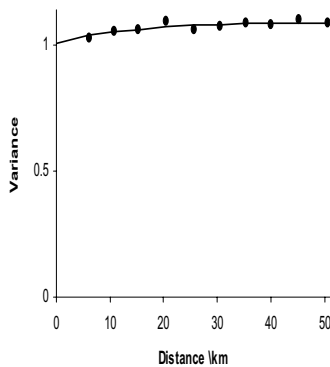
Figure 2. Estimated variogram of transformed normalized change in OC.

As stated in section 3.2, a relationship between the rate of change of organic carbon and the original level of organic carbon was identified. Using the methodology described, the variogram of the error term was shown to have a very weak spatial dependence. Given that the spatially structured variance was very small, the benefits of kriging the residuals and adding them to the regression predictions would also have been very small. So the estimation of the organic carbon at the sites that were not resampled was made directly from the equation relating the rate of change of organic carbon to the original organic carbon content (Bellamy et al., 2005).

5. Conclusions

It is important to use robust statistics for analysis of change variables as the effects of outliers cause the conventional methods to under-estimate the spatial dependence in the data. Cross-validation using robust variograms suggested that in almost all cases a normally distributed random variable with outliers is a suitable statistical model of the change variable. It is apparent that levels of metal concentration are higher in England and Wales than in other European countries for which data are available (Utermann et al., unpub). This is mainly due to the variety of parent materials and the early industrial revolution in Great Britain. It is important therefore to study the spatial structure in the change variables before decisions on long term monitoring schemes can be made.

For organic carbon change, the contaminated normal model was not appropriate and an alternative methodology has been suggested based on a relationship in the data. This analysis gave very large estimates of decline in organic carbon which occurred across the country and across land uses (Bellamy et al., 2005). There is no reason to suggest that this decline in organic carbon has not occurred across all temperate regions and has serious implications in terms of climate change and carbon sequestration. The geostatistical procedures used in these studies have wide applicability to soil monitoring across Europe.

Acknowledgments

References

Bellamy, P.H., Loveland, P.J., Bradley, R.I, Lark, R.M., and Kirk, G.J.D., 2005, Carbon losses from all soils across England and Wales. *Nature* **437**: 245–248.

Blum W.E.H., 1993, Soil Protection Concept of the Council of Europe and Integrated Soil Research. In Soil and Environment Vol. 1, H.J.P. Eijsackers and T. Hamers, eds., Integrated Soil and Sediment Research: A basis for Proper Protection. Dordrecht: Kluwer Academic Publishers, pp. 37– 47.

Brys, G., Hubert, M., and Struyf, A., 2004, A robust measure of skewness *Journal of Computational and Graphical Statistics* **13** (4): 996–1017.

EC, 2002, Communication of 16 April 2002 from the Commission to the Council, the European Parliament, the Economic and Social Committee and the Committee of the Regions: Towards a Thematic Strategy for Soil Protection [COM (2002) 179 final, 35 p.]. (At: http://europa.eu.int/scadplus/printversion/en//lvb/l28122.htm; last accessed: 27.10.2005).

Lark, R.M., 2000, A comparison of some robust estimators of the variogram for use in soil survey. *European Journal of Soil Science* **51**: 137–157.

Lark, R.M., 2002, Modelling complex soil properties as contaminated regionalized variables. *Geoderma*. **106**: 171–188.

Lark, R.M., and Ferguson, R.B., 2004, Mapping the conditional probability of deficiency or excess of soil phosphorous, a comparison of ordinary indicator kriging and disjunctive kriging. *Geoderma* **118**: 39–53.

Jones, R.J.A, Hiederer, R., Rusco, E., Loveland, P.J., and Montanarella, L., 2005, Estimating organic carbon in the soils of Europe for policy support. *European Journal of Soil Science* **56**: 655–671.

McGrath, S.P., and Loveland, P.J., 1992, *The Soil Geochemical Atlas of England and Wales*. Blackie Academic and Professional, Glasgow. 101 p.

Scholz, M., Oliver, M.A., Webster, R., Loveland, P.J., and McGrath, S.P., 1999, Sampling to monitor soil in England and Wales. In: Proceedings of 2nd European Conference on Geostatistics for Environmental Applications, Valencia, Spain, 18–20 November 1998, pp. 465–476.

Rousseeuw, P.J., and Croux, C., 1992, Explicit scale estimators with high breakdown point. In: *L₁ Statistical Analysis and Related Methods* (ed. Y. Dodge), pp. 77–92. North Holland, Amsterdam.

Rousseeuw, P.J., and Croux, C., 1993, Alternatives to the median absolute deviation. *Journal of the American Statistical Association* **88**: 1273–1283.

Utermann, J., Duwel, O., and Nagel, I., unpub, Trace Element and Organic Matter Contents of European Soils. Final Report (2003) to the Joint Research Centre, European Commission. 41 p.

Webster, R., and Oliver, M.A., 1989, Optimal interpolation and isarithmic mapping of soil properties. VI. Disjunctive kriging and mapping the conditional probability. *Journal of Soil Science* **40**: 497–512.

EFFECT OF A HAZARDOUS WASTE LANDFILL AREA ON GROUNDWATER QUALITY

SEVGI TOKGÖZ GÜNES*, AYSEN TURKMAN
Dokuz Eylül University, Department of Environmental Engineering, Izmir, Turkey

Abstract. In 1992, uncontrolled landfills in Izmir were closed on the ground that they threat the public health and Harmandalı Hazardous Wastes Landfill Area has been put into service by İzmir Metropolitan Municipality. Harmandalı Region, which was selected as a sanitary landfill area, has an area of approximately 900 000 m² and is located in the border of the city Izmir. Izmir is the third biggest city of Turkey with a population of 3.5 million. In this study, the probable impacts of Harmandalı Sanitary Landfill Area on groundwater quality have been investigated. In order to predict the effect land disposal site, "Computer Model of Two-Dimensional Solute Transport and Dispersion in Groundwater" has been applied to the Harmandalı area by using the available data. The results of the model have been controlled after eight years by groundwater analysis in the area.

Keywords: hazardous waste landfill; groundwater; contamination; computer model.

1. Introduction

Harmandali Sanitary Landfill Area has been put into service in 1992 to bury industrial and domestic wastes. The Mediterranean Climate affects Harmandali Sanitary Landfill Area (Fig. 1), which is hot and dry in summer

_____

 *To whom correspondence should be addressed. Sevgi Tokgöz Güneş, Dokuz Eylül University, Department of Environmental Engineering, Izmir, Turkey

and warm and rainy in winter. In the study area, the annual mean
temperature and precipitation are 17.6°C and 700 mm, respectively. To
prevent the groundwater pollution that could be caused by leachate,
hydrological and geological investigation drillings have been carried out in
the landfill area and its surroundings (UKAM, 1990).

The soil investigations were carried to evaluate the suitability of the
area. 24 boreholes have been opened in the area and the geological map,
with a scale of 1/5000 has been prepared. At the end of in-situ studies, types
and characteristics of geological layers and positions of faults have been
determined. According to the results, locations of the test bores with
"carrot" have been drilled. Standard penetration and rock quality tests have
been done to determine their geotechnical characteristics of Harmandalı
Sanitary Landfill Area. According to these studies, alluvium consists of
clays that are classified as hard or semi-hard and sands as semi-tight. To
observe the effect of leachate, which would originate from solid wastes, 4
observation wells, having a depth of 30 m and a diameter of 2″, have been
drilled. The results obtained from the boring tests and observations of the
area have been evaluated and the geotechnical cross-section has been
prepared.
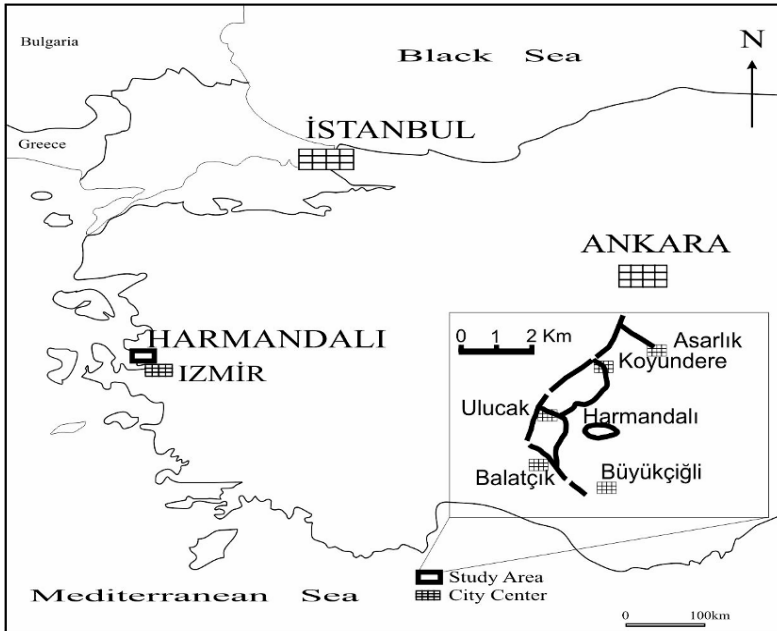
Figure1. Map of the Harmandalı Sanitary Landfill Area.

To determine the hydraulic conductivity of land on the consolidated materials and/or on the rocky structure that spread out in the area pressurised and unpressurised (gravity) Packer test have been done. The results can be listed as follows (Çoban, 1992):

- It has been determined that there is an impermeable layer above the pyroclastic unit;
- Groundwater table is not close to ground level, geological structures included impermeable layers;
- The Harmandalı Sanitary Landfill Area is not located in the region used for drinking water supply of villages.

Hydraulic conductivity coefficients of the layers have been determined in the range of between 10^{-7} to 10^{-10} m/sec. According to these data, the degree of hydraulic conductivity of the soil layers have been determined to vary from very low to practically impermeable, but generally it can be considered as impermeable.

2.   Experimental studies

2.1.   GROUNDWATER QUALITY ANALYSIS

In the sanitary landfill area, it is necessary to know the chemical quality of water samples to estimate the effects on the groundwater and surroundings from the wastes. For this reason, water samples have been taken from the observation wells and other wells before the landfill was put into operation (Fig. 2).

2.2.   GEOLOGICAL STUDIES

In Harmandalı Sanitary Landfill Area, three lithostratigraphic units were determined. These are classified from bottom to top as Harmandalı flysch, pyroclastic unit and alluvium. The Harmandalı flysch lies from the elevation of 30 m to 200 m and covers approximately half of studied area. The predominant lithology is mudstone that has no clear layer as a visible structure. In the most structure of Harmandalı Sanitary Landfill Area, there are thin laminations as mudstone. Their colors change from dark grey-black to light brown-red. Sandstones show a structure as a thin layer. It has been determined that a fault lies into northwest, north-north-west and south-south-east direction. Groundwater table has not been found in the test bores that is cut into the Harmandalı flysch. Mudstone layer of the Harmandalı flysch is impermeable and sandstone layer is relatively permeable (UKAM, 1990).

The Harmandalı flysch is covered by pyroclastic structure irregularly on a large scale in the studied area. According to their pore and cell structure, pyroclastic rocks could be divided into three lithologies; volcanic rocks, agglomerates and andesites. It has been determined that pyroclastic rocks spread out depending on paleotopograpy. Alluvium is located into the west side of investigation area and was occurred by transportation of pyroclastic material. Their thickness is 19 m. According to standard penetration studies, clays are classified as hard and semi-hard, sands as semi-tight.
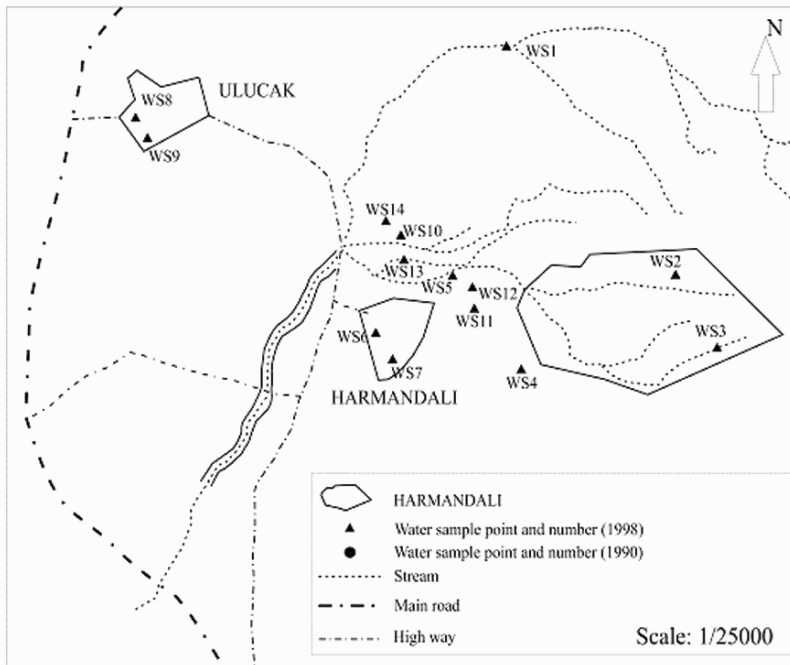
Figure 2. Sampling points in Harmandali Sanitary Landfill Area.

Organic matter content of soil samples of the area change between 2.27-5.39% in surface horizons. Generally organic matter is in humus form and contains the specific forms of plant wastes. In deeper layers organic matter content falls to 0.26% (Çoban, 1992). Soil pH values ranges between 5.21-6.67.

2.3. WASTE INVESTIGATIONS IN HARMANDALI SANITARY LANDFILL AREA

The Aegean region is the second most important industrial area in Turkey. There are many industries within the border of İzmir Metropolitan Municipality such as detergent, oil, chemical, textile, leather, engine, automobile, metal and slaughterhouses. The Municipality had accepted treatment sludges until the end of 1992 to Harmandalı Sanitary Landfill Area. After this date, a regulation has been put into force which brings an obligation that water content of biological sludges must be below 65% and of chemical sludges below 75% in industrial plants since the beginning of 1993.

Heavy metal contents of treatment sludges of the industries within the border of İzmir Metropolitan Municipality have been determined and are given in Table1.

TABLE 1. The Characteristics of treatment sludge from industrial plants (mg/kg).

Parameter	Concen-tration	Parameter	Concen-tration	Parameter	Concen-tration
Pb	8-4120	Ca^{+2}	56340	Cl^-	98360
Cd	5	Mg^{+2}	29810	Total P	500-1850
Cr	23-170000	SiO_2	16500	Total N	0.3-4.9
Ni	44-6900	S^-	500	Al_2O_3	15.3
Hg	0.05-0.3	Fe	2644	NaOH	1.2
Zn	85	Oil and grease	13560	SO_4^{-2}	82160

Industrial wastes that have similar properties with the domestic wastes are being stored together with domestic solid wastes. Until Management of Hazardous Wastes Regulation (1995) becomes effective, these kinds of wastes were stored in a part of the landfill area which has minimum permeability and covered with soil in Harmandalı Sanitary Landfill Area. Hospital wastes are buried into deep pits, which have an impermeable layer and covered with soil after the addition of lime.

According to 8th paragraph of the Soil Pollution Control Regulation (2001), special wastes like hospital, laboratory, radioactive, batteries, pills etc. must be separately disposed. For this purpose, İzmir Metropolitan Municipality has started a campaign to collect used batteries. Batteries contain heavy metals such as cadmium, nickel, mercury that are very toxic to the environment and human health. For this reason, batteries are solidified and buried into deep pits.

Four sampling points are selected for heavy metal analysis between The Harmandalı Sanitary Landfill Area and Harmandalı Village. Results of analysis of water samples are given in Tables 2 and 3.

TABLE 2. Anion and cation content of groundwater samples in the study area in November 1990 (Öztuna, 1993).

Sample No	Cations (mg/l)				Anions (mg/l)		
	Na^+	K^+	Ca^{+2}	Mg^{+2}	HCO_3^-	Cl^-	SO_4^{-2}
WS-1	59.93	11.63	90.00	23.47	305.06	127.66	86.67
WS-2	33.37	5.93	72.10	22.85	274.56	95.74	13.56
WS-3	15.00	5.71	45.00	8.81	158.63	21.28	12.90
WS-4	16.17	4.71	201.58	9.17	170.84	40.78	30.66
WS-5	61.84	5.11	91.05	19.71	475.59	74.47	20.49
WS-6	45.29	5.52	112.11	22.25	396.58	67.38	60.04
WS-7	207.40	59.11	472.63	101.15	457.60	1.003.55	311.82
WS-8	20.47	4.71	59.47	12.83	268.46	35.46	7.26
WS-9	173.50	13.49	213.68	56.30	396.58	698.58	86.51
WS-10	107.13	3.89	117.37	54.11	616.23	1.173.76	4.20
WS-11	41.25	5.79	71.43	12.38	231.86	74.45	22.98
WS-l2	42.70	5.79	97.96	43.65	414.80	145.35	22.10
WS-13	58.54	13.89	29.59	15.20	183.00	92.17	10.18
WS-14	46.46	10.84	44.89	23.75	298.90	14.18	50.52

TABLE 3. Results of heavy metal analysis of samples in November 1990 (Öztuna, 1993).

Sample No	Cd mg/l	Cu mg/l	Cr mg/l	Fe mg/l	Mn mg/l	Ni mg/l	Pb mg/l	Zn mg/l
WS-6	-	-	-	0.015	0.010	0.007	-	0122
WS-11	0.0018	0.022	0.015	2.074	0.548	0.028	0.163	0.029
WS-l2	0.0020	0.005	0.005	0.127	0.025	0.023	-	0.017
WS-13	0.0110	0.008	0.005	0.179	0120	0.033	0.125	0.011

Leachate samples have been taken from Harmandalı Sanitary Landfill Area and analyses have been done for pH, chemical oxygen demand (COD), total suspended solids (TSS), chloride and sulfate ions (Table 4).

TABLE 4. Composition of leachate from Harmandalı Sanitary Landfill Area, (Öztuna, 1993).

Parameter	Concentration (mg/l)	Parameter	Concentration (mg/l)
PH	5.95	Pb	0.86
COD	72000	Cd	0.07
TSS	1450	Cr	0.83
Cl^-	9500	Ni	3.66
SO_4^{-2}	2233	Oil and Grease	1000

3.   Transport modelling

"Two-Dimensional Solute Transport and Dispersion in Groundwater Model" (Konikow and Bredehoeft, 1978) simulates solute transport in flowing groundwater and computes changes in concentration over time caused by the mixing (or dilution) from fluid sources. The model can be applied to a wide range of problem types and it is one of the most used models for solute-transport problems. It is applicable to one-or two-dimensional problems involving steady state or transient flow. The model assumes that the solute is nonreactive and that gradients of fluid density, viscosity, and temperature do not effect the velocity distribution. Computer model solves two simultaneous partial differential equations. One equation is the groundwater flow equation another is the solute-transport equation. The groundwater flow equation describes the head distribution in the aquifer and the solute-transport describes the chemical concentration in the system. The model can be used in aquifers that may be heterogeneous and/or anisotropic. The model uses an alternating direction implicit procedure to solve a finite-difference approximation to the groundwater flow equation.

There are four distinct processes in the model (Konikow and Bredehoeft, 1978):

- Convective transport, in which dissolved chemicals are moving with the flowing groundwater;
- Hydrodynamic dispersion, in which molecular and ionic diffusion and small-scale variations in the velocity of flow through the porous media cause the paths of dissolved molecules and ions to diverge or spread from the age direction of groundwater flow;
- Fluid sources, where water of one composition is introduced into water of a different composition;
- Reactions, in which some amount of a particular dissolved chemical species may be added to or removed from the groundwater due to chemical and physical reactions in the water or between the water and the solid aquifer materials.

The model is based on a rectangular, block-centred, finite-difference grid. It allows the specification of any number of injection or withdrawal wells and of spatially varying diffuse recharge or discharge, saturated thickness, transmissivity, boundary conditions, and initial heads and concentrations. It contains up to five observation points. The numerical procedure used in this model requires that the area of interest be surrounded

by a no-flow boundary. No-flow boundaries can also be located elsewhere in the grid to simulate natural limits or barriers to groundwater flow. A constant-head boundary in the model can be applied to parts of the aquifer where the head will not change with time, such as recharge boundaries or areas beyond the influence of hydraulic stresses. In the model, adjusting the leakage term at the appropriate nodes simulates constant-head boundaries.

Assumptions related to the model are given as follows:

- Darcy's law is valid and hydraulic-head gradients are the only significant driving mechanism for fluid flow;
- No chemical reactions occur that affect the concentration of the solute, the fluid properties or the aquifer properties;
- The porosity and hydraulic conductivity of the aquifer are constant with time, and porosity is uniform in space;
- The aquifer is homogeneous and isotropic with respect to the coefficients of longitudinal and transverse dispersivity;
- Gradients of fluid density, viscosity and temperature do not effect the velocity distribution;
- Ionic and molecular diffusion are negligible contributors to the dispersive flux;
- Vertical variations in head and concentration are negligible.

These assumptions affect the applicability and reliability of the model. In the study, two different model areas (A- and B- model areas) have been determined. They have been established on 16*19 grids, and consist of four observations wells and a pumping well (Figure 3). Since the flow was assumed to be steady state, the storage coefficient was set equal to zero. Although there are many parameters to monitor the groundwater pollution; chloride, oil and grease and cadmium were selected to be used in the model and the transport of heavy metal and chloride concentrations have been investigated in groundwater.

The A and B-model areas were simulated for a period of 400 years. This option consists of one pumping well located in a regional flow field that is controlled by two constant-head boundaries. For the A-model area, the contamination sources were defined in three central nodes along the up-gradient constant-head boundary and one node is in front of them in the model. For the B-model area, pollution sources are only three central nodes along the up-gradient constant-head boundary.
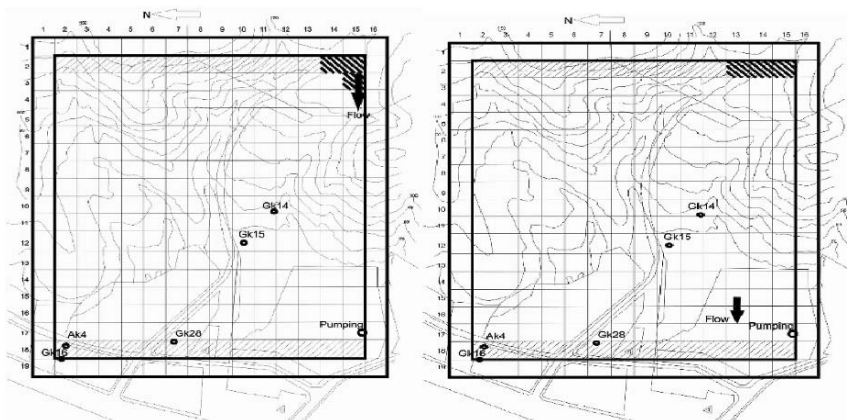
Figure 3. The grid and boundary conditions defined the A- and B-model area.

The first situation was established to evaluate the application of Cl⁻ on the A and B-model areas, since Cl⁻ has a high mobility in groundwater. A second situation was designated on A-model area to evaluate application of Cd, which can be adsorbed onto soil, and oil and grease can decay. In soil media, situation of adsorption is different than activated carbon so, a value is accepted as 10 to be suitable to soil of Harmandalı Sanitary Landfill Area.

4. The model results

According to the results of the computer program, there will be no contamination in observation wells at Harmandalı Sanitary Landfill Area for a long time. Fig. 3 shows the A-model area where Cl⁻ (9500 mg/l) moves 100 m (328 ft) during the next 400 years in the groundwater. The result of the model indicates that chloride does not reach to observation wells (WS11, WS12, WS13 and WS14) during this time. The model results also indicate that Cd (10 mg/l) cannot move very long distance in groundwater. When Cd concentration is 100 mg/l, transportation of Cd in groundwater is observed but it cannot reach to observation wells. Oil and grease has also been applied on the A-model area, according to this study oil and grease cannot reach to observation wells since it decays and was adsorbed on soil particles.

Cl⁻ parameter has been applied on the B-model area. Also prediction indicates Cl⁻ will not be transported to the observation wells but it has shown a small dispersion in this study area. Cd has not been applied to the

B-model area because; they have not transported and dispersed in the A-model area where contaminants originate from the larger contaminated area than the B-model area. It was found that no transportation and dispersion of oil and grease have occurred in this B-model area.

5. Changes of groundwater quality in time

The results of the model have been controlled after eight year by groundwater analysis in 1998. One observation well (WS12) that is between the Harmandalı Sanitary Landfill Area and Harmandalı Village is selected for this reason. Results of analysis are given in Table 5.

TABLE 5. The Results of water chemistry and heavy metal analysis of WS12 in November 1998 (Baba and Güneş, 1999).

Parameter	Concentration mg/l	Parameter	Concentration mg/l	Parameter	Concentration mg/l	Parameter	Concentration mg/l
Na^+	125	Si	22.9	Cd	0.008	Mn	0.018
K^+	30	Cl^-	175	Cu	0.026	Ni	0.036
Ca^+	150	SO_4^{-2}	155	Cr	0.008	Zn	0.084
Mg^{+2}	44	HCO_3^-	400	Fe	0.135		

In evaluating the experimental data, it is determined that Cd concentration of groundwater exceeded 0.005 mg/l of Turkish Standards (TSE, 1997) for drinking water. According to the Water Pollution Control Regulation (1988) Cd concentration must be below 0.01 mg/l for irrigation water. 0.008 mg/l of Cd concentration is very close of the standard and it is possible that it exceed the standard value after a short period of time. The chloride concentration is also above the standards. Analysis results of groundwater samples after eight years are given in Figures 4 and 5 to compare the pollution effect.

The impact of The Harmandalı Sanitary Landfill Area on groundwater can be easily seen from the figures in the period of eight years.
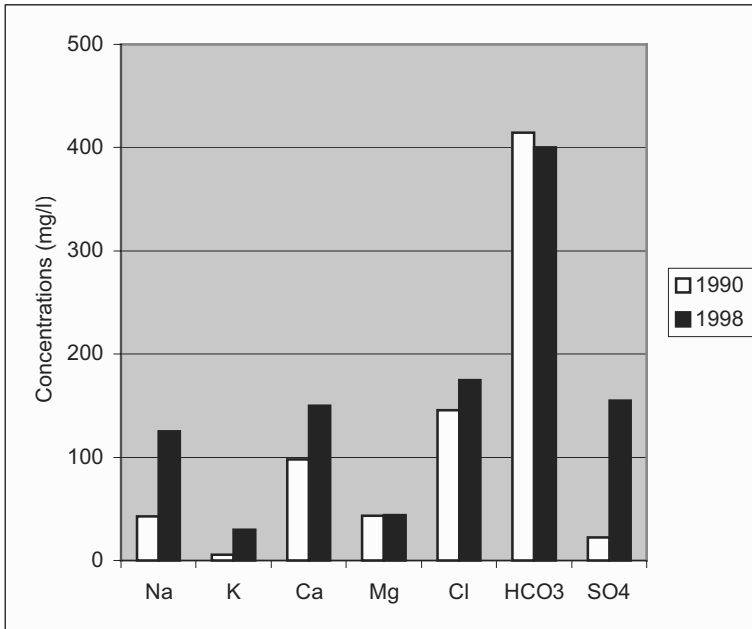
Figure 4. Comparison of the ions in well WS12 in 1990 and 1998.
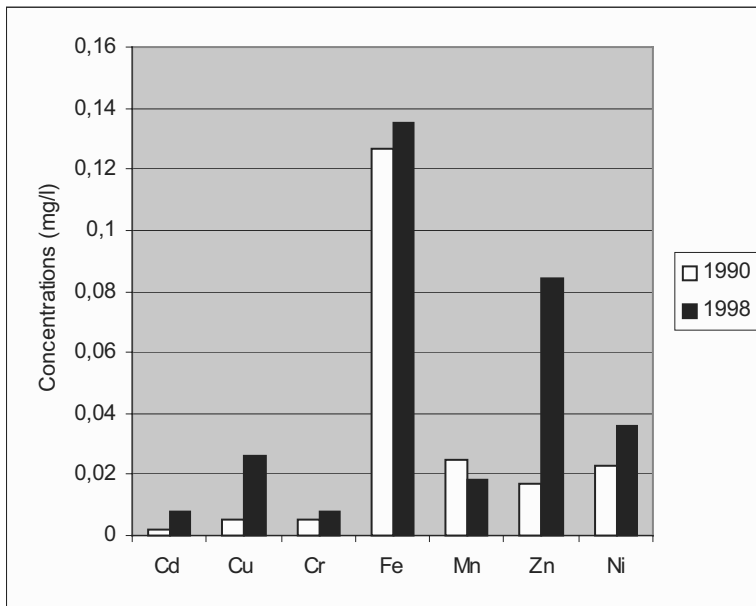
Figure 5. Comparison of the heavy metals well WS12 in 1990 and 1998.

6. Result and discussion

Harmandalı Sanitary Landfill Area has been evaluated with respect to mobility of contaminants by using two-dimensional solute transport and dispersion model in 1993. Although the prediction results of the computer model indicated very safe results and the contamination would take place after more than 100 years, the contamination has taken place earlier then expected. This might be attributed the permeability of the soil since the impermeable layer below the landfill area may not be uniform.

Another reason for the prediction to be not verified may be surface flow from the landfill area during the heavy rainy period. In fact, in the creek nearby, some pollutants have been detected originating from the landfill leachate.

At present no hazardous wastes are accepted to the Harmandali landfill area.

References

Baba, A., Tokgöz Güneş, S., 1999, İzmir Harmandalı Düzenli Atık Depolama Sahasının yüzeysel ve yeraltısularına etkisi (Impacts of İzmir Harmandalı Sanitary Landfill Area on surfacewater and groundwater), 4–5 Haziran, İzmir, İzmir Su Kongresi, pp. 263–275.

Çoban, S., 1992, An approach to the environmental impact assessment of solid waste disposal plant", Master Degree Thesis, Advisor: Prof. Dr. E. Erdin, İzmir.

Hacettepe Üniversitesi Uluslararası Karst Su Kaynakları Uygulama ve Araştırma Merkezi (UKAM), İzmir Harmandalı Çöp Depolama Alanı zemin araştırmaları raporu, Aralık 1990, Ankara.

Konikow, L.F., Bredehoeft, J.D., 1984, Computer model of dimensional solute and dispersion in ground water, 2nd. ed., Techniques of Water Resources Investigations of The United States Geological Survey, Washington, Book 7, Chapter C2.

Management of Hazardous Wastes Regulation, Official Gazette, No: 22387, 1995.

Oztuna, B., 1993, Evaluation of an Industrial Sludge Discharge Site With Respect to Mobility of Contaminants, DEU, M.Sc. Thesis, Advisor: Prof. Dr. A. Türkman, İzmir.

Soil Pollution Control Regulation, Official Gazette, No: 24609, 2001.

Turkish Standards Organization, TSE 266, 1997.

Water Pollution Control Regulation, Official Gazette, No: 19919, 1988.

COMPUTATIONAL AND NUMERICAL BACKGROUND OF THE UNIFIED DANISH EULERIAN MODEL

ZAHARI ZLATEV
National Environmental Research Institute, Frederiksborgvej 399, P. O. Box 358, DK-4000 Roskilde, Denmark, E-mail address: zz@dmu.dk.

Abstract. The necessity to handle efficiently large-scale air pollution models in order to be able to resolves a series of comprehensive environmental tasks is discussed. It is emphasized that the choice of fast and, at the same time, sufficiently accurate numerical methods is very important, but not sufficient. It is also necessary to exploit efficiently the cache memory of the computer under consideration and/or to be able to carry out parallel computations. The particular model used is the Unified Danish Eulerian Model (UNI-DEM), but most of the results can also be applied when other large-scale models are used. The use of UNI-DEM in several comprehensive air pollution studies is discussed in the end of this paper. The investigation of the impact of future climate changes on air pollution levels in some European countries is among the most important studis in which UNI-DEM has until now been used.

1. PDEs arising in environmental modelling

Many environmental models are described mathematically with a system of partial differential equations (PDEs) of the following type:

$$\frac{\partial \mathbf{c}_s}{\partial \mathbf{t}} = -\frac{\partial (\mathbf{u}\,\mathbf{c}_s)}{\partial \mathbf{x}} - \frac{\partial (\mathbf{u}\,\mathbf{c}_s)}{\partial \mathbf{y}} - \frac{\partial (\mathbf{u}\,\mathbf{c}_s)}{\partial \mathbf{z}}$$

$$+ \frac{\partial}{\partial \mathbf{x}}\left(\mathbf{K}_x \frac{\partial \mathbf{c}_s}{\partial \mathbf{x}}\right) + \frac{\partial}{\partial \mathbf{y}}\left(\mathbf{K}_y \frac{\partial \mathbf{c}_s}{\partial \mathbf{y}}\right) + \frac{\partial}{\partial \mathbf{z}}\left(\mathbf{K}_z \frac{\partial \mathbf{c}_s}{\partial \mathbf{z}}\right)$$

$$+ \mathbf{E}_s + \mathbf{Q}_s(\mathbf{c}_1, \mathbf{c}_2, \ldots, \mathbf{c}_q) - (\mathbf{k}_{1s} + \mathbf{k}_{2s})\mathbf{c}_s ,$$

$$\mathbf{s} = 1, 2, \ldots, \mathbf{q},$$

The number $\mathbf{q}$ of equations is equal to the number of chemical species. The other quantities in the above formula can be described as follows:

- the concentrations of the chemical species are denoted by $\mathbf{c}_s$,
- $\mathbf{u},\ \mathbf{v}$ and $\mathbf{w}$ are wind velocities,
- $\mathbf{K}_x,\ \mathbf{K}_y$ and $\mathbf{K}_z$ are diffusion coefficients,
- $\mathbf{E}_s$ are emission sources,
- $\mathbf{k}_{1s}$ and $\mathbf{k}_{2s}$ are deposition coefficients,
- the chemical reactions are denoted by $\mathbf{Q}_s(\mathbf{c}_1, \mathbf{c}_2 \ldots, \mathbf{c}_q)$.

A particular model, the Unified Danish Eulerian Model (UNI-DEM), is consistently used in this paper in order to facilitate the exposition of the results. However, the main ideas are applicable to many other environmental models (and also for many models arising in other fields of science and engineering).

The space domain of UNI-DEM is a 4800 km x 4800 km square containing Europe and parts of Africa, Asia, the Arctic area and the Atlantic Ocean. Initial and boundary conditions are read from a file (being either prepared during another run of UNI-DEM or by running a hemi-spherical model). Initial and boundary conditions used in UNI-DEM are discussed in Havasi and Zlatev (2002), Zlatev (1995, 2002).

Only basic ideas used when the system of PDEs (1) is handled on computers will be discussed in this paper (full description of the methods used in the numerical treatment of such models can be found in Zlatev, 1995, 2002). Applications are discussed in Ambelas Skjøth et al. (2000), Bastrup-Birk et al., (1997), Havasi and Zlatev (2002), Zlatev et al. (2001).

2.   Need for splitting procedures

It is difficult to handle directly the systems of PDEs by which an environmental model is described mathematically. This is why splitting procedures are normally to be implemented and used. The splitting procedure currently used in UNI-DEM leads to three sub-models:

- horizontal advection + horizontal diffusion,
- vertical exchange (i.e. vertical advection +vertical diffusion),
- chemical reactions + emissions + deposition.

Splitting allows us to apply different numerical methods in the different sub-models and, thus, to reduce considerably the computational work and to exploit better the properties of each sub-model. These are the main advantages of using splitting. Unfortunately, there are drawbacks also: the splitting procedure is introducing errors, and it is difficult to control these errors. Attempts to evaluate the splitting errors were recently carried out; see Lanser and Verwer (1999), Dimov et al., (2001, 2004).

3. Spatial discretization

Finite elements are used to discretize the spatial derivatives in the system of partial differential equations. This particular method used in UNI-DEM is described in Pepper and Baker (1979) and Pepper et al., (1979). Its implementation in UNI-DEM is discussed in Georgiev and Zlatev (1999). Other numerical methods can also be used:

- **Pseudo-spectral discretization,** Zlatev (1995). The pseudo-spectral discretization is based on expanding the unknown function in Fourier series and truncating this series after some finite number of terms. This method requires periodicity on the boundaries, which causes problems, because in many realistic situations this condition is not satisfied. Special techniques are to be used in order to satisfy this requirement (Fornberg, 1996). The method is able to produce very accurate results when the requirement for periodicity on the boundaries is satisfied; Fornberg (1975), Kreiss and Oliger (1972) and Zlatev (1995).
- **Semi-Lagrangian discretization** (can be used to discretize only the first-order derivatives, i.e. the advection part should not be combined with the diffusion part when this method is to be applied). This method is well-know under the name method of characteristics among the mathematicians.
- **Methods producing non-negative values of the concentrations.** The method proposed in Bott (1989) is often used in air pollution modelling. The method from Hundsdorfer et al., (1995) is based on a solid theoretical foundation. A thorough description of the principle used in many methods of this type is given in the monograph of Hundsdorfer and Verwer (2003).

4. Time discretization

The ODE system after the discretization of the vertical exchange sub-model (vertical advection + vertical diffusion) can be solved by using many classical time-integration methods. The so-called θ-method (see, for example, Lambert, 1991) is currently used in UNI-DEM. The choice of numerical method is not very critical in this part, because it is normally not very expensive computationally.

Predictor-corrector methods with several different correctors are used in the solution of the ODE system arising after the discretization of the advection-diffusion sub-model. The correctors are carefully chosen so that the stability properties of the method are enhanced; see Zlatev (1984). The reliability of the algorithms used in the advection part was verified by using the well-known rotational test proposed simultaneously in 1968 in Crowley (1968) and Molenkampf (1968).

The solution of the ODE system arising from the chemical sub-model is much more complicated, because this system is both time-consuming and stiff. Very often the QSSA method is used in this part of the model. The QSSA (quasi-steady-state approximation; see, for example, Hesstvedt et al., 1978, or Hov et al., 1988) is simple and relatively stable but not very accurate (therefore it has to be run with a small time-stepsize). The QSSA method can be viewed as an attempt to transform dynamically, during the process of integration, the system of ODEs into two systems: a system of ODEs and a system of non-linear algebraic equations. These two systems, which have to be treated simultaneously, can be written in the following generic form:

In this way we arrive at a system of differential-algebraic equations (DAEs). There are special methods for treating such systems as, for example, the code DASSL (see Brenan et al., 1996). Problem-solving environments (such as MATLAB or Simulink) can be used in the preparation stage (where a small chemical system at only one grid-point is used in the tests). More details about the use of such problem solving environments can be found in Shampine et al., (1999). A method based on the solution of DAE for air pollution models was recently proposed in Djouad and Sportisse (2003).

The classical numerical methods for stiff ODE systems (such as the Backward Euler Method, the Trapezoidal Rule and Runge-Kutta algorithms) lead to the solution of non-linear systems of algebraic equations and, therefore, they are more expensive; Lambert (1991). On the other hand, these methods can be incorporated with an error control and perhaps with larger time-steps. The extrapolation methods, Deuflhard (1985), are also promising. It is easy to calculate an error estimation and to carry out the integration with large time-steps when these algorithms are used.

However, it is difficult to implement such methods in an efficient way when all three sub-models, which are obtained by the splitting procedure selected, are to be treated successively.

Partitioning can also be used (Alexanrov et al., 1997). Convergence problems related to the implementation of partitioning are studied in Zlatev (2001).

It is important to apply good algorithms for treating general sparse matrices when the chemical sub-model is treated. The methods that are discussed in Zlatev (1980, 1982, 1987, 1991) can successfully be used. Methods for sparse matrices developed especially for atmospheric chemistry sub-models are discussed in Alexandrov et al., (1997).

The experiments with different integration methods for the chemical sub-model are continuing. The QSSA, with some enhancements based on ideas from Verwer and van Loon (1996) and Verwer and Simpson (1995), has actually been used in the experiments. The method is described in Alexandrov et al., (1997). There are still very open questions related to the choice of method for the chemical part. The choice of the improved QSSA was made to get well-balanced parallel tasks.

5. High erformance computing

Many tasks, which several years ago had to be handled on powerful supercomputers, can be handled at present on PCs or work-stations. However, there are still many tasks that can be run only on parallel computers. It will be shown in this section that large air pollution models are to be treated on parallel computers. This statement is especially true for the 3-D versions of UNI-DEM when these are discretized on a fine grid. If a 480x480x10 grid is used (this correspond to 10 km × 10 km surface cells, while the thickness of the layers is not equidistant) and if the number of chemical species is 35, then the semi-discretization of the system of PDEs leads to the solution of several huge systems of ODEs, each of them containing $480×480×10×34=80\ 640\ 000$ equations. If the model has to be run over a time period of one year, then more of 200 000 time-steps are needed. Furthermore, it is normally necessary to run the model with many scenarios in order to study the dependence of the results on the variation of some key parameters (as for example, the emissions).

Exploiting the cache memory: In the modern computers the time needed for performing arithmetic operations is reduced dramatically (compared with computers available 10-15 years ago). The reductions of both the time needed to bring the numbers which are participating in the arithmetic operations from the memory to the place in the computer where the arithmetic operation is to be performed and the time needed to store the results back in the memory are much smaller. This is why most of the

computers have different caches. It is much more efficient to use data which are in cache than to make references to the memory. It is very difficult for the user (if at all possible) to control directly the utilization of the cache. Nevertheless, there are some common rules by the use of which the performance can be improved. Division of the data into chunks has been used in Owczarz and Zlatev (2001, 2002), Alexandrov et al., (2004). Some results obtained by using chunks of different sizes are given in Table 1. It is seen that the use of very big chunks is a good choice when old-fashioned vector processors (Fugitsu) are used. On parallel machines (IBM, SGI) medium chunks give best results (even if only one processor, as in Table 1, is used).

TABLE 1. Computing times in seconds obtained when the data arrays are divided into different chunks. The 96x96 2-D model is used. All runs were performed by using one processor only.

Size of the chunks	Fugitsu	SGI Origin 2000	IBM SMP
1	76964	14847	10313
48	2611	12114	5225
9216	494	18549	19432

6. Achieving Parallelism

It is very important to prepare parallel codes which run efficiently on modern parallel computers. The preparation of such a code is by no means an easy task. Moreover, it may happen that when the code is ready the computing centre exchanges the computer which has been used in the preparation of the code with another (hopefully, more powerful) computer. This is why it is desirable to use only standard tools in the preparation of the code. This will facilitate the transition of the code from one computer to another when this becomes necessary. Only standard tools, OpenMP (WEB-site for OpenMP, 1999) and MPI (Gropp et al., 1994), are used in UNI-DEM. The algorithms used in order to obtain efficient parallel runs are described in detail in Alexandrov et al., (2004), Georgiev and Zlatev (1999), Owczarz and Zlatev (2001,2002). Some results obtained by using of the most demanding 3-D version of UNI-DEM are given in Table 2.

The Sun computers used in the runs, results of which are shown in Table 2, are shared memory machines. Therefore, one should expect the OpenMP versions of the code to be more efficient than the MPI versions. In fact, the MPI versions are more efficient. The reasons for this phenomenon are explained in Alexandrov et al., (2004). Some results which illustrate this fact are given in Table 3.

Table 2. Results obtained by running UNI-DEM discretized on a 480x480x10 grid on the SUN computers of DCSC (WEB-site of DCSC, 2004). The time interval is one 48 hours.

Number of processors	Computing time	Speed-up
1	372173	-
15	12928	28.79
30	7165	51.94
60	4081	91.20

TABLE 3. Results obtained in the comparison of the MPI version with the OpenMP version. UNI-DEM is discretized on a 480x480x1 grid and all runs are performed on the SUN computers of DCSC (WEB-site of DCSC, 2004). The time interval is one year. ADV, CHEM, COMM and TOTAL refer to the computing times spent in the advection-diffusion sub-model, the chemistry sub-model (together with emissions and depositions), in the communication part and in the whole run respectively.

Process	MPI version	OpenMP version
ADV	822291	1663812
CHEM	393158	596920
COMM	255785	-
TOTAL	1782752	2614983

7. Applications of UNI-DEM

UNI-DEM was run with different options and different scenarios in a long series of comprehensive studies. Several of these studies are listed below (see more details in Havasi and Zlatev, 2002, as well as in the references there):

- impact of climate changes on air pollution levels (Dimov et al., 2002 based on climate scenarios from the IPCC report prepared by Houghton et al., 2001),
- influence of the biogenic emissions on the creation of high ozone concentrations (Geernaert and Zlatev, 2004),
- long-term variations of the air pollution levels in different parts of Europe (Ambelas Skjøth et al., 2000, Bastrup-Birk et al., 1997),
- influence of European sources outside Denmark on the Danish pollution levels (Zlatev et al., 2001),
- exceedance of critical levels established by EU in Denmark and in other parts of Europe (Zlatev, 1995, Zlatev et al., 2001),
- evaluation of damages caused by high pollution levels (Zlatev et al., 2001).

8.   Plans for further improvements

The improvement of the fine resolution versions of UNI-DEM, especially the 3-D fine resolution version, is an important task, which must be resolved in the near future (indeed, the results presented in this paper show that we are not able to use this version when (a) the time-interval is long and/or (b) many scenarios are to be run. Thus, it is necessary both to improve the performance of the different versions of the model and to have access to more processors (and/or to more powerful computers) in order to be able to run operationally fine resolution versions of UNI-DEM.

Improvements of the performance of the model on high-speed computers are important because the computational work will be further increased by introducing additional options, such as (i) an option for treating particles (see Ackermann, and Schell et al., 2001) and (ii) options for integrating measurements in the computational process by using variational data assimilation techniques (see Elbern et al., 1997).

Acknowledgements

References

Ackermann, I., Hass, H., Schell, B., and Binkowski, F. S., 1999, Regional modelling of particulate matter with MADE, *Environmental Management and Health* **10:**201–208.

Alexandrov, V. N., Owczarz, W., Thomsen, P. G. and Zlatev, Z., 2004, Parallel runs of a large air pollution model on a grid of Sun computers, *Mathematics and Computers in Simulations* **65:** 557–577.

Alexandrov, V. N. Sameh, A., Siddique, Y., and Zlatev, Z., 1997, Numerical integration of chemical ODE problems arising in air pollution models, *Environmental Modelling and Assessment* **2:** 365–377.

Ambelas Skjøth, C., Bastrup-Birk, A., Brandt, J., and Zlatev, Z., 2000, Studying variations of pollution levels in a given region of Europe during a long time-period, *Systems Analysis Modelling Simulation* **37:**297–311.

Bastrup-Birk, A., Brandt, J., Uria, I., and Zlatev, Z., 1997, Studying cumulative ozone exposures in Europe during a seven-year period, *Journal of Geophysical Research* **102:**23917–23935.

Bott, A., 1989, A positive definite advection scheme obtained by non-linear renormalization of the advective fluxes, *Monthly Weather Review* **117:**1006–1015.

Brenan, K., Campbell, S., and Petzold, L., 1996, Numerical solution of initial value problems in differential-algebraic equations, *SIAM*, Philadelphia.

Crowley, W. P., 1968, Numerical advection experiments, *Monthly Weather Review* **96:**1–11.

Deuflhard, P., 1985, Recent progress in extrapolation methods for ordinary differential equations, *SIAM Review* **27:**505–535.

Dimov, I., Faragó, I., Havasi, Á., and Zlatev, Z., 2001, L-Commutativity of the operators in splitting methods for air pollution models, *Annales Univ. Sci. Budapest* **44:**129–150.

Dimov, I., Faragó, I., Havasi, Á. and Zlatev, Z., 2004, Operator splitting and commutativity analysis in the Danish Eulerian Model, *Mathematics and Computers in Simulation* **67:**217–233.

Dimov, I., Geernaert, G., and Zlatev, Z., 2002, Influence of future climate changes in Europe on exceeded ozone critical levels. In: *Nordic Meteorological Meeting 23, 2002,* H. E. Jørgensen, ed., http://www.dams.dk/nmm2002/proceedings.htm.

Djouad, R., and Sportisse, B., 2003, Solving reduced chemical models in air pollution modelling, *Applied Numerical Mathematics* **40:**49–61.

Elbern, H., Schmidt, H., and Ebel, A., 1997, Variational data assimilation for tropospheric chemistry modelling, *Journal of Geophysical Research* **104:**15967–15985.

Fornberg, B., 1975, On a Fourier Method for the integration of hyperbolic equations, *SIAM J. Numer. Anal.*, 12, 509–528.

Fornberg, B., 1996, A practical guide to pseudospectral methods, *Cambridge Monographs on Applied and Computational Mathematics*, Cambridge University Press, Cambridge.

Geernaert, G., and Zlatev, Z., 2004, Studying the influence of the biogenic emissions on the AOT40 levels in Europe, *International Journal of Environment and Pollution* **22:**29–42.

Georgiev, K., and Zlatev, Z., 1999, Parallel Sparse Matrix Algorithms for Air Pollution Models, *Parallel and Distributed Computing Practices* **2:**429–442.

Gropp, W., Lusk, E., and Skjellum, A., 1994, *Using MPI: Portable Programming with the Message Passing Interface,* MIT Press, Cambridge, Massachusetts.

Havasi, Á., and Zlatev, Z., 2002, Trends of Hungarian air pollution levels on a long time-scale, *Atmospheric Environment* **36:**4145–4156.

Hesstvedt, E., Hov, Ø., and Isaksen, I. A., 1978, Quasi-steady-state approximations in air pollution modelling: comparison of two numerical schemes for oxidant prediction, *International Journal of Chemical Kinetics* **10:**971–994.

Houghton, J. T., Ding, Y., Griggs, D. J, Noguer, M., van der Linden, P. J., Dai, X., Maskell, K., and Johnson, C. A., eds., 2001, *Climate Change 2001: The Scientific Basis*, Cambridge University Press, Cambridge, New York, Melbourne, Madrid, Cape Town.

Hov, Ø., Zlatev, Z., Berkowicz, R., Eliassen, A., and Prahm, L. P., 1988, Comparison of numerical techniques for use in air pollution models with non-linear chemical reactions, *Atmospheric Environment*, **23:**967–983.

Hundsdorfer, W., Koren, B., van Loon, M., and Verwer, J. G., 1995, A positive finite difference advection scheme, *J. Comput. Phys.* **117:**35–46.

Hundsdorfer, W., and Verwer, J. G., 2003, *Numerical Solution of Time-Dependent Advection-Diffusion-Reaction Equations,* Springer, Berlin.

Kreiss, H. O. and J. Oliger, J., 1972, Comparison of accurate methods for the integration of hyperbolic equations, *Tellus* **24:**199–215.

Lambert, J. D., 1991, *Numerical Methods for Ordinary Differential Equations,* Wiley, New York.

Lanser, D., and Verwer, J. G., 1999, Analysis of operators splitting for advection-diffusion-reaction problems in air pollution modelling, *J. Comput.Appl. Math.* **111:**201–216.

Molenkampf, C. R., 1968, Accuracy of finite-difference methods applied to the advection equation, *Journal of Applied Meteorology* **7:**160–167.

Owczarz, W., and Zlatev, Z., 2001, Running a large air pollution model on an IBM SMP computer, *International Journal of Computer Research* **10:**321–330.

Owczarz, W., and Zlatev, Z., 2002, Parallel matrix computations in air pollution modelling, *Parallel Computing* **28:**355–368.

Pepper, D. W., and Baker, A. J., 1979, A simple one-dimensional finite element algorithm with multidimensional capabilities, *Numerical Heath Transfer* **3:**81–95.

Pepper, D. W., Kern, C. D., and Long, P. E. Jr., 1979, Modelling the dispersion of atmospheric pollution using cubic splines and chapeau functions, *Atmospheric Environment* **13:**223–237.

Schell, B., Ackermann, I. J., Hass, H., Binkowski, F. S., and Ebel, A., 2001, Modelling the formation of secondary organic aerosol within a comprehensive air quality model system, *Journal of Geophysical Research* **106:**28275–28293.

Shampine, L. F., Reichelt, M., W., and Kierzenka, J. A., 1999, Solving Index-1 DAEs in MATLAB and Simulink, *SIAM Rev.* **41:**538–552.

Verwer, J. G., and van Loon, M., 1996, An evaluation of explicit pseudo-steady state approximation for stiff ODE systems from chemical kinetics, *J. Comp. Phys.* **113:**347–352.

Verwer, J. G., and Simpson, D., 1995, Explicit methods for stiff ODE's from atmospheric chemistry, *Appl. Numer. Math.* **18:**413–430.

WEB-site for OPEN MP tools, 1999, http://www.openmp.org.

WEB-Site of DCSC, 2004, Danish Centre for Scientific Computing, Sun High Performance Computing Systems, http://www.hpc.dtu.dk.

Zlatev, Z., 1980, On some pivotal strategies in Gaussian elimination by sparse technique, *SIAM J. Numer. Anal.* **17:**18–30.

Zlatev, Z., 1982, Use of iterative refinement in the solution of sparse linear systems, *SIAM J. Numer. Anal.* **19:**381–399.

Zlatev, Z., 1984, Application of predictor-corrector schemes with several correctors in solving air pollution problems, *BIT* **24:**700–715.

Zlatev, Z., 1987, Survey of the advances in exploiting the sparsity in the solution of large problems, *J. Comput. Appl. Math.* **20:**83–105.

Zlatev, Z., 1991, *Computational Methods for General Sparse Matrices,* Kluwer Academic Publishers, Dordrecht-Boston-London.

Zlatev, Z., 1995, *Computational Treatment of Large Air Pollution Models,* Kluwer Academic Publishers, Dordrecht-Boston-London.

Zlatev, Z., 2001, Partitioning ODE systems with an application to air pollution models, *Computers and Mathematics with Applications* **42:**817–832.

Zlatev, Z., 2002, Massive data set issues in air pollution modelling, In: *Handbook on Massive Data Sets*, J. Abello, P. M. Pardalos and M. G. C. Resende, eds., Kluwer Academic Publishers, Dordrecht-Boston-London, pp. 1169–1220.

Zlatev, Z., Dimov, I. Ostromsky, Tz. Geernaert, G., Tzvetanov, I. and Bastrup-Birk, A., 2001, Calculating loses of crops in Denmark caused by high ozone levels, *Environmental Modeling and Assessment* **6:**35–55.

FINITE VOLUME SCHEMES ON CUBED SPHERE

RAMAZ BOTCHORISHVILI

*Institute of Mechanics and Mathematics & VIAM,Tbilisi State
University, 2 University Str., 380043 Tbilisi, Georgia*

Abstract. Some typical drawbacks are analyzed for numerical schemes
used in environmental modeling. A new approach for constructing finite
volume schemes on a cubed sphere is presented. A locally one-dimensional
implicit scheme for the linear advection equation is developed and studied
in detail.

1. Introduction

We consider here some numerical aspects related with environmental
modeling. In particular, we consider issues on numerical resolution of first
order hyperbolic equations of the following type:

$$\frac{\partial u}{\partial t} + \sum_{i=1}^{N} \frac{\partial A_i(u,x,t)}{\partial x_i} = f(t,x,u), \tag{1}$$

where t is time variable, N is space dimension, x=$(x_1, x_2, ..., x_N)$ is space
variable, *u(t,x)* is an unknown function; flux functions A_i,*i=1,2,...,N,* and
source term *f* are sufficiently smooth functions.

Equations used in environmental modeling are far more complicated
then the equation presented above, though usually these complicated
equations comprise the terms that constitute the Eq. (1). Recall that operator
splitting is still a widespread and useful technique when solving

complicated partial differential equations. When applying operator splitting, e.g. to an advection-diffusion-reaction system then at one stage one arrives to the need of numerically solving of the advection equation. The latter is a particular case of the Eq. (1). Therefore considerations presented below are also relevant to the wider class of equations then Eq. (1) that are used in environmental modeling.

The rest of the paper is organized as follows. The next section is devoted to the analysis of some approaches used in environmental modeling. This analysis is performed from the standpoint of theoretical considerations on convergence of numerical schemes. In particular, issues are considered such as conservativeness, change of variables and conservation of equilibrium states. The danger that is associated with improper handling of these properties will be clarified. Notice that all this is well known to the scientific community working on hyperbolic conservation laws or CFD but sometimes they are ignored when modeling environmental problems, climate or meteorology. For instance, some insufficiently accurate approaches are implemented even in some operational codes. In the third section finite volume schemes on a cubed sphere are developed. Locally one-dimensional schemes for the linear advection equation are studied in detail. These schemes are in accordance with theoretical properties of the Eq. (1). In the last section some conclusions and short overview of future work are given.

2.   Analysis of some approaches

2.1.   NONCONSERVATIVE SCHEMES CONVERGE TO WRONG SOLUTION

Different opinions exist on the usefulnsess of using conservative discretizations in numerical schemes. Typical arguments against using conservative discretization are of the following style: "conservative discretization is important just for climate modelling, for short time intervals it does not matter, errors will not be accumulated", "the governing equations contain source terms and why should one care about conservativeness, if the quantity is not conserved? " etc. In response we can say that such judgments are not correct for Eq. (1). The reason is that, e.g., the Cauchy problem for Eq. (1) does not have classical smooth solution in general and even in case of smooth initial data discontinuties may develop rapidly. Therefore equations in conservative form are necessary for defining a generalized solution in integral form that contains no derivatives of the solution of Eq. (1). Thus if Eq. (1) written in nondivergent form has no classical solution, then evidently it does not make sense to use nonconservative space discretization in numerical schemes. Therefore using nonconservative schemes in this case means that one is trying to find a solution that does not exist. It is mathematically proven that if

nonconservative schemes for Eq. (1) are convergent then usually they converge to wrong solutions. In particular, if a nonconservative scheme converges then it converges to an Eq. differing from the original Eq. (1) with an artificial nonphysical source term. Notice that the bounded variation estimate is available in the scalar case. For details we refer to Hou and LeFloch (1994). Notice that such convergence to wrong solutions can be observed in the case of nonlinear flux functions or insufficiently smooth inputs in the equations, e.g. insufficiently smooth wind fields in the linear advection equation written in conservative form. Because of all the arguments given above we conclude that using conservative schemes is important for the accuracy of computations, if equations of type (1) are involved in a model that has to be solved.

2.2. TRANSFORMATION OF DEPENDENT VARIABLES RESULTS IN WRONG PROPAGATION SPEED

Transformation of dependent variables is a widespread technique when solving various problems. Sometimes, suitable selection of variables leads to some simplification of the problem under consideration and thus it is very important for finding an efficient way of solution. But for the equations of type (1) transformation of dependent variables may be dangerous. For demonstrating this we consider the particular case of Eq. (1), the inviscid Burgers equation in two space dimensions, that writes

$$\frac{\partial u}{\partial t} + \sum_{i=1}^{2} \frac{\partial u^2 / 2}{\partial x_i} = 0. \tag{2}$$

Let us introduce the transformation of variables $v = u^2$. Formally Eq. (2) "equivalently" writes

$$\frac{\partial v}{\partial t} + \sum_{i=1}^{2} \frac{\partial (2v^{3/2} / 3)}{\partial x_i} = 0. \tag{3}$$

But in fact Eqs. (2) and (3) are not equivalent. The reason is that they have different entropy functions and therefore different entropy inequalities that define physically relevant unique solutions to the problem under consideration. For details on entropy solutions and numerical entropy condition we refer to Godlewski, Raviart (1996), LeVeque (1992) and to references therein. Analysis of the same Riemann problem for the Eqs. (2) and (3) shows that they ensure different propagation speeds. This can also be observed numerically. Consider the test problem on unit circle with initial condition 0 and prescribed boundary value 1. The same upwind Engquist-Osher scheme and the same finite volume mesh are used for

Eqs. (2) and (3). Numerical results for the same time moment are given in Figure 1. One can easily observe that, arriving from the border, shock waves have different propagation speeds, in accordance with theoretical considerations. Thus we conclude that transformation of variables can result in wrong propagation speed.

Equation (2) can be also written in non-conservative form as follows.

$$\frac{\partial u}{\partial t} + \sum_{i=1}^{2} u \frac{\partial u}{\partial x_i} = 0. \tag{4}$$

The same problem as considered above was also solved with a first order upwind non-conservative scheme for the Eq. (4). In this case the numerical solution is also different from numerical solutions of Eqs. (2) and (3). In particular, the numerical solution is identically constant 0 inside the computational domain, if the coefficient in Eq. (4) is discretized at the cell center. The reason of this is that the non-conservative scheme also has a wrong propagation speed. Therefore for the time moment corresponding to the steady state shown in Figure 1 is already established in the numerical solution computed by the non-conservative scheme. Thus here we also get numerical evidence of the validity of the conclusion in Subsection 2.1. Because of all the above we conjecture that for accurate numerical computations it is better to obtain governing equations in primitive variables and to perform their discretization without any transformation of dependent variables.
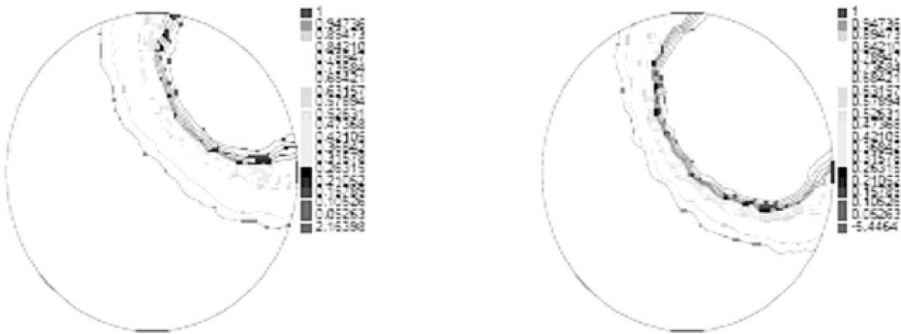
Figure 1. Test problem for inviscid Burgers equation, original variable -left, transformed variable –right.

2.3. LACK OF ACCURACY OF NUMERICAL SCHEMES CAN NOT BE COMPENSATED BY INCREASING THE COMPUTATIONAL POWER

The importance of computational power is evident for numerical modeling. This is so clear that some people even believe that if computers are fast enough then there is no need to care about the quality of numerical methods and one can get good results when using "bad" numerical methods and fast computers. But to rely too much just on computational power is dangerous and here we provide an example for this. One of the typical numerical difficulties is associated with maintaining exact steady states, equilibrium states, at a discrete level. This problem arises when an equation under consideration contains the so called geometric source terms or the governing equation is obtained after transformation of dependent variables. Notice that usually the same numerical scheme for original and transformed equations has different equilibrium states. When modeling the environment, climate or meteorology, transformation of independent variables is a widespread technique and source terms, e.g. due to gravity acceleration, are also present in governing equations. Here we recall example from Botchorishvili (2005) where the inviscid Burgers equation with source terms of the type

$$b(u)\sum_{i=1}^{2}\frac{\partial z(x)}{\partial x_i},$$

is considered *where b(u), z(x)* are smooth functions. For the solution of this problem, in particular, for the computation of the steady state solution two different numerical schemes on two different platforms were considered. In the first case a standard upwind scheme with cell centered discretization of source terms was used on a powerful PC cluster with 16 CPUs, Intel Pentium 4 FOSTER Xeon 2Ghz, 2GB RDRAM. In the second case a standard upwind scheme with equilibrium type discretization of source terms was used on a laptop with an Intel Pentium 3 processor, 128MB DRAM. The numerical scheme used in the second case was designed in Botchorishvili and Pironneau (2003), and it is well suited for computations of equilibrium states. So in the first case a "bad" numerical scheme is used on a fast computer and in the second case a "good" numerical scheme on a slow computer. To ensure more advantage in computational power in the first case the problem was solved in one space dimension, i.e. with $N = 1$. In the second case the same problem was solved on a unit circle with initial and boundary conditions as in the previous example. Problems were selected so that the equilibrium state of the one- dimensional problem was the same as the steady state solution along a diagonal for the two-dimensional problem in space. Some results of computations are given in Table 1 which confirm the validity of the title of this subsection. For more

results see Botchorishvili (2005). Notice that explicit numerical schemes
were used in the above mentioned numerical experiments. Probably the
results would be different, if suitable implicit time discretizations were
used, since in explicit schemes the time step is restricted by the so called
Courant-Friedrichs-Levy condition. The considered example suggests that
despite of the large variety of different standard approaches it is worth to
design special computational schemes for the numerical solution of difficult
problems.

TABLE. Laptop vs. PC cluster.

Computer	Number of nodes	Error	Computing time
PC cluster	16 000	2.4×10^{-4}	512 seconds
Laptop	98	8.9×10^{-5}	25 seconds

3.   Cubed sphere and finite volumes

3.1.   GENERAL APPROACH

Here we propose an approach to the construction of numerical schemes that
are free of the drawbacks of discretization discussed in the previous section.
In particular we propose numerical methods that are conservative, that do
not use any transformation of dependent or independent variables, and that
are stable for large time steps. First we choose the coordinate system, i.e.
independent variables, as global Cartesian coordinate system. The
computational domain is defined as domain between two spheres of
different radius centered at the origin of the global Cartesian system. We
assume that all governing equations are derived directly in global Cartesian
coordinates in primitive variables in conservative form. This is one of the
cores of our approach since in this case the implementation of well
developed approaches for constructing of finite volume schemes for the
equations of type (1) is straightforward. Thus several problems related with
the construction of finite volume schemes can be solved by means of
selection of a suitable coordinate system, derivation of governing equations
in conservative form and use of existing approaches. But even in this case
there are still problems, e.g. related with spherical borders of the
computational domain or related with stability when using large time steps.
These points will be addressed in the next subsections. In Subsection 3.2
the construction procedure of a finite volume mesh for the computational
domain will be considered. In Subsection 3.3 a general approach will be
presented for building semi-discrete locally one-dimensional schemes on a
cubed sphere. Since the advection algorithm is one of the fundamental

building blocks of atmospheric flow simulations we concentrate on it in subsection 3.4 where operator splitting and implicit schemes are combined in order to ensure stability for large time steps.

3.2. CONSTRUCTION OF FINITE VOLUME MESH

For meshing of the computational domain one of the important stages is meshing of borders, i.e. sphere in the case under consideration. For this purpose one can use traditional latitude-longitude grid, see e.g. Jablonowski et al., (2005), icosahedral-hexagonal mesh, Majewski et al., (2002) or cubed sphere, Ronchi et al., (1996). For our purposes the latter approach seems to be most suitable since it is free of the associated latitude-longitude grid pole problems, has quadrilateral cells that are simpler then hexagonal or pentagonal cells of the icosahedral grid. The most important point is for us that it has usual Cartesian type data structure and that is simple and efficient. There exist different ways of constructing a cubed sphere mesh, see e.g. Adcroft et al., (2004). Since mesh quality is not so important for the development of numerical schemes we choose the simplest approach. Our construction starts from a cube with vertices on the surface of the inner sphere of computational domain. Each face of this cube is meshed using standard technique. The obtained mesh is projected onto inner and outer spheres in the radial directions. Thus borders of the computational domain are meshed. Connecting corresponding projected points on inner and outer spheres we get a first finite volume mesh that in each radial direction contains one finite volume cell only. Notice that such cells have six faces and two opposite faces are placed on the surfaces of the inner and outer spheres. The desired number of cells along the radius of the sphere can be easily obtained by means of intersection of the obtained finite volume mesh with spheres placed in between the inner and outer borders. The last stage in our construction is the identification of the nodal points of our finite volume mesh. This is done by means of averaging of vertices of the finite volume cells. Thus the construction of our cell centered finite volume mesh using cubed sphere technique is finished. For referring to nodal points we introduce the multi-index $j=(j^1,j^2,j^3,j^4)$, where the first three indices refer to Cartesian coordinates and the fourth index refers to faces of the cube, i.e. $0 \leq j^4 \leq 5$. As usual the term "horizontal mesh" will be used for denoting a mesh on the surface of a sphere and the term "vertical" will be used for denoting the radial direction. Finally notice, that we have developed a cell centered finite volume mesh; and nodal points of this mesh do not represent itself projections of the nodal points of the initial mesh on the faces of the starting cube. Advantage of such construction will become evident in the next subsection when defining splitting directions.

3.3. LOCALLY ONE-DIMENSIONAL FINITE VOLUME SCHEMES

The approach presented below uses a block Cartesian data structure of the finite volume mesh on cubed sphere. Schematically, the horizontal data structure can be represented by means of 6 squares as it is shown in Figure 2. Indexing of nodal points at each square starts from the left low corner cell, index j^1 corresponds to the direction of the abscissa and index j^2 corresponds to the direction of the ordinate.

Locally one-dimensional finite volume schemes on a cubed sphere are constructed in the following three steps:

1. Discretization in space.
2. Operator splitting.
3. Discretization in time.
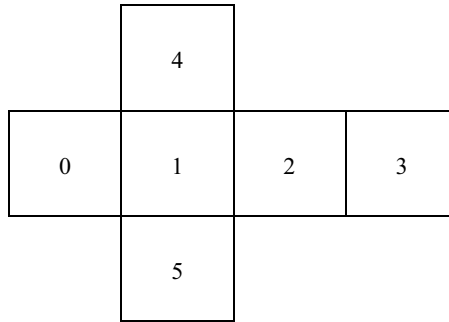
Figure 2. Schematic representation of horizontal mesh.

For the development of a locally one-dimensional algorithm the source term is not important. Therefore for the convenience of further exposition it is assumed that $f = 0$ in Eq. (1). Then the typical first order semidiscrete finite volume scheme for Eq. (1) writes:

$$\frac{du_j}{dt} + \frac{1}{\left|C_j\right|}\sum_{k\in I_j}\left|\Gamma_{jk}\right|A(u_j, u_k, \vec{n}_{jk}, x_j, x_k, t) = 0, \qquad (5)$$

where I_j is a set of reference numbers of cells having a common interface with the cell C_j, $\vec{n}_{jk}$ is the unit vector normal to the cell interface, directed from cell C_j to cell C_k, Γ_{jk} is the interface between cells C_j and C_k, $A(u_j, u_k, \vec{n}_{jk}, x_j, x_k, t)$ is the consistent numerical flux function satisfying

$$A(u, u, \vec{n}_{jk}, x, x, t) = <\vec{A}(u, x, t), \vec{n}_{jk}>, \quad \vec{A}(u, x, t) = (A_1, A_2, A_3), \qquad (6)$$

where $< .,. >$ denotes the scalar product.

Operator splitting is applied to the system of ordinary differential Eq. (5) that is obtained after semi-discretization of the governing equation. Notice that our finite volume mesh is well structured; each finite volume cell has six interfaces. We wish split equations, i.e. equations obtained after splitting, to be similar to equations in one space dimension. For this purpose system (5) is split into the following 4 systems of equations on account of the cubed mesh structure:

$$\frac{du_{jm}}{dt} + \frac{1}{|C_j|} \sum_{k \in I_{jm}} |\Gamma_{jk}| \mathrm{A}(u_j, u_k, \vec{n}_{jk}, x_j, x_k, t) = 0, \ \ 1 \le m \le 4, \quad (7)$$

where I_{jm} defines directional splitting for a given j and m. In fact it is a set of opposite cell interfaces and satisfies

$$I_j = \bigcup_{m=1}^{4} I_{jm}.$$

Splitting directions in terms of reference number to squares are given in Table 2. From this table and from the schematic shown in Figure 2 one can easily trace locally one-dimensional splitting directions for each m.

TABLE 2. Splitting directions on cubed sphere.

m	Reference number to squares			
1	0	1	2	3
2	1	4	3	5
3	0	4	2	5
4	vertical directions for all squares			

The splitted Eq. (5) can be combined in different ways in order to get an approximate solution to the original equation, e.g. one can use first order sequential or second order symmetrized strang splitting. Evidently locally one-dimensional splitting (7) makes sense if at the final stage of our construction implicit time discretization is used. This aspect will be considered in the next subsection for the linear advection equation.

3.4. LOCALLY ONE-DIMENSIONAL MONOTONE SCHEMES FOR THE LINEAR ADVECTION EQUATION

Here we concentrate on studying properties of locally one-dimensional finite volume schemes for the following linear advection equation

$$\frac{\partial u}{\partial t} + \sum_{i=1}^{3} \frac{\partial (v_i(t,x)u)}{\partial x_i} = 0, \tag{8}$$

where the so called wind field $\vec{v}(t,x) = (v_1(t,x), v_2(t,x), v_3(t,x))$ is a sufficiently smooth given function.

For the convenience of further exposition denote via Ω the computational domain and via $\partial\Omega$ its border. Suppose that the wind field satisfies the following inequality

$$< \vec{v}(t,x), \vec{n}(x) > \leq 0, \quad x \in \partial\Omega, \ t > 0, \tag{9}$$

where $\vec{n}(x)$ is the unit vector normal to the outer border at point x. In this case Eq. (8) is supplied with initial and boundary conditions:

$$u(0,x) = u_0(x), x \in \Omega, \quad u(t,x) = u_b(t,x), x \in \partial\Omega, t > 0, \tag{10}$$

where $u_0(x)$ and $u_b(t,x)$ are sufficiently smooth given functions. Notice that the problem (8) - (10) is well posed.

Let us decompose the wind field at cell interfaces in the following way:

$$< \vec{v}, \vec{n} > = < \vec{v}, \vec{n} >^+ + < \vec{v}, \vec{n} >^-, \quad < \vec{v}, \vec{n} >^+ \geq 0, < \vec{v}, \vec{n} >^- \leq 0. \tag{11}$$

Then monotone numerical flux function for Eq. (8) writes

$$A(u_j, u_k, \vec{n}_{jk}, x_j, x_k, t) = < \vec{v}(t,x_j), \vec{n}_{jk} >^+ u_j + < \vec{v}(t,x_k), \vec{n}_{jk} >^- u_k. \tag{12}$$

Notice that thanks to Eq. (11) the numerical flux function defined by Eq. (12) satisfies the consistency condition (6), it is non-decreasing in u_j and non-increasing in u_k. Let us apply the sequential splitting model and perform time discretization of Eq. (7) in implicit way. We get the following implicit scheme:

$$\frac{u_j^{n+\frac{m}{4}} - u_j^{n+\frac{m-1}{4}}}{\Delta t} + \frac{1}{|C_j|} \sum_{k \in I_{jm}} |\Gamma_{jk}| A(u_j^{n+\frac{m}{4}}, u_k^{n+\frac{m}{4}}, \vec{n}_{jk}, x_j, x_k, t_{n+\frac{m}{4}}) = 0, \tag{13}$$

where $1 \leq m \leq 4$ and Δt is the discretization step in time; superscript $n+m/4$ refers to the time moment $t_{n+m/4}$, $t_{n+m/4} = t_n + m\Delta t / 4$. Notice that the set I_{jm} consists of two elements only. Therefore we conclude that numerical schemes (12) - (13) represent a linear system of band diagonal algebraic equations. In particular for $m=1,2,3$, the system is cyclic tridiagonal, for $m=4$ the system is tridiagonal. Notice that in both cases the matrices have diagonal dominance and therefore Eq. (13) can efficiently be solved for all $m, 1 \leq m \leq 4$.

Under supposition of sufficient smoothness of the input data and sufficient smoothness of the numerical flux function (12) one can obtain

unconditional stability of the numerical scheme (13) in a finite time interval in maximum and L^1 norms. By analogy with monotone schemes we can conjecture that the scheme (13) is at most first order accurate in the sense of the local truncation error. But directly proving this is not trivial, e.g. by using the standard technique of Taylor's expansion in the nodal point. One of the reasons is that the cell interfaces are curvilinear surfaces, and therefore the normal to cell interface vector depends on the space variables. Here we mention some key moments for computing the truncation error of the locally one-dimensional scheme (13). First we define point x_{jk} for each cell interface Γ_{jk} so that the following relation holds:

$$\int_{\Gamma_{jk}} f(x)dx = \left|\Gamma_{jk}\right| f(x_{jk}) + O(h^2)\left|\Gamma_{jk}\right|, \qquad (14)$$

where f is an arbitrary smooth function, h is the characteristic size of the cell interface. Then we compute $\vec{n}_{jk}$, normal to the cell interface Γ_{jk}, in the point x_{jk}.

The Eqs. (13) are summed up with respect to m and all the members of obtained equation are expanded in Taylor's series with respect to the time variable in the same point. After this step it remains to show that the term, similar to the second term in the Eq. (5), approximates space derivatives in the governing equation. This can be shown by means of Taylor's expansion of the numerical flux functions at corresponding points x_{jk}, using Eq. (14) and the Gauss theorem.

Properties of the numerical scheme (12) - (13) are summarized in the following proposition.

PROPOSITION. Suppose the input data and the numerical flux function (12) are sufficiently smooth. Then the locally one-dimensional scheme (12) - (13) has the following properties:

1. First order accuracy in the sense of local truncation error.

2. Unconditional stability in maximum and L^1 norms.

3. Conservativeness.

4. Requires $0(M)$ arithmetic operation per time step, where M is the number of mesh nodes.

5. Converges to the solution of (8) - (10).

Numerical tests also confirm the validity of the proposition. Locally the one-dimensional scheme (12) - (13) is fast and stable for large time steps

but at the same time it "smears" the numerical solution what is typical for first order schemes.

4.   Conclusions and future work

A general approach for building conservative finite volume schemes on cubed sphere has been proposed. In the particular case conservativeness, large time steps and low computational cost per time step make the developed locally one-dimensional scheme (12) - (13) an efficient computational tool on cubed sphere for the numerical solution of the linear advection equation written in conservative form (7) in global Cartesian coordinates. Its drawback is low accuracy and typical smearing of approximate solutions. For improving the scheme the development of high order space discretizations, e.g. of MUSCL type, is necessary. Implementation of similar locally one-dimensional splitting seems to be possible for other structured meshes, e.g. for hexagonal meshes, and even for some unstructured meshes. All this will be addressed in future work.

References

Adcroft, A., Campin, J.-M., Hill, C., and Marshall, J., 2004, Implementation of an atmosphere-ocean general circulation model on the expanded spherical cube, *Mon. Wea. Rev.* **132 (12):**2845–2863.

Botchorishvili, R., and Pironneau, O., 2003, Finite volume schemes with equilibrium type discretization of source terms for scalar conservation laws. *J. Comput. Phys.* **187**:391–427.

Botchorishvili, R., 2005, Notes on laptop computing vs parallel computing, to appear in *Appl. Mathem. Inform. Mech.*, vol. **10** , No. 2.

Godlewski, E., and Raviart, P. A., 1996, *Numerical approximations of hyperbolic systems of conservation laws*, Applied Mathematics Sciences 118, Springer, New York.

Hou, T. Y., and LeFloch P.G., 1994, Why nonconservative schemes converge to wrong solutions: error analysis, *Mathematics of Computation,* Vol. **62, 206:**497–530.

Jablonowski, C., Herzog, M., Penner, J. E., Oehmke, R. C., Stout, Q. F., van Leer B., and Powell, K. G., 2005, Block-structured adaptive grids on the sphere: advection experiments, submitted to *Mon. Wea. Rev*.

LeVeque, R., 1992*, Numerical Methods for Conservation Laws, Lectures in Mathematics*, Birkhauser, ETH Zurich.

Majewski, D., Liermann, D., Prohl, P., Ritter, B., Buchhold, M., Hanisch, T., Paul, G., Wergen, W., and Baumgardner, J., 2002, The operational global icosahedral-hexagonal gridpoint model GME: description and high resolution tests. *Mon Wea Rev* **130:**319–338.

Ronchi, C., Iacono, R., and Paolucci, P. S., 1996, The "cubed sphere": a new method for the solution of partial differential equations in spherical geometry, *J. Comp. Phys.,* **124.**

CHEMICAL WEATHER ANALYSIS OPTIMISATION WITH EMISSION IMPACT ESTIMATION USING NESTED FOUR-DIMENSIONAL VARIATIONAL CHEMISTRY DATA ASSIMILATION

HENDRIK ELBERN*, ACHIM STRUNK
Rhenish Institute for Environmental Research at the University of Cologne (RIU), Aachener Str. 209, 50931 Cologne (Koeln), Germany

Abstract. Combined emission rate and chemical state optimization by four-dimensional variational data assimilation is presented. Using an adjoint nesting technique, a model setup focussing on the Berlin area is employed, enabling to analyze constituents with strong spatial gradients like NO and NO_2. Possible requirements for satellite observations to be used for tropospheric chemical state estimation are shortly discussed.

1. Introduction

The adjoint modelling approach for emission estimates has been pioneered by Marchuk and co-workers as early as the seventies, where sulphur

---

*To whom correspondence should be addressed. Hendrik Elbern, Rhenish Institute for Environmental Research at the University of Cologne (RIU), Aachener Str. 209, 50931 Cologne (Koeln), Germany; e-mail: he@eurad.uni-koeln.de

emission rates were assessed. In this case, observations of sulphur were used for the analysis. In the present paper the approach is generalised for other observed, reactive product constituents, where emission rates of not observed precursor species are estimated.

In general, data assimilation focus on the optimal exploitation of observations by combination with other information sources like chemistry transport models and climatological information. The objective is to infer a chemical state analysis, specifically a chemical weather state, as precise as possible. The feasibility of the four-dimensional variational data assimilation methodology to optimise chemical state estimates has been successfully demonstrated by Elbern et al. (1997) for a chemical box model, and for a full 3 dimensional model set up (Elbern and Schmidt, 1999, 2001). This is a practical basis for integrating chemistry transport models a better way, producing more reliable forecasts based on more reliable initial values. However, chemical state analyses of the atmosphere are of interest of its own right and helpful in many ways: To name but a few items, budget assessments with hardly observable tracer fluxes, and exposure time estimates will be more reliable, while scientific field campaigns can be complemented with an additional wealth of external data, in combination with chemistry transport models. The underlying model system used at the RIU group is the EURopean Air pollution Dispersion model EURAD.

The EURAD data assimilation system will be used to support measurement campaigns, focussed both on surface level and aircraft campaigns. A suite of presently ongoing studies include the following objectives: boundary layer ozone formation (postprocessing BERLIOZ), updrafted pollutants in cyclonic warm conveyor belts (CONTRACE), upper tropospheric chemistry (SPURT), and others. In nearly all cases, the use and benefits of satellite retrievals will be assessed, namely NO_2 tropospheric columns and NNORSY neural network based ozone profiles. The focus of this paper is placed on the nested grid application for emission rate optimisation, assimilating BERLIOZ data. The feasibility to extend the optimisation space also for emission rates has been demonstrated by Elbern et al., (2000) for idealised identical twin conditions. A first use of this concept for a real world application is given in Elbern and Schmidt (2002).

2. The variational inversion system

2.1. VARIATIONAL ASSIMILATION AND MODEL SET-UP

The EURAD CTM is a comprehensive tropospheric Eulerian model operating on the mesoscale-α (Jakobs et al., 1995). The chemistry transport

model calculates the transport, diffusion, and gas phase transformation of about 60 chemical species with 158 reactions. The present mother grid configuration is $77 \times 67 \times 15$ with 54 km grid resolution and 100 hPa model top. The associated adjoint operators include the gas phase mechanism, the transport schemes and an implicit vertical diffusion scheme.

The emission data in this study are taken from EMEP (co-operative programme for monitoring and evaluation of the long range transmission of air pollutants in Europe) and further processed as presented in Memmesheimer et al., (1995).

The general methodology rests on advanced data assimilation algorithms, most prominently the four-dimensional variational technique (4Dvar). With this method it is possible to ingest direct and remote sensing observations, scattered in space and time, into a model based data assimilation system. Most prominently, recently available tropospheric satellite data can be assimilated, even when only given in terms of tropospheric columns, as in the case of NO_2. The research focus for chemical weather forecasting is placed on multi-scale forecasts, starting with a European scale grid with 54 km horizontal resolution, down to a fourth generation nested grid, with 2 km resolution.

Initial values are not necessarily the least known parameter. Rather, the emission rates are also considered as insufficiently known, while, at the same time, exerting a strong influence on the chemical evolution. Consequently, the flexibility of the variational approach is and will further be used for emission rate related inversions.

For the implementation of the variational approach a distance function or objective function, which penalises both discrepancies with observations and a priori knowledge of emission rates, may be defined as follows:

$$J(x, e(t)) = \frac{1}{2} \int_0^N (e_b(t) - e(t))^T K^{-1} (e_b(t) - e(t)) dt$$

$$+ \frac{1}{2} \int_0^N (y(t) - Hx(t))^T R^{-1} (y(t) - Hx(t)) dt$$

where J is a scalar functional defined on the time interval $0 \leq t \leq N$ dependent on the vector valued state variables $x(t)$ and $e(t)$ to be optimised. Here, observations y are compared with their model equivalent Hx at time t. The error covariance matrices of the first guess or background emission rates $e_b(t)$ and observations are denoted K and R, respectively. The chemistry transport model (CTM) with inclusion of emissions is given by $\frac{dx}{dt} = M(x) + e$, where M acts as a generally non-linear model

operator and e is in our case the vector of emission rates. Both terms uniquely define the state variable $x(t)$ at time t, after an ever fixed initial state $x(0)$ is provided. A detailed description of the theoretical background and implementation may be found in Elbern et al., (2000).

The variational chemistry data assimilation algorithm is composed of four components: (1) the forward model, (2) the adjoint of its tangent linear version, (3) the background error covariance matrix, making use of the diffusion paradigm (Weaver and Courtier, 2001), and (4) the minimisation routine, where the quasi-Newton L-BFGS method is selected (Nocedal, 1980). Further numerical and implementation details are given in Elbern et al., (1999) and Elbern and Schmidt (2002).

2.2. ADJOINT NESTING TECHNIQUE

Apart from traditional necessities invoking nested model applications, the poor representativity of many observations of important air quality related species mandates the use of highly resolving grid design. For example, observation sites are often not far from point and line sources of NO_x emissions, reflecting only a very limited domain leeward of the emission source. No representativity can be attributed to these measurements in coarse grid applications. To address this issue, major work has been devoted to the development of the first adjoint nesting technique in chemical 4d-var data assimilation. The nesting technique is used for succeeding grid refinements while each nested model domain is a horizontal subspace of the respective mother domain. This facilitates to simulate large-scale features together with rather detailed structures by telescoping down to smaller scales in the region of interest. This technique is employed in two different modes, namely one-way and two-way nesting. The difference of these modes is the way the simulations on the nested domains are performed. Doing two-way nesting, the simulations on the different grids are carried out simultaneously, with information flow in both directions: from mother domain to daughter domain and vice versa. If a model sequence uses one-way nesting, the information flow is only from mother domain to daughter domain, thus the simulations on the daughter domain do not feedback the results on the mother domain. Therefore, one-way nesting can be performed sequentially.

In both modes, the coarser grid serves for the initial and boundary values for the finer grid. This is achieved by interpolation, which is one of the crucial properties of the refinement approach, since it needs to preserve the systems shape and monotonicity properties. Applying two-way nesting, additionally the model state of the coarser domain is updated at each time step by averaged values of the finer grid.

The EURAD-CTM admits to be run in a multiple, one-way nested mode following a scheme devised by Pleim et al., [1991]. It has been first introduced by Jakobs et al., [1995] and in the following been employed in various model studies (see, e.g., Memmesheimer et al., [2004] and citations therein). This technique has been adapted to the 4d-var data assimilation system in the framework of SATEC4D. On each nest level (here coarse grid CG and nest N1), the background knowledge of the initial values is retrieved by a forecast F on the same nest level using the analysed model parameters from the previous day, called analysis run hereafter. The background knowledge of the emission factors (if optimised) is equal to the analysis of the previous day.

Dynamical boundary values are provided by the analysis run of the respective mother domain. This scheme of inheritance of information is chosen due to two reasons:

1) The analysis on the CG for the current day already comprises the knowledge about the system coded in the observations from the current day and, thus, is a step beyond any forecast resting on an analysis from the previous day. However, following the principle of nesting,

2) the forecast on the nested domain can contain physical and chemical features which are not feasible by a coarse grid simulation and thus are not destroyed by taking the initial values from a model simulation on the same nest level. Inflow regions of the nested domain will always gain the information already contained in the mother domain.

The principle of initial value optimisation is that integrating the analysis model state will lead to an improved forecast skill. To put it simple, the information of an observation is integrated backward in time and at the resulting position the model state is changed. If this location lies outside the model domain, there is no direct possibility to use this observation for adjusting the initial model state. This applies for all parts of a model domain, which are influenced by boundary conditions during the forward integration. Consequently, this will happen even more often on a much smaller, nested domain. One direct conclusion is, that initial value optimisation will lose its information gain under strong inflow conditions, when the domain is too small compared to the length of the assimilation window. This will lead to a stronger focus on emission factor optimisation on nested domains. Future developments should therefore focus on the model design and to assure that the main region of interest is always far enough from lateral boundaries. This can be achieved, e.g, by analysing the current dynamics on the coarse grid and to decide the size and location of a nested domain afterwards. Concerning possible benefits of data assimilation in nested applications, it has to be stressed, that the observational errors comprise measurement errors as well as representativeness errors, which are due to the limitations given by Hx generating the model equivalence to y.
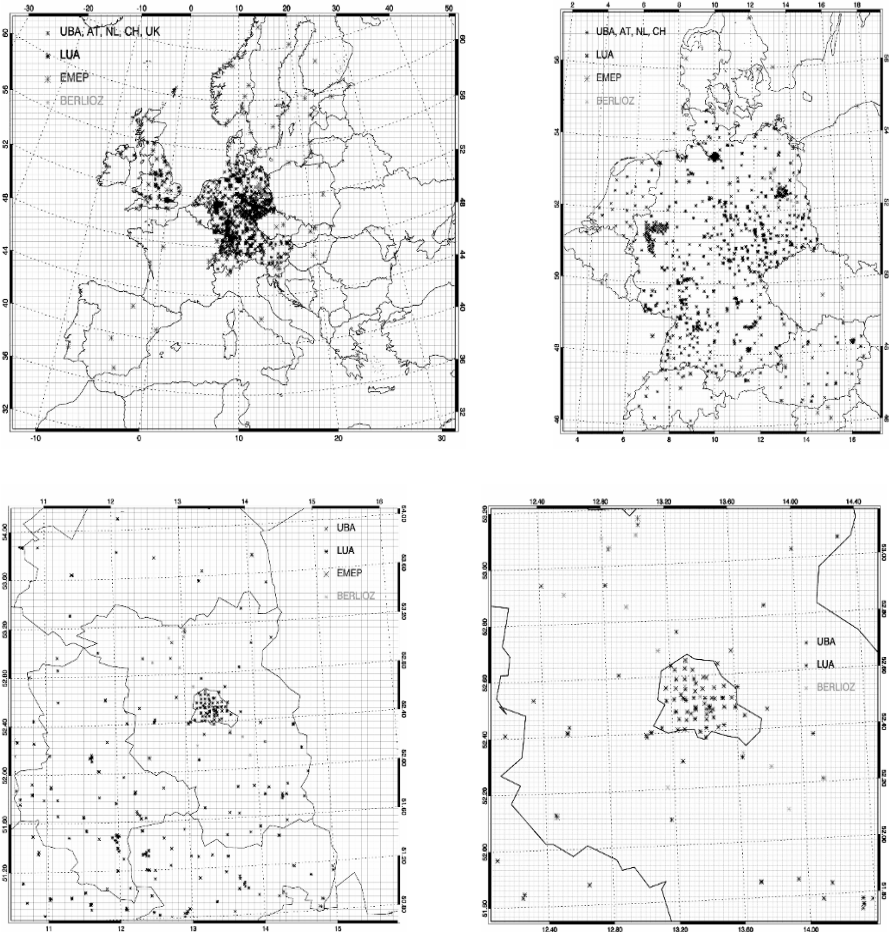
Figure 1. BERLIOZ grid designs and observational sites with the observation configuration for 20 – 21 July 1998. The horizontal resolution is 54, 18, 6 and 2 km, respectively, from the upper left to the lower right panel. The stations of the operational networks of the German Federal Environmental Agency (UBA) and the corresponding institutions from The Netherlands, Switzerland, Austria, and the United Kingdom are shown together with the campaign stations of UBA, EMEP and BERLIOZ.

The telescoping facilities of the nesting technique allow to successively enhance the horizontal resolution of a model simulation.

Due to the finer discretization in x, this will lead to a stepwise improved quality of *Hx*. The benefits of the nesting technique in simulating trace gases with a high spatial variability like nitrogen oxides has been shown in various model simulations and will be expanded here to data assimilation. In addition to the possible benefits of nested forecasting, the application of the nesting technique in an advanced chemical data assimilation system supplies the feasibility of high-quality spatio-temporal model state analyses at an almost arbitrary horizontal resolution. This enables possibly the variational calculus to identify wrong process treatment or inappropriate discretization. With increasing computer power and high resolving campaign data supported by satellite based earth observations, these issues will be at hand.

2.3. CASE STUDY SET-UP

The simulations for the BERLIOZ campaign include a coarse grid (CG), encompassing Europe and parts of North-Africa. Three domains (N1,N2,N3) have been nested with a nesting ratio of three, resulting in a sequence of 54-18-6-2 km, telescoping from regional scale down to urban scale. Nest 3 covers the greater Berlin area, being the region of main interest. The nesting sequence is shown in Figure 1, together with the locations of in-situ measurements. The BERLIOZ campaign stations were located in a SE-NW line, due to a high probability of this wind direction during July and thus the possibility to trace the plume. However, the meteorological situation during BERLIOZ was exceptionally dominated by westerly wind regimes (Volz-Thomas et al., 2003),and intensive observational periods (IOPs) took place only on July 20 and 21 and August 4 and 5, due to the then given observability of the plume by the campaign stations. The days analysed by the EURAD 4d-var data assimilation system are July 20 to 21, 1998.

3. Results

The nested simulations presented here are based on assimilation procedures applying joint optimisation, where both, the initial values and the emission rates are optimised jointly with the same calculation. This proved to be superior to the single initial value or only emission factor optimisation. It must be noted, that the time series include the forecast for quality control, while only observations from the first 14 hours (from 06 to 20 UTC) have been assimilated (grey shaded areas in the time series plots of Fig. 2).

NO_x data proved to be difficult to assimilate, due to its highly reactive character and localized emissions (Elbern and Schmidt, 2001). Urban street level conditions with channelling conditions of buildings are at the limits of

Eulerian modelling with the traditional vertical coordinate designs. Fig. 2 presents selected NO$_2$ and NO observations (red crosses) and the model simulation results for the second nested domain N2. The simulation skill is very good to excellent, not only for the assimilation window but also for the subsequent forecast. Concentration peaks, which have not been predicted by the control run (and partly neither by the first guess run), can be reproduced in a fully satisfying way by the analysis run. Hence, observed time series of species which have a strong local variability have become sufficiently predicted by optimised model simulations with a spatial resolution of 6 km. Consequently, besides the facility of improving the horizontal resolution by nesting, the feature of joint initial value and emission rate optimisation appears to be prerequisite for skilful forecast of emitted species.
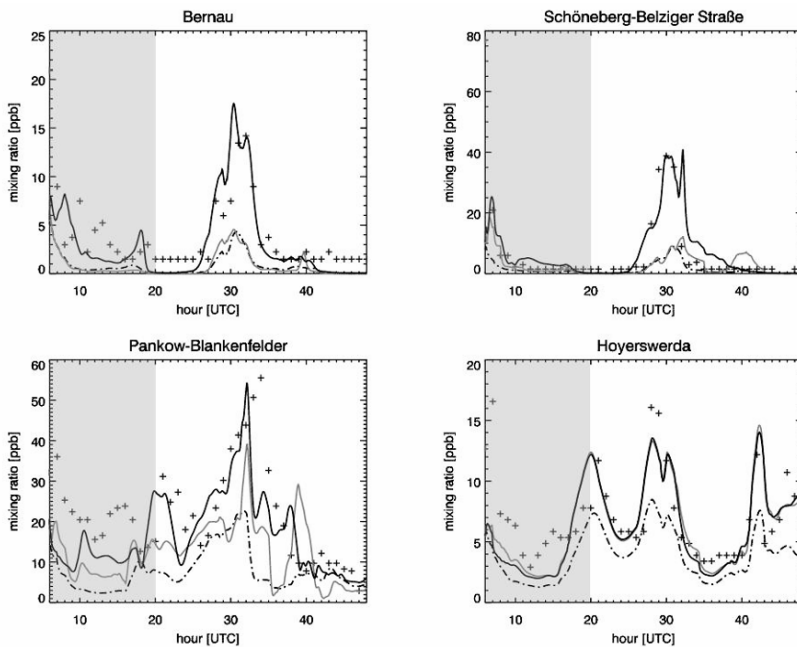
Figure 2. Examples of NO$_x$ observations at BERLIOZ stations and calculations in nested domains with subsequent forecasts from 20 to 21 July 1998. Top row: NO at stations Berrnau (left) and Schönefeld - Belziger Straße. Bottom row: NO$_2$ at stations Pankow, Blankenfelder Straße (left), and Hoyerswerda (right). Observations are given by crosses. The assimilation interval is indicated by grey shading. Observations outside the assimilation interval serve for forecast performance control. Light solid line: first guess on N2 (6 km resolution) after assimilation on coarser grids CG (54 km) and N1 (18 km). Dark solid line: analysis run after data assimilation on CG/N1/N2. Dash-dotted line: control run without data assimilation on any grid, for reference only.
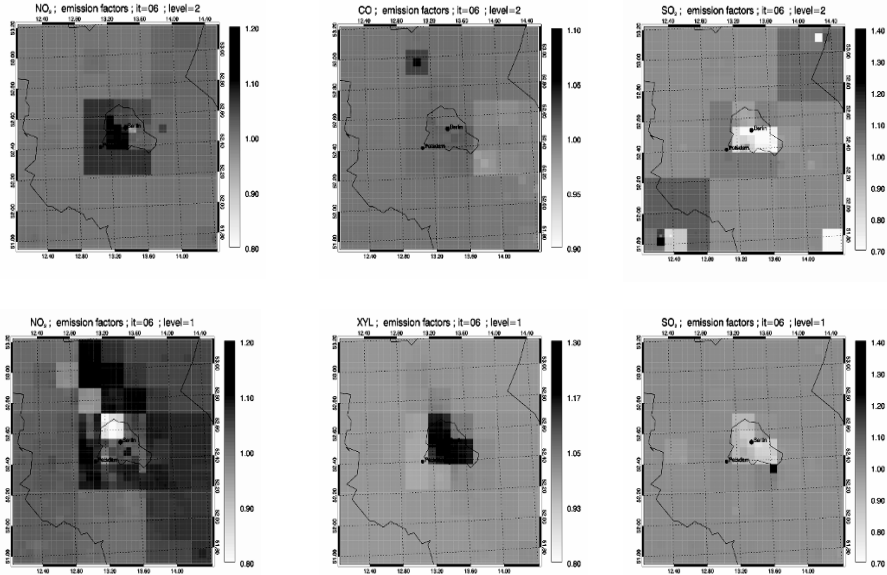
Figure 3. Emission source strength estimates by nested variational inversion. Optimised emission factors for nest 3 are given for the surface layer (bottom panels) and first height layer ~76m (top panels). Left panels NO$_2$, middle panels xylene (bottom), CO (top), and right panels SO$_2$.

As a result of the assimilation procedure, emission correction factors are inferred, which serve to optimise absolute emission values. Each nest level contributes to refinements of the emission strength, with values for each emitted species at each grid cell affected by emissions. The analysed emission factors for sulphur dioxide, nitrogen dioxide, carbon monoxide and xylene on Nest 3 are given in Fig. 3. While only surface emission scaling factors are given for CO and xylene, both the surface and next higher level values for SO$_2$ and NO$_2$ are shown additionally. The different optimisation stages in terms of boxes of coarse grid and nests 1, 2 and 3 are still visible by their respective grid cell size. Each nest level refines the previously determined emission scaling factors. The resulting emission factors show moderate values, thus the analysis runs do not enforce a vigorous change in emission inventory to reproduce the observational information. Rather, factors remain in the limits of 0.5 and 1.5 on extreme occasions. These are given for SO$_2$ in the eastern part of Berlin, where obviously the emission inventory does not fully capture the progress made in reduction of sulphur emissions after economic transition of the former

GDR areas. These optimised emission rates are a direct estimate of improved surface fluxes and exert control of the simulated chemical evolution to perform considerably improved forecasts, as has been shown in Figure 2.

4.   Conclusions

Emission rate and forecast optimisation by estimation of the chemical state and emission rate correction factors by data assimilation is crucially dependent on the spatial representativity of the data. As emission patterns are often characterized by point and line sources, measurements in the vicinity of the sources have only a very limited representativity. On the other hand, most of available stations are deployed in densely populated areas with associated crowding of sources and related fine scale structures. In response to this problem only nesting techniques are able to exploit data close to structured emissions. Success could be demonstrated for NO and NO_2 assimilation in densely populated areas of Berlin and vicinity. It turned out that a step forward in forecast skill could be observed with a spatial resolution of 6 km. This could also indicate the target resolution to be aspired by satellite instruments for a fully useful application in highly industrialised regions. With a scan size of 24 km × 13 km, OMI (Ozone Monitoring Experiment) is a huge step forward from SCIAMACHY (60 km × 30 km) and GOME-2 (80 km × 40 km). While all these instruments clearly give evidence of highly elevated NO2 levels by tropospheric column amounts, spectral sensitivity of these instruments is low at the lowest atmospheric levels, where air quality really matters. Therefore, improvements for forecasting pollution levels at street level will rest on in situ observations, unless further progress is made in satellite instrumentation.

References

Elbern, H., Schmidt, H., and Ebel, A., 1997, Variational data assimilation for tropospheric chemistry modeling*, J. Geophys. Res*. **102, D13:**15,967-15,985.

Elbern, H., and Schmidt, H., 1999, A four--dimensional variational chemistry data assimilation scheme for Eulerian chemistry transport modeling, *J. Geophys. Res.* **104:**18,583-18,598.

Elbern, H., Schmidt, H., and Ebel, A., 1999, Implementation of a parallel 4D-variational Data Assimilation scheme, *Environ. Manag. Health* **10:**236-244.

Elbern, H., Schmidt, H., Talagrand, O., and Ebel, A., 2000, 4D-variational data assimilation with an adjoint air quality model for emission analysis*, Environ. Mod. Softw.* **15:**539–548.

Elbern, H., and Schmidt, H., Ozone episode analysis by four-dimensional variational chemistry data assimilation, *J. Geophys. Res,* **106, D4:**3569–3590.

Elbern, H., and Schmidt, H., 2002, Chemical 4D variational data assimilation and its numerical implications for case study analyses, in: *IMA Volumes in Mathematics and its Applications, Volume 130: Atmospheric Modeling,* D. P. Chock and G. R. Carmichael, eds, Minneapolis, Minnesota, pp. 165–184.

Jakobs, H.J., Feldmann, H., Hass, H., and Memmesheimer, M., 1995, The use of nested models for air pollution studies: An application of the EURAD model to a SANA episode, *J. Applied Meteor.* **34:**1301–1319.

Nocedal, J., 1980, Updating quasi--Newton matrices with limited storage*. Mathem. Comp.* **35:**773–782, 1980.

Volz-Thomas, A., Geiss, H., Hofzumahaus, A., and Becker, K.H., Introduction to spezcial section: Photochemistry Experiment in BERLIOZ*, J. Geophys. Res,* **108, D4:** 8285, 2003.

Weaver, A., and Courtier, P., 2001, Correlation modelling on the sphere using a generalized diffusion equation, Quart. J. Roy. Meteor. Soc. 127:1815–1846.

OPTIMIZATION PROBLEMS OF ALGORITHMS CONNECTED WITH DIFFERENT CALCULATION SCHEMES OF DIFFERENCE EQUATIONS

KARTLOS KACHIASHVILI*
I. Vekua Institute of Applied Mathematics of the Tbilisi State University, 2,University st., Tbilisi, 380143, Georgia,
kartlos5@yahoo.com

D. I. MELIKDZHANIAN
Center of Ecological Safety of the Georgian Technical University, 77, Kostava st., Tbilisi 380178, Georgia

Abstract. The problems related to practical realization (as a computer program) of difference schemes for solving the diffusion equations that describe pollutants transport in river water are considered in this paper. In particular, the problem of optimum choosing of the algorithm parameters on which depend the accuracy, the time and the possibility of practical realization of the equation solution are considered. The demand to reduce as much as possible the time and the errors of calculations, and also the simplicity of the functions of certain classes used in mathematical models and the degree of correspondence to real physical conditions are considered as criteria of optimality.

———
To whom correspondence should be addressed. K.J. Kachiashvili, I. Vekua Institute of Applied Mathematics of the Tbilisi State University, 2,University st., Tbilisi, 380143, Georgia; e-mail: kartlos5@yahoo.com

1. Introduction

The dynamics of transport of polluting substances in river water is described by diffusion equations. These equations are needed for numerical treatment of environmental risk and impact assessment problems. Usually we have to solve these equations numerically by means of difference schemes. Thus the problem of correct choice of ratios between spatial steps of the grid, and also between them and the time step in the difference scheme for increasing the accuracy of calculation at the given number of nodal points arises there.

2. Boundary problem

For solving the diffusion equation, a boundary problem is considered as auxiliary. In this problem, the unknown function $\Phi(x)$ is defined at $x \in X$, where X is an interval (in a one-dimensional problem) or a region (in a multi-dimensional problem). The problem contains the differential equation

$$\hat{\alpha}\, \Phi(\boldsymbol{x}) = f(\boldsymbol{x})$$

with boundary conditions on the border of the region X

$$\hat{\beta}\, \Phi(\boldsymbol{x}) = \psi(\boldsymbol{x}),$$

where $f(x)$ and $\psi(x)$ are given numerical functions; $\hat{\alpha}$ is a linear elliptic differential operator; $\hat{\beta}$ is a first-order linear differential operator.

Solving the boundary problem, the differential equation for internal points of the region X is replaced by the difference equation

$$\hat{\alpha}_h\, \Phi(\boldsymbol{x}) = f(\boldsymbol{x}),$$

where $\hat{\alpha}_h$ is the difference operator depending on an additional parameter h, which is the maximum spatial step of the grid. The accuracy of approximation of the differential operator $\hat{\alpha}$ by the difference operator $\hat{\alpha}_h$ is characterized by the residual $\rho(x,h)$:

$$\hat{\alpha}_h\, \Phi(\boldsymbol{x}) = \hat{\alpha}\, \Phi(\boldsymbol{x}) + \rho(\boldsymbol{x},h).$$

In the difference schemes[1] considered below this approximation has the order h^2, i.e. at $h \to 0$

$$\rho(x,h) = O\!\left(h^2\right).$$

2.1. ESTIMATION OF THE RESIDUAL IN ONE-DIMENSIONAL DIFFERENCE SCHEMES

The residual corresponding to the difference operator $\hat{\alpha}_h$ can be determined as follows: $\rho(x,h) = h^2 \cdot \rho_h(x,h)$, where

$$\rho_h(x,h) =$$

$$\frac{1}{24}\left(\frac{\partial}{\partial h'}\right)^4 \left(G_{dn}(x,h')\cdot\Phi(x-h')+G_{md}(x,h')\cdot\Phi(x)+G_{up}(x,h')\cdot\Phi(x+h')\right).$$

h' is some number from the interval $(0,h)$.

Accurate to the terms of order h^3, one has $\rho(x,h)\approx h^2\cdot\rho_h(x,0)$, and

$$\rho_h(x,0) = -\frac{1}{12}A(x)\cdot\frac{d^4}{dx^4}\Phi(x)+\frac{1}{6}\tilde{B}(x)\cdot\frac{d^3}{dx^3}\Phi(x)+$$

$$+U(x)\cdot\frac{d^2}{dx^2}\Phi(x)+\left(V_{up}(x,0)-V_{dn}(x,0)\right)\cdot\frac{d}{dx}\Phi(x)$$

If the coefficients of the difference operator are determined by the relation

$$G_{dn}(x,h) = -A(x-h/2)-\frac{h}{2}B(x); \quad G_{up}(x,h) = -A(x+h/2)+\frac{h}{2}B(x),$$

then

$$\rho_h(x,0) = -\frac{1}{12}A(x)\frac{d^4}{dx^4}\Phi(x)+$$

$$+\frac{1}{6}\tilde{B}(x)\frac{d^3}{dx^3}\Phi(x)-\frac{1}{8}\ddot{A}(x)\frac{d^2}{dx^2}\Phi(x)-\frac{1}{24}\dddot{A}\frac{d}{dx}\Phi(x).$$

With $A(x)=A=const$

$$\rho_h(x,0) = -\frac{1}{12}A\cdot\frac{d^4}{dx^4}\Phi(x)+\frac{1}{6}B(x)\cdot\frac{d^3}{dx^3}\Phi(x).$$

2.2. MULTIDIMENSIONAL BOUNDARY PROBLEM

Let us consider the *m*-dimensional boundary problem in the case when the region X is a hyper parallelepiped the coordinates of the points of which satisfy the inequalities:

$$a_k \leq x_k \leq b_k, \quad (k=1,...,m).$$

The operator $\hat{\alpha}$ is represented in the form of

$$\hat{\alpha} = -\nabla\cdot\left(\mathbf{A}(x)\cdot\nabla\right)+B(x)\cdot\nabla+C(x),$$

where $C(x)$, $B(x)$ and $A(x)$ are the second-rank scalar, vector and tensor depending on *x*; the tensor $A(x)$ is considered as diagonal, which essentially simplifies the difference schemes. The boundary conditions are set in the form of

$$\left(p_k^{(a)}\,\Phi(\boldsymbol{x}) + q_k^{(a)}\,\nabla_k\Phi(\boldsymbol{x})\right)\Big|_{x_k=a_k} = \psi_k^{(a)}(x_1,\ldots,x_{k-1},x_{k+1},\ldots,x_m);$$

$$\left(p_k^{(b)}\,\Phi(\boldsymbol{x}) + q_k^{(b)}\,\nabla_k\Phi(\boldsymbol{x})\right)\Big|_{x_k=b_k} = \psi_k^{(b)}(x_1,\ldots,x_{k-1},x_{k+1},\ldots,x_m).$$

$(k = 1,\ldots,m)$. Here $p_k^{(a)}$, $q_k^{(a)}$, $p_k^{(b)}$, $q_k^{(b)} = const$, $\psi_k^{(a)}$, $\psi_k^{(b)}$ are the given numerical functions.

The m-dimensional rectangular grid with equidistant nodes along the coordinate axes is used in the considered difference scheme. Thus the difference equation is equivalent to the set of N linear equations for the values of function $\Phi(x)$ at nodal points with coordinates $x_k = a_k + j_k h_k$ ($k = 1,\ldots,m$; $j_k = 0,1,\ldots,N_k$), where $h_k = (b_k$ - $a_k)/n_k$ are the spatial steps of the grid; $(n_k + 1)$ is the number of nodal points along the k-th coordinate axis;

$$N = (n_1 + 1)\cdots(n_m + 1)$$

is the total number of nodal points which coincides with the order of the matrix corresponding to the difference operator $\hat{\alpha}_h$.

Diagonality of the tensor $\mathbf{A}(x)$ means that $\hat{\alpha}$ is equal to the sum of m operators, each of which contains the derivatives only by one variable. The difference operator $\hat{\alpha}_h$ approximating $\hat{\alpha}$, can also be presented in the form of the sum of one-dimensional difference operators, the expressions for which can be derived from the corresponding formulae of the previous item.

In this case, the residual of the equation can also be presented in the form of the sum of m residuals corresponding to different coordinate axes:

$$\rho(\boldsymbol{x},h) = \sum_{k=1}^{m} h_k^2 \cdot \rho_k(\boldsymbol{x},h_k),$$

and, correct to the terms of order h^3, it is possible to replace the functions $\rho_k(\boldsymbol{x},h_k)$ with their values $\rho_k(\boldsymbol{x},0)$ in the equation above. Expressions for $\rho_k(\boldsymbol{x},h_k)$ and $\rho_k(\boldsymbol{x},0)$ for each value $k = 1,\ldots,m$ are similar to the corresponding expressions for the residuals in the one-dimensional problem (in these expressions it is necessary to replace the scalar functions $A(x)$ and $B(x)$ with corresponding components $A_{kk}(\boldsymbol{x})$ and $B_k(\boldsymbol{x})$). In particular, at $A(\boldsymbol{x}) = A = const$,

$$\rho_k(\boldsymbol{x},0) = -\frac{1}{12}A_{kk}\cdot\nabla_k^4\Phi(\boldsymbol{x}) + \frac{1}{6}B_k(\boldsymbol{x})\cdot\nabla_k^3\Phi(\boldsymbol{x}).$$

2.3. OPTIMIZATION OF THE CHOICE OF NUMBERS $n_1,...,n_m$

The total number of nodal points N determines the time necessary for the numerical treatment of the algorithm; the accuracy of the obtained result depends on it. Naturally, there arises the question how the numbers $n_1,...,n_m$ at the given value N should be chosen so that the algorithm would be optimum.

In conformity with the considerations above, the upper bound of the module of the residual $\rho(x,h)$ can be presented in the form of

$$\sum_{k=1}^{m} \rho_k \, h_k^2 \text{ , where } \rho_1,...,\rho_m = const \text{ .}$$

Let us introduce an auxiliary parameter

$$H = \prod_{k=1}^{m} h_k^2 = \left(\frac{V}{n_1...n_m}\right)^2 \approx \left(\frac{V}{N}\right)^2 ,$$

where

$$V \equiv \prod_{k=1}^{m}(b_k - a_k)$$

is the volume of the hyper parallelepiped limiting the region X.

The optimization consists in that, at the given value N (i.e. at the given value H), there are defined such values $h_1,...,h_m$ for which the upper bound of the module of the residual assumes the minimum value:

$$\begin{cases} \displaystyle\sum_{k=1}^{m} \rho_k \, h_k^2 \to \min \\ \displaystyle\prod_{k=1}^{m} h_k^2 = H = \text{const} \end{cases}.$$

The solution of this optimization problem is given by

$$h_k^2 = \frac{1}{\rho_k}\left(H \prod_{k=1}^{m} \rho_k\right)^{1/m}, \qquad (k = 1,...,m).$$

Thus, at the optimum choice of spatial steps of the grid along different coordinate axes, the upper bound of the residual proves to be the sum of m equal components, each of which is proportional to the square of the corresponding step h_k. In other words, each of parameters h_k brings an identical "contribution" to the error of the result.

The main difficulty for practical realization of the described optimization scheme is the necessity of estimation of the upper bound of partial derivatives of the function $\Phi(x)$ with respect to the spatial

coordinates in terms used to express the parameters ρ_k (see Section 3) without solving the differential equation.

3. Diffusion equation

In the so-called mixed problem containing the diffusion equation, the unknown function $\Phi(t, x)$ is assumed to be defined at $t \geq 0$ and $x \in X$, where X is the interval (in the one-dimensional problem) or the region (in the multivariable problem). The problem involves the differential equation

$$D(t, x)\frac{\partial}{\partial t}\Phi(t, x) + \hat{\alpha}(t)\,\Phi(t, x) = f(t, x),$$

with $\Phi(0, x) = \Phi_0(x)$ and boundary conditions on the border of the region X

$$\hat{\beta}(t)\,\Phi(t, x) = \psi(t, x),$$

where $D(t, x), f(t, x), \psi(t, x)$ and $\Phi_0(x)$ are given numerical functions; $\hat{\alpha}(t)$ is a linear elliptic differential operator depending on t; $\hat{\beta}(t)$ is a first-order linear differential operator depending on t.

3.1. ESTIMATION OF THE RESIDUAL

Let the difference operator $\hat{\alpha}_h(t)$ approximating $\hat{\alpha}(t)$ be known:
$$\hat{\alpha}_h(t)\,\Phi(t, x) = \hat{\alpha}(t)\,\Phi(t, x) + h^M\,\rho_h(x, t, h).$$

The accuracy of approximation of the diffusion equation by the difference equation is characterized by the residual $\rho(t, x, \tau, h)$:

$$\frac{1}{\tau}D(t + v\tau, x)\cdot\big(\Phi(t + \tau, x) - \Phi(t, x)\big) + \sigma\cdot\hat{\alpha}_h(t + v\tau)\,\Phi(t + \tau, x) +$$

$$+ (1 - \sigma)\cdot\hat{\alpha}_h(t + v\tau)\,\Phi(t, x) = f(t + v\tau, x) + \rho(t + v\tau, x, \tau, h).$$

The last equation is exact; it transforms into the difference equation which can be used for the approximate solution of the initial diffusion equation if we neglect the function $\rho(...)$ on the right side.

The last equation can also be rewritten in the form of the equation for layers:

$$\hat{\alpha}_{lau}^{(h)}\,\Phi_{lau}(x) = f_{lau}(x) + \rho(t', x, \tau, h),$$

where

$$\hat{\alpha}_{lau}^{(h)} = \sigma\cdot\hat{\alpha}_h(t') + \frac{1}{\tau}D(t', x)\cdot\hat{I}; \qquad t' = t + v\tau.$$

For the symmetric scheme:

$$\rho(t, \boldsymbol{x}, \tau, h) = h^{M} \rho_{h}(t, \boldsymbol{x}, h) + \tau^{2} \rho_{\tau}(t, \boldsymbol{x}, \tau, h),$$

where

$$\rho_{\tau}(t, \boldsymbol{x}, \tau, h) = \frac{1}{48} D(t, \boldsymbol{x}) \left(\Phi^{(3)}(t + \tau'/2, \boldsymbol{x}) + \Phi^{(3)}(t - \tau'/2, \boldsymbol{x}) \right) +$$

$$+ \frac{1}{16} \hat{\alpha}_{h}(t) \left(\Phi^{(2)}(t + \tau''/2, \boldsymbol{x}) + \Phi^{(2)}(t - \tau''/2, \boldsymbol{x}) \right);$$

τ' and τ'' are values from the interval $(0, \tau)$;

$$\Phi^{(k)}(t, \boldsymbol{x}) \equiv (\partial / \partial t)^{k} \Phi(t, \boldsymbol{x}).$$

The residual has the order $\tau^{2} + h^{M}$. one finds, correct to the terms of order τ,

$$\rho_{\tau}(t, \boldsymbol{x}, \tau, h) = \frac{1}{24} D(t, \boldsymbol{x}) \Phi^{(3)}(t, \boldsymbol{x}) + \frac{1}{8} \hat{\alpha}_{h}(t) \Phi^{(2)}(t, \boldsymbol{x}).$$

For all other schemes, except the symmetric one,

$$\rho(t, \boldsymbol{x}, \tau, h) = h^{M} \rho_{h}(t, \boldsymbol{x}, h) + \tau \rho_{\tau}(t, \boldsymbol{x}, \tau, h),$$

where

$$\rho_{\tau}(t, \boldsymbol{x}, \tau, h) =$$

$$= \frac{1}{2} D(t, \boldsymbol{x}) \left((1 - v)^{2} \cdot \Phi^{(2)}(t + (1 - v)\tau', \boldsymbol{x}) - v^{2} \cdot \Phi^{(2)}(t - v\tau', \boldsymbol{x}) \right) +$$

$$+ \hat{\alpha}_{h}(t) \left(\sigma(1 - v) \cdot \Phi^{(1)}(t + (1 - v)\tau'', \boldsymbol{x}) - v(1 - \sigma) \cdot \Phi^{(1)}(t - v\tau'', \boldsymbol{x}) \right);$$

τ' and τ'' are some numbers from the interval $(0, \tau)$;

$$\Phi^{(k)}(t, x) \equiv (\partial / \partial t)^{k} \Phi(t, x).$$

The residual has the order $\tau + h^{M}$. Correct to the terms of order τ

$$\rho_{\tau}(t, \boldsymbol{x}, \tau, h) = (1/2 - v) D(t, \boldsymbol{x}) \Phi^{(2)}(t, \boldsymbol{x}) + (\sigma - v)\hat{\alpha}_{h}(t) \Phi^{(1)}(t, \boldsymbol{x}).$$

3.2. OPTIMIZATION OF THE CHOICE OF PARAMETER τ FOR THE SCHEME OF THE ORDER τ^{2}

Similar to the solution of boundary problems, there arises the question with regard to the solution of difference schemes for the diffusion equation: how to choose the parameters of the algorithm in an optimum way. In this case, it is the question of the optimum choice of the parameter τ at the given spatial steps of the grid.

We shall consider that the mean time it takes the computer to solve the set of N linear equations at big values of N is proportional to N^k, where k is some positive constant.

If the method of scrolling is used to solve the set of equations, then $k \approx 1$.

If the Seidel method is used to solve the set of equations and the number of nonzero elements in each row of the matrix of the considered set is fixed and does not depend on N, then $k \approx 1$.

Treating the problem in the same way as in Section 3.1 we find that, at the given value of the upper bound of the module of the residual of the equation which is equal to ε, there are specific values τ and N for which the time of calculation assumes the minimum value:

$$\begin{cases} N^\kappa / \tau \to \min \\ \rho_\tau \, \tau^2 + P \, N^{-2/m} = \varepsilon = \mathrm{const} \end{cases}.$$

The solution of this optimization problem is given by

$$N = \left(\frac{P\,(\kappa + 1/m)}{\kappa \varepsilon} \right)^{m/2}; \qquad \tau^2 = \frac{1}{\rho_\tau} \frac{\varepsilon}{1 + \kappa m};$$

$$\rho_1 \, h_1^2 = ... = \rho_m \, h_m^2 = \kappa \, \rho_\tau \, \tau^2 = \frac{\kappa \varepsilon}{1 + \kappa m}.$$

In the case when $k = 1$, at the optimum choice of grid spacing and time step, the upper bound of the residual proves to be the sum of $m + 1$ equal components, each of which only depends on one of the parameters: $\tau, h_1, ..., h_m$. This result is similar to the one obtained in Section 2.3.

3.3. OPTIMIZATION OF THE CHOICE OF PARAMETER τ FOR THE SCHEME OF THE ORDER τ

Let us consider the same problem as in the previous section provided that the used difference scheme is not symmetric. In this case, the upper bound of the module of the residual $\left| \rho(t, x, \tau, h) \right|$ of the considered diffusion equation can be written in the form $\rho_\tau \, \tau + \sum_{k=1}^{m} \rho_k \, h_k^2$, where $\rho_\tau, \rho_1, ..., \rho_m = const$.

We can repeat the procedure outlined in the previous section with minor changes. The condition of optimization is written in the form

$$\begin{cases} N^{\kappa} / \tau \to \min \\ \rho_{\tau}\, \tau + P\, N^{-2/m} = \varepsilon = \text{const} \end{cases}.$$

The solution of this optimization problem is determined by

$$N = \left(\frac{P\,(\kappa + 2/m)}{\kappa \varepsilon} \right)^{m/2}; \qquad \rho_{\tau}\, \tau = \frac{\varepsilon}{1 + \kappa m/2};$$

$$\rho_1\, h_1^2 = \ldots = \rho_m\, h_m^2 = \frac{1}{2}\kappa\, \rho_{\tau}\, \tau^2 = \frac{\varepsilon \kappa/2}{1 + \kappa m/2}.$$

4. Estimation of unknown function derivatives

As already mentioned in the previous two sections, it is necessary for practical use of the described optimization schemes to somehow estimate the upper bounds of the modules of partial derivatives of the unknown function with respect to independent variables without solving the boundary or the mixed problem.

It should be borne in mind that the derivatives of these functions can be estimated up to a common constant multiplier.

One of the ways of the solution of this problem consists in the following: for some values of the parameters h_k and τ (used for the solution of the diffusion equation) the values of the function Φ are determined as a first approximation, then, by means of numerical differentiation the required derivatives are determined and the values sought for the parameters are calculated. After that, using these values there are determined new values of the function Φ and so on until the difference between the last two calculated values of the function are less than a given value. Regarding the solution of the diffusion equation it is possible to use the explicit scheme at the first stage. Further it is necessary to determine the values of the sought function with higher accuracy.

In this case, an iteration method similar to the one used in[2] for the calculation of the multidimensional integral by the Monte-Carlo method can be employed for determination of the unknown function values.

It is known that the operations of numerical differentiation are not steady, but this should not prevent the application of the proposed method since it only requires the rough estimate of unknown derivatives.

The obvious draw-back of the given method is necessity of performance of a large number of additional calculations.

Undoubtedly, there are also other methods of estimations of the parameters ρ_k and ρ_{τ}. This is the theme of further studies.

5. Conclusions

The essence of this work is solving the problems related to the numerical solution of the diffusion equation that describes transport of pollutants in rivers. In particular, the problem of optimum choice of the algorithm parameters on which the accuracy depends, the required time and the possibility of practical computation of the solution are considered. The demand to reduce the time and errors of calculation as much as possible is considered as the criterion of optimality. The discussed algorithms are used in the program package "Application package for realization of mathematical models of pollutants transport in rivers" for the integration of one-, two- and three-dimensional transport models for the treatment of river water quality in the presence of pollution sources[3]. Using of this package annual mean values of some polluting substances deposited in the Black Sea by rivers of the Khbistskali basin (western Georgia) are calculated.

Acknowledgement

References

1. B.P. Samarsky, A.V. Gulin, *Numerical methods* (Science, Moscow, 1989).
2. Primak, A.V., Kafarov, V.V., KachiashviIi, K.J., *System analysis of air and water quality control*. Naukova Dumka, Kiev, 1991, 360 p. (Science and technical progress).
3. Kachiashvili K.J., Gordeziani D.G., Melikdzhanian D.Y., Khuchua V.I., Stepanishvili V.A. Software Packages for Automation of Environmental Monitoring and Experimental Data Processing // Proceedings of the third international conference advances of computer methods in geotechnical and geoenvironmental engineering, Moscow, 1–4 February, 2000, pp. 273–278.

CONTROL THEORY AND MODELS (WORKING GROUP 1)

VLADIMIR PENENKO*
Institute of Computational Mathematics and Mathematical Geophysics, Siberian Branch of Russian Academy of Sciences, Lavrentieva 6, 630990, Novosibirsk, Russia

ALEXANDER BAKLANOV, ALEXANDER MAHURA
Danish Meteorological Institute, Lyngbyvej 100, DK-2100, Copenhagen, Denmark

ARTASH ALOYAN
Institute of Numerical Mathematics, Russian Academy of Sciences, Gubkina 8, 117334, Moscow, Russia

Abstract. This paper reports on the existing approaches, needs and priority issues related to the control theory and models and their applications to environmental risk assessments, as discussed in Working Group 1 during the NATO Advanced Research Workshop (ARW) on Air, Water and Soil Quality Modelling for Risk and Impact Assessment. These include the methods of forward and inverse modelling, methods using adjoint equations, perturbation theory, and variational methods. Their applicability, advantages and shortcomings are underlined.

_____

 *To whom correspondence should be addressed. Prof. Vladimir Penenko, Institute of Computational Mathematics and Mathematical Geophysics, Siberian Branch of Russian Academy of Sciences, Lavrentieva 6, 630990, Novosibirsk, Russia; e-mail: penenko@sscc.ru.

1. Introduction

Increased interest was shown during the ARW with respect to quantitative methods of analysis of environmental processes. These methods are required for analysis of environmental quality which is connected with the problems of population health. The interest also concerns the methods of comparative analysis of the strategies to reduce risks and expenses for practical realization of such approaches. Quantitative studies of risks are important to reveal and identify the levels of chemical, biological, radioactive pollution of the environment and its influence on the population taking into account the changes of the climate and weather conditions. The term "risk assessment" is a general one, and sometimes it does not have a clear qualitative meaning. Most often, it is used for applications of a combination of tools designed for assessing the damage caused to the environment. In this sense risk assessment has an interdisciplinary character. From the point of view of the environmental sciences, it is well known that atmospheric gas pollutants and aerosols have a significant impact not only on soil, water, and vegetation, but also on the human health. Until recently, the damage due to primary emissions of different pollutants has mainly been estimated. However, secondary pollutants together with aerosol particles are also of great importance in this respect. Besides, in many cases (e.g. the hot summer 2003 in Paris) it is important to consider even more complex and combined effects of meteorological and pollution factors on human health. Hence, there is a necessity to develop comprehensive models of environmental risk assessment taking into account as many factors as possible. This will allow formulating and solving multi-criteria optimization problems within combined models with specific constraints of economical, ecological, or health essences. These problems are especially important for elaboration of mitigation strategy and minimisation of risk.

At the research institutions, represented at this workshop, a set of the comprehensive models of non-linear dynamics were developed, tested, and verified for the analysis of environmental processes. These models consist of the systems of partial differential and integral equations. They take into account a wide spectrum of acting factors of natural and anthropogenic character with different temporal and spatial scales. The combined use of forward and inverse modelling approaches is fruitful in such models. But there are some shortcomings in this methodology which should be eliminated. Namely, there is a lack of analytical tools for operational consideration of current changes in safety restriction and criteria, as well as for assimilation of current observations and measurements into the models of very high dimensions. These are so called "real time" problems. The principal difficulty in the integrated analyses of risks, socio-economical and

population health problems is the limitation or even absence of general metrics for differential consideration of various agents and factors.

Problems also exist with respect to a specific set of the objective functionals for analysis of mutual relations of the end-points, state functions' behaviour and parameters of the models.

In particular, the last two points are important for comparative analysis of management strategy of the current behaviour of the environment in order to reach the final aims and to obtain quantitative estimates of cumulative risks. The latter depends on the individual pollutants with multiple ways of impact on the environment and population health, and joint influence of multiple effects.

The formulation of such general metrics and target functionals will require additional efforts which should be done in multidisciplinary studies. Moreover, such studies need to be done in parallel and in cooperation with research and development of mathematical models and methods required to achieve optimal or compromise results.

2. Approaches and methods

During the workshop, several approaches were presented for the tasks of the risk assessment and control theory.

First, there are the methods of forward modelling based on the analysis of ensembles of scenarios for different variants of input data and acting factors. These methods can be realized with deterministic and stochastic (for example, Monte-Carlo method) algorithms.

Secondly, it is the methods that use adjoint equations generated for the evaluation of linear functionals such as inner products defined in spaces of both the state functions of models and weight functions with limited supports.

Thirdly, it is the variational method for linear and non-linear dynamical systems and functionals in combination with methods of control theory, risk theory and sensitivity theory. These methods can be realized using a combination of the forward and inverse modelling approaches taking into account the uncertainties of models, parameters and observational data.

A simplified scheme of variational methods and control theory approach for environmental risk assessment and mitigation strategy optimisation is presented in Figure 1 choosing atmospheric chemistry transport (ACT) modelling as an example.
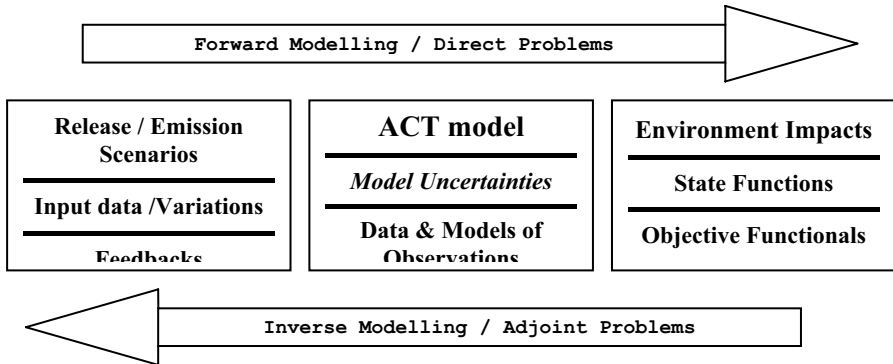
Figure 1. Simplified scheme of the variational methods and control theory approach for the environmental risk assessment and mitigation strategy optimization.

The methods of forward modelling can be applied to a given set of input parameters and data for simulation of the spatial and temporal behaviour of the state functions. Then the values of the objective functionals are calculated.

It should be noted, that the feedback in these models is usually realized by means of new runs with changed parameters. The variational methods and others using the adjoint problems can give the backward propagation of information which is contained in the target functionals to parameters of models through the sensitivity functions. This gives a basis for realization of the feedback algorithms and methods of the control theory.

The variational technique in combination with the methods of the control, risk, and sensitivity theories has a wide area for applications. In particular, among these applications are the following:

- diagnosis of the model quality,
- data assimilation,
- reconstruction of state functions using models and observational data,
- sensitivity studies,
- parameter identification,
- design of measurements,
- ecological prospecting,
- estimation of risk and vulnerability areas,
- problems of "receptor-source" and "source-receptor" types,
- detection of pollutant sources,
- environmental quality and risk control,
- optimisation of the environmental protection or mitigation strategy.

The advantages of the variational methods with adjoint problems are the following. First, they have a flexible structure which can be easily adjusted to diverse mathematical models. Secondly, they are also

conveniently adapted to sets of functionals and restrictions, as well as to different means of assimilation of observational data. The variational technique gives the possibility to incorporate a priori knowledge into the modelling technology with the help of the special functionals. Moreover, if splitting and decomposition methods are used, algorithms of simple structure and effective realization can be obtained. They are easily coordinated at different stages of the solution of the problem in the forward (principal) and adjoint (inverse) modes.

The methods of the control and optimization theories have actively been developed in different areas of science and technology during the last four decades. From the mathematical point of view they are of variational nature. As a consequence, the methods of the sensitivity theory generated from variational principles give a powerful formalism for estimating the variations of functionals of general form and particularly for evaluating risks and vulnerability of territories with respect to disturbances of acting factors in the models.

Using modern computing resources, the adjoint variational algorithms can effectively be realized at relatively reduced computational cost. Usually, one cycle of simulation includes the integration of forward and inverse models. The additional cost of inverse runs for sensitivity studies for one functional or for an ensemble of functionals, that generate just one adjoint problem, is approximately equal to the cost of the forward model run. If we need to calculate the sensitivity functions (SF) with respect to parameter variations, the additional cost of each SF is proportional to the dimension of the space-time grid domain. The total cost is obtained as the sum of the partial SF's costs over the number of parameters.

In new methods of data assimilation using splitting and decomposition techniques, the cost of one cycle of assimilation is proportional to the cost of the run for sensitivity studies of quality functionals. As regards control and optimization algorithms, the cost depends on the formulation of the problem and the approach used for its solution. For the adjoint-based gradient method using of the sensitivity relations, the cost of one iteration cycle is equivalent to the required computational costs of sensitivity relations for all target functionals and constraints defining the task formulation.

Note that optimization and identification of parameters and sources belong to the class of inverse and ill-posed problems. This requires increased quality of the numerical approximations of the models and algorithms used for forward and inverse modelling.

3. Conclusion

Future evolution of the above mentioned variational methodology will be directed toward creation of new methods for the management of

environmental quality and control of risks aiming at sustainable development, possible mitigation measures and socio-economic impact assessment. It is a new class of problems of the multi-criteria optimization of high dimensions in which the constraints of the state functions and parameters originating from inherent conditions of an application are taken into account. These constraints could arise from economical, ecological, medical, social, etc. factors. Because it is a multidisciplinary task, the involvement of the scientific community from different research fields will be essential.

CLEMENS MENSINK
VITO - Flemish Institute for Technological Research,
Boeretang 200, B-2400 Mol, Belgium

INTEGRATED MODELLING AND APPLICATIONS (WORKING GROUP 2)

Abstract. This paper reports on the ideas, needs and priority issues related to integrated modelling and applications, as discussed in working group 2 during the NATO Advanced Research Workshop on Air, Water and Soil Quality Modelling for Risk and Impact Assessment. The discussion paper presents a multi-disciplinary view on the motivation for integrated modelling in the area of environmental pollution, its objectives, the state of the art and the relevance of the work that has been presented and discussed during the workshop. The paper concludes with a reflection on the challenges and future research needs for integrated modelling.

Keywords: air, water, soil, health impacts, economical evaluation, models, risk assessment, integrated assessment

1. Introduction

What does *integrated* mean, when we discuss integrated modelling? After a first round table discussion, it was clear that integrated modelling does not mean: one machine, one unified model. Models connected to each other with a common objective, would be a better way of understanding the word integrated in terms of modelling. One of the major objectives of integrated modelling in the area of environmental modelling is to support decision makers. Models can help to make scientifically sound decisions and to

evaluate policies, e.g. as a part of a decision support system. In such a system, not only the models have to be integrated, but data bases should be integrated as well.

On the process level, integration of models is needed to couple different processes within one medium (e.g. transport, heat transfer and chemistry). On the other hand, the coupling of different media, e.g. through boundary conditions at the surface interfaces is another challenging form of integration.

Beyond the scope of individual models or decision support systems, there is a need for more integration among the modellers. To what extend can approaches and standards be integrated and harmonized? How can indicators and measures used by policy makers, - and very often composed by means of model results -, be developed in a more integrated way?

With this initial assumptions and questions on integrated modelling, we first discussed the objectives of integrated modelling. The common framework of the DPSIR approach was found to be useful in this context. The objectives and different levels of integration are discussed in section 2. A limited overview of the state of the art in integrated modelling and its applications, as from the point of view of the workshop participants, is given in section 3. In section 4 the relation with the topics and papers presented in this workshop are investigated. Where did we see efforts to integrate models or model results ? What are the issues that urgently need a continuation of these efforts ? Section 5 focuses on this last question by exploiting the challenges and future research needs.

2.   The objectives of integrated modelling

To a large extend, the objectives of integrated modelling coincide with those of integrated assessments. Models play an important role in such assessments. Integrated assessment can be defined (Munn, 2002) as an interdisciplinary process of combining, interpreting and communicating knowledge from diverse scientific disciplines in such a way that the whole cause-effect chain of a problem can be evaluated from a synoptic perspective with two characteristics:

> (i) it should have added value compared to single disciplinary assessment, and
> (ii) it should provide useful information to decision makers

Integrated assessment thus can be seen as an interactive process that links science and policies. This interactive process can be visualized by means of the DPSIR chain, shown in Figure 1.

DPSIR is a general framework for organizing information about state of the environment (OECD, 1993). The idea of the framework was however originally derived from social studies and only then widely applied

internationally, in particular for organizing systems of indicators in the context of environment and, later, sustainable development.

The framework assumes cause-effect relationships between interacting components of social, economic, and environmental systems, which are

- **D**riving forces of environmental change (e.g. industrial production),
- **P**ressures on the environment (e.g. discharges of waste water),
- **S**tate of the environment (e.g. water quality in rivers and lakes),
- **I**mpacts on population, economy, ecosystems (e.g. water unsuitable for drinking),
- **R**esponse of the society (e.g. watershed protection).
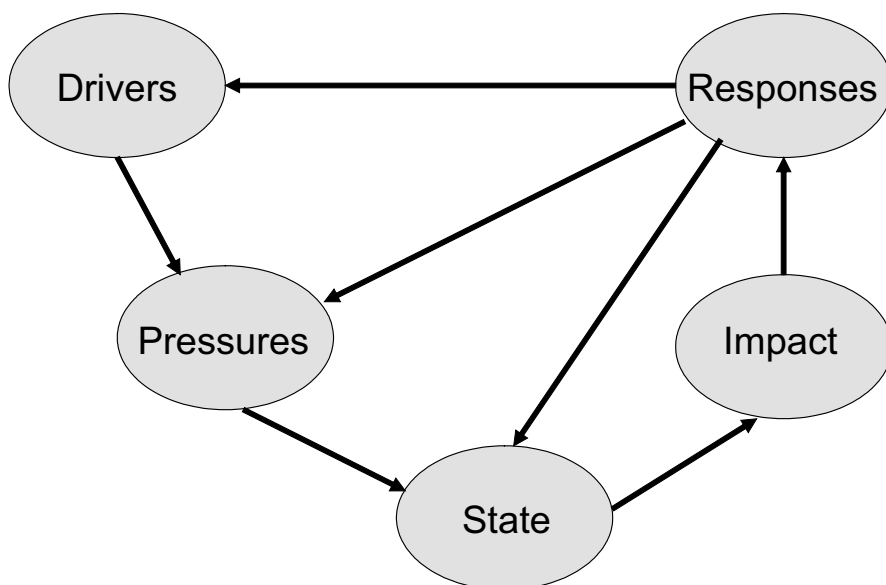
Figure 1. DPSIR chain for integrated assessments and integrated modelling.

The cycle thus starts with analyzing the human activities that are cause the problem (Drive). These anthropogenic activities will result in a pressure on the environment, e.g. by emissions or discharges into air, water or soil (Pressure). These pressures will lead to a change in the state or the quality of the environmental compartment (State). As a result we can expect certain health impacts or impacts on ecosystems. These impacts sometimes can be evaluated economically (Impact). In order to act and adjust the cause-effect chain, effective policies are needed (Response).

In this context the role of models becomes very clear. In order to take part in the process of providing policy support to decision makers, the models should be useful and integrated through the whole DPSIR chain. Examples of such approaches are the RAINS model (IIASA, 2005), the ExternE methodology (Friedrich and Bickel, 2001) and the UNECE Task Force on Integrated Assessment Modelling (UNECE, 2005).

Other motivations for model integration are more specifically dealing with different modelling aspects. However they can always be related to the DPSIR chain. Specific issues for integration are:

- Integration over different compartments (Air, Water, Soil, …),
- Integration of different scales within a compartment (time, space),
- Integration of various physical/chemical processes (transport, chemistry, boundaries),
- Integration of societal issues (policies, economical, social, decision making, health, …),
- Integration of tools and data,
- Integration of scientific disciplines.

Of course it is realized by the participants that integration of all these aspects has its limitations. Not only from a point of view of knowledge and effort management, but also from a more scientific point of view (e.g. complex multi-phase flows).

3.   State of the art in integrated modelling and its applications

Discussing the activities related to integrated modelling among the participants of the workshop, the following issues were found to be very relevant: (i) processes at the boundary interfaces and scale interactions, (ii) modelling of economical impacts and (iii) modelling multi-media exposure & health impacts. Without being complete , the following subsections give a very brief overview of the main issues discussed in the working group.

3.1.   BOUNDARY PROCESSES & SCALE INTERACTIONS

For environmental problems in air, water and soil, first of all the coupling of processes within one medium is to be described by the models (e.g. the transport of aerosols in relation to temperature and chemistry). Coupling of other media or compartments usually happens through boundary conditions. An important problem in coupling of media are the scales. Time scales

and spatial scales on which the individual processes take place are usually not compatible. Boundary layers that couple atmosphere, soil, oceans and vegetation need to be described and resolved in detail. This means that higher resolution models are needed that require a better description of exchange processes.

3.2. MODELLING OF ECONOMICAL IMPACTS

A large effort is put nowadays in trying to include economical impacts. Optimization algorithms, economical impact evaluation (damage costs) and cost & benefit analysis are integrated into environmental models in order to support the decision making process (e.g. Markal, ExternE, RAINS, Economics and water flow optimization).

3.3. MODELLING MULTI-MEDIA EXPOSURE & HEALTH IMPACTS

Pollution and health is becoming more and more relevant in all compartments. Multi-media exposure (i.e. exposure of pollutants transported through soil, water and air into the food chain) is a good example of where different modelling approaches are trying to integrate. Some examples of exposure and health impact applications are given below:

- particulate matter exposure modelling, as an input to health impact assessments and as a basis for external costs.
- Development of an ecological health index
- Modelling exposure to UV radiation (ozone depletion)
- Modelling the fate of e.g. PCB from air to soil, water and plants into the food chain
- Modelling transport of hormones in fertilizers to surface waters and ground waters; evaluation of the effects on fish and health effects (food chain).

3.4. AN EXAMPLE: AIR QUALITY ASSESSMENT BY INTEGRATION OF MONITORING AND MODELLING

An example of the state of the art in integrated air quality assessment is given in the project AIR4EUROPE. This project deals with research on integrated air quality (AQ) assessment by combining monitoring and modelling at different temporal and spatial scales for regulated pollutant components in Europe: PM_{10} (and $PM_{2.5}$), NO_2, O_3, CO, SO_2, and benzene. AIR4EUROPE strengthens the links between research and policy, which has been recognised as a priority within the "Clean Air for Europe" (CAFE)

programme. There are a wide variety of assessment methods to provide
reliable and accurate AQ data, but the methods depend on the spatial and
temporal scales, and are often not or only partially compatible. Monitoring
and modelling methods are usually used separately and consequently yield
results that are not mutually consistent.
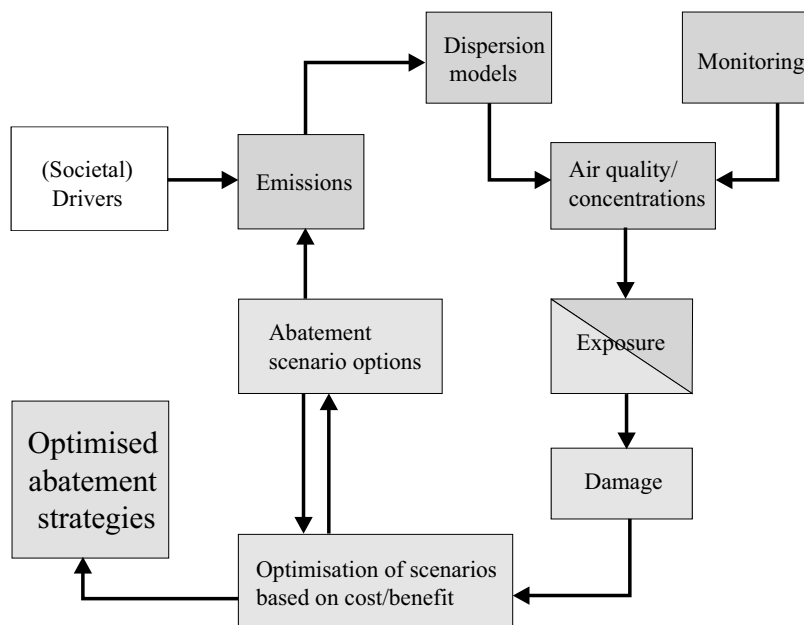
Figure 2. Functional structure of modules in an integrated AQM system.

Traditionally, urban air quality management efforts are time - and
resource-consuming, due to the large amounts of data needed for the
analysis, as well as large amounts of computer resources. In parallel with
scientific developments in the various air quality related fields, software
systems have been developed, which more or less efficiently link the
various modules needed by the system, in order to reduce the resource
consumption. GIS tools have been integrated in the systems, facilitating the
geographical presentation and visualisation of results. Internet and other
modes to make data public has been utilised as well.

The key feature of a modern environmental information and
management system is the integrated approach that enables the user in an
efficient way to access the air quality data quickly and use them directly in
the assessment and planning of actions. The demands to the integrating
features of the system, i.e. enabling monitoring, forecasting and warning,
strategic planning, as well as visualisation and presentation, will be

increasing in the future. A typical structure of an urban air quality management system is shown in Figure 2 (Moussiopoulos, 2003). In the figure, the air quality assessment section is shown by dark grey boxes, where the air quality in an area (e.g. a city) is assessed either by monitoring, by modelling, or a combination of both. The air quality abatement section is illustrated by light grey boxes. Here the damage costs and abatement costs are assessed and compared/optimised.

4. Relations with presented work

During the workshop, several issues discussed in the previous sections were addressed. Scale issues were addressed by Zilitinkevich, Alpert, Bourgeat and Baklanov. Coupling of transport and chemistry within one medium was addressed by Simunek, Ebel, and Finzi. Kordzadze and Gordeziani were focusing on integration of compartments through boundary conditions. Multiphase flows and their complexities were also addressed.

Further exploitation of computer resources and efficient use of computational power (parallel computing, grid, …) is needed. These topics were exploited by Zlatev, Elbern and others.

Methodological issues related to integrated assessment and integrated modelling were discussed in papers by Bashmakova and Mensink. Health issues were addressed by Ali-Khodja. Economical optimization was addressed by Timchenko. Integration of model output for decision support was presented by Bashmakova, Jenderedjian and San José.

5. Challenges and future research needs

What are the challenges in order to reach the objectives in integrated modelling, discussed in section 2? At the moment we have the feeling that models are only partially integrated in the different environmental compartments and there is a strong need to continue and strengthen this integration. One way of strengthening the exchange of information between different compartments is to give more attention to boundary layer processes. Boundary layers couple atmosphere, soil, oceans and vegetation. A better understanding of these processes using higher resolution models will allow a better description. Integration of heterogeneous surface fluxes is another issue which will allow a better understanding and description of the exchange processes.

Providing and improving tools for (and communication with) decision makers (law makers, policy development and evaluation) is another challenge for the future. Information offered to policy makers must provide an integrated picture, including the uncertainties, which is not always

the case. For example: when emission inventories are set up in order to support emission reduction strategies, emissions from soil should be integrated as well. This is actually not the case.

What are the research needs? In air quality modelling further integration is still hampered by the large gap between atmospheric modelling, data resolution and physical understanding on one hand and the needs for interactions with soil and water on the other hand (e.g. how do we go down from 150 km resolution to the detailed urban level). As for water quality, there is a strong need of indicators and measures characterizing an ecosystem as a whole.

There is also a need for further integration at the policy (political) level. "AIR4EUROPE" is an attempt to integrate air quality policies for cities. As mentioned in section 3.4 the methods and models have different spatial and temporal scales, which makes them not always compatible and consistent. Guidance and recommendations on how to integrate measuring and modelling techniques into internally consistent, comprehensive and cost effective assessment methods is needed. Handling and especially communicating on uncertainties is another gap. Different uncertainties should be taken into account when reporting to decision makers.

Aknowledgement

References

Friedrich, R. and Bickel, P. (ed.), 2001, *Environmental External Costs of Transport*, Springer Verlag, Heidelberg.

IIASA, 2005, www.iiasa.ac.at/~rains/

Moussiopoulos, N. (ed.), 2003, Air Quality in cities, *SATURN EUROTRAC-2 Subproject Final report*, Springer Verlag, Berlin, Heidelberg, New York, 292 p.

Munn, T., 2002, *Encyclopedia of Global Environmental Change*.

UNECE, 2005, www.unece.org/env/tfiam/welcome.html

OECD, 1993, OECD core set of indicators for environmental performance reviews. OECD Environment Monographs No. 83. OECD/GD(93)179, 39 p.

ENVIRONMENTAL MODELLING FOR SECURITY: FUTURE NEEDS AND DEVELOPMENT OF COMPUTER NETWORKING, NUMERICS AND ALGORITHMS (WORKING GROUP 3)

ZAHARI ZLATEV*
National Environmental Research Institute, Frederiksborgvej 399, P. O. Box 358, DK-4000 Roskilde, Denmark

ADOLF EBEL
Rhenish Institute for Environmental Research (RIU), EURAD-Project, University of Cologne, Cologne, Germany

KRASSIMIR GEORGIEV
Institute for Parallel Processing, Bulgarian Academy of Sciences, Sofia, Bulgaria
.

Abstract. The need of (i) more powerful computers, (ii) faster and more robust numerical methods and (iii) better utilization of the computer memory were considered in Working Group 3. Also different types of tasks, which require increased computer power for environmental risk and impact assessment, were considered during the discussion. The major conclusions are presented in this paper.

Keywords: Large-scale environmental models; numerical algorithms; efficient utilization of powerful computers; cache memory; large-scale environmental problems

———

*To whom correspondence should be addressed. National Environmental Research Institute, Frederiksborgvej 399, P. O. Box 358, DK-4000 Roskilde, Denmark; e-mail: zz@dmu.dk

1. Are the available computers sufficient in the efforts to improve the output of different environmental models?

The participants in Working Group 3 agreed very quickly that most of the problems, which several years ago were solved on supercomputers, can now be successfully treated on powerful PCs. Moreover the class of scientific problems that can be handled on the presently available PCs will become larger and larger, because the PCs are becoming more and more powerful (this is so both because the PCs are becoming faster and because the memory discs are becoming larger). This means that a growing number of modellers are now able and/or will able in the near future to run their problems on PCs (or on clusters of PCs). This possibility gives some very clear advantages, because it is possible to plan better runs that are needed in the study under consideration and, thus, to utilize better the available computer (computers).

On the other hand, the demands of the modern society for obtaining more detailed information and, what is even more important, more reliable information about environmental pollution are becoming more and more stringent. It is permanently necessary to improve the models in order to meet the increasing demands. The improvements are achieved by

- improving the description of the chemical and physical mechanisms used in the model,
- refining the resolution by using finer grids and/or different kinds of nesting,
- developing new modules (as, for example, modules for calculating aerosols),
- utilizing the available observations by applying different data assimilation algorithms.

This list of improvements of the models can be continued. It is more important, however, to emphasize the fact that any of these improvements leads to an increase of both the computing time and the storage needed in the runs of the improved models. As an illustration of this fact, it is worthwhile to point out that the application of data assimilation techniques may lead to an increase of the computing time by a factor of more than 100 (and in many cases by a factor much greater than 100). This means that tasks can become much more time and storage consuming when different improvements are incorporated in the models. This fact indicates that some large-scale problems are to be run on efficient modern computer architectures (parallel computers and/or computing grids). This is why the

demand for more powerful computers is steadily increasing in spite of the possibility, discussed in the beginning of this section, to run more tasks and more models on PCs.

The conclusion from the discussion on this topic was that

although more and more scientists will be able to use their own PCs or clusters of PCs in the solution of their tasks, the increased demands

- *for better quality of the information about our environment,*
- *for studying the future trends of the pollution levels in relation to climatic changes and*
- *for more details with regard to the spatial resolution*

will require availability and efficient exploitation of powerful super-computers and/or computing grids.

2.   Need for faster but sufficiently accurate numerical algorithms

The performance of the models with regard to computing time and data storage can be improved not only by running them on bigger and faster computers, but also by implementing more efficient numerical algorithms. This is not a very easy task because most of the scientists working in this area are already using very efficient algorithms. Nevertheless considerable advancement can still be achieved. And recently developed improved numerical methods can lead to big savings. One should especially be careful with regard to the stability of the numerical methods used in the chemical part. The selection of stable, sufficiently accurate and fast numerical algorithms in the treatment of the chemical reactions is very important.

The importance of the choice of good numerical algorithms is increased when new modules (as, for example, modules for treatment of aerosols, modules for local refinement of the grids, modules for data assimilation, etc.) are implemented in the existing model. It must be stressed here that sometimes quite new types of numerical methods are needed. If a variational data assimilation technique is used, then it is necessary to select and to implement in an efficient way some minimization algorithm (optimization algorithms are not used in the models when no data assimilation technique is applied).

The main conclusion of the discussion on this topic can be formulated as follows:

- not only is the choice of better numerical methods important in the efforts to reduce the computing time and the data storage needed in the existing models,
- but selecting quite new types of numerical algorithms might be crucial when new modules are developed and added to the models.

The choice of efficient numerical methods in the latter case is both much more needed and much more important.

3. Utilization of the cache memory of the available computer

In old computers the speed of performance of arithmetic operations was much slower than the speed of references to computer memory (i.e. than loading numbers from the computer memory to the device in the computer where the arithmetic operations are to be performed and storing back in the memory the numbers when the arithmetic operation under consideration is performed). The ratio

$$\frac{\textit{Computing time for performing arithmetic operations}}{\textit{Computing time for the needed references to memory}}$$

was as a rule greater than several hundreds. In the new computers the speed of arithmetic operations has increased tremendously (many thousand times). The speed of performing references to the computer memory was also increased, but the rate of increase was much smaller. This leads to an overall degradation of the performance. To compensate for smaller speed of references to computer memory, computers with multi-hierarchical memories, consisting of several levels of caches, are nowadays produced. It is worthwhile to point out here that cache memories are also available on all modern PCs.

If the problem is becoming large, then the efficient exploitation of the caches becomes very important. The main principle is quite simple: use the same data in the computations as long as possible (then the data will stay in cache and the computations will be fast). However, it is not easy to achieve this in practice. It should be mentioned here that subroutines in many standard libraries (also libraries which are public domain) try automatically to exploit efficiently different caches in the computers.

The main conclusion on this topic was the following: *When the problem solved becomes very large, one can achieve very good results by smart utilization of the cache memory, but such efforts do not pay too much when the problem is not very large.*

4.   Major Tasks That Require Increased Computer Power

At the end of the discussion the major tasks which require increased computer power were classified. The following three tasks were the main topic of this part of the discussion.

The first and, according to most of the participants in the discussion, the most important task, which requires to prepare and to deliver promptly reliable information, is *the evaluation of the consequences of an accident*. The accident could either be a result of human activities (as, for example, explosion in a nuclear power plant) or a result of natural catastrophe (say, storm, floating, etc.). The accident could also be a combination of human activities and specific natural conditions (as, for example, the appearance of a smoke episode in a heavy industrialized area under certain critical meteorological conditions). In all these cases, it will be necessary to inform the responsible authorities as quickly as possible about the consequences of the accident and also about the area where the consequences of the accident will be harmful for the population. Powerful computers will often be needed, because the computations should be performed and the results should be analyzed as quickly as possible. It might be appropriate to apply analyses performed by several independent groups.

Using *ensembles* (for different purposes) is another task that requires increased computer power. Indeed, the performance of 50-100 runs and preparing an ensemble on the basis of all these runs is a quite challenging task even for the best high–performance computers available at present. On the other hand, the results obtained by using ensembles are normally much more reliable than the results obtained in separate runs of a model.

Implementation of *data assimilation* techniques is another task that requires a lot of computations and storage. Therefore, as already mentioned above, also this task can only properly be solved when powerful computers are available and, moreover, efficiently used.

It was emphasized, that many other improvements of the models might lead to the necessity to use a powerful computer architecture because the computing time is increased considerably, the storage requirements become very demanding and/or both the computing time and the storage needed are highly increased.

LIST OF PARTICIPANTS

AND MEMBERS OF THE SCIENTIFIC COMMITTEE

Ali-Khodja, Hocine
Département de Chimie, Faculté
des Sciences, Université
Mentouri, Constantine, Algeria,
hocine_ak@yahoo.fr

Aloyan, Artash
Environmental Research Group,
Russian Academy of Sciences,
Institute of Numerical
Mathematics, 8 Gubkin str., GSP-1,
117334 Moscow, Russia,
aloyan@inm.ras.ru

Alpert, Pinhas
Dept. Geophysics and Planetary
Sciences,
Tel-Aviv University, Israel
Tel-Aviv, 69978
pinhas@cyclone.tau.ac.il

Baklanov, Alexander
Danish Meteorological Institute,
Lyngbyvej 100, 2100
Copenhagen, Denmark,
alb@dmi.dk

Bashmakova, Irina
Odessa State Environmental
University (OSEU)
Lvovskaja str. 15.
Odessa 65016, Ukraine
luft_vatten@yahoo.com

Bellamy, Pat
National Soil Resources Institute,
Cranfield University, Silsoe,
Bedfordshire MK45 4DT,
United Kingdom,
p.bellamy@Cranfield.ac.uk

Borrego, Carlos
Dept. of Environment and
Planning, University of Aveiro,
3810-193 Aveiro, Portugal,
borrego@ua.pt

Botchorishvili, Ramaz
I. Vekua Institute of Applied
Mathematics (VIAM), State
University of Tbilisi, 2,
University str., Tbilisi 380043,
Georgia,
ramaz.botchorishvili@gmd.de

Bourgeat, Alain
UCB Lyon, UMR 5208 – MCS,
Bât. ISTIL, Domaine de la Doua;
15 Bld. Latarjet, F-69622
Villeurbanne Cedex, France,
Alain.Bourgeat@cdcsp.univ-
lyon1.fr

Costa, Ana Manganida
Dept. of Environment and
Planning, University of Aveiro,
3810-193 Aveiro, Portugal,
anamang@dao.ua.pt

Davitashvili, Teimuraz
I. Vekua Institute of Applied
Mathematics (VIAM), State
University of Tbilisi, 2,
University str., Tbilisi 380043,
Georgia, tedav@viam.hepi.edu.ge

Ebel, Adolf
RIU, University of Cologne,
Aachener Str. 209,
50931 Cologne, Germany,
eb@eurad.uni-koeln.de

Efendiev, Yalchin
Department of Mathematics,
608K Blocker Hall, Texas A&M
University, College Station,
TX 77843, USA,
efendiev@math.tamu.edu

Elbern, Hendrik
RIU, University of Cologne,
Aachener Str. 209,
50931 Cologne, Germany,
he@eurad.uni-koeln.de

Finzi, Giovanna
Facolta' di Ingegneria, Università
degli Studi di Brescia,
via Branze, 38, Brescia, I-25123,
Italy, finzi@ing.unibs.it

Georgiev, Krassimir
Bulgarian Academy of Sciences,
Central Laboratory for Parallel
Processing, Acad. G. Bonchev
str., bl. 25A, 1113 Sofia,
Bulgaria,
georgiev@parallel.bas.bg

Gordeziani, David
I. Vekua Institute of Applied
Mathematics (VIAM), State
University of Tbilisi, 2,
University str., Tbilisi 380043,
Georgia, gord@viam.hepi.edu.ge

Gordeziani, Ekaterine
I. Vekua Institute of Applied
Mathematics (VIAM), State
University of Tbilisi, 2,
University str., Tbilisi 380043,
Georgia,
egord@viam.hepi.edu.ge

Jenderedjian, Arpine
Yerevan State University, 8
Byron str., apt. 5, Yerevan,
375009, Armenia.,
arpinej@yahoo.com

Joppich, Wolfgang
Fachhochschule Bonn-Rhein-
Sieg, University of Applied
Sciences, Grantham-Allee 20,
53757 Sankt Augustin, Germany,
wolfgang.joppich@fh-bonn-
rhein-sieg.de

Kachiashvili, Kartlos
I. Vekua Institute of Applied
Mathematics (VIAM), State
University of Tbilisi, 2,
University str., Tbilisi 380043,
Georgia,
kartlos@viam.hepi.edu.ge

Kochoradze, Givi
TSU Innovation Teaching Center,
State University of Tbilisi,3,
Chavchavadze Av., Tbilisi 0128,
Georgia, gcp@ip.osgf.ge

Kordzadze, Avtandil
Institute of Geophysics, State
University of Tbilisi, 2,
University str., Tbilisi 380043,
Georgia,
avtokor@ig.acnet.ge

Krysta, Monika
CEREA, Ecole Nationale des
Ponts et Chaussées, 6-8 Avenue
Blaise Pascal, Cité Descartes,
Champs sur Marne, 77455 Marne
la Vallée, CEDEX 2, France
krysta@cereve.enpc.fr

Mahura, Alexander
Institute of Northern Environ-
mental Problems, Kola Science
Center, Russian Academy of
Sciences, 14 A, Fersman str.,
Apatity, Murmansk Region,
184200, Russia,
mahura@inep.ksc.ru

Penenko. Vladimir
Institute of Computational
Mathematics and Mathematical
Geophysics, SB RAS, Prospekt
Lavrentieva 6, Novosibirsk
630090, Russia,
penenko@sscc.ru

Mensink, Clemens
VITO, Boeretang 200,
2400 Mol, Belgium,
clemens.mensink@vito.be

San José, Roberto
Technical University of Madrid,
Campus de Montegancedo –
Boadilla del Monte-,
28660 Madrid, Spain,
roberto@fi.upm.es

Shardakova, Ludmila
Uzhydromet, NIGMI,
72, K. Makhsumov str.,Tashkent,
700052, Uzbekistan,
sanigmi@Albatros.uz

Silva, José Matos
Instituto Superior Técnico
(CEHIDRO), Av. Rovisco Pais,
1049-001 Lisboa, Portugal,
jmsilva@civil.ist.utl.pt

Simunek, Jirka
Department of Environmental
Sciences, University of California
Riverside, Riverside, CA, 92521,
USA, Jiri.Simunek@ucr.edu

Tavkhelidze, Ilya
I. Vekua Institute of Applied
Mathematics (VIAM), State
University of Tbilisi, 2,
University str., Tbilisi 380043,
Georgia,
iliko@viam.hepi.edu.ge

Tridvornov, Alexander
Institute of Computational
Modelling, SB RAS,
Constitutions str. 9, Apartment 28,
Krasnoyarsk, 660049, Russia,
tridvornov_alexander@yahoo.co.
uk

Turkman, Aysen
Dokuz Eylul University, Dept. of
Environmental Engineering,
Kaynaklar Kampus,
35160 Buca Izmir, Turkey,
aysen.turkman@deu.edu.tr

Udovyk, Oleg
Environmental Institute,
Ukrainian Academy of Sciences,
3 Dobrohotov str., room 71,
Kyiv 03142, Ukraine,
oleg_udovyk@hotmail.com

Vereecken, Harry
Institut Agrosphaere, FZ Juelich,
52425 Juelich, Germany,
h.vereecken@fz-juelich.de

Zilitinkevich, Sergej
Finnish Meteorological Institute
(FMI), Vuorikatu 15 A,
P.O. Box 503, 00101 Helsinki,
Finland,
Sergej.Zilitinkevich@fmi.fi

Zlatev, Zahari
National Environmental Research
Institute, Frederiksborgvej 399,
P.O.Box 358, DK-4000 Roskilde,
Denmark, zlatevi@adslhome.dk

SUBJECT INDEX